

8-2017

The Functionalization of N-cyclobutylanilines under Photoredox Catalysis

Jiang Wang
University of Arkansas, Fayetteville

Follow this and additional works at: <https://scholarworks.uark.edu/etd>

 Part of the **Organic Chemistry Commons**

Citation

Wang, J. (2017). The Functionalization of N-cyclobutylanilines under Photoredox Catalysis. *Graduate Theses and Dissertations* Retrieved from <https://scholarworks.uark.edu/etd/2416>

This Dissertation is brought to you for free and open access by ScholarWorks@UARK. It has been accepted for inclusion in Graduate Theses and Dissertations by an authorized administrator of ScholarWorks@UARK. For more information, please contact scholar@uark.edu.

The Functionalization of *N*-cyclobutylanilines under Photoredox Catalysis

A dissertation submitted in partial fulfillment
of the requirements for the degree of
Doctor of Philosophy in Chemistry

by

Jiang Wang
Lanzhou University
Bachelor of Science in Chemistry, 2010

August 2017
University of Arkansas

The dissertation is approved for recommendation to the Graduate Council.

Nan Zheng, Ph.D.
Dissertation Chair

Matthias McIntosh, Ph.D.
Committee Member

Bill Durham, Ph.D.
Committee Member

Jingyi Chen, Ph.D.
Committee Member

Abstract

While transition metal catalyzed cross coupling reactions have become one of the most useful strategies in constructing carbon-carbon and carbon-heteroatom bond formations, major disadvantages such as high reaction temperature, expansive metal catalysts input and limited reaction substrates scope have significantly downshifted the applications of those two electron involved transformations. Comparably, the studies on the redox coupling reactions are less investigated. Derived from single electron transfer process, the redox coupling reactions can be used to construct otherwise challenging chemical bonds efficiently, such as Csp^3 - Csp^3 bond. Recently, visible light mediated photoredox catalysis has merged as a highly prominent tool in the development of many unconventional organic transformations. Those transformations are typically conducted in an extremely mild reaction conditions only by irradiating reaction mixtures under visible light or sunshine at room temperature and without any ligand addition. Hence, exceptional efforts are needed for further exploration of those photoredox catalyzed organic transformations. This work described an innovation approach of using visible light photoredox catalysis to develop efficient one-step syntheses for the construction of structurally diverse amine substituted novel cyclic and acyclic organic motifs from easily prepared starting materials.

Amines are typically used as a sacrificial electron donor in a photoredox derived reaction. Nan Zheng recently revealed that by incorporating amine into a reductive quenching photoredox catalytic cycle, amine can be used as both the sacrificial electron donor and substrate. To accomplish this, *N*-cyclobutylanilines were oxidized to its corresponding amine radical cation by a photoredox catalyst upon irradiation under visible light, which would lead to a distonic radical cation through a C-C bond cleavage of cyclobutyl ring. The distonic radical cation can be

trapped by a pi bond such as alkene or alkyne to reveal a novel amine substituted six membered carbon cycle through a [4+2] annulation reaction. Alternatively, by introducing a nucleophile such as trimethylsilyl cyanide and a radical acceptor such as allylsulfone derivative, a difunctionalization of *N*-cyclobutylanilines has been realized through a multicomponent reaction fashion. The method was further expanded to the success difunctionalization of fused cyclopropylanilines. Structurally important α -cyano pyrrolidines were synthesized with the generation of a quaternary carbon center on the α positin of pyrrolidines.

© 2017 by Jiang Wang
All Rights Reserved

Acknowledgments

I thank my mom and dad for their support and love since I was born. I would not be where I am without your unconditional love and support. I also thank my old brother, Bairong Wang for his love, support and encouragement.

I am forever grateful to my advisor, Dr. Nan Zheng, for his guidance, his words and deeds throughout my graduate program, as a great mentor and advisor. His broad knowledge in chemistry and cautious attitude towards science will benefit me for my entire life as a chemist. Without his encouragement and continual support, I would not have survived in the graduate program. I express my sincere gratitude to Dr. Matt McIntosh for his excellent advice in my researches. I thank Drs. Bill Durham, Jingyi Chen for serving on my committee and for all the helpful advice and suggestions. I thank Dr. James Hinton and KZ Shein for their assistance with NMR Spectroscopy. I also thank Dr. Colin Heyes for his assistance with Fluorescence Spectroscopy and all the good suggestions.

I thank Dr. Yongmin Liang from Lanzhou University and Dr. Aiqin Wang from Lanzhou Institute of Chemical Physics, Chinese Academy of Science for their guidance on my undergraduate study and their ultimate support since then.

I thank the members of the Zheng group, especially Dr. Samaresh Jana, Dr. Jie Hu and Scott Morris for being such great friends to me. I also thank Lucas Whisenhunt for being a great friend and roommate.

I thank my wonderful wife, Tianshu Zhang, for her unconditional love and support. Thanks for showing up in my life and being my life partner.

Last, I thank Chemistry & Biochemistry department for all the support.

Dedication

I dedicate this dissertation to my dearest parents, Shulan Zhang and Xiaoyi Wang.

Table of Contents

Chapter 1: Visible Light Mediated Photoredox Catalysis

1.1. Photoredox Chemistry.....	1
1.2. Photoredox Catalyst.....	4
1.3. Homogeneous Photoredox Catalysis in Organic Synthesis.....	7
1.3.1. Oxidative Quenching Cycle.....	10
1.3.2. Reductive Quenching Cycle.....	14
1.3.3. Energy Transfer Process.....	19
1.4. Amine Radical Cations.....	21
1.5. Ring Opening Strategies of Cyclobutanes.....	27
1.5.1. Transition Metal Catalyzed Activation of C-C Bond on Cyclobutane.....	28
1.5.2. Radical Mediated C-C bond cleavage on Cyclobutane.....	32
1.5.3. Donor-Acceptor (DA) Mediated Ring Opening of Cyclobutane.....	35
1.6. Conclusion.....	37
1.7 References.....	38

Chapter 2: Intermolecular [4+2] Annulation of *N*-Cyclobutylanilines with Alkynes

2.1. Introduction.....	49
2.2. [4+2] Annulation of N-cyclobutylanilines with Alkynes under Photoredox Catalysis.....	50
2.2.1. Reaction Optimization of the [4+2] Annulation.....	50
2.2.2. Substrates Scope of Monocyclic and Bicyclic <i>N</i> -Cyclotbulanilines.....	52
2.2.3. Mechanism Study.....	58
2.2.4 Experimental Section.....	61
2.2.5 Summary	87

2.3. [4+2] Annulation of <i>N</i> -Cyclobutylanilines with <i>Pi</i> bonds under Continuous Flow.....	88
2.3.1. Results and Discussion.....	89
2.3.2. Gram Scale Synthesis.....	93
2.3.3 Experimental Section.....	93
2.3.4 Summary.....	102
2.4. [4+2] Annulation under Heterogeneous $Ti^{3+}@\text{TiO}_2$ Catalysis.....	102
2.4.1. Reaction Optimization.....	106
2.4.2. Substrates Scope.....	109
2.4.3. Catalyst Recycle and Stability Study.....	111
2.4.4. Reaction Mechanism Study.....	113
2.3.5. Experimental Section.....	120
2.3.6 Summary.....	130
2.5. References.....	131

Chapter 3: Difunctionalization of *N*-Cyclobutylanilines under Photoredox Catalysis

3.1. Introduction.....	139
3.2 Results and Discussion.....	141
3.2.1. Reaction Optimization.....	141
3.2.2. Substrates Scope.....	143
3.2.3. Products Derivatization.....	146
3.2.4. Reaction Mechanism Study.....	147
3.2.5. Experimental Section.....	148
3.3. Summary.....	182
3.4. References.....	183

List of Tables

Table 2.2.1 Optimization of [4+2] Annulation	52
Table 2.2.2 Scope of [4+2] Annulation with Phenylacetylene.....	53
Table 2.2.3 Scope of [4+2] Annulation with various Alkynes.....	55
Table 2.2.4 [4+2] Annulation with Bicyclic cyclobutylanilines.....	57
Table 2.3.1 Optimization of [4+2] Annulation under Flow.....	90
Table 2.3.2 [4+2] Annulation with various <i>pi</i> bonds.....	91
Table 2.4.1 Optimization of $Ti^{3+}@\text{TiO}_2$ Catalyzed [4+2] Annulation.....	107
Table 2.4.2 Evaluation of Ti^{3+} influence in $Ti^{3+}@\text{TiO}_2$	109
Table 3.1 Difunctionalization Reaction Optimization.....	142
Table 3.2 The absorbance of the Actinometry at 510 nm.....	179

List of Figures

Figure 1.1 The Synthesis of Carvone Camphor under Sunlight.....	1
Figure 1.2. Different Pathways of Photoexcited Molecules.....	2
Figure 1.3. Absorption Spectrum of Ru(bpy) ₃ (PF ₆) in CH ₃ CN.....	4
Figure 1.4. Depiction of Working Protocol of Ru(bpy) ₃ (PF ₆) ₂	5
Figure 1.5. Ligand Effects on Redox Properties.....	7
Figure 1.6. Oxidative Quenching Cycle and Reductive Quenching Cycle.....	8
Figure 2.4.1. Catalyst Recycle.....	112
Figure 2.4.2. TEM Images of Self-doped Ti ³⁺ @TiO ₂ before Reactions.....	112
Figure 2.4.3. TEM Images of Self-doped Ti ³⁺ @TiO ₂ after 5 Runs.....	112
Figure 2.4.4. Trapping of ¹ O ₂ by TEMP without Cyclobutylaniline 1a	116
Figure 2.4.5. Trapping of ¹ O ₂ by TEMP with Cyclobutylaniline 1a	117
Figure 2.4.6. Control: Trapping of ¹ O ₂ without Ti ³⁺ @TiO ₂	117
Figure 2.4.7. Fluorescence Spectra of SOSG.....	118
Figure 2.4.8. Light source Flux Graph.....	122
Figure 2.4.9. Catalyst Recycling experiment.....	125
Figure 2.4.10a. ¹ O ₂ from T3 trapped by TEMP.....	127
Figure 2.4.10b. ¹ O ₂ trapped by TEMP without T3	127
Figure 2.4.10c. Control experiment of addition of 1a	127
Figure 3.1. The Distonic Radical Cation: Generation and Reactivity.....	140

List of Schemes

Scheme 1.1. Direct Asymmetric α -Alkylation under Photoredox Catalysis.....	9
Scheme 1.2. Photoredox Catalyzed Pschorr Reaction.....	11
Scheme 1.3. [2+2] Cycloaddition under Photoredox Catalysis.....	12
Scheme 1.4. Reductive Deiodination under Photoredox Catalysis.....	13
Scheme 1.5. Reduction of Electron-Deficient Olefins under Photoredox Catalysis.....	15
Scheme 1.6. Photoredox Catalyzed Radical Michael Addition Reaction.....	16
Scheme 1.7. Photoredox catalyzed Hydroamination Reactions.....	17
Scheme 1.8. Photoredox Catalyzed [3+2] Annulation Reaction.....	18
Scheme 1.9. Photoredox Catalyzed [2+2] Cycloadditions Through Energy Transfer.....	21
Scheme 1.10. Amine Radical Cations' Mode of Reactivity.....	24
Scheme 1.11. Photoredox aza-Henry Reaction.....	25
Scheme 1.12. Radical Michael Addition of α -Amine Radicals Derived from Anilines.....	26
Scheme 1.13. Photoredox Cleavage of C-C bonds of 1,2-Diamines.....	27
Scheme 1.14. Direct Insertion of Rh(I) Complex into Cyclobutanone.....	28
Scheme 1.15. Ito's Reductive Cylobutanone Ring Cleavage.....	29
Scheme 1.16. Nickel Catalyzed [4+2] Cycloaddition of Cyclobutanones and Alkynes.....	30
Scheme 1.17. Palladium Catalyzed Ring Opening of <i>tert</i> -Cyclobutanols.....	31
Scheme 1.19 Rhodium Catalyzed Enatioselective [4+2] Cycloaddition.....	32
Scheme 1.19. Silver Catalyzed Ring Opening of Cyclobutanol.....	33
Scheme 1.20. Cyclobutanol Ring Opening for Azadations.....	34
Scheme 1.21. Reactions of Activated Vicinal DA Cyclobutane.....	35
Scheme 1.22. Formal [2+2+2] Cycloaddition.....	36

Scheme 1.23. [4+2] Annulation of Aminocyclobutanes.....	37
Scheme 2.1 The Ring Opening Rate Studies and Our Proposed Reaction Pathway.....	50
Scheme 2.2. Proposed Reaction Mechanism.....	58
Scheme 2.3.1. Gram Scale Reaction.....	93
Scheme 2.4.1. [4+2] Annulation of Cyclobutylanilines with Alkynes.....	105
Scheme 2.4.2. Oxidation of Primary Amines to Imines on UV-irradiated TiO ₂	106
Scheme 2.4.3. Scope of the [4+2] Annulation Catalyzed by Self-doped Ti ³⁺ @TiO ₂	110
Scheme 2.4.4. Proposed Catalytic Cycle.....	114
Scheme 2.4.5. Chemical Probes for the Involvement of ¹ O ₂	115
Scheme 2.4.6. Comparison of Self-doped Ti ³⁺ @TiO ₂ against Rose Bengal.....	119
Scheme 3.1 Difunctionalization of Monocyclic Substrates.....	144
Scheme 3.2 Difunctionalization of Bicyclic cyclopropylaniline Substrates.....	146
Scheme 3.3 Derivatization of 3.3q.....	147
Scheme 3.4 Proposed Reaction Mechanism.....	148

List of Charts

Chart 2.1 Photoredox Catalysts.....	51
Chart 2.2 Cyclic Voltammograms of 1a and 3a.....	60
Chart 2.3 Fluorescence Quenching Studies.....	61
Chart 2.4 Diastereomer Identification.....	87
Chart 3.1a Using <i>N</i> -cyclobutylaniline to quench $\text{Ir}(\text{ppy})_2(\text{dtbbpy})\text{PF}_6$	176
Chart 3.1b Using allylsufone to Quench $\text{Ir}(\text{ppy})_2(\text{dtbbpy})\text{PF}_6$	177
Chart 3.1c Using TMSCN to Quench $\text{Ir}(\text{ppy})_2(\text{dtbbpy})\text{PF}_6$	177
Chart 3.2 The moles of Fe^{2+} as a Function of Time (t).....	179
Chart 3.3. Absorbance of the Ferrioxalate Actinometer Solution.....	180
Chart 3.4 Absorbance of Catalyst.....	182

List of Published Papers

Chapter 2

Wang, J.; Zheng, N., The cleavage of a C-C Bond in cyclobutylanilines by visible-light photoredox catalysis: Development of a [4+2] annulation method. *Angew. Chem., Int. Ed.* **2015**, *54* (39), 11424-11427.

Wang, J.; Nguyen, T. H.; Zheng, N., Photoredox-catalyzed [4+2] annulation of cyclobutylanilines with alkenes, alkynes, and diarynes in continuous flow. *Science China Chemistry* **2016**, *59* (2), 180-183.

Wang, J.; Mao, C.; Feng, P.; Zheng, N., Visible light mediated [4+2] annulation of *N*-cyclobutylanilines with alkynes catalyzed by self-doped $Ti^{3+}@\text{TiO}_2$. *Chem. Euro. J.* **2017**, DOI: 10.1002/chem.201701587.

Chapter 1. Visible Light Mediated Photoredox Catalysis

1.1. Photoredox Chemistry

The use of sunlight to mediate organic synthesis can be traced back to as early as the twentieth century when the brilliant Italian chemist, Giacomo Luigi Ciamician revealed the elegant synthesis of carvone camphor by exposing carvone under sunlight (Figure 1.1).¹ He predicted in one of his lecture that since sunlight is abundant, renewable and inexpensive, it is optimal energy source not only for the use in synthetic chemistry, but also it can be generally applied to all the fields such as solar materials and solar fuel.

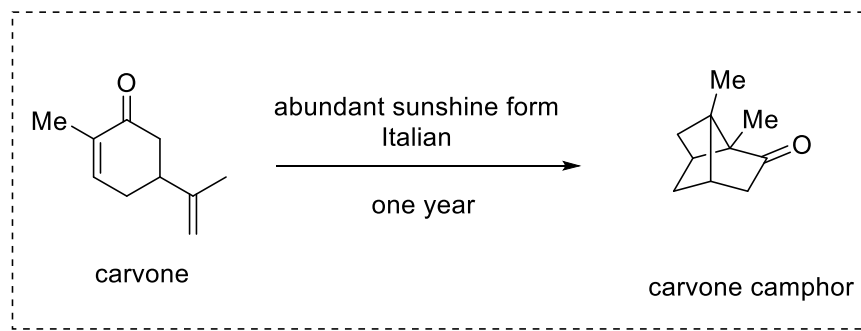


Figure 1.1. The Synthesis of Carvone Camphor under Sunlight.

Followed by his ambitious prediction and elegant synthetic application, the use of sunlight or photon as the driving force in organic synthesis has interested synthetic chemists for decades.² Such photo reactions are typically initiated by the absorption of light in the form of photons by one of the reaction components and the consequent promotion of an electron to the singlet excited state (Figure 1.2). Since the life time of the singlet excited state of the reaction component is generally rather short, it can either undergo direct vibrational relaxation to the ground state by a radiative process known as fluorescence, or rapid conversion to its lowest-

energy triplet excited state **T₁** through an intersystem crossing (ISC) process, which has been shown to possess a longer lifetime.³ The longer lived triplet excited state of the molecule can then be engaged in single-electron transfer with other organic reactants to reveal organic transformations. Alternatively, the triplet excited state of the molecule can also go through a radiative decay back to a singlet state known as phosphorescence, which has been shown to proceed at a significantly slower rate.

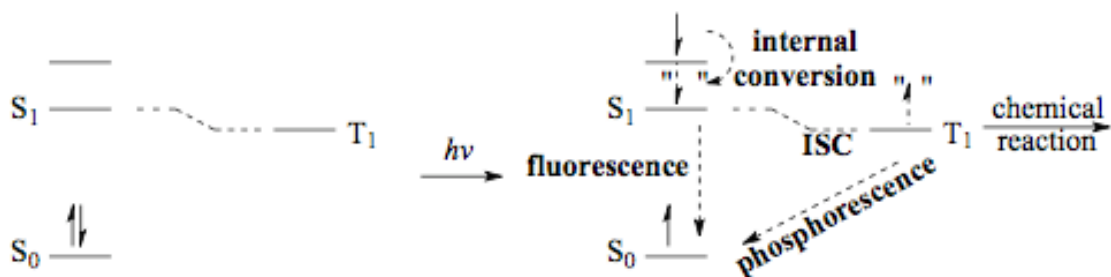


Figure 1.2. Different Pathways of Photoexcited Molecules.

Since the majority of organic molecules are not capable of absorbing visible light efficiently, earlier works of photo induced organic syntheses were mainly focused on using ultraviolet (UV) as the light source. The use of UV in organic synthesis, however, has always suffered from several major drawbacks such as functional group compatibility and chemoselectivity under UV light are generally worse than lower-energy visible light.⁴ Moreover, the requirement of intensive UV input for the generation of high-energy UV-irradiation has always increased the cost of light source and ecological footprint. The specialized and expensive photoreactors such as quartz glass wares are typically required for the transmission of UV light, which are also impractical for industry scales. To address the issues as mentioned above, organic chemists recently have turned their attentions to use visible light in synthesis.⁵ The advantages of using visible light over UV are rooted not only in its abundance and benign environmental

impact, but also milder reaction conditions allowing for greater functional group compatibility. However, due to the poor absorption of organic molecules in visible light region, chromophores/photoredox catalysts capable of absorbing visible light are typically required. A variety of photoredox catalysts have been developed to mediate electron transfer with organic molecules under direct excitation by visible light.

To date, there are two major classes of photoredox catalysts which have been constantly used in synthetic organic chemistry, metal polypyridyl complexes and metal free organic photoredox catalysts. Since metal polypyridyl complexes are used as the only class of photocatalysts in the research, the discussions will be focused only on them. However, it is important to note that the discussed concepts can be applied to both types of photo catalysts. Among all the metal polypyridyl complexes, ruthenium (II)⁻⁶ and iridium (III)⁻⁷ based complexes are particularly popular because their straightforward preparation methods, excellent stability, tolerance for harsh reaction conditions, and their unique photophysical and chemical properties. For instance, $\text{Ru}(\text{bpy})_3^{2+}$, one of the most used photoredox catalysts, possesses a strong and broad absorption band between 400-500 nm that corresponds to a metal to ligand charge transfer (MLCT) transition to yield a redox active triplet photoexcited state (Figure 1.3).⁸ This type of excited state can also be considered as the promotion of an electron from the metal-based orbital to the ligand-based orbital to produce a reactive charge separation described as $[\text{Ru}^{\text{III}}(\text{bpy}^{\cdot-})(\text{bpy})_2]^{2+*}$. As the structure of the excited $\text{Ru}(\text{bpy})_3^{2+}$ implies, it can engage in either one-electron oxidation reactions or one-electron reduction reactions via outer-sphere electron transfer processes with organic molecules to initialize radical chemistries. Seminal works by McMillan,^{9,10} Stephenson,^{11,12} Yoon,¹³ and others have¹⁴ shown great potential of visible light photoredox catalysis in organic synthesis.

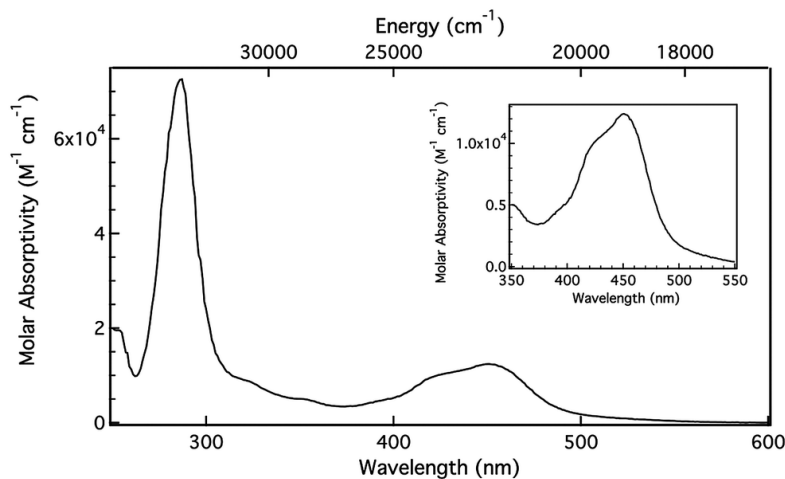


Figure 1.3. Absorption spectrum of $\text{Ru}(\text{bpy})_3(\text{PF}_6)$ in CH_3CN .

1.2. Photoredox Catalysts

The central role of a photoredox catalyst is to harvest visible light energy and then transfer it to reactants to activate them. Hence, certain characteristics such as stability over harsh reaction conditions, broad absorption spectra in the visible light region, high oxidation and/or reduction potential, longer lifetime of excited states, facile synthesis, and tunability of ground- and excited- state properties all need to be taken into consideration when choosing a proper photoredox catalyst for a targeted organic transformation. Ruthenium- and iridium-based polypyridyl complexes are two major classes of photoredox catalysts that have been widely used and studied because they possess most if not all the characteristics. It is worth noting that in addition to organic synthesis, those metal polypyridyl complexes are also widely used in a variety of applications including water splitting,¹⁵ CO_2 reduction,¹⁶ solar cell synthesis,¹⁷ and polymerization reactions.^{18,19} Metal polypyridyl complexes generally rely on electron transfer or energy transfer to activate organic molecules. Using $\text{Ru}(\text{bpy})_3(\text{PF}_6)_2$ as an example(Figure 1.4),

upon exposure to visible light irradiation, an electron in one of the metal-centered d orbitals is excited to the ligand-centered π^* orbital, generating a Ru(III) center with a radical anion of the ligand formally that is termed as metal to ligand charge transfer (MLCT). The initially generated singlet excited state of the catalyst is rather short-lived, and a rapid intersystem crossing (ISC) is followed to provide the longer-lived triplet excited state that can be further engaged in single-electron oxidation and reduction reactions or energy transfer with organic molecules. Notably, the excited state is both more oxidizing and more reducing than the ground state. This feature is likely attributed to the photocatalyst's ability to readily engage in single-electron oxidation or reduction reaction.

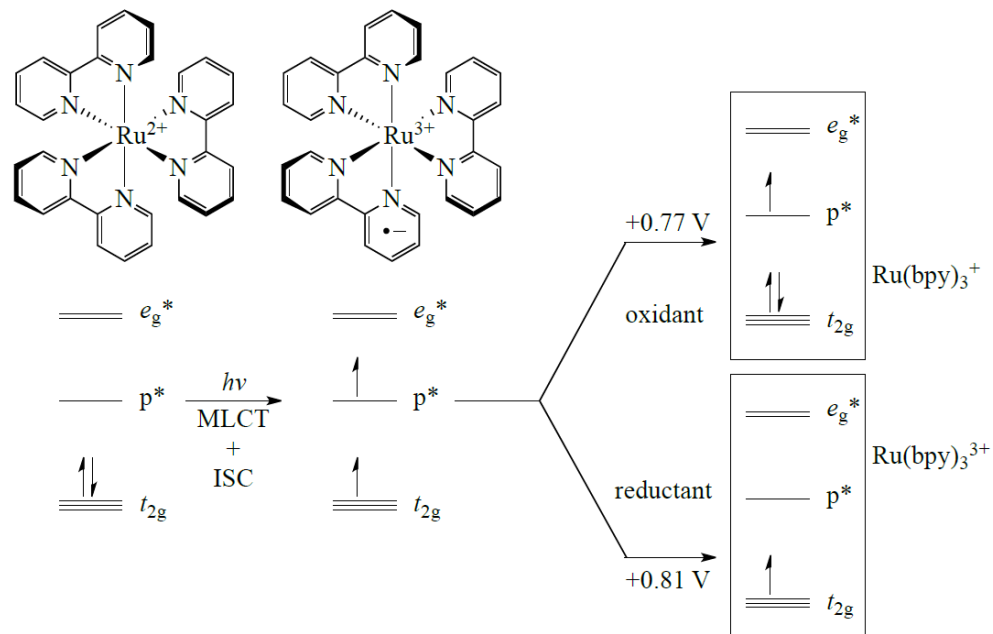


Figure 1.4. Depiction of working protocol of $\text{Ru}(\text{bpy})_3(\text{PF}_6)_2$.

One of the significant advantages for using Ru(II) and Ir(III) polypyridyl complexes as photocatalysts is their tunable redox properties. By modifying electronic properties of the ligands

as well as the metal center, the redox properties of the complex can be tuned for a targeted reaction.²⁰ Generally speaking, by making the ligands electron richer, the metal complex tends to be more reducing whereas the electron poorer ligands render the metal complex more oxidizing.^{21,22} Figure 1.5 illustrates the electronic effect of the ligand on the iridium center's redox properties. For instance, $\text{Ir}(\text{ppy})_2(\text{dtbbpy})^+$ has a ground state oxidation potential of +1.21 V [$\text{Ir}^{4+}/\text{Ir}^{3+}$] and a ground state reduction potential of -1.51 V [$\text{Ir}^{3+}/\text{Ir}^{2+}$]. By decorating electron withdrawing substituents such as F and CF_3 to the 2-phenylpyridine ligand, the resulting complex, $\text{Ir}[\text{dF}(\text{CF}_3)\text{ppy}]_2(\text{dtbbpy})^+$, shifts its reduction potential to -1.37 V for [$\text{Ir}^{3+}/\text{Ir}^{2+}$] and +1.69 V for [$\text{Ir}^{4+}/\text{Ir}^{3+}$] respectively. The less negative reductive potential indicates that the catalyst is harder to be oxidized, allowing the oxidation of the catalyst to become more difficult, and therefore is a stronger oxidation species compared to $\text{Ir}(\text{ppy})_2(\text{dtbbpy})^+$. On the other hand, less electron deficient ligands facilitate the metal-centered oxidation and make the complex more reducing. For example, when replacing 2-phenylpyridine ligand to less electron deficient 3,4'-dimethyl-2-phenylpyridine to form $\text{Ir}(3,4'\text{-dmppy})_2(\text{dtbbpy})^+$, the complex's reduction potential is shifted to -1.524 V for [$\text{Ir}^{3+}/\text{Ir}^{2+}$] and +1.20 V for [$\text{Ir}^{4+}/\text{Ir}^{3+}$] respectively. The more negative reduction potential, in this case, indicates that the catalyst is a more reducing than $\text{Ir}(\text{ppy})_2(\text{dtbbpy})^+$. Several research groups including: Yoon and Stephenson have also demonstrated the potential to fine-tune the ligands to better serve in the reaction design. Detailed discussions regarding this aspect are listed in the paragraphs below (section 1.3).

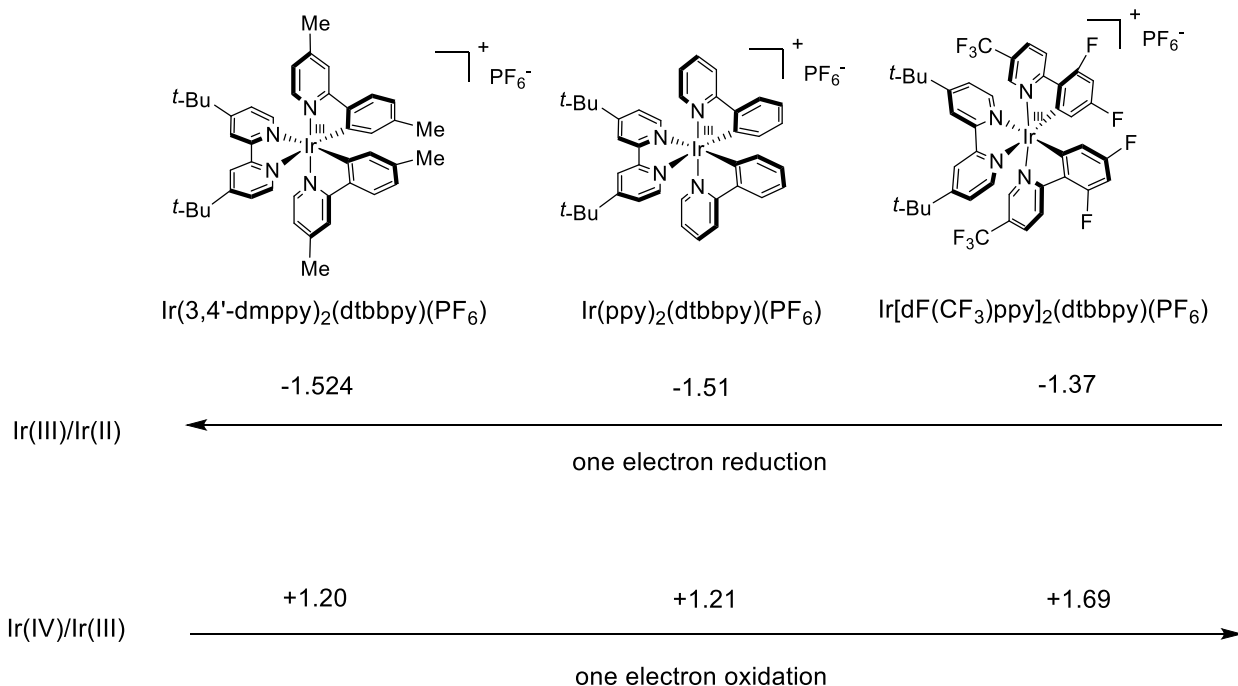


Figure 1.5. Ligand effects on redox properties.

1.3. Homogeneous Photoredox Catalysis in Organic Synthesis

Derived from photoredox catalysts' unique property of being both oxidizing and reducing when being excited to their triplet excited states by visible light, organic molecules can either be oxidized or reduced through one electron transfer manner. The pathway that organic molecules being oxidized is called reductive quenching cycle and the pathway that organic molecules being reduced is named oxidative quenching cycle (Figure 1.6). In addition to the two major pathways described above, there are rare cases that the photoexcited state of the catalysts were proposed to engage in energy transfer with organic substrates.^{13g,23,24}

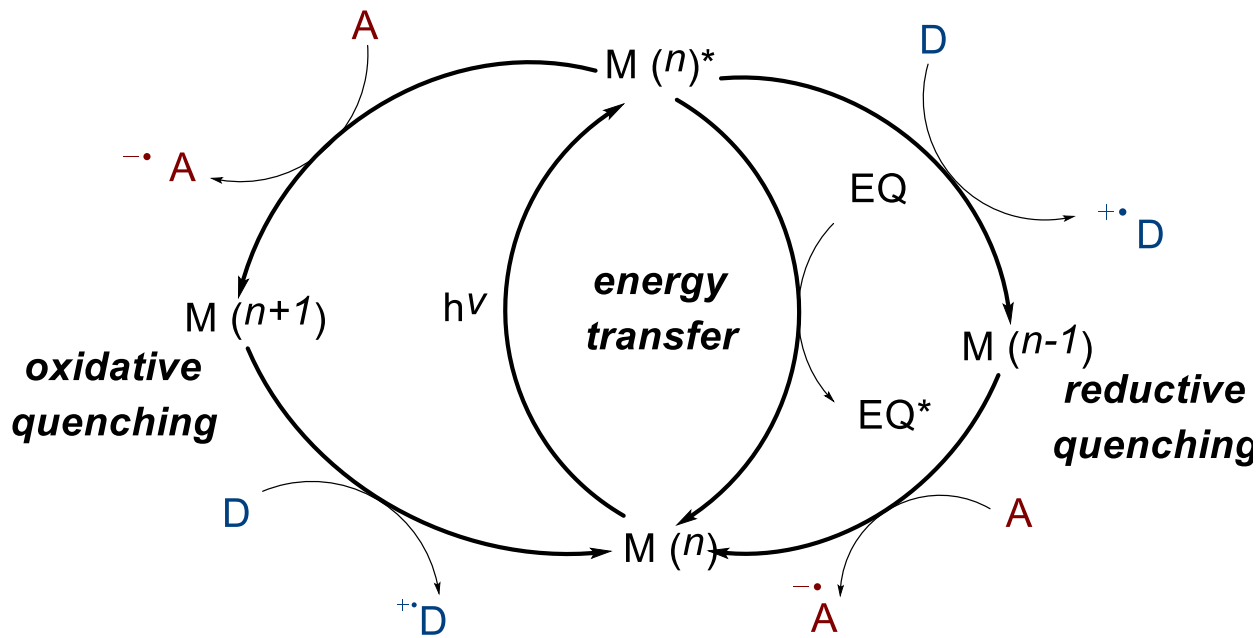
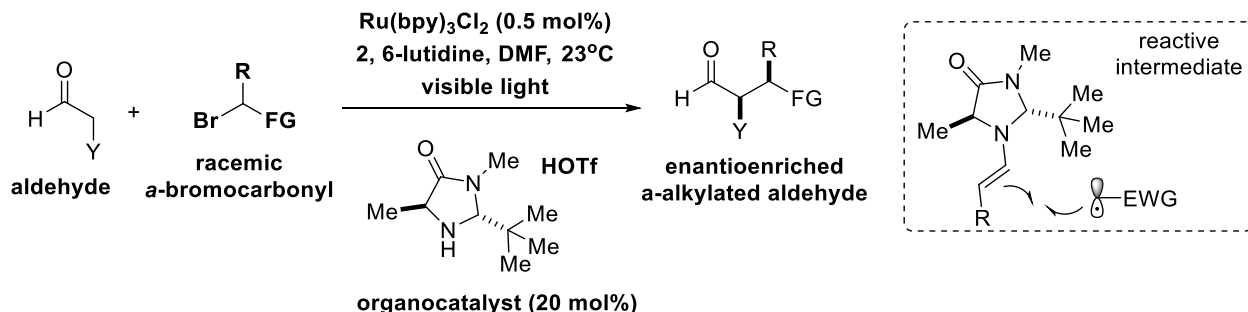


Figure 1.6. Oxidative Quenching Cycle and Reductive Quenching Cycle

Early contributions of utilizing photoredox catalysis in organic synthesis that developed by Fukuzumi²⁵, Kellogg²⁶, Tanaka²⁷, Pac²⁸ and others²⁹ were focused on the reduction of carbon-halogen bonds, olefins, carbonyls and diazonium salts with the aid of $\text{Ru}(\text{bpy})_3\text{Cl}_2$ as photoredox catalysts. A “photo rush”, however, occurred since 2008 when MacMillan demonstrated the elegant concept on the dual catalysis by merging photoredox catalysis and organocatalysis to accomplish direct asymmetric α -alkylation of aldehydes (Scheme 1.1)^{9a}. A working protocol was proposed by Nicewicz and MacMillan: excited triplet $\text{Ru}(\text{bpy})_3^{2+}$ that generated under photoredox pathway could potentially initiate an reductive cleavage of C-Br bond and furnishing an electron deficient carbon radical which can further add to the enamine, upon merging of the organocatalytic cycle. The method was shown to generate a wide scope of enantioenriched α -alkylated aldehydes efficiently with good to high reaction yields.



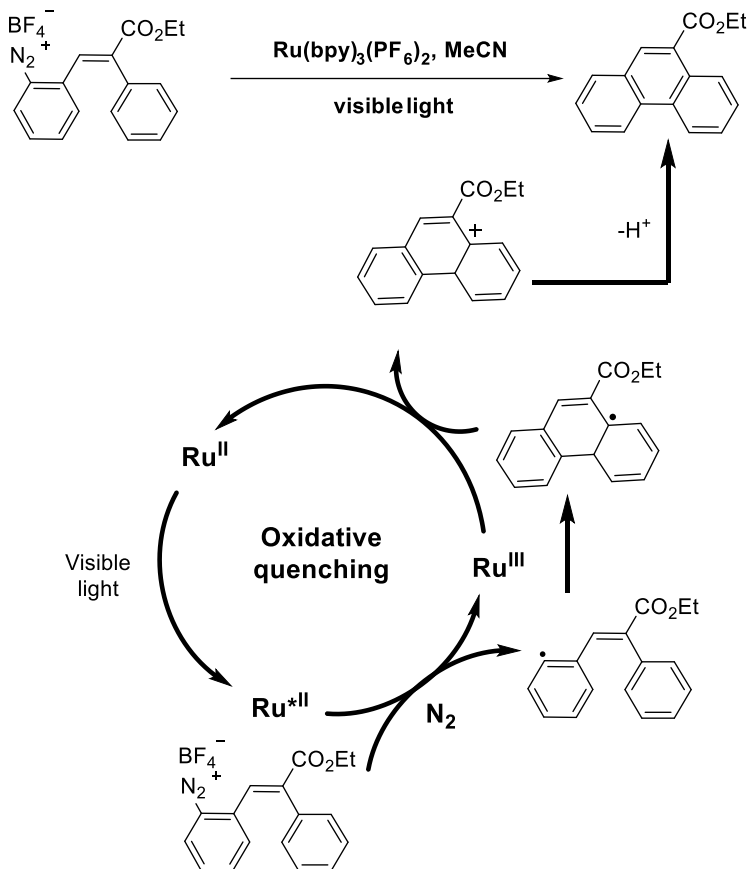
Scheme 1.1. Direct Asymmetric α -Alkylation of Aldehydes under Photoredox Catalysis.

$\text{Ru}(\text{bpy})_3\text{Cl}_2$ as a photoredox catalyst has drawn significant attention as mentioned above. Its unique photophysical properties, enabling the use of abundant, inexpensive source of visible light not only have provided extremely mild reaction conditions for organic reactions to occur, but also have suggested new thoughts on the development of environmental friendly synthetic chemistry. Its relevance in organic synthesis has impacted the further of synthetic chemistry with the growing number of novel synthetic methods for the constructions of synthetically challenging molecules and bonds formation. Along with Macmillan, Yoon and Stephenson and others have capitulated the application of photoredox catalysis by demonstrating the versatility of ruthenium and iridium complexes that participates in an oxidative, reductive or energy transfer quenching cycle. By tuning the ligands of the ruthenium or iridium complexes with the decoration of different electronic characters to achieve desired redox potentials is one of the major advantages for those photoredox catalysts. Selected examples on the synthetic applications of using the three quenching cycles have been listed in the following section.

1.3.1 Oxidative Quenching Cycle

As is mentioned previously, oxidative quenching cycle refers to a photoredox process that an excited photoredox catalyst donates an electron to an organic molecule (or oxidative quencher), resulting a reduced organic molecule for further desired redox transformation. The oxidized catalyst then can be regenerated by getting another electron from an electron donor to its ground state. The overall process can be referred to as outlined in Figure 1.6.

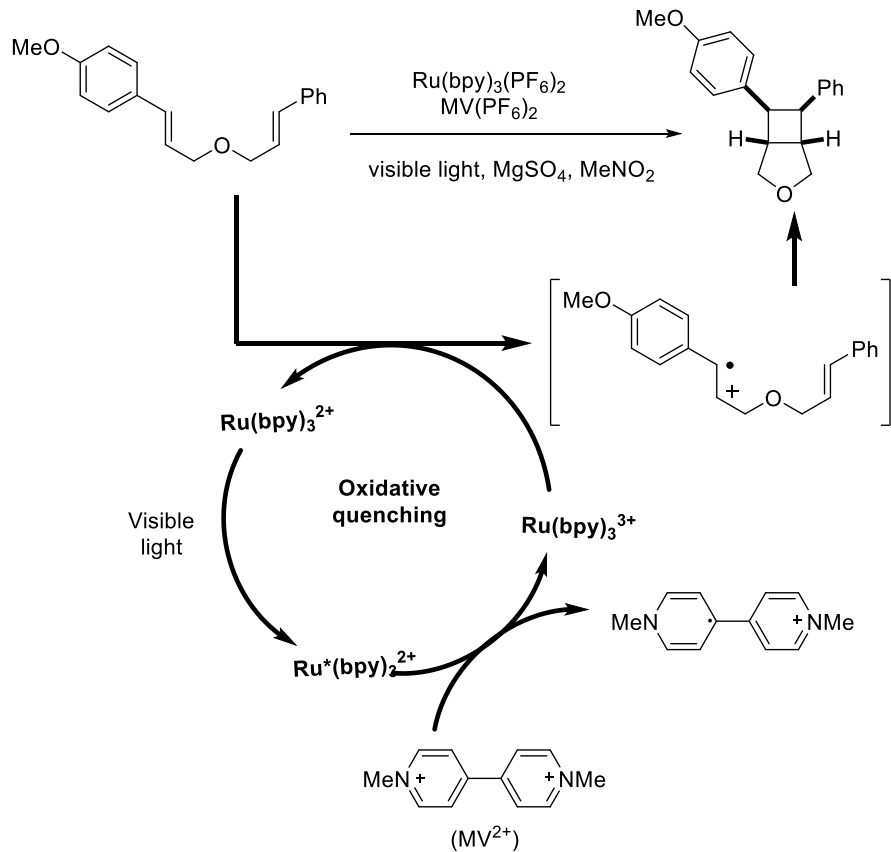
Early pioneer Deronzier and coworkers have reported one of the earliest works based on photoredox catalysis that would fit into this reaction category³⁰. In 1984, Deronzier and Cano-Yelo have disclosed the Pschorr reaction that catalyzed by $\text{Ru}(\text{bpy})_3^{2+}$ under photoredox catalysis (scheme 1.2). In the reported reaction, aryl diazonium salts were proposed to be reduced by excited $\text{Ru}(\text{bpy})_3^{2+*}$ complex to yield aryl radical. Intramolecular radical addition of the aryl radical to the pendent arene gives a cyclic adduct radical intermediate which was oxidized by $\text{Ru}(\text{bpy})_3^{3+}$ to provide the cyclized carboncation and the regeneration of the catalyst. By deprotonation of the carboncation, phenanthrene was yield as final product.³¹



Scheme 1.2. Photoredox Catalyzed Pschorr Reaction

In 2010, Yoon and coworkers have reported an intramolecular [2+2] cycloaddition of electron-rich bis(styrenes) under photoredox catalysis (scheme 1.3).^{13d} By employing an oxidation quenching cycle, they have successfully addressed the limitation of their previous report on the requirement of electron-deficient bis(styrenes) for the [2+2] cycloaddition to occur. Using methyl viologen (MV^{2+}) as single electron oxidation reagent, $\text{Ru}(\text{bpy})_3^{3+}$ species was generated from excited $\text{Ru}(\text{bpy})_3^{2+}$. Subsequent oxidation of the electron rich bis(styrene) to afford its corresponding radical cation for the initiation of the [2+2] cycloaddition process to yield the desired cyclobutane adducts with high diastereoselectivities (cis: trans > 10:1) and regeneration of the $\text{Ru}(\text{bpy})_3^{2+}$ catalyst. Limitation of the reaction was also reported as electron

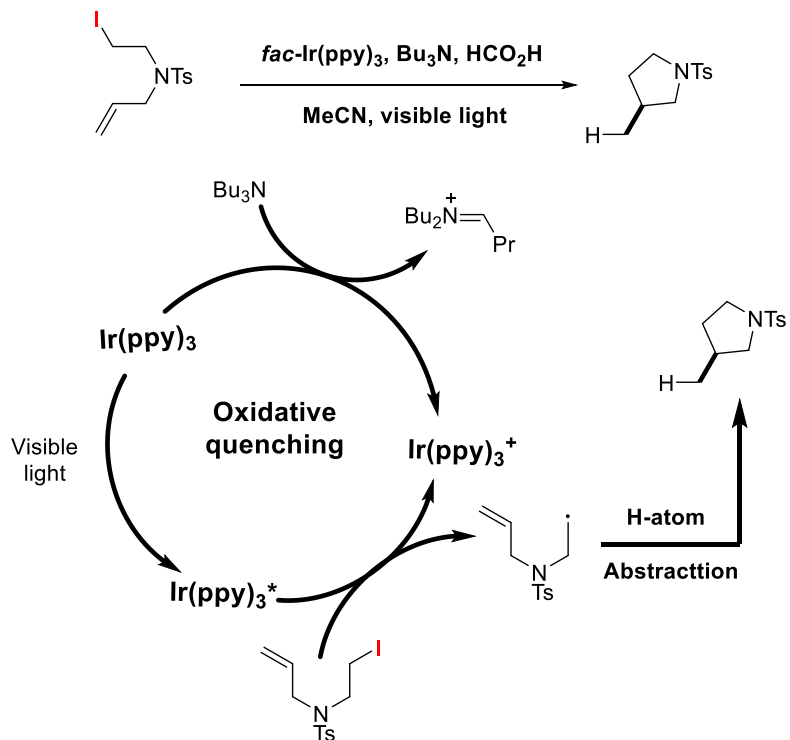
donating substituent must be incorporated at least in one of the styrenes to ensure the success of the oxidation to occur.



Scheme 1.3. [2+2] Cycloaddition under Photoredox Catalysis

Stephenson and coworkers have also demonstrated the power of oxidative quenching process under photoredox catalysis in reductive dehalogenation reactions in 2012 (Scheme 1.4).³² Due to the high reduction potentials of the alkyl iodide, alkenyl iodide and aryl iodide (for example, the reduction potential of *s*-butyl iodide has been determined to be between -1.61 V and -2.10 V versus SCE, the reduction potential of iodobenzene is between -1.59 V to -2.25 V versus SCE), the reduction of those carbon-iodide bonds would be always difficult to achieve. Stephenson and coworkers realized that by the incorporation of highly reductive $\text{Ir}(\text{ppy})_3$

photoredox complex ($\text{Ir}^{4+}/\text{Ir}^{3+*}$: -1.73 V versus SCE) into the reductive system could potentially be an ideal solution to those challenges on the reduction of iodine. They were further encouraged by MacMillan's work on the reduction of electron-deficient benzyl bromides. Using a combination of tributylamine and Hantzsch ester as their electron/hydrogen donor, $\text{Ir}(\text{ppy})_3$ as the photoredox catalyst and acetonitrile as reaction solvent, they were able to conduct the deiodination reactions over a handful of alkyl iodides. By switching the hydrogen donor combination to tributylamine and formic acid, they have also accomplished the reductive deiodination reactions of various aryl iodide and alkenyl iodide. Meanwhile, the reduction of aryl iodides in the presence of aryl bromides, aryl chlorides and distal olefins even highlighted the versatile utilities of the mild photoredox reduction methods. The authors further engaged flow chemistry to the reductive deiodination reactions to realize gram scale synthesis using this method.

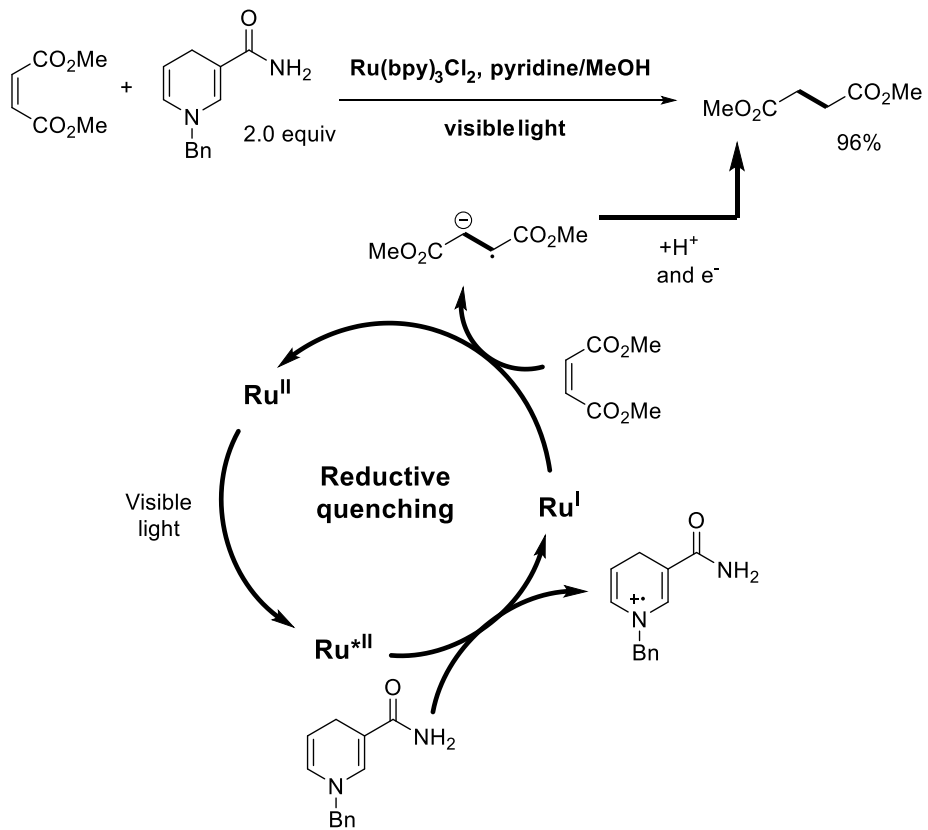


Scheme 1.4. Reductive Deiodination under Photoredox Catalysis.

1.3.2 Reductive Quenching Cycle

A reductive quenching cycle referred as those that in a photoredox reaction, the photoredox catalyst acts as an electron acceptor to accept an electron from an organic molecule, resulting an oxidized organic molecule for further organic transformation. The reduced photoredox catalyst can then be oxidized by an oxidation reagent to regenerate the ground state of the catalyst back. The overall process can be referred to Figure 1.6.

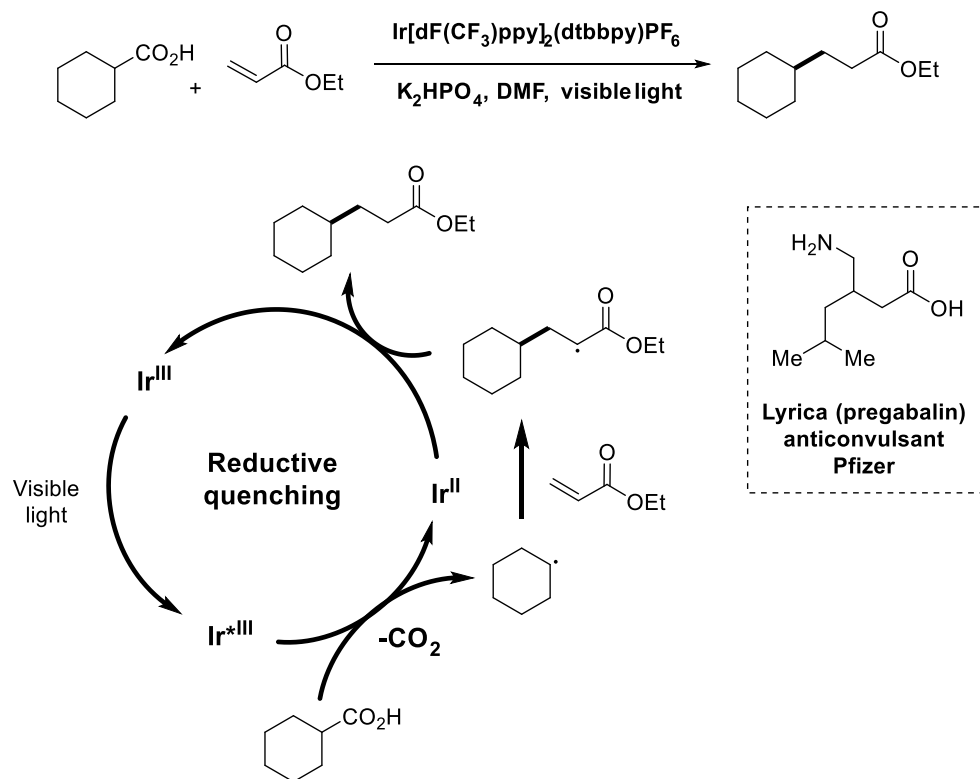
As early as 1981, Pac and co-workers have already reported the first example of photoredox catalyzed reduction of electron deficient olefins (Scheme 1.5).^{28a} Adopted a reductive quenching cycle of photoredox catalysis, they have successfully reduced dimethyl maleate to the saturated product dimethyl succinate with the aid of 2 equiv of 1-benzyl-1,4-dihydronicotinamide (BNAH) and catalytic amount of $\text{Ru}(\text{bpy})_3\text{Cl}_2$ as photoredox catalyst. Possessing an oxidation potential of +0.77 V vs SCE, the excited $\text{Ru}(\text{bpy})^{2+}$ is proposed to oxidize BNAH ($E_{1/2}^{\text{red}} = +0.76$ V vs SCE) to generate the BNAH radical cation along with a reduced form of $\text{Ru}(\text{bpy})_3^+$, which is highly reducing ($E_{1/2}^{\text{II/I}} = -1.33$ V vs SCE). This Ru(I) intermediate further donates an electron to dimethyl maleate to yield its corresponding radical anion as well as generating the catalyst back to its ground state to complete the catalytic cycle. The generated radical anion intermediate is then believed to undergo a second single-electron reduction and a protonation step for the further formation of dimethyl succinate as the final reduction product. Further substrates scope study revealed the general utility of this method, as it is amenable to the reduction of alkenes bearing a range of electron-deficient groups, such as ketones, nitriles and esters.



Scheme 1.5. Reduction of Electron-Deficient Olefins under Photoredox Catalysis.

In 2014, MacMillan and coworkers have demonstrated a photoredox catalyzed radical Michael Addition reaction using carboxylic acid as radical precursors (Scheme 1.6)³³. In detail, they proposed that base-promoted deprotonation of a carboxylic acid substrate (hexanoate ion, $E_{1/2}^{\text{red}} = +1.16$ V vs SCE in CH_3CN) would potentially be oxidized by the excited bphotoredox catalyst $\text{Ir}^*[\text{dF}(\text{CF}_3)\text{ppy}_2]_2(\text{dtbbpy})^+$ ($E^*_{1/2}^{\text{III/II}} = +1.21$ V vs SCE in CH_3CN), leading to an extrusion of CO_2 to further yield an alkyl radical species for the radical nucleophilic reaction to occur. Using proline as their decarboxylation precursor, K_2HPO_4 as the base, and dimethylethylidenemalonate as the Michael acceptor, they found that the proposed reaction can be conducted smoothly with the irradiation of a 26 W CFL bulb, a reaction yield of 92% was furnished. Further incorporation of structurally divergent Michael acceptors as well as carboxylic

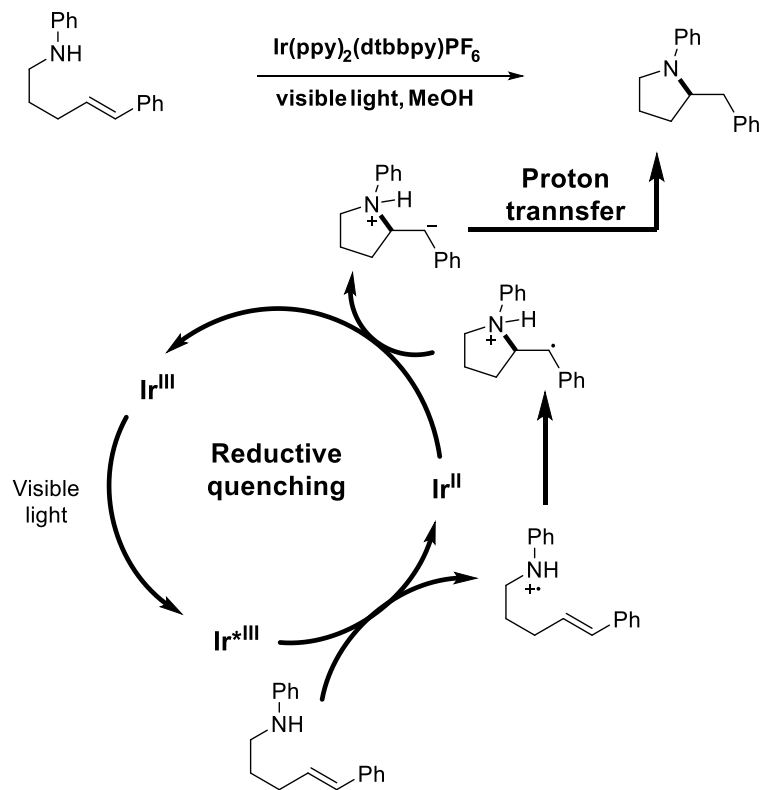
acid fragments revealed a broad substrates scope for this method. In order to demonstrate the operational simplicity and generality of this new method, they further conducted a three-step racemic synthesis of pregabalin, an anticonvulsant drug which has been commercialized by Pfizer (Scheme 1.6).



Scheme 1.6. Photoredox Catalyzed Radical Michael Addition Reaction.

A catalytic olefin hydroamination through direct intramolecular C-N bond formation reaction has been accomplished by Knowles and coworkers (Scheme 1.7).³⁴ The reaction was proposed to initiate through a single electron oxidation of amine to its corresponding amine radical cation by an excited triplet $\text{Ir}(\text{ppy})_2(\text{dtbbpy})\text{PF}_6$ complex under photoredox reductive quenching cycle. Unlike traditional Hofmann-Löffler-Freytag reaction which require a pre-installation of N-halogenated or N-nitrosylated analogues and in the presence of a strong

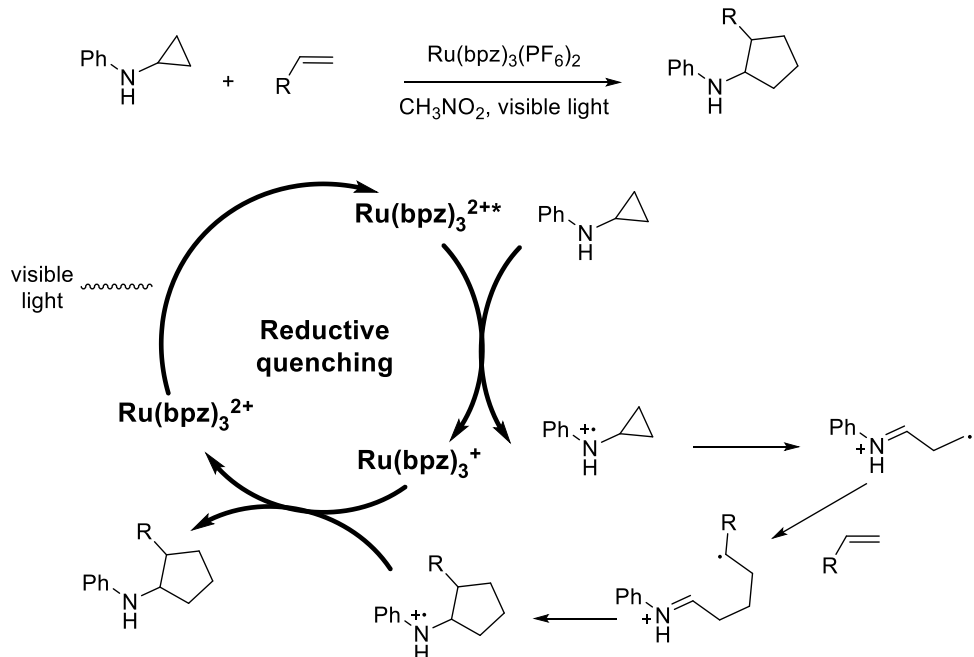
Bronsted acid under ultraviolet irradiation, the reported reaction was operated through a sequential single electron transfer from a simple secondary amine precursor to the excited triplet $\text{Ir}(\text{ppy})_2(\text{dtbbpy})\text{PF}_6$ complex under extremely mild visible light irradiation condition. Further substrates scope studies revealed that this method can be applied to a handful of structurally divergent aniline substitutes as well as the styrenyl acceptors. This work represents a rare example of the use of amine radical cations that generated from simple amine precursors for further C-N bond constructions.



Scheme 1.7. Photoredox catalyzed Hydroamination Reactions.

Another example of the direct oxidation of amines to its corresponding amine radical cations under photoredox catalysis for further organic transformations was demonstrated by Zheng and coworkers.³⁶ By this approach, they have successfully developed a series of novel

[3+2] annulation reactions of *N*-cyclopropylanilines with various *pi*-bonds. Unlike a typical photoredox reductive quenching cycle in which amines were used only as sacrificial electron donor, Zheng and coworkers realized that amine could also be used as one of the reactants for further synthesis of some structurally important amino compounds. They further turned their attention on *N*-cyclopropylamine, which is pre-installed with severe ring strain energy. By the oxidation of *N*-cyclopropylamine to its corresponding amine radical cation, the three membered carbon cycle would further refragment to a ring opened reactive intermediate by a radical C-C bond cleavage. The ring opening intermediate, distonic radical cation, is further reacted with various *pi* bonds and a subsequent ring close to yield the final [3+2] annulation product. Further substrates scope study revealed that this method is quite fruitful and can be applied to a scope of *pi* bonds such as alkenes, alkynes, symmetrical diynes, unsymmetrical diynes and enynes. However, an electron withdrawing substituent on the *pi* bond side is required for ensuring the [3+2] annulation reaction to occur.



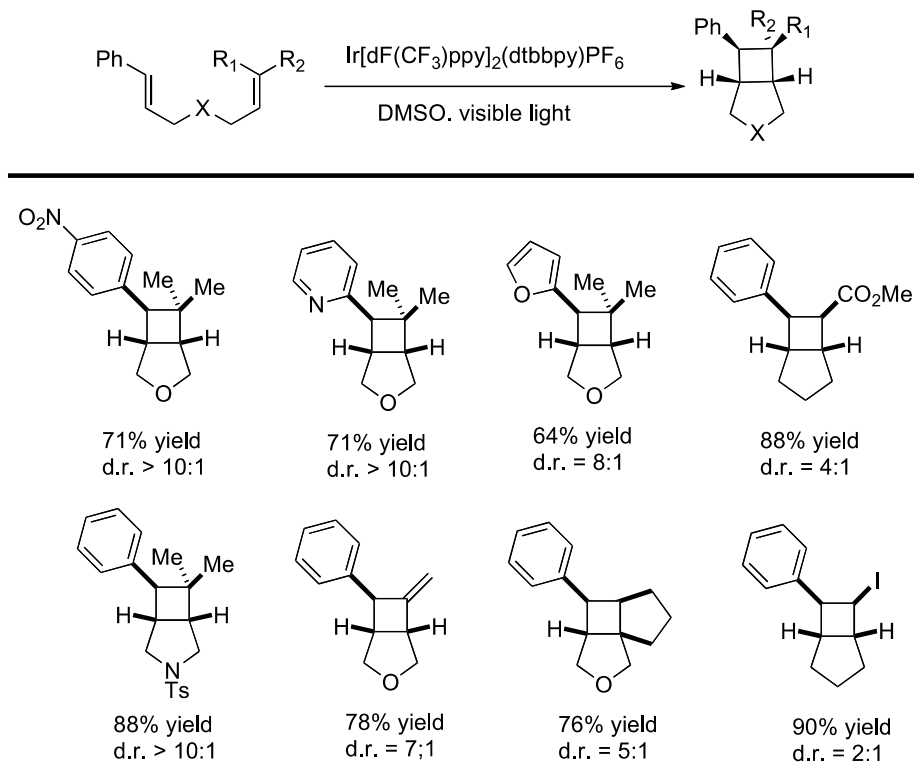
Scheme 1.8. Photoredox Catalyzed [3+2] Annulation Reaction.

1.3.3 Energy Transfer Process

As is mentioned above, depending on whether the excited triplet state of a photoredox catalyst being oxidized first or reduced the first, the photoredox reactions can be included into either an oxidative quenching cycle or a reductive quenching cycle. Those reactive quenching cycles are all relied on the efficient electron transfer process from a photoredox catalyst to a reactive intermediate or an organic molecule. To this end, the limitation of the above mentioned photoredox quenching processes is obvious as inefficient electron transfers from catalyst to reactant would greatly inhibited the reaction process. For instance, in the oxidative quenching cycle, the substrate's reduction potential needs to be more positive than the reduction potential of a photoredox catalyst to ensure the success oxidation of catalyst by substrate; Alternatively, in the reductive quenching cycle, the substrate's reduction potential has to be less positive than the reduction potential of the photoredox catalyst to support the reduction of catalyst by substrate. To address the above issues in certain photoredox initiated organic synthesis, pioneer chemists have developed an additional pathway, termed energy transfer, which doesn't involve a direct energy transfer between photoredox catalyst and reactant. In energy transfer process, the excited triplet state energy (E_T) of the photoredox catalyst directly transfer energy to an organic substrate or an reactive intermediate through a triplet energy to triplet energy transfer process and yield an excited triplet organic reactive intermediate for further fragmentation and reveal the reactivity. Through this energy transfer process, the constraint on matching the potential of catalyst and substrate is effectively avoided. The overall process is depicted in Figure 1.6.

One of the synthetic applications which utilizing the energy transfer process in photoredox catalysis was demonstrated by Yoon and coworkers (Scheme 1.9).^{13g} In a previous

report from the same group on the [2+2] cycloaddition of styrenes under photoredox catalysis, they found that the reaction was extremely limited only on those electron-rich styrene substituents. The presented limitation was caused by the inefficient electron transfer between the photoredox catalyst and the styrene as only those electron rich styrene can be oxidized by the tested photoredox catalysts for further [2+2] cycloadditions to occur. In order to circumvent this limitation, the authors designed an energy transfer pathway for the [2+2] cycloadditions of those electron neutral and electron deficient styrene. Their reaction screening indicated that the proposed [2+2] cycloadditions could proceed smoothly when using $\text{Ir}[\text{dF}(\text{CF}_3)\text{ppy}_2](\text{dtbbpy})\text{PF}_6$ as energy transfer catalyst and DMSO as the solvent. In order to support their proposed energy transfer mechanism, they compared the potentials of *p*-nitrostyrene precursor ($E_{1/2}^{\text{red}} = +1.68$ V vs SCE) and oxidation potential of $\text{Ir}^*[\text{dF}(\text{CF}_3)\text{ppy}_2](\text{dtbbpy})\text{PF}_6$ ($E^*_{1/2}^{\text{III/II}} = +1.21$ V vs SCE), which strongly suggested the insufficient redox potential of the catalyst to the organic molecule. On the other hand, the excited triplet energy of the $\text{Ir}[\text{dF}(\text{CF}_3)\text{ppy}_2](\text{dtbbpy})\text{PF}_6$, 61 Kcal/mol, along with styrene's excited state triplet energy of approximately 60 Kcal/mol, would thus enable the triplet to triplet energy transfer of the catalyst and styrene. Further exploration of the reaction substrates scope showed that a handful of substituents with different characteristic such as electron characters and heteroatom characters all compatible in the reaction. Other functional groups such as enones, enoates, enol ether, haloalkenes and allenes were also found to suitable as another [2+2] cycloaddition partners.



Scheme 1.9. Photoredox Catalyzed [2+2] Cycloadditions Through Energy Transfer.

1.4. Amine Radical Cations*

* Portion of this chapter has been published in Hu, J.; Wang, J.; Nguyen, T. H.; Zheng, N.

Beilstein J. Org. Chem. **2013**, 9, 1977-2001.

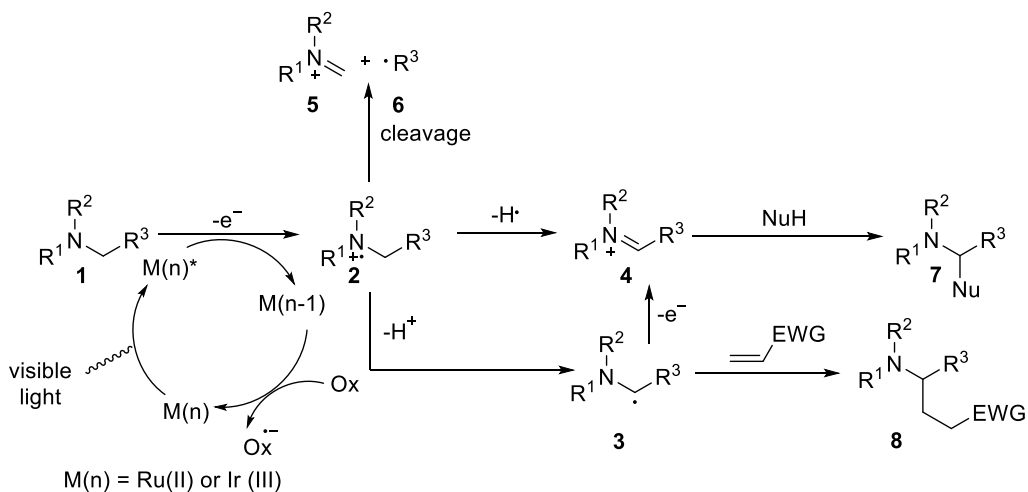
Amine radical cations are odd- electron species that are formed by loss of an electron from the corresponding amines.³⁶ Multiple methods have been developed for the formation of those single electron species including electrochemistry,³⁷ chemical oxidation,³⁸ metal-catalyzed oxidation,³⁹ UV light-mediated photochemistry⁴⁰ and more recently, photoredox catalysis.⁴¹ Since those visible light photoredox catalysis processes are typically conducted under extremely mild reaction conditions such as room temperature, this approach has become a major research

focus in the synthesis of those amine radical cations. Like most organic molecules, most amines do not absorb visible light efficiently. Therefore, photoredox catalysts such as ruthenium and iridium polypyridyl complexes, organic dyes are often required for initiating the electron-transfer reactions with amines. Since the formation of amine radical cations from neutral amines is an oxidation process, typically a photoredox reductive quenching cycle is operable for such reactions to occur. It is also worth noting that amines are also routinely used as reductive quenchers to quench the excited photoredox catalyst and subsequently being oxidized to its corresponding amine radical cations.

Actually, the use of amines as sacrificial electron donors can be traced back to as early as 1970s when they were constantly used in water splitting⁴² and reduction of carbon dioxide.⁴³ However, it is not until recently that pioneers, such as MacMillan, Stephenson and Zheng, have reinvigorated the field of visible light photoredox catalysis and started to use amines as both the electron donor and the reaction substrates, rather than just the electron donor, to harvest structurally divergent amine substituted organic molecules.

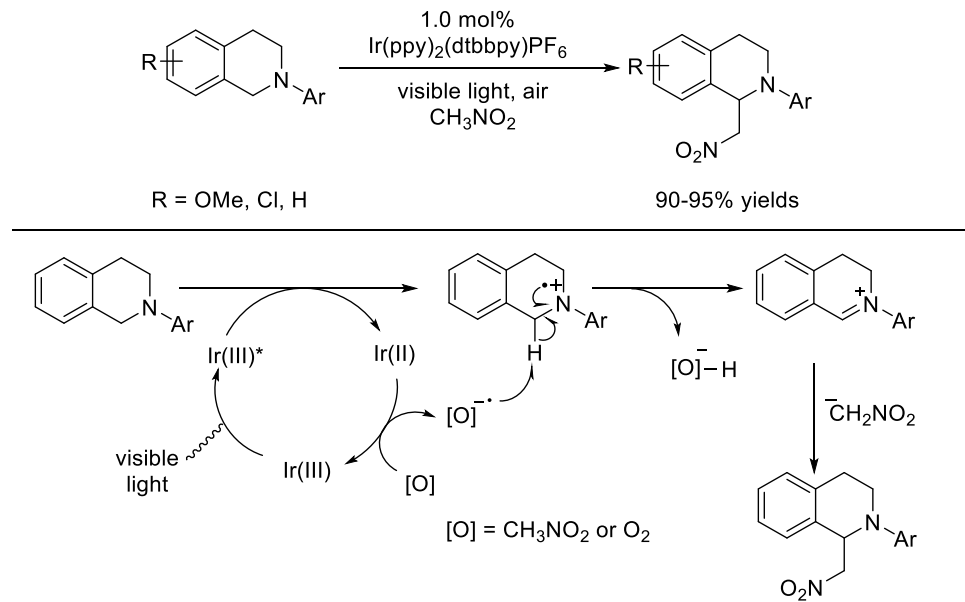
The single electron oxidation of amine by a photoredox catalyst is governed by the reduction potential of the excited photoredox catalyst. The amine's reduction potential, which can be readily measured by cyclic voltammetry, should be less positive than that of the excited photoredox catalyst. On the other hand, the reaction solvent also has a significant influence on the electron transfer step as well as the subsequent organic transformations. It is proposed that a polar solvent is generally beneficial for the single electron transfer between the amines and photoredox catalysts for the formation of amine radical cations. Once formed, the amine radical cation was shown to have four modes of reactivity, as shown in scheme 1.10. The first mode is the back electron transfer reaction, in which the formed amine radical cation 2 is given back an

electron form the reduced photoredox catalyst $M(n-1)$ to generate the ground state of the catalyst as well as the amine starting material. This is a major side reaction which is competing with other productive downstream reactions of 2. To deactivate this side reaction, two approaches are typically exploited. The first approach is mainly focused on the ligand modification of the catalysts to retard the back electron transfer.⁴⁴ The second approach involves the designation of fast and/or irreversible downstream reaction of 2. The second mode of the amine radical cations involves a hydrogen atom abstraction from 2 to furnish iminium ion 4 when presenting in front of a good hydrogen atom acceptor. The use of amine radical cation 2 as the hydrogen radical source has been widely used to a number of visible light mediated reductions such as reductive radical cyclization, reductive dehalogenation and reduction of activated ketones. Meanwhile, the newly formed iminium ion 4 can further react with a variety of nucleophiles to furnish α -amino substituted products like 7. The third mode involves deprotonation of amine radical cation 2 to further yield α -amino radical 3, which can be converted to iminium ion 4 by another single electron oxidation. The newly formed radical can further react with radical acceptors, such as electron-deficient pi bond, for further construction of C-X bond, and yield α -amino substituted product such as 8. The last mode involves cleavage of a C-C bond α to the nitrogen atom, leading to a neutral free radical 6 and a corresponding iminium ion 5. Compared to the well documented pathways of 2 and 3 under photoredox catalysis, the synthetic utility of pathway 4 has rarely been reported. Selected examples of above pathways are discussed in the following sections.



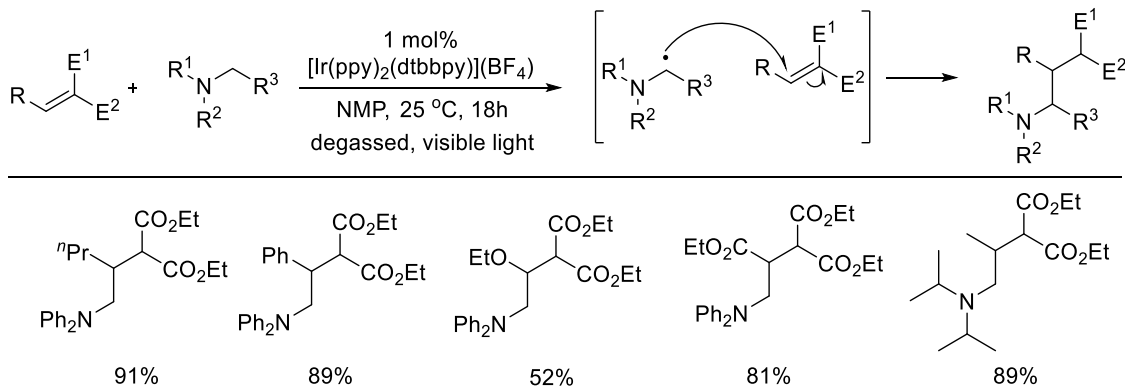
Scheme 1.10. Amine Radical Cations' Mode of Reactivity.

In 2010, Stephenson and coworkers have reported a photoredox catalysis aza-henry reaction (Scheme 1.11).⁴⁵ The reported reaction was proposed to go through the pathway 2 that derived from single electron oxidation of *N*-arylterahydroisoquinolines to the corresponding iminium ion as described above. It was proposed that under photo irradiation, a variety of *N*-aryltetrahydroisoquinolines could be oxidatively coupled with nitroalkanes to furnish the aza-Henry products with good yields. Further mechanistic studies suggested that *N*-aryltetrahydroisoquinolines was oxidized by excite $\text{Ir}^*(\text{ppy})_2(\text{dtbbpy})\text{PF}_6$ complex to its corresponding amine radical cation. The reduced Ir(II) catalyst then reduces nitromethane or oxygen to a radical anion that may abstract a hydrogen atom from amine radical cation to form the iminium ion which was further intercepted by the anion of nitromethane to afford the final product.



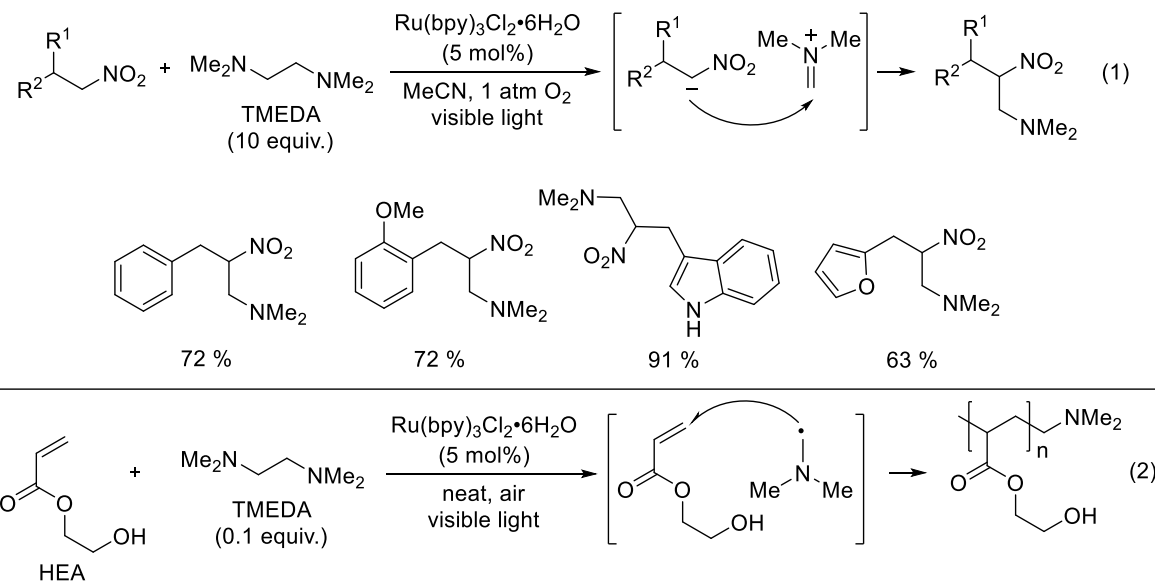
Scheme 1.11. Photoredox aza-Henry Reaction.

As is mentioned above, α -amino radicals could also be generated from amine radical cations under photoredox conditions. Compared to those photoredox generated electrophilic iminium ions, α -amino radicals are quite nucleophilic and they tend to add to Michael acceptors in a 1,4 addition fashion. For instance, the Nishibayashi group has reported that α -amino radicals that generated from anilines under photoredox catalysis could be added intermolecularly to Michael acceptors such as acrylate type molecules (Scheme 1.12).⁴⁷ The Michael acceptor, however, was found to be limited to those activated by two electron-withdrawing groups. Further reaction screening revealed that while $\text{Ir}(\text{ppy})_2(\text{dtbbpy})\text{PF}_6$ complex was the most effective catalyst, NMP as the solvent was critical for the reaction to occur.



Scheme 1.12. Radical Michael Addition of α -Amine Radicals Derived from Anilines.

Except for the domain reaction pathway of involving the hydrogen atom abstraction of amine radical cation to form the iminium ion, there is a much less exploited reaction pathway concerning amine radical cations which is cleavage of the C-C bond α to the nitrogen atom for the generation of iminium ion as well as a neutral carbon radical as described above as pathway 4. Few applications were reported based on this particular approach including Zheng (Scheme 1.8) and others. Li and Wang also applied this cleavage reaction to 1,2-dimaines, simultaneously creating two types of synthetically useful intermediates, iminium ions and α -amine radicals (Scheme 1.13).⁴⁷ The iminium ions were then trapped with nitroalkanes for further reveal of aza-Henry reaction. Separately, irradiation of 2-hydroxyethylacrylate (HEA), TMEDA and Ru(bpy)₃Cl₂ in air produced a polymer incorporating a dimethylamino group. The dimethylamino radical, the other intermediate generated by cleaving TMEDA, most likely induced the polymerization. The chemistries involving the iminium ions and α -amine radicals, generated under visible light photoredox conditions, are often limited by the substrate scope of the amine precursors, since aromatic amines are typically required.



Scheme 1.13. Photoredox Cleavage of C-C bonds of 1,2-Diamines.

1.5. Ring Opening Strategies of Cyclobutanes

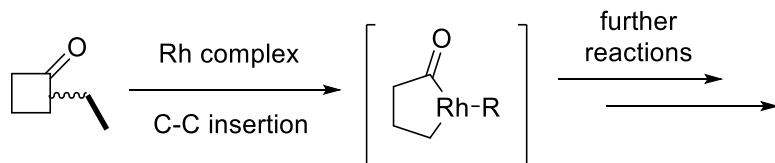
Strained molecules have caught the interest of chemists in both theoretical studies and synthetic applications. For instance, cyclopropane has been constantly used in synthetic organic chemistry as ideal three membered carbon synthon.⁴⁸ When compared to cyclopropane, cyclobutane remained underutilized for a long time.⁴⁹ This difference is surprising, as cyclobutane was always considered to possess similar properties and reactivity to those of cyclopropane.⁵⁰ As a result, the strain energy of cyclopropane (27.5 kcal/mol) is found incredibly similar with that of cyclobutane (26.7 kcal/mol).^{50c,50d} The surprising similarity of strain energy of those two carbon cycles has been rationalized by the dissection of the strain into C-C and C-H bond energy contributions. Although the total C-C bond strain of cyclopropane is 10.1 kcal/mol higher than that of cyclobutane, the stronger C-H bonds (8.0 kcal/mol) of cyclopropane almost compensate the overall difference. The ring strain embedded in the four membered carbon cycle

is a well appreciated driving force that enables and accelerate otherwise rather sluggish ring opening process. To this end, the development of novel methods towards the activation of cyclobutane through a C-C bond cleavage fashion for the further reveal of this synthetically important four membered carbon synthon is crucially demanded.^{49b,49c}

Depending on the different substituents or functional groups that decorated on the cyclobutane ring, three different reaction pathways have been reported for the ring opening of cyclobutane. Selected examples on the activation of cyclobutane are documented below.

1.5.1. Transition Metal Catalyzed Activation of C-C Bond on Cyclobutane

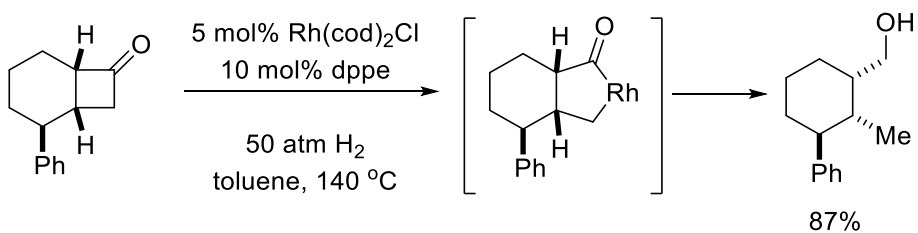
Rhodium (I) complexes have been largely used in the direct oxidative insertion into the acyl-carbon bond of cyclobutanone based organic motifs for the formation of a rhodacycle reactive intermediate.^{49c} A variety of novel transformations have been disclosed depending on the substrate substitution pattern, the metal complex used and the reaction conditions.⁵¹



Scheme 1.14. Direct Insertion of Rh(I) Complex into Cyclobutanone.

As early as 1994, Ito and coworkers have reported the first example on the activation of cyclobutanones with rhodium (I) catalyst (Scheme 1.15).⁵² The proposed reaction cycle starts with the oxidative addition of rhodium complex to a less steric hindered acyl-carbon bond to form the organorhodium reactive intermediate. Under an atmosphere of hydrogen, reductive ring

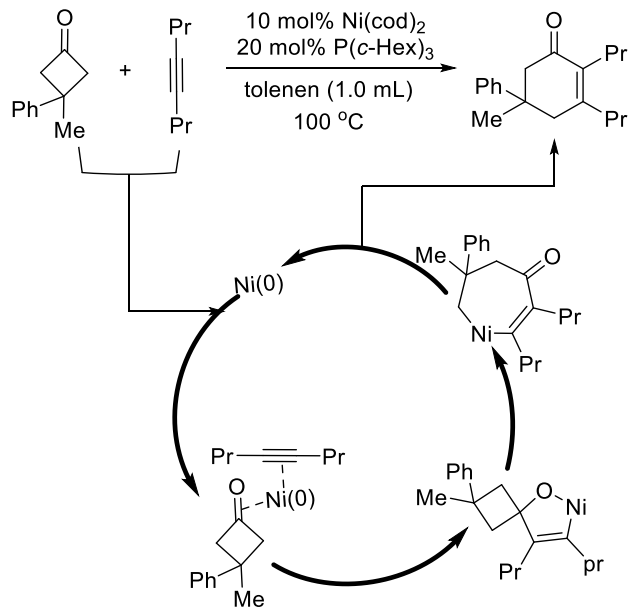
cleavage takes place through the aldehyde key intermediate to deliver alcohol as the final product.



Scheme 1.15. Ito's Reductive Cylobutanone Ring Cleavage.

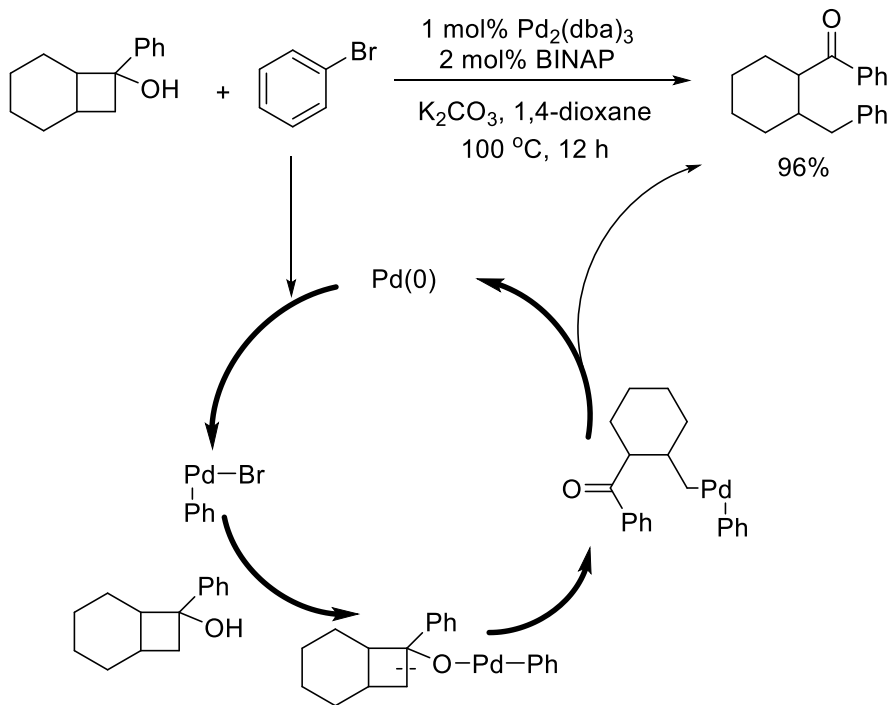
In 2005, Murakami and coworkers have discovered a formal [4+2] cycloaddition reaction of cyclobutanones with various alkynes (Scheme 1.16).⁵³ Using 3-methyl-3-phenylcyclobutanone and 4-octyne as two cycloaddition partners, the [4+2] cycloaddition can be conducted rather smooth when using bis(1,5-cyclooctadiene)nickel(0) as the catalyst, tricyclohexylphosphine as ligand and toluene as solvent. A scope of structurally divergent cyclohexenones was synthesized with good yields and high regioselectivities. A mechanism is proposed to start with the coordination of the cyclobutanone and alkyne to a nickel complex. Subsequent oxidative cyclization of the carbonyl group of the cyclobutanone and alkyne with nickel further yields oxanickelacyclopentene intermediate. The four membered ring is then opened by β -carbon elimination, resulting in ring expansion to form seven-membered nickelacycle for the final reductive elimination and generate the final product. Reaction substrates scope study revealed that the [4+2] cycloaddition reaction can be generally applied to a variety of different substrates both on cyclobutanone side and alkyne side. For instance, both aliphatic and aromatic substituents at 3-position of cyclobutanones are well tolerated in the reaction. Also, symmetrical and unsymmetrical internal alkynes with both aliphatic and aromatic

substituents can be well reacted in the [4+2] cycloaddition reaction. However, one shortage is also observed that terminal alkynes, such as 1-octyne and phenylacetylene, failed to participate in the reaction due to rapid oligomerization of the alkynes.



Scheme 1.16. Nickel Catalyzed [4+2] Cycloaddition of Cyclobutanones and Alkynes.

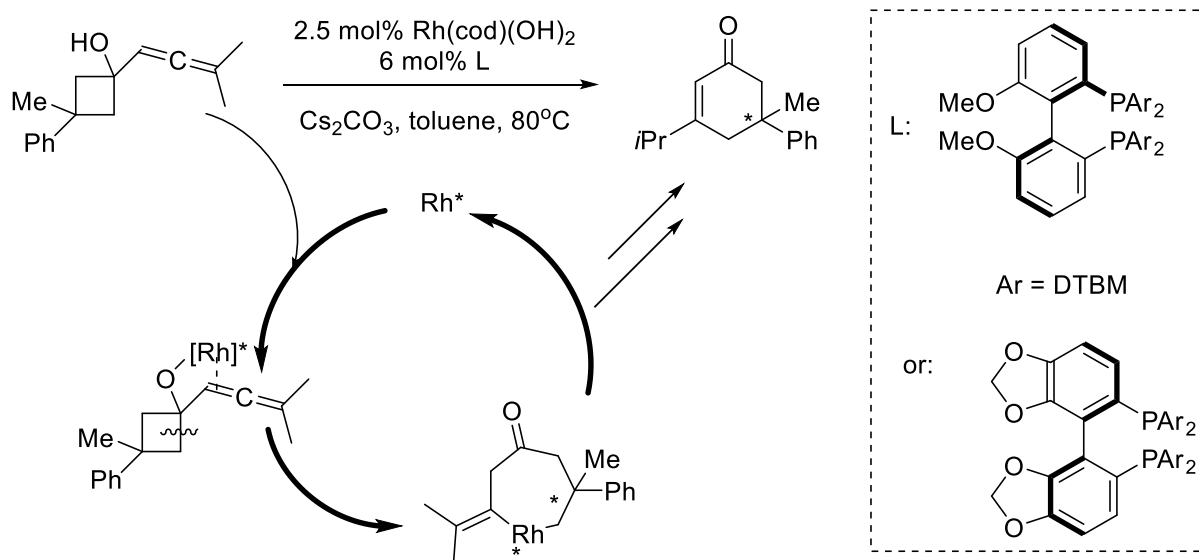
Palladium has also been shown to efficiently catalyze the ring opening of cyclobutane. In 1999, Uemura and coworkers reported palladium-catalyzed arylation of *tert*-cyclobutanols with various aryl bromides through a C-C bond cleavage process.⁵⁴ The reaction is proposed to initiate with the oxidative addition of Pd(0) to an aryl halide to generate the requisite Pd(II) species. Ligand exchange of the Pd(II) intermediate with *tert*-cyclobutanol further generate a palladium alcoholate intermediate, which yield an alkylpalladium intermediate through β -carbon elimination. A reductive elimination finally occurred on the alkylpalladium to give the final product as well as the regeneration of the palladium catalyst.



Scheme 1.17. Palladium Catalyzed Ring Opening of *tert*-Cyclobutanols.

In 2008, Cramer and coworkers reported an enantioselective rhodium-catalyzed intramolecular [4+2] cycloaddition of allenyl cyclobutanols (Scheme 1.18)⁵⁵. The transformation leads to a variety of highly substituted cyclohexenones with excellent enantioselectivity. A reaction mechanism is proposed to start with the coordination of the Rh(I) center to both the hydroxyl group and the proximal double bond of the allene which is followed by an oxidative insertion of Rh(I) to the cyclobutanol to yield a seven-membered metallacycle as key intermediate. During the insertion of rhodium, a pre-installed chiral phosphine ligand ensured the overall enantioselectivity of the reaction. Final reductive elimination and isomerization along lead to the formation of the final cyclohexenone product. Several phosphine based ligand were screened in the reaction condition screening, and all of them showed modest to good enantioselectivity. Sterically demanding homologues (R)-DTBM-MeObiphep and (S)-DTBM-

segphos were proven the best two ligands with the reported reaction with 96% ee and 95% ee respectively. Remarkably, further study of the catalyst loading suggest that the catalyst loading of the reaction could be lowered down to 0.1 mol% without any yield loss.



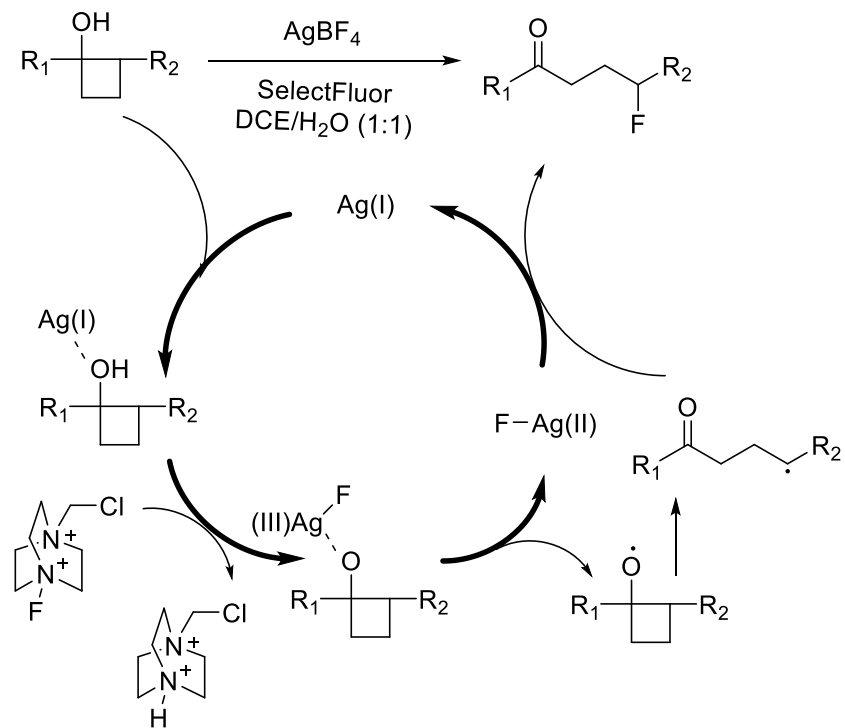
Scheme 1.18. Rhodium Catalyzed Enantioselective [4+2] Cycloaddition.

1.5.2. Radical Mediated C-C bond Cleavage on Cyclobutane.

Compared to the transition metal catalyzed activation of cyclobutane, the use of single electron pathway for the cleavage of a C-C bond on cyclobutane is rare. To date, only a handful of results are published on this approach. The majority of those results were all based on the oxidation of the particular organic motif, cyclobutanol.^{49c}

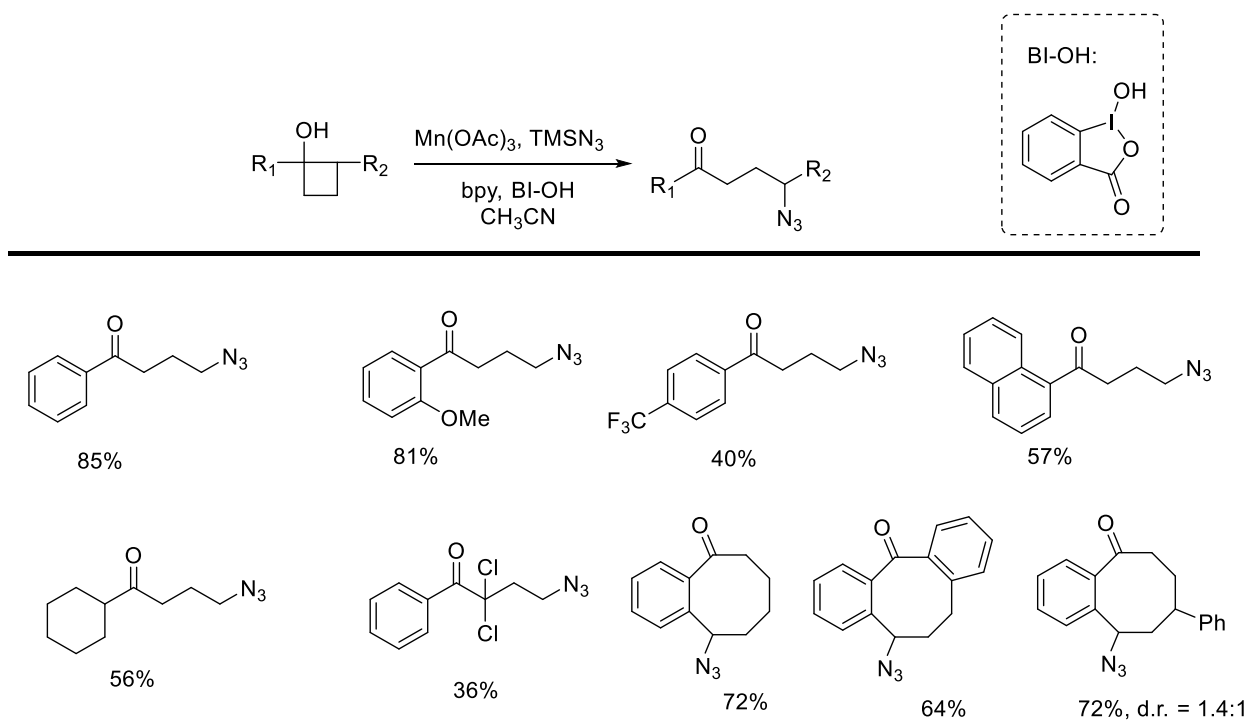
In 2015, Zhu and coworkers have reported a silver catalyzed ring opening of cyclobutanol for the synthesis of various γ -fluorinated ketones (Scheme 1.19).⁵⁶ Using SelectFluor as their fluorine source, and AgBF_4 as their silver catalyst, a handful of aromatic and

aliphatic substituted cyclobutanols are found to be compatible in the transformation. A mechanism is proposed to start with the incorporation of Ag(I) with the hydroxyl group of cyclobutanol to generate a silver complex. By interacting with SelectFluor, Ag(I) complex is oxidized to generate a F-Ag(III) complex which is further gone for a radical cleavage to generate F-Ag(II) complex along with a cyclobutoxy radical. The cyclobutoxy radical is quite unstable since it suffered from the cyclobutane ring strain and is gone for a rapid C-C bond cleavage on one of the C-C bond in a radical cleavage fashion for the further formation of ring opened alkyl radical. The product is then generated by the oxidation of the F-Ag(II) intermediate to the alkyl radical along with the regeneration of Ag(I) catalyst.



Scheme 1.19. Silver Catalyzed Ring Opening of Cyclobutanol.

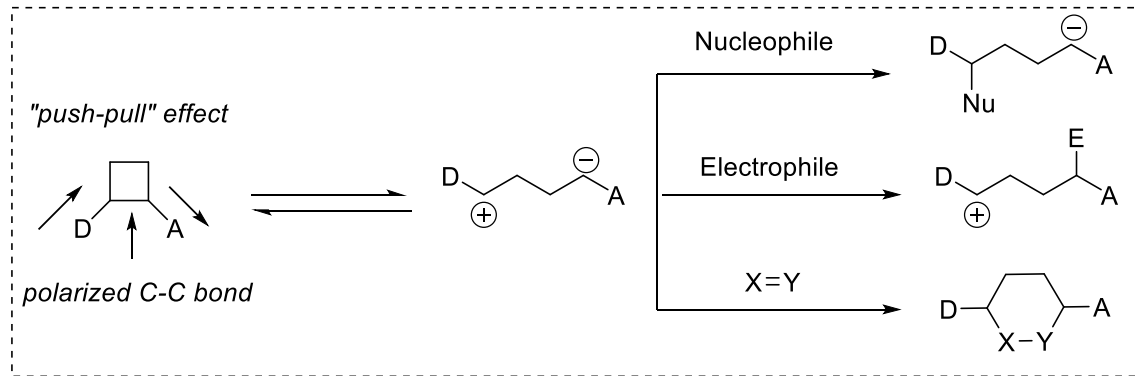
Using the same strategy, Zhu and coworkers have realized an oxidative azidation reaction on cyclobutanols (Scheme 1.20).⁵⁷ A wide range of primary, secondary and tertiary alkyl azides are generated in synthetically useful yields and exclusive regioselectivity. Along with linear alkyl azides, other medium sized cyclic azides are also prepared with the methods. Unlike the synthesis of previous γ -fluorinated ketones that using AgBF_4 as the catalyst, it is found that Mn(OAc)_3 as the catalyst works the best in the azidation reaction. TMSN_3 is used as the azide source, along with a hypervalent iodine reagent (BI-OH) as the oxidant.



Scheme 1.20. Cyclobutanol Ring Opening for Azadations.

1.5.3. Donor-Acceptor (DA) Mediated Ring Opening of Cyclobutane

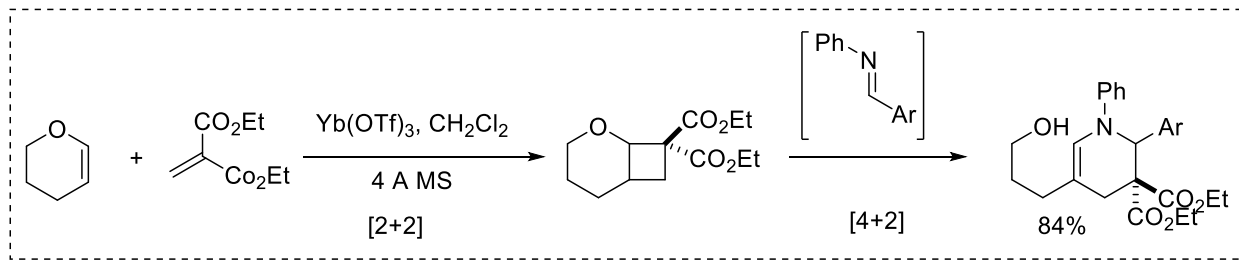
The use of donor-acceptor strategy (DA) represents another major approach for the activation of cyclobutane ring. The increased reactivity of DA cyclobutanes results from the vicinal relationship between both the donor and acceptor groups, which work in a synergistic manner for the cleavage of the C-C bond. The push-pull effect, which is created by the substituents of both electron donating group and electron withdrawing group that decorated on the cyclobutane, is responsible for stabilizing the dipolar reactive sites. The dipolar reactive sites are capable of reacting with electrophiles, nucleophiles or dipolarophiles, and hence be a promising four carbon synthon (Scheme 1.21).⁵⁸ Additionally, the acquired umplung reactivity is advantageous to reveal transformations that are challenging with previous methods. The major approach to ring opening reaction of DA cyclobutanes is nucleophilic addition of heteroatom nucleophiles or electron rich arenes, which is often mediated by a Lewis acid.



Scheme 1.21. Reactions of Activated Vicinal DA Cyclobutane.

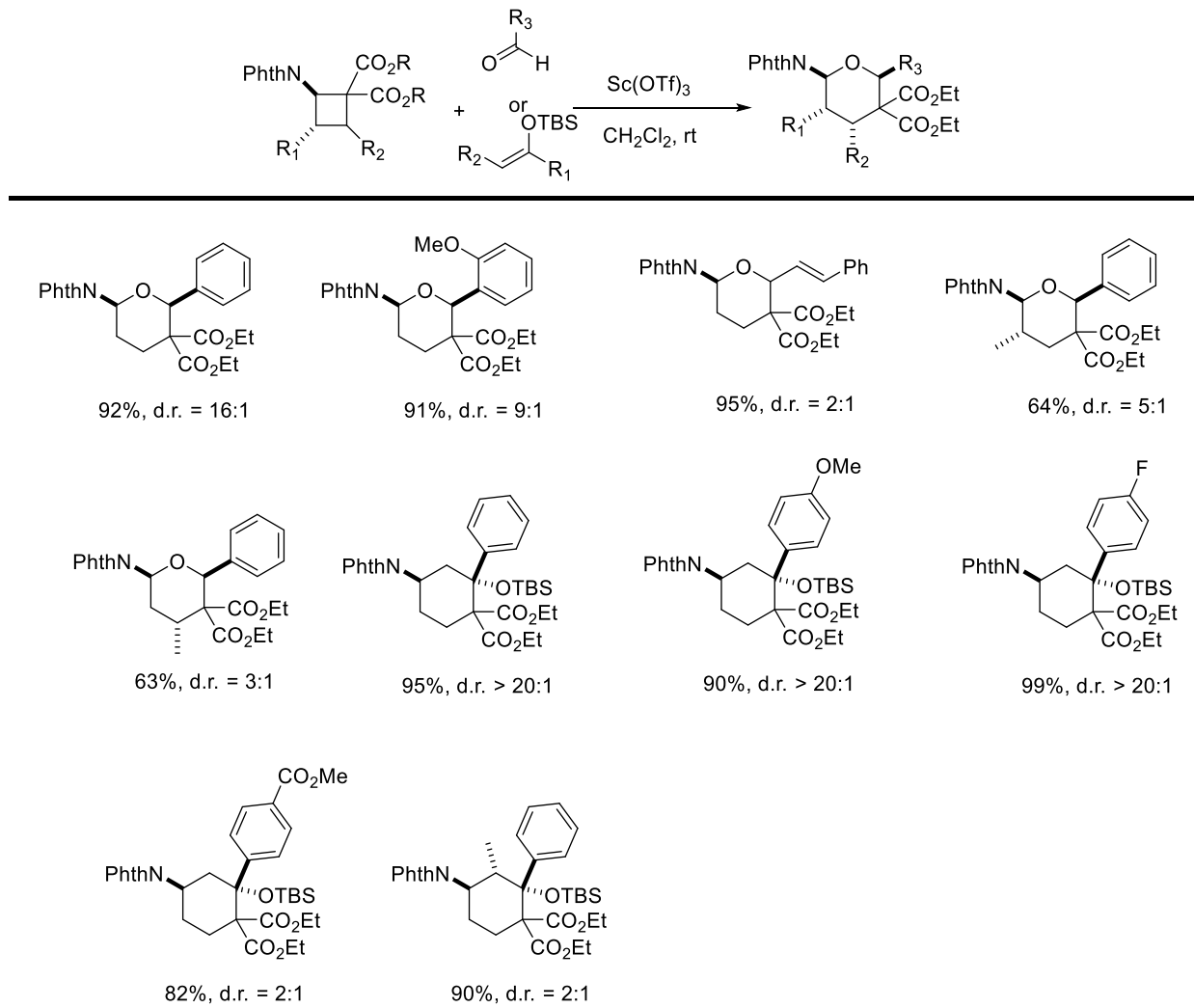
Using $\text{Yb}(\text{OTf})_3$ as catalyst, Pagenkopf and coworkers have demonstrated a formal [4+2] cycloaddition of alkoxy-substituted DA cyclobutanes with imines.⁵⁹ A handful of highly substituted piperidines and piperideines are prepared with good reaction yields. Reaction

screening revealed that a temperature of -50°C was ideal for the [4+2] cycloaddition to occur. They further conducted a one pot [2+2+2] cycloaddition for the synthesis of piperidines (Scheme 1.22). The one pot synthesis started with the [2+2] cycloaddition between disubstituted enol ether and 3,4-dihydropyran to yield a fused cyclobutane structure, which upon meeting with aryl-imine to reveal an [4+2] addition to furnish the final piperideine product.



Scheme 1.22. Formal [2+2+2] Cycloaddition.

In 2015, Waser and coworkers reported an [4+2] annulation of aminocyclobutanes with enol ethers (Scheme 1.23).⁶⁰ Unlike previous reports of using oxygen and carbon as electron donating groups in the activation of DA cyclobutane molecule, nitrogen is used in the reported reaction and revealed superior reactivity for the synthesis of a handful of heavily substituted tetrahydropyranyl amines.



Scheme 1.23. [4+2] Annulation of Aminocyclobutanes.

1.6 Conclusion

Photoredox catalysis has emerged as an essential tool in synthetic organic chemists toolbox for enabling novel organic transformations as is demonstrated by various groups around the world. The advantages of those photoredox methods not only build in its extremely mild single electron oxidation conditions, but also, or more importantly, it is incredibly easy to tune and modulate its photophysical properties of the photocatalysts has lead to novel reaction discovery. The three catalytic cycle, oxidative quenching cycle, reductive quenching cycle, energy transfer quenching cycle, can be specifically designed or utilized into initial redox

reaction design which would lead to the synthetically challenging building blocks. On the other hand, the single electron oxidation of amine to its corresponding amine radical cation, has been constantly used in photoredox catalysis. However, it is not until recently, the use of photoredox catalysis for the oxidation of an amine has been discovered to be a powerful tool for the construction of those amine related structures. As a result, the finding of a ring-opening strategy of *N*-cyclobutylanilines was disclosed, which prompted the discovery of a reactive intermediate, distonic radical cation, for further reactivity of several structurally diverse nitrogen containing organic motifs.

1.7 References

1. (a) Ciamician, G.; Silber, P., Chemical Action of Light (XIII). *Ber. Dtsch. Chem. Ges.* **1908**, *41*, 1928-35; (b) Ciamician, G., Photochemistry of the Future. *Science (Washington, DC, U. S.)* **1912**, *36*, 385-94.
2. (a) Salomon, R. G., homogeneous metal-catalysis in organic-photochemistry. *Tetrahedron* **1983**, *39* (4), 485-575. (b) Liu, R. S. H.; Asato, A. E., photochemistry and synthesis of stereoisomers of vitamin-a. *Tetrahedron* **1984**, *40* (11), 1931-1969. (c) Ramamurthy, V., organic-photochemistry in organized media. *Tetrahedron* **1986**, *42* (21), 5753-5839. (d) Hegedus, L. S., Chromium carbene complex photochemistry in organic synthesis. *Tetrahedron* **1997**, *53* (12), 4105-4128. (e) Kumar, A.; Sun, S. S.; Lees, A. J., Photophysics and Photochemistry of Organometallic Rhenium Diimine Complexes. In *Photophysics of Organometallics*, Lees, A. J., Ed. 2010; Vol. 29, pp 1-35. (f) Reckenthaler, M.; Griesbeck, A. G., Photoredox Catalysis for Organic Syntheses. *Advanced Synthesis & Catalysis* **2013**, *355* (14-15), 2727-2744.
3. (a) Hoffmann, N., Photochemical Reactions as Key Steps in Organic Synthesis. *Chem. Rev. (Washington, DC, U. S.)* **2008**, *108* (3), 1052-1103; (b) Palmisano, G.; Augugliaro, V.; Pagliaro, M.; Palmisano, L., Photocatalysis: A promising route for 21st century organic chemistry. *Chem. Commun. (Cambridge, U. K.)* **2007**, *(33)*, 3425-3437; (c) Fagnoni, M.; Dondi, D.; Ravelli, D.; Albini, A., Photocatalysis for the Formation of the C-C Bond. *Chem. Rev. (Washington, DC, U. S.)* **2007**, *107* (6), 2725-2756.

4. Ischay, M. A.; Anzovino, M. E.; Du, J.; Yoon, T. P., Efficient Visible Light Photocatalysis of [2+2] Enone Cycloadditions. *J. Am. Chem. Soc.* **2008**, *130* (39), 12886-12887.
5. (a) Furst, L.; Matsuura, B. S.; Narayanan, J. M. R.; Tucker, J. W.; Stephenson, C. R. J., Visible Light-Mediated Intermolecular C-H Functionalization of Electron-Rich Heterocycles with Malonates. *Organic Letters* **2010**, *12* (13), 3104-3107. (b) Hari, D. P.; Konig, B., Eosin Y Catalyzed Visible Light Oxidative C-C and C-P bond Formation. *Organic Letters* **2011**, *13* (15), 3852-3855. (c) Maji, T.; Karmakar, A.; Reiser, O., Visible-Light Photoredox Catalysis: Dehalogenation of Vicinal Dibromo-, alpha-Halo-, and alpha,alpha-Dibromocarbonyl Compounds. *Journal of Organic Chemistry* **2011**, *76* (2), 736-739. (d) Singh, A.; Arora, A.; Weaver, J. D., Photoredox-Mediated C-H Functionalization and Coupling of Tertiary Aliphatic Amines with 2-Chloroazoles. *Organic Letters* **2013**, *15* (20), 5390-5393. (e) Tyson, E. L.; Ament, M. S.; Yoon, T. P., Transition Metal Photoredox Catalysis of Radical Thiol-Ene Reactions. *Journal of Organic Chemistry* **2013**, *78* (5), 2046-2050. (f) Xi, Y. M.; Yi, H.; Lei, A. W., Synthetic applications of photoredox catalysis with visible light. *Organic & Biomolecular Chemistry* **2013**, *11* (15), 2387-2403. (g) Hopkinson, M. N.; Sahoo, B.; Glorius, F., Dual Photoredox and Gold Catalysis: Intermolecular Multicomponent Oxyarylation of Alkenes. *Advanced Synthesis & Catalysis* **2014**, *356* (13), 2794-2800. (h) Kaldas, S. J.; Cannillo, A.; McCallum, T.; Barriault, L., Indole Functionalization via Photoredox Gold Catalysis. *Organic Letters* **2015**, *17* (11), 2864-2866. (i) Karakaya, I.; Primer, D. N.; Molander, G. A., Photoredox Cross-Coupling: Ir/Ni Dual Catalysis for the Synthesis of Benzylic Ethers. *Organic Letters* **2015**, *17* (13), 3294-3297. (j) Pratsch, G.; Lackner, G. L.; Overman, L. E., Constructing Quaternary Carbons from N-(Acyloxy)phthalimide Precursors of Tertiary Radicals Using Visible-Light Photocatalysis. *Journal of Organic Chemistry* **2015**, *80* (12), 6025-6036. (k) Shaw, M. H.; Twilton, J.; MacMillan, D. W. C., Photoredox Catalysis in Organic Chemistry. *Journal of Organic Chemistry* **2016**, *81* (16), 6898-6926.
6. (a) Juris, A.; Balzani, V.; Barigelletti, F.; Campagna, S.; Belser, P.; Von Zelewsky, A., Ruthenium(II) polypyridine complexes: photophysics, photochemistry, electrochemistry, and chemiluminescence. *Coord. Chem. Rev.* **1988**, *84*, 85-277. (b) Kalyanasundaram, K.; Gratzel, M., Applications of functionalized transition metal complexes in photonic and optoelectronic devices. *Coord. Chem. Rev.* **1998**, *177*, 347-414. (c) Kalyanasundaram, K., Photophysics, photochemistry and solar energy conversion with tris(bipyridyl)ruthenium(II) and its analogs. *Coord. Chem. Rev.* **1982**, *46*, 159-244.
7. (a) Lowry, M. S.; Bernhard, S., Synthetically tailored excited states: phosphorescent,cyclometalated iridium(III) complexes and their applications. *Chem. - Eur. J.* **2006**, *12* (31), 7970-7977. (b) Flamigni, L.; Barbieri, A.; Sabatini, C.; Ventura, B.; Barigelletti, F., Photochemistry and photophysics of coordination compounds: iridium. *Top. Curr. Chem.* **2007**, *281* (Photochemistry and Photophysics of Coordination Compounds II), 143-203.

8. Arias-Rotondo, D. M.; McCusker, J. K., The photophysics of photoredox catalysis: a roadmap for catalyst design. *Chem. Soc. Rev.* **2016**, *45* (21), 5803-5820.
9. (a) Nicewicz, D. A.; MacMillan, D. W. C., Merging Photoredox Catalysis with Organocatalysis: The Direct Asymmetric Alkylation of Aldehydes. *Science (Washington, DC, U.S.)* **2008**, *322* (5898), 77-80; (b) Shih, H.-W.; Vander Wal, M. N.; Grange, R. L.; MacMillan, D. W. C., Enantioselective α -Benzylation of Aldehydes via Photoredox Organocatalysis. *J. Am. Chem. Soc.* **2010**, *132* (39), 13600-13603; (c) Nagib, D. A.; Scott, M. E.; MacMillan, D. W. C., Enantioselective α -Trifluoromethylation of Aldehydes via Photoredox Organocatalysis. *J. Am. Chem. Soc.* **2009**, *131* (31), 10875-10877; (d) Pham, P. V.; Nagib, D. A.; MacMillan, D. W. C., Photoredox Catalysis: A Mild, Operationally Simple Approach to the Synthesis of α -Trifluoromethyl Carbonyl Compounds. *Angew. Chem., Int. Ed.* **2011**, *50* (27), 6119-6122, S6119/1-S6119/32; (e) Petronijevic, F. R.; Nappi, M.; MacMillan, D. W. C., Direct β -Functionalization of Cyclic Ketones with Aryl Ketones via the Merger of Photoredox and Organocatalysis. *J. Am. Chem. Soc.* **2013**, *135* (49), 18323-18326; (f) Cecere, G.; Konig, C. M.; Alleva, J. L.; MacMillan, D. W. C., Enantioselective Direct α -Amination of Aldehydes via a Photoredox Mechanism: A Strategy for Asymmetric Amine Fragment Coupling. *J. Am. Chem. Soc.* **2013**, *135* (31), 11521-11524; (g) Nagib, D. A.; MacMillan, D. W. C., Trifluoromethylation of arenes and heteroarenes by means of photoredox catalysis. *Nature (London, U. K.)* **2011**, *480* (7376), 224-228.
10. Prier, C. K.; Rankic, D. A.; MacMillan, D. W. C., Visible Light Photoredox Catalysis with Transition Metal Complexes: Applications in Organic Synthesis. *Chem. Rev. (Washington, DC, U. S.)* **2013**, *113* (7), 5322-5363.
11. Narayanan, J. M. R.; Tucker, J. W.; Stephenson, C. R. J., Electron-Transfer Photoredox Catalysis: Development of a Tin-Free Reductive Dehalogenation Reaction. *J. Am. Chem. Soc.* **2009**, *131* (25), 8756-8757.
12. (a) Tucker, J. W.; Stephenson, C. R. J., Tandem Visible Light-Mediated Radical Cyclization-Divinylcyclopropane Rearrangement to Tricyclic Pyrrolidinones. *Org. Lett.* **2011**, *13* (20), 5468-5471; (b) Furst, L.; Narayanan Jagan, M. R.; Stephenson Corey, R. J., Total synthesis of (+)-gliocladin C enabled by visible-light photoredox catalysis. *Angew Chem Int Ed Engl* **2011**, *50* (41), 9655-9; (c) Tucker, J. W.; Zhang, Y.; Jamison, T. F.; Stephenson, C. R. J., Visible-Light Photoredox Catalysis in Flow. *Angew. Chem., Int. Ed.* **2012**, *51* (17), 4144-4147, S4144/1-S4144/24; (d) Konieczynska, M. D.; Dai, C.; Stephenson, C. R. J., Synthesis of symmetric anhydrides using visible light-mediated photoredox catalysis. *Org. Biomol. Chem.* **2012**, *10* (23), 4509-4511; (e) Nguyen, J. D.; Matsuura, B. S.; Stephenson, C. R. J., A Photochemical Strategy for Lignin Degradation at Room Temperature. *J. Am. Chem. Soc.* **2014**, *136* (4), 1218-1221; (f) Bergonzini, G.; Schindler, C. S.; Wallentin, C.-J.; Jacobsen, E. N.; Stephenson, C. R. J., Photoredox activation and anion binding catalysis in the dual catalytic enantioselective synthesis of β -amino esters. *Chem. Sci.* **2014**, *5* (1), 112-116; (g) Freeman, D. B.; Furst, L.; Condie, A. G.; Stephenson, C. R. J., Functionally Diverse Nucleophilic Trapping of Iminium Intermediates Generated Utilizing Visible Light. *Org. Lett.* **2012**, *14* (1), 94-97; (h)

Nguyen, J. D.; Reiss, B.; Dai, C.; Stephenson, C. R. J., Batch to flow deoxygenation using visible light photoredox catalysis. *Chem. Commun. (Cambridge, U. K.)* **2013**, 49 (39), 4352-4354; (i) Dai, C.; Narayanan, J. M. R.; Stephenson, C. R. J., Visible lightmediated conversion of alcohols to halides. *Nat. Chem.* **2011**, 3 (2), 140-145.

13. (a) Du, J.; Yoon, T. P., Crossed Intermolecular [2+2] Cycloadditions of Acyclic Enones via Visible Light Photocatalysis. *J. Am. Chem. Soc.* **2009**, 131 (41), 14604-14605; (b) Lu, Z.; Shen, M.; Yoon, T. P., [3+2] Cycloadditions of Aryl Cyclopropyl Ketones by Visible Light Photocatalysis. *J. Am. Chem. Soc.* **2011**, 133 (5), 1162-1164; (c) Tyson, E. L.; Farney, E. P.; Yoon, T. P., Photocatalytic [2 + 2] Cycloadditions of Enones with Cleavable Redox Auxiliaries. *Org. Lett.* **2012**, 14 (4), 1110-1113. (d) Ischay, M. A.; Lu, Z.; Yoon, T. P., [2+2] cycloadditions by oxidative visible light photocatalysis. *J. Am. Chem. Soc.* **2010**, 132 (25), 8572-8574. (e) Lin, S.; Ischay, M. A.; Fry, C. G.; Yoon, T. P., Radical Cation Diels-Alder Cycloadditions by Visible Light Photocatalysis. *J. Am. Chem. Soc.* **2011**, 133 (48), 19350-19353; (f) Parrish, J. D.; Ischay, M. A.; Lu, Z.; Guo, S.; Peters, N. R.; Yoon, T. P., Endoperoxide Synthesis by Photocatalytic Aerobic [2 + 2 + 2] Cycloadditions. *Org. Lett.* **2012**, 14 (6), 1640-1643. (g) Lu, Z.; Yoon, T. P., Visible Light Photocatalysis of [2+2] Styrene Cycloadditions by Energy Transfer. *Angew. Chem., Int. Ed.* **2012**, 51 (41), 10329-10332, S10329/1-S10329/128.

14. (a) Hari, D. P.; Schroll, P.; Koenig, B., Metal-free, visible-light-mediated direct C-H arylation of heteroarenes with aryl diazonium salts. *J. Am. Chem. Soc.* **2012**, 134 (6), 2958-2961; (b) Zou, Y.-Q.; Chen, J.-R.; Liu, X.-P.; Lu, L.-Q.; Davis, R. L.; Joergensen, K. A.; Xiao, W.-J., Highly Efficient Aerobic Oxidative Hydroxylation of Arylboronic Acids: Photoredox Catalysis using Visible Light. *Angew. Chem., Int. Ed.* **2012**, 51 (3), 784-788, S784/1-S784/80; (c) Kalyani, D.; McMurtrey, K. B.; Neufeldt, S. R.; Sanford, M. S., Room-Temperature C-H Arylation: Merger of Pd-Catalyzed C-H Functionalization and Visible-Light Photocatalysis. *J. Am. Chem. Soc.* **2011**, 133 (46), 18566-18569; (d) Larraufie, M.-H.; Pellet, R.; Fensterbank, L.; Goddard, J.- P.; Lacote, E.; Malacria, M.; Ollivier, C., Visible-Light-Induced Photoreductive Generation of Radicals from Epoxides and Aziridines. *Angew. Chem., Int. Ed.* **2011**, 50 (19), 4463-4466, S4463/1-S4463/74; (e) Neumann, M.; Fueldner, S.; Koenig, B.; Zeitler, K., Metal-Free, Cooperative Asymmetric Organophotoredox Catalysis with Visible Light. *Angew. Chem., Int. Ed.* **2011**, 50 (4), 951-954, S951/1-S951/28; (f) Andrews, R. S.; Becker, J. J.; Gagne, M. R., Intermolecular addition of glycosyl halides to alkenes mediated by visible light. *Angew. Chem., Int. Ed.* **2010**, 49 (40), 7274-7276, S7274/1-S7274/16; (g) Ye, Y.; Sanford, M. S., Merging Visible-Light Photocatalysis and Transition-Metal Catalysis in the Copper-Catalyzed Trifluoromethylation of Boronic Acids with CF₃I. *J. Am. Chem. Soc.* **2012**, 134 (22), 9034-9037.

15. (a) Graetzel, M., Artificial photosynthesis: water cleavage into hydrogen and oxygen by visible light. *Acc. Chem. Res.* **1981**, 14 (12), 376-84; (b) Sala, X.; Romero, I.; Rodriguez, M.; Escriche, L.; Llobet, A., Molecular catalysts that oxidize water to dioxygen. *Angew. Chem., Int. Ed.* **2009**, 48 (16), 2842-2852.

16. Takeda, H.; Ishitani, O., Development of efficient photocatalytic systems for CO₂ reduction using mononuclear and multinuclear metal complexes based on mechanistic studies. *Coord. Chem. Rev.* **2010**, 254 (3-4), 346-354.

17. Kalyanasundaram, K.; Gratzel, M., Applications of functionalized transition metal complexes in photonic and optoelectronic devices. *Coord. Chem. Rev.* **1998**, 177, 347-414.

18. (a) Lalevee, J.; Blanchard, N.; Tehfe, M.-A.; Morlet-Savary, F.; Fouassier, J. P., Green Bulb Light Source Induced Epoxy Cationic Polymerization under Air Using Tris(2,2'-bipyridine)ruthenium(II) and Silyl Radicals. *Macromolecules (Washington, DC, U. S.)* **2010**, 43 (24), 10191-10195; (b) Lalevee, J.; Peter, M.; Dumur, F.; Gigmes, D.; Blanchard, N.; Tehfe, M. A.; Morlet-Savary, F.; Fouassier, J. P., Subtle Ligand Effects in Oxidative Photocatalysis with Iridium Complexes: Application to Photopolymerization. *Chem. - Eur. J.* **2011**, 17 (52), 15027-15031, S15027/1-S15027/13; (c) Fors, B. P.; Hawker, C. J., Control of a Living Radical Polymerization of Methacrylates by Light. *Angew. Chem., Int. Ed.* **2012**, 51 (35), 8850-8853.

19. (a) Xiao, P.; Zhang, J.; Dumur, F.; Tehfe, M. A.; Morlet-Savary, F.; Graff, B.; Gigmes, D.; Fouassier, J. P.; Lalevee, J., Visible light sensitive photoinitiating systems: Recent progress in cationic and radical photopolymerization reactions under soft conditions. *Progress in Polymer Science* **2015**, 41, 32-66. (b) Shao, J. Z.; Huang, Y.; Fan, Q. U., Visible light initiating systems for photopolymerization: status, development and challenges. *Polymer Chemistry* **2014**, 5 (14), 4195-4210. (c) Pan, X. C.; Tasdelen, M. A.; Laun, J.; Junkers, T.; Yagci, Y.; Matyjaszewski, K., Photomediated controlled radical polymerization. *Progress in Polymer Science* **2016**, 62, 73-125. (d) Dadashi-Silab, S.; Aydogan, C.; Yagci, Y., Shining a light on an adaptable photoinitiator: advances in photopolymerizations initiated by thioxanthones. *Polymer Chemistry* **2015**, 6 (37), 6595-6615.

20. Singh, A.; Teegardin, K.; Kelly, M.; Prasad, K. S.; Krishnan, S.; Weaver, J. D., Facile synthesis and complete characterization of homoleptic and heteroleptic cyclometalated Iridium(III) complexes for photocatalysis. *Journal of Organometallic Chemistry* **2015**, 776, 51-59.

21. Tordera, D.; Serrano-Pérez, J. J.; Pertegás, A.; Ortí, E.; Bolink, H. J.; Baranoff, E.; Nazeeruddin, M. K.; Frey, J., Correlating the Lifetime and Fluorine Content of Iridium(III) Emitters in Green Light-Emitting Electrochemical Cells. *Chemistry of Materials* **2013**, 25 (16), 3391-3397.

22. Okada, S.; Okinaka, K.; Iwawaki, H.; Furugori, M.; Hashimoto, M.; Mukaide, T.; Kamatani, J.; Igawa, S.; Tsuboyama, A.; Takiguchi, T.; Ueno, K., Substituent effects of

iridium complexes for highly efficient red OLEDs. *Dalton Transactions* **2005**, (9), 1583-1590.

23. Heitz, D. R.; Tellis, J. C.; Molander, G. A., Photochemical Nickel-Catalyzed C–H Arylation: Synthetic Scope and Mechanistic Investigations. *Journal of the American Chemical Society* **2016**, 138 (39), 12715-12718.

24. Welin, E. R.; Le, C.; Arias-Rotondo, D. M.; McCusker, J. K.; MacMillan, D. W. C., Photosensitized, energy transfer-mediated organometallic catalysis through electronically excited nickel(II). *Science* **2017**, 355 (6323), 380-385.

25. Fukuzumi, S.; Mochizuki, S.; Tanaka, T., Photocatalytic reduction of phenacyl halides by 9,10-dihydro-10-methylacridine: control between the reductive and oxidative quenching pathways of tris(bipyridine)ruthenium complex utilizing an acid catalysis. *J. Phys. Chem.* **1990**, 94 (2), 722-726.

26. Van Bergen, T. J.; Hedstrand, D. M.; Kruizinga, W. H.; Kellogg, R. M., Chemistry of dihydropyridines. 9. Hydride transfer from 1,4-dihydropyridines to sp³-hybridized carbon in sulfonium salts and activated halides. Studies with NAD(P)H models. *J. Org. Chem.* **1979**, 44 (26), 4953-4962.

27. Tanaka, H.; Tsuda, M.; Nakanishi, H.; Photochemistry of poly(vinyl cinnamylideneacetate) and related compounds. *J. Polym. Sci. A-1 Polym. Chem.* **1972**, 10, 1729–1743.

28. (a) Pac, C.; Ihama, M.; Yasuda, M.; Miyauchi, Y.; Sakurai, H., Tris(2,2'-bipyridine)ruthenium(2+)-mediated photoreduction of olefins with 1-benzyl-1,4-dihydronicotinamide: a mechanistic probe for electron-transfer reactions of NAD(P)H-model compounds. *J. Am. Chem. Soc.* **1981**, 103 (21), 6495-6497; (b) Pac, C.; Miyauchi, Y.; Ishitani, O.; 141 Ihama, M.; Yasuda, M.; Sakurai, H., Redox-photosensitized reactions. 11. Ru(bpy)₃²⁺-photosensitized reactions of 1-benzyl-1,4-dihydronicotinamide with aryl-substituted enones, derivatives of methyl cinnamate, and substituted cinnamonnitriles: electron-transfer mechanism and structure-reactivity relationships. *J. Org. Chem.* **1984**, 49 (1), 26-34; (c) Ishitani, O.; Yanagida, S.; Takamuku, S.; Pac, C., Redox-photosensitized reactions. 13. Ru(bpy)₃²⁺-photosensitized reactions of an NADH model, 1-benzyl-1,4-dihydronicotinamide, with aromatic carbonyl compounds and comparison with thermal reactions. *J. Org. Chem.* **1987**, 52 (13), 2790-2796.

29. (a) Cano-Yelo, H.; Deronzier, A., Photooxidation of some carbinols by the ruthenium(II) polypyridyl complex-aryl diazonium salt system. *Tetrahedron Lett.* **1984**, 25 (48), 5517-5520; (b) Cano-Yelo, H.; Deronzier, A., Photocatalysis of the Pschorr reaction by tris(2,2'-bipyridyl)ruthenium(II) in the phenanthrene series. *J. Chem. Soc., Perkin Trans. 2* **1984**, (6), 1093-1098. (c) Okada, K.; Okamoto, K.; Morita, N.; Okubo, K.; Oda, M., Photosensitized decarboxylative Michael addition through N-(acyloxy)phthalimides via an electron-transfer mechanism. *J. Am. Chem. Soc.* **1991**, 113 (24), 9401-9402. (d) Willner, I.; Tsfania, T.; Eichen, Y., Photocatalyzed and electrocatalyzed reduction of vicinal dibromides and activated ketones using ruthenium(I) tris(bipyridine) as electron-transfer mediator. *J. Org. Chem.* **1990**, 55 (9), 2656-2662; (e) Maidan, R.; Goren, Z.; Becker, J. Y.; Willner, I., Application of multielectron charge relays in chemical and photochemical debromination processes. The role of induced disproportionation of N,N'-dioctyl-4,4'-bipyridinium radical cation in two-phase systems. *J. Am. Chem. Soc.* **1984**, 106 (21), 6217-6222; (f) Maidan, R.; Willner, I., Photochemical and chemical enzyme catalyzed debromination of meso-1,2-dibromostilbene in multiphase systems. *J. Am. Chem. Soc.* **1986**, 108 (5), 1080-1082.

30. Cano-Yelo, H.; Deronzier, A., Photocatalysis of the Pschorr reaction by tris-(2,2[prime or minute]-bipyridyl)ruthenium(II) in the phenanthrene series. *Journal of the Chemical Society, Perkin Transactions 2* **1984**, (6), 1093-1098.

31. Cano-Yelo, H.; Deronzier, A., Photocatalysis of the pschorr reaction by Ru(bpy) 3^{2+} . *Journal of Photochemistry* **1987**, 37 (2), 315-321.

32. Nguyen, J. D.; D'Amato, E. M.; Narayanan, J. M. R.; Stephenson, C. R. J., Engaging unactivated alkyl, alkenyl and aryl iodides in visible-light-mediated free radical reactions. *Nat Chem* **2012**, 4 (10), 854-859.

33. Chu, L.; Ohta, C.; Zuo, Z.; MacMillan, D. W. C., Carboxylic Acids as A Traceless Activation Group for Conjugate Additions: A Three-Step Synthesis of (\pm)-Pregabalin. *Journal of the American Chemical Society* **2014**, 136 (31), 10886-10889.

34. Musacchio, A. J.; Nguyen, L. Q.; Beard, G. H.; Knowles, R. R., Catalytic Olefin Hydroamination with Aminium Radical Cations: A Photoredox Method for Direct C–N Bond Formation. *Journal of the American Chemical Society* **2014**, 136 (35), 12217-12220.

35. Maity, S.; Zhu, M.; Shinabery, R. S.; Zheng, N., Intermolecular [3+2] Cycloaddition of Cyclopropylamines with Olefins by Visible-Light Photocatalysis. *Angewandte Chemie International Edition* **2012**, 51 (1), 222-226.

36. Chow, Y. L.; Danen, W. C.; Nelsen, S. F.; Rosenblatt, D. H., Nonaromatic aminium radicals. *Chem. Rev.* **1978**, *78* (3), 243-74; Bauld, N. L., Cation radical cycloadditions and related sigmatropic reactions. *Tetrahedron* **1989**, *45* (17), 5307-63; Schmittel, M.; Burghart, A., Understanding reactivity patterns of radical cations. *Angew. Chem., Int. Ed. Engl.* **1997**, *36* (23), 2551-2589; Fallis, A. G.; Brinza, I. M., Free radical cyclizations involving nitrogen. *Tetrahedron* **1997**, *53* (52), 17543-17594; Moeller, K. D., Synthetic Applications of Anodic Electrochemistry. *Tetrahedron* **2000**, *56* (49), 9527-9554; Hoffmann, N., Photochemically induced radical addition of tertiary amines to C=C and C=O double bonds: a green chemistry contribution to organic synthesis. *Pure Appl. Chem.* **2007**, *79* (11), 1949-1958.

37. Shono, T.; Matsumura, Y.; Tsubata, K., Electroorganic chemistry. 46. A new carbon carbon bond forming reaction at the α -position of amines utilizing anodic oxidation as a key step. *J. Am. Chem. Soc.* **1981**, *103* (5), 1172-6; Basle, O.; Borduas, N.; Dubois, P.; Chapuzet, J. M.; Chan, T.-H.; Lessard, J.; Li, C.-J., Aerobic and Electrochemical Oxidative Cross-Dehydrogenative-Coupling (CDC) Reaction in an Imidazolium-Based Ionic Liquid. *Chem. - Eur. J.* **2010**, *16* (27), 8162-8166, S8162/1-S8162/8.

38. Tsang, A. S. K.; Todd, M. H., Facile synthesis of vicinal diamines via oxidation of Nphenyltetrahydroisoquinolines with DDQ. *Tetrahedron Lett.* **2009**, *50* (11), 1199-1202; Richter, H.; Garcia Mancheno, O., Dehydrogenative functionalization of C(sp³)-H bonds adjacent to a heteroatom mediated by oxoammonium salts. *Eur. J. Org. Chem.* **2010**, (23), 4460-4467, S4460/1-S4460/32; Shu, X.-Z.; Xia, X.-F.; Yang, Y.-F.; Ji, K.-G.; Liu, X.-Y.; Liang, Y.-M., Selective Functionalization of sp³ C-H Bonds Adjacent to Nitrogen Using (Diacetoxyiodo)benzene (DIB). *J. Org. Chem.* **2009**, *74* (19), 7464-7469.

39. Murahashi, S.-I.; Zhang, D., Ruthenium-catalyzed biomimetic oxidation in organic synthesis inspired by cytochrome P-450. *Chem. Soc. Rev.* **2008**, *37* (8), 1490-1501; Boess, E.; Schmitz, C.; Klussmann, M., A Comparative Mechanistic Study of Cu-Catalyzed Oxidative Coupling Reactions with N-Phenyltetrahydroisoquinoline. *J. Am. Chem. Soc.* **2012**, *134* (11), 5317-5325; Ratnikov, M. O.; Doyle, M. P., Mechanistic Investigation of Oxidative Mannich Reaction with tert-Butyl Hydroperoxide. The Role of Transition Metal Salt. *J. Am. Chem. Soc.* **2013**, *135* (4), 1549-1557.

40. Cho, D. W.; Yoon, U. C.; Mariano, P. S., Studies Leading to the Development of a Single-Electron Transfer (SET) Photochemical Strategy for Syntheses of Macrocyclic Polyethers, Polythioethers, and Polyamides. *Acc. Chem. Res.* **2011**, *44* (3), 204-215; Pandey, G.; Gadre, S. R., Sequential two electron photooxidation of t-amines: generation of a regiospecific iminium cation and its application in organic synthesis. *ARKIVOC (Gainesville, FL, U. S.)* **2003**, (3), 45-54; Hoshikawa, T.; Yoshioka, S.; Kamijo, S.; Inoue, M., Photoinduced direct cyanation of C(sp³)-H bonds. *Synthesis* **2013**, *45* (7), 874-887.

41. (a) Shi, L.; Xia, W., Photoredox functionalization of C-H bonds adjacent to a nitrogen atom. *Chem. Soc. Rev.* **2012**, *41* (23), 7687-7697. (b) Maity, S.; Zheng, N., A photo touch on amines: new synthetic adventures of nitrogen radical cations. *Synlett* **2012**, *23* (13), 1851-1856.

42. Bard, A. J.; Fox, M. A., Artificial Photosynthesis: Solar Splitting of Water to Hydrogen and Oxygen. *Acc. Chem. Res.* **1995**, *28* (3), 141-145.

43. Willner, I.; Maidan, R.; Mandler, D.; Duerr, H.; Doerr, G.; Zengerle, K., Photosensitized reduction of carbon dioxide to methane and hydrogen evolution in the presence of ruthenium and osmium colloids: strategies to design selectivity of products distribution. *J. Am. Chem. Soc.* **1987**, *109* (20), 6080-6086.

44. (a) DeLaive, P. J.; Foreman, T. K.; Giannotti, C.; Whitten, D. G., Photoinduced electron transfer reactions of transition-metal complexes with amines. Mechanistic studies of alternate pathways to back electron transfer. *J. Am. Chem. Soc.* **1980**, *102* (17), 5627-31.(b) DeLaive, P. J.; Lee, J. T.; Sprintschnik, H. W.; Abruna, H.; Meyer, T. J.; Whitten, D. G., Photoinduced redox reactions of hydrophobic ruthenium(II) complexes. *J. Am. Chem. Soc.* **1977**, *99* (21), 7094-7.

45. Liang, B.; Kalidindi, S.; Porco, J. A.; Stephenson, C. R. J., Multicomponent Reaction Discovery: Three-Component Synthesis of Spirooxindoles. *Organic Letters* **2010**, *12* (3), 572-575.

46. Miyake, Y.; Nakajima, K.; Nishibayashi, Y., Visible-Light-Mediated Utilization of α -Aminoalkyl Radicals: Addition to Electron-Deficient Alkenes Using Photoredox Catalysts. *Journal of the American Chemical Society* **2012**, *134* (7), 3338-3341.

47. Cai, S.; Zhao, X.; Wang, X.; Liu, Q.; Li, Z.; Wang, D. Z., Visible-Light-Promoted C \square C Bond Cleavage: Photocatalytic Generation of Iminium Ions and Amino Radicals. *Angewandte Chemie International Edition* **2012**, *51* (32), 8050-8053.

48. (a) Reissig, H. U., Donor-acceptor-substituted cyclopropanes: versatile building blocks in organic synthesis. *Top. Curr. Chem.* **1988**, *144* (Small Ring Compd. Org. Synth. 3), 73-135. (b) Salaun, J. R. Y., Synthesis and synthetic applications of 1-donor substituted cyclopropanes with ethynyl, vinyl, and carbonyl groups. *Top. Curr. Chem.* **1988**, *144* (Small Ring Compd. Org. Synth. 3), 1-71; (c) Paquette, L. A., Silyl-substituted cyclopropanes as versatile synthetic reagents. *Chem. Rev.* **1986**, *86* (5), 733-50; (d) Wong, H. N. C.; Hon, M. Y.; Tse, C. W.; Yip, Y. C.; Tanko, J.; Hudlicky, T., Use of

cyclopropanes and their derivatives in organic synthesis. *Chem. Rev.* **1989**, *89* (1), 165-98.

49. (a) Conia, J. M.; Salaun, J. R., CYCLOBUTANE RING CONTRACTIONS NOT INVOLVING CARBONIUM-IONS. *Accounts of Chemical Research* **1972**, *5* (1), 33-+.; (b) Wong, H. N. C.; Lau, K. L.; Tam, K. F., THE APPLICATION OF CYCLOBUTANE DERIVATIVES IN ORGANIC-SYNTHESIS. *Topics in Current Chemistry* **1986**, *133*, 83-157. (c) Namyslo, J. C.; Kaufmann, D. E., The application of cyclobutane derivatives in organic synthesis. *Chemical Reviews* **2003**, *103* (4), 1485-1537.

50. (a) Wu, W.; Ma, B.; I-Chia Wu, J.; Schleyer, P. v. R.; Mo, Y., Is Cyclopropane Really the σ -Aromatic Paradigm? *Chemistry – A European Journal* **2009**, *15* (38), 9730-9736. (b) Bach, R. D.; Dmitrenko, O., Strain Energy of Small Ring Hydrocarbons. Influence of C–H Bond Dissociation Energies. *Journal of the American Chemical Society* **2004**, *126* (13), 4444-4452. (c) Khouri, P. R.; Goddard, J. D.; Tam, W., Ring strain energies: substituted rings, norbornanes, norbornenes and norbornadienes. *Tetrahedron* **2004**, *60* (37), 8103-8112. (d) Wiberg, K. B., Cyclobutane—Physical Properties and Theoretical Studies. In *The Chemistry of Cyclobutanes*, John Wiley & Sons, Ltd: **2006**; pp 1-15.

51. Souillart, L.; Cramer, N., Enantioselective Rhodium-catalyzed C–C Bond Activation of Cyclobutanones. *Chimia* **2015**, *69* (4), 187-190. (b) Nemoto, H.; Shiraki, M.; Nagamochi, M.; Fukumoto, K., A CONCISE ENANTIOCONTROLLED TOTAL SYNTHESIS OF (-)-ALPHA-BISABOLOL AND (+)-4-EPI-ALPHA-BISABOLOL. *Tetrahedron Letters* **1993**, *34* (31), 4939-4942. (c) Matsuda, T.; Shigeno, M.; Murakami, M., Activation of a cyclobutanone carbon–carbon bond over an aldehyde carbon–hydrogen bond in the rhodium-catalyzed decarbonylation. *Chemistry Letters* **2006**, *35* (3), 288-289. (d) Matsuda, T.; Makino, M.; Murakami, M., Addition/ring-opening reaction of organoboronic acids to cyclobutanones catalyzed by rhodium(I)/P(t-Bu)(3) complex. *Bulletin of the Chemical Society of Japan* **2005**, *78* (8), 1528-1533. (e) Lund, E. A.; Kennedy, I. A.; Fallis, A. G., Dihydrofurans from alpha-diazoketones due to facile ring opening - cyclisation of donor-acceptor cyclopropane intermediates. *Canadian Journal of Chemistry-Revue Canadienne De Chimie* **1996**, *74* (12), 2401-2412. (f) Chung, L. W.; Wiest, O.; Wu, Y. D., A theoretical study on the trans-addition intramolecular hydroacylation of 4-alkynals catalyzed by cationic rhodium complexes. *Journal of Organic Chemistry* **2008**, *73* (7), 2649-2655.

52. (a) Murakami, M.; Amii, H.; Ito, Y., Selective activation of carbon–carbon bonds next to a carbonyl group. *Nature* **1994**, *370* (6490), 540-541.(b) Murakami, M.; Amii, H.; Shigeto, K.; Ito, Y., Breaking of the C–C Bond of Cyclobutanones by Rhodium(I) and Its Extension to Catalytic Synthetic Reactions. *Journal of the American Chemical Society* **1996**, *118* (35), 8285-8290.

53. Murakami, M.; Ashida, S.; Matsuda, T., Nickel-Catalyzed Intermolecular Alkyne Insertion into Cyclobutanones. *Journal of the American Chemical Society* **2005**, *127* (19), 6932-6933.

54. Nishimura, T.; Uemura, S., Palladium-Catalyzed Arylation of tert-Cyclobutanols with Aryl Bromide via C–C Bond Cleavage: New Approach for the γ -Arylated Ketones. *Journal of the American Chemical Society* **1999**, *121* (47), 11010-11011.

55. Seiser, T.; Roth, O. A.; Cramer, N., Enantioselective Synthesis of Indanols from tert-Cyclobutanols Using a Rhodium-Catalyzed C \square C/C \square H Activation Sequence. *Angewandte Chemie International Edition* **2009**, *48* (34), 6320-6323.

56. Zhao, H.; Fan, X.; Yu, J.; Zhu, C., Silver-Catalyzed Ring-Opening Strategy for the Synthesis of β - and γ -Fluorinated Ketones. *Journal of the American Chemical Society* **2015**, *137* (10), 3490-3493.

57. Ren, R.; Zhao, H.; Huan, L.; Zhu, C., Manganese-Catalyzed Oxidative Azidation of Cyclobutanols: Regiospecific Synthesis of Alkyl Azides by C \square C Bond Cleavage. *Angewandte Chemie International Edition* **2015**, *54* (43), 12692-12696.

58. (a) Reissig, H.-U.; Zimmer, R., Thrilling Strain! Donor–Acceptor-Substituted Cyclobutanes for the Synthesis of (Hetero)Cyclic Compounds. *Angewandte Chemie International Edition* **2015**, *54* (17), 5009-5011. (b) Wang, L. J.; Tang, Y., Asymmetric Ring-Opening Reactions of Donor-Acceptor Cyclopropanes and Cyclobutanes. *Israel Journal of Chemistry* **2016**, *56* (6-7), 463-475. (c) O'Connor, N. R.; Wood, J. L.; Stoltz, B. M., Synthetic Applications and Methodological Developments of Donor-Acceptor Cyclopropanes and Related Compounds. *Israel Journal of Chemistry* **2016**, *56* (6-7), 431-444.

59. Moustafa, M. M. A. R.; Pagenkopf, B. L., Ytterbium Triflate Catalyzed Synthesis of Alkoxy-Substituted Donor–Acceptor Cyclobutanes and Their Formal [4 + 2] Cycloaddition with Imines: Stereoselective Synthesis of Piperidines. *Organic Letters* **2010**, *12* (21), 4732-4735.

60. Perrotta, D.; Racine, S.; Vuilleumier, J.; de Nanteuil, F.; Waser, J., [4 + 2]-Annulations of Aminocyclobutanes. *Organic Letters* **2015**, *17* (4), 1030-1033.

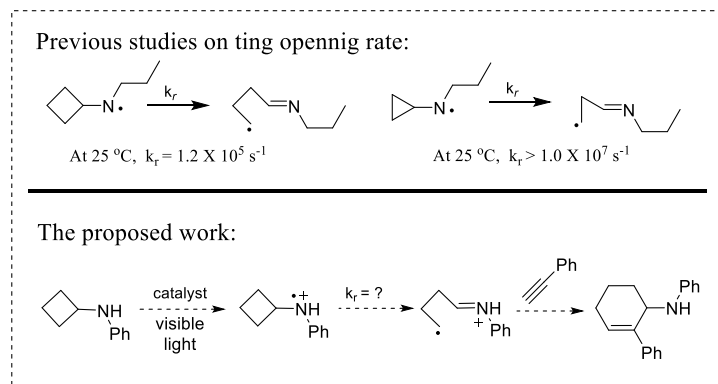
Chapter 2. Intermolecular [4+2] Annulation of Cyclobutylanilines with Alkynes

2.1 Introduction

Release of ring strain has often been exploited as a driving force by organic chemists to promote cleavage of typically unreactive bonds such as carbon-carbon bonds.¹ This strategy has been successfully applied to ring opening of cyclopropanes, which leads to the wide use of cyclopropanes in organic synthesis.² We recently reported visible light promoted [3+2] annulation reactions of cyclopropylanilines with various pi bonds.³ In these reactions, the cleavage of cyclopropyl rings is promoted by photooxidation of the parent amine to the corresponding amine radical cation. Since the oxidation potentials of cyclopropylaniline and cyclobutylaniline were found to be similar,⁴ we were intrigued by the possibility of using cyclobutylanilines in the annulation reactions in a similar manner. We were further encouraged by the fact that cyclobutane's strain energy is almost identical to that of cyclopropane.^{5,6}

Still, ring opening of cyclopropanes is generally much faster than that of cyclobutanes. Newcomb reported that the rate constant for ring opening of a cyclobutylcarbonyl radical was $1.5 \times 10^3 \text{ s}^{-1}$ at 20 °C compared to $7 \times 10^7 \text{ s}^{-1}$ at 20 °C for ring opening of a cyclopropylcarbonyl radical.⁷ Ingold reported the rate constant for ring opening of the cyclobutyl-*n*-propylaminyl radical to be $1.2 \times 10^5 \text{ s}^{-1}$ at 25 °C while the rate constant was estimated to be greater than 10^7 s^{-1} at 25 °C for ring opening of the cyclopropyl-*n*-propylaminyl radical (Scheme 2.1).⁸ The proposed ring opening of the cyclobutylaniline radical cation was expected to be faster than the neutral aminyl radical,⁹ which lent further credence to the proposed annulation reaction (Scheme 2.1). Surprisingly, to the best of our knowledge, there have been no reports of using cyclobutylanilines in the tandem ring opening and annulation sequence to construct six-membered carbocycles. This is in contrast to the increasing use of other types of cyclobutanes in

the tandem sequence.¹⁰ Successful ring opening of these cyclobutanes usually relies on the decoration of the cyclobutyl ring with donor-acceptors¹¹ or ketone/hydroxyl functionality.¹² Herein we describe the successful development of the [4+2] annulation of cyclobutylanilines with alkynes enabled by visible light photoredox catalysis, which greatly broadens the use of cyclobutanes as a four-carbon synthon in organic synthesis. We hope that this method will add to the growing pool of synthetic methods based on photocatalysis.¹³



Scheme 2.1 The Ring Opening Rate Studies and Our Proposed Reaction Pathway.

2.2. [4+2] Annulation of *N*-Cyclobutylanilines with Alkynes under Photoredox Catalysis.

2.2.1. Reaction Optimization of the [4+2] Annulation

We chose 4-*tert*-Butyl-*N*-cyclobutylaniline **1a** and phenylacetylene **2a** as the standard substrates to optimize the [4+2] annulation. The optimized conditions of our previous [3+2] annulation of *N*-cyclopropylanilines with alkynes, which are composed of Ru(bpz)₃(PF₆)₂ **4b** as the photoredox catalyst, CH₃NO₂ as the reaction solvent and under the irradiation with one 18 W white LED, were incorporated in the initial screening. We found that only traceable amount of the desired [4+2] annulation product **3a** was observed in the condition after a standard 16 h irradiation (Table 2.2.1, entry 1). Further screening of more photon flux by adding an extra one

18 W LED increased the yield of **3a** to 30% (Table 2.2.1, entry 2). Meanwhile, the reaction yield was further improved by switching the catalyst **4b** to a more stable $\text{Ir}(\text{ppy})_2(\text{dtbbpy})\text{PF}_6$ **4a** (Table 2.1, entry 3). However, other common iridium based photoredox catalysts, such as $\text{Ir}(\text{ppy})_3$ (**4c**) and $\text{Ir}(\text{dF}(\text{CF}_3)\text{ppy})_2(\text{dtbbpy})\text{PF}_6$ (**4d**) all failed in improving the reaction yield. Solvent and other reaction parameters' screening revealed that $[\text{Ir}(\text{dtbbpy})(\text{ppy})_2](\text{PF}_6)$ **4a** in MeOH with two 18 W LEDs was optimal conditions for the proposed [4+2] annulation, providing the desired product **3a** in 97% GC yield (90% isolated yield) (Table 2.2.1, entry 6). Conducting the experiment without degassing the reaction mixture led to significant decrease in the yield (Table 2.2.1, entry 7). Two control studies showed that omitting either the photocatalyst or light produced a negligible amount of **3a** (entries 11 and 12). The beneficial effect of using two lights could include increasing exposure to light and raising the reaction temperature. An internal temperature of 55 °C was measured with two bulbs while 25 °C was recorded with one bulb. To further probe this phenomenon, we performed a temperature control study in which the test tube was placed in a 55 °C water bath with one LED light (entry 14). Though not as high as using two LED lights, product **3a** was detected in 68% yield. The yield improvement, comparing to one LED light at room temperature (entry 6), suggests that higher temperature and photon output are both beneficial to the reaction.

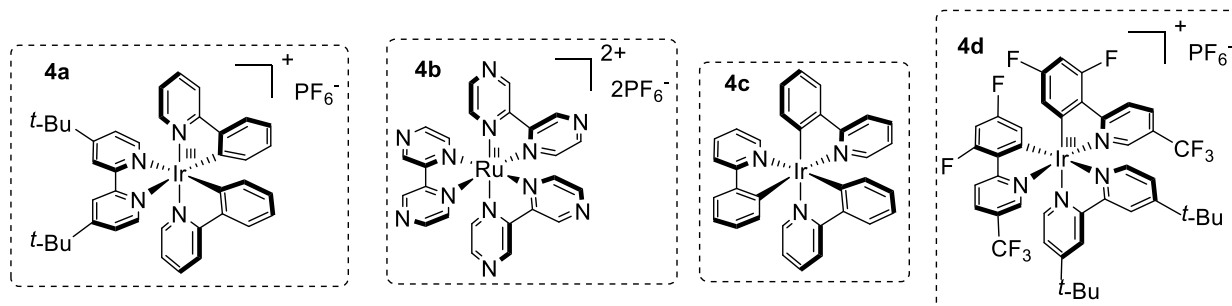
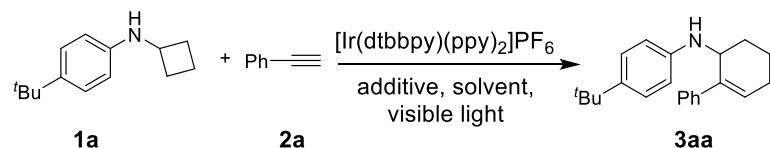


Chart 2.1 Photoredox catalysts.

Table 2.2.1 Optimization of [4+2] annulation



Entry ^[a]	Condition	t [h]	Conv. of 1 a [%] ^[b]	Yield of 3 a [%] ^[b]
1 ^[c]	4b (2mol%), CH ₃ NO ₂	16	11	9
2	4b (2mol%), CH ₃ NO ₂	16	40	30
3	4a (2 mol%), CH ₃ NO ₂	16	100	47
4	4a (2 mol%), DMF	16	90	86
5	4a (2 mol%), DMSO	16	100	90
6	4a (2 mol%), MeOH	12	100	97 (90) ^[d]
7	4a (2 mol%), Air, MeOH	16	100	42
8	4b (2mol%), MeOH	16	52	37
9	4c (2mol%), MeOH	16	82	60
10	4d (2mol%), MeOH	16	11	8
11	without 4a , MeOH	16	7	3
12	4a (2mol%), MeOH, light bulb off	16	10	7
13 ^[c]	4a (2 mol%), MeOH	16	29	27
14 ^[e]	4a (2 mol%), MeOH	12	70	68

[a] Reaction conditions: **1a** (0.2 mmol, 0.1 M in degassed solvent), **2a** (1mmol), irradiation with two 18 W LED lightbulb at room temperature.

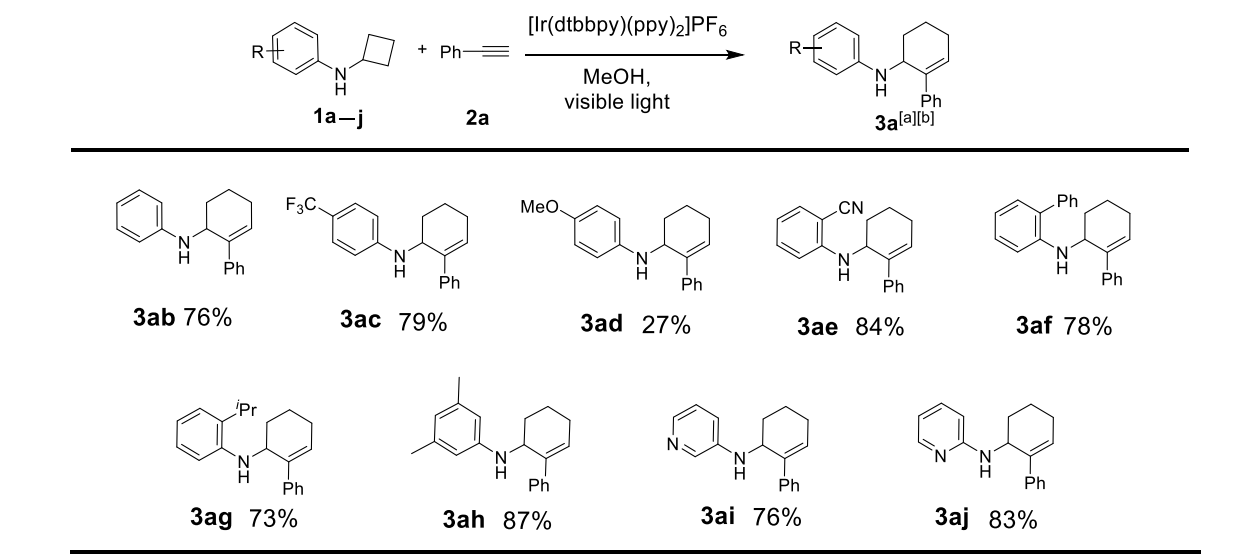
[b] Yields determined by GC analysis using dodecane as an internal standard unless noted. [c] One 18 W LED light. [d] Isolated yield by silica gel column chromatography. [e] One 18 W LED light, reaction tube in a 55 °C water bath.

2.2.2. Substrates Scope of Monocyclic and Bicyclic *N*-Cyclotbulanilines

We next examined the scope of cyclobutylaniline derivatives with phenylacetylene **2a** as the annulation partner under the optimized conditions (Table 2.2.2). Cyclobutylanilines were readily prepared by the Buchwald-Hartwig amination of cyclobutylamine with aryl halides.¹⁴

The annulation reaction generally tolerated both electron-withdrawing (e.g., CF₃ and CN) and electron-donating substituents (e.g., OMe, Ph, and alkyl) on the aryl ring. The low yield of **3ad** was due to the low solubility of **1d** in MeOH. Use of a cosolvent, such as DMF, helped solubilize **1d** but failed to improve the yield. Steric hindrance was also well tolerated as ortho substituents with various sizes (**1e-1g**) showed little effect on the reaction. Moreover, it is worth noting that heterocycles can be easily incorporated into the annulation products. The cyclobutylanilines (**1i** and **1j**) substituted by a pyridyl group at the 2- or 3- position underwent the annulation reaction uneventfully, affording the desired product (**3ai** and **3aj**) in good yields.

Table 2.2.2 Scope of [4+2] Annulation with Phenylacetylene.

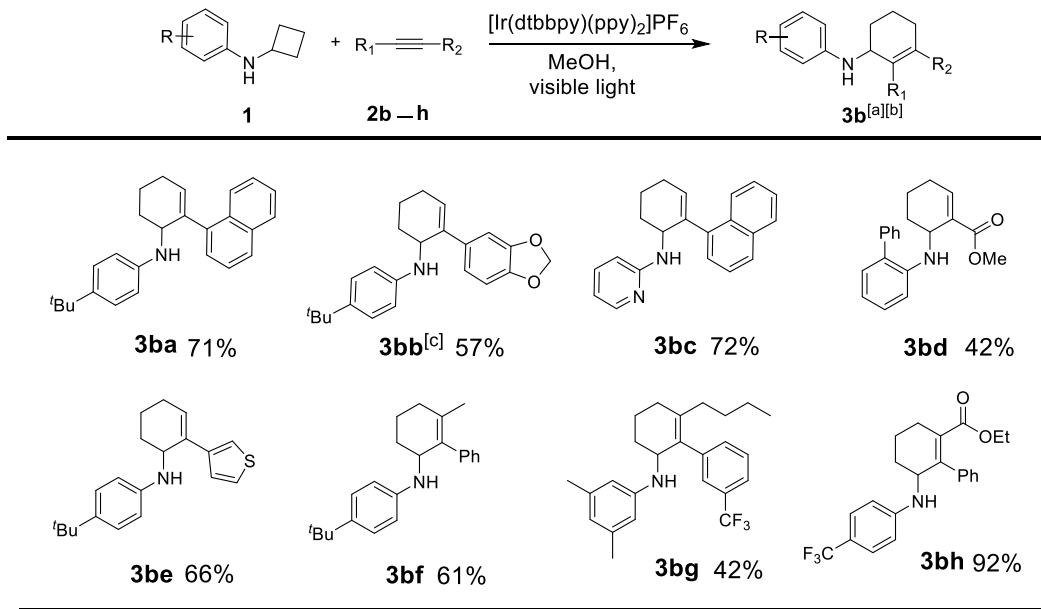


[a] Reaction condition: substrate (0.2 mmol, 0.1 M in degased MeOH), 2 a (1 mmol), 4 a (2 mol%), irradiation with two 18 W LED lightbulb. [b] Isolated yield by silica gel column chromatography.

Encouraged by the success in the initial scope studies, we turned our attention to the generality of alkynes (Table 2.2.3). The reactivity pattern displayed by alkynes in the annulation reaction generally resembles that in the intermolecular addition of non-polar nucleophilic alkyl

radicals to alkynes.¹⁵ Terminal alkynes substituted with a functional group, capable of stabilizing the incipient vinyl radical, were found to be viable annulation partners (*vide infra*). The functional group included a list of quite diverse groups such as naphthyl (**2b**), 1,3-benzodioxole (**2c**), methyl ester (**2d**), and thiophene (**2e**). The annulation of these alkynes with several cyclobutylanilines showed complete regioselectivity, affording a range of six-membered carbocycles in good yields. A notable side reaction occurred when less hindered cyclobutylanilines were used in conjunction with methyl propiolate **2d**. 1,4-Addition of cyclobutylaniline **1k** to **2d** completely suppressed the desired [4+2] annulation reaction.¹⁶ An ortho substituent on the *N*-aryl ring (e.g., **1f**) was needed to inhibit the side reaction. Typically, internal alkynes are less reactive than terminal alkynes in intermolecular addition of carbon radicals to alkynes due to steric hindrance.¹⁵ Internal alkynes were unsuccessful in the annulation with cyclopropylanilines.^{3b,3c} Surprisingly, divergent reactivity emerged between cyclopropylanilines and cyclobutylanilines with respect to this class of alkynes. Several internal alkynes (**2f-h**) successfully underwent the annulation reaction with cyclobutylanilines in complete regiocontrol. A limitation of utilizing internal alkynes is that at least one of the two substituents must be capable of stabilizing the vinyl radical. The regiochemistry of the annulation products (**3bf-bh**) were assigned based on 2D NMR spectroscopy. The annulation product (**3bh**) was further confirmed by X-ray crystallography.¹⁷ The regioselectivity can be rationalized based on the substituent's ability to stabilize the incipient vinyl radical.

Table 2.2.3 Scope of [4+2] Annulation with various Alkynes.

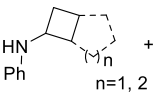
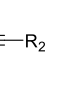
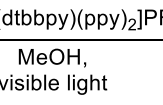
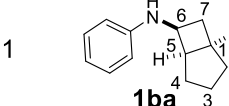
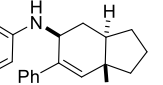
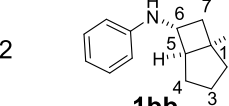
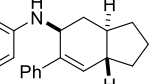
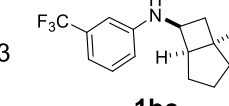
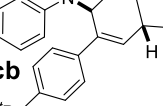
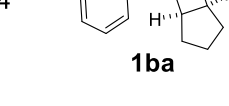
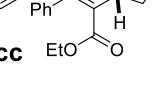
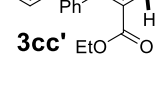
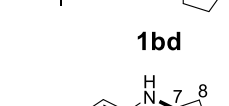
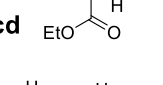
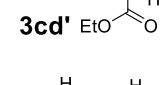
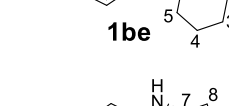
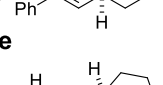
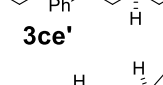
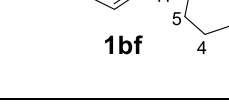
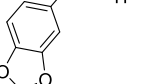
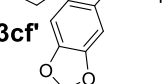


[a] Reaction condition: substrate (0.2 mmol, 0.1 M in degassed MeOH), 2b-2h (0.6 mmol), 4a (2 mol%), irradiation with two 18 W LED lightbulb. [b] Yield was measured after column chromatography. [c] Solvent mixture of MeOH and CH_3NO_2 (1:1)

Bicyclo[4.3.0]nonane (hydrindan) and bicyclo[4.4.0]decane (decalin) are two common structural motifs in small organic molecules. Yet, only a handful of methods such as the Diels-Alder reaction¹⁸ and the Robinson annulation¹⁹ are available for their preparation. Hence, these structures are ideal targets to test the scope of the [4+2] annulation reaction (Table 2.2.4). The requisite starting materials, *cis*-fused 5,4-membered (**1ba-bd**) and 6,4-membered (**1be** and **1bf**) bicycles, were readily accessible in four steps from commercially available cyclopentene and cyclohexene, respectively.^{20,21} Under the optimized conditions, a pair of diastereomeric 5-4 membered bicycles (**1ba** and **1bb**), which differ in the stereochemistry at C6, underwent the annulation with phenylacetylene **2a** to provide **3ca** as the major product in similar yields and almost identical drs (entries 1 and 2). High diastereoselectivity was achieved (>10:1) with **3ca**

being *trans*-fused. This data is consistent with regioselective ring opening of **1ba** or **1bb** at the C5-C6 bond, which leads to formation of the identical distonic radical iminium ion²² and subsequent loss of the stereochemical integrality of the C6 stereocenter. The observed regioselective ring opening was probably driven by the formation of a more stable secondary carbon radical versus a primary radical. Incorporation of a strong electron-withdrawing group (e.g., CF₃) (entry 3) into the *N*-aryl ring showed little effect on both the yield and diastereoselectivity. Internal alkyne **2h** successfully participated in the annulation reaction, affording the annulation products **3cc** and **3cc'** in excellent yield albeit lower diastereoselectivity when compared to terminal alkynes (entries 1-3). The annulation of 6,4-membered bicycles (**1be** and **1bf**) with terminal alkynes (**2a** and **2c**) furnished *cis*-fused decalin derivatives (**3ce**, **3ce'** and **3cf**, **3cf'**) in excellent yields, although a decrease in diastereoselectivity was observed in comparison to 5,4-membered bicycles (entries 6 and 7). Two *cis*-fused decalin derivatives were obtained along with a third diastereomer whose relative configuration was unidentified in both examples (**1be** and **1bf**).²³ The structure and stereochemistry of the annulation products were assigned by 2D NMR spectroscopy. X-ray crystallographic analysis of **3cd** was also obtained to further support our assignments.²⁴

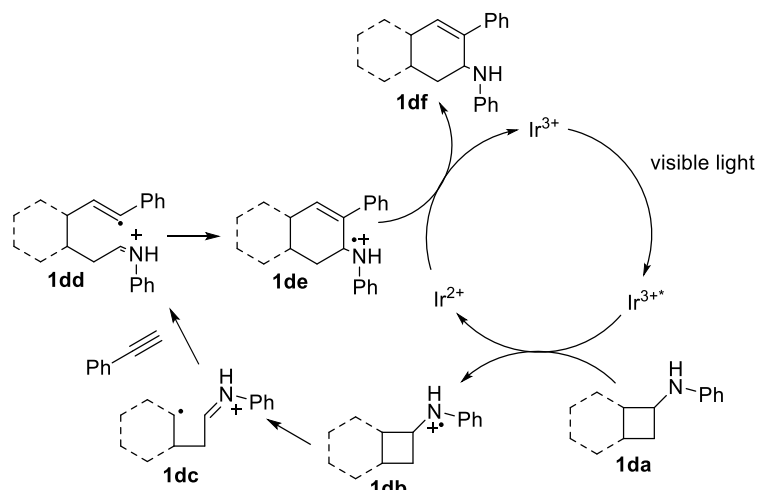
Table 2.2.4 [4+2] Annulation with Bicyclic Cyclobutylanilines.

Entry ^[a]	Substrate 	Alkyne 	Product		Yield[%] ^[b] d.r. ^[c]
			major 	minor n.a.	
1				n.a.	95 13:1
2				n.a.	97 11:1
3				n.a.	89 20:1
4					98 4:1
5					89 4:1
6					94 6:1
7					92 4:1

[a] Reaction condition: substrate (0.2 mmol, 0.1 M in degassed MeOH), 2a, 2c, 2h and 2i (0.6 mmol), 4a (2 mol%), irradiation with two 18 W LED lightbulb for 12 h. [b] Combined yields of the two isomers after column chromatography. [c] Determined by ¹H NMR analysis of the crude products.

2.2.3 Mechanism Study

A proposed catalytic cycle for the [4+2] annulation is shown in **Scheme 2.2**. Exposure of $[\text{Ir}(\text{dtbbpy})(\text{ppy})_2](\text{PF}_6)$ **4a** to two white LEDs produces the photoexcited $[\text{Ir}(\text{dtbbpy})(\text{ppy})_2]^{1+*}$, which is reductively quenched by cyclobutylaniline **1da** to generate $[\text{Ir}(\text{dtbbpy})(\text{ppy})_2]$ with the concomitant formation of amine radical cation **1db**. Subsequent ring opening generates distonic radical iminium ion **1dc**, which undergoes intermolecular addition to phenylacetylene **2a** to yield vinyl radical **1dd**. Intramolecular addition of the vinyl radical to the iminium ion in **1dd** closes the six-membered ring and produces amine radical cation **1de**. Finally, reduction of amine radical cation **1de** by $[\text{Ir}(\text{dtbbpy})(\text{ppy})_2]$ furnishes product **1df** and regenerates $[\text{Ir}(\text{dtbbpy})(\text{ppy})_2]^{1+}$, thus completing the catalytic cycle.



Scheme 2.2. Proposed Reaction Mechanism.

We have measured the oxidation peak potential of **1a** to be 0.8 V vs. SCE, which is more positive than the reduction potential of the photoexcited **4a** ($\text{Ir}^{3+*}/\text{Ir}^{2+}$: 0.66 V vs. SCE). Although thermodynamically unfavorable, such SET processes have been reported as long as

there is overlap between the substrate's oxidation (or reduction) peak potential and the redox potential of the photocatalyst's excited state. Furthermore, if the SET processes are subsequently coupled with an irreversible chemical reaction, they will more likely proceed to completion. In our case, presumably the irreversible C-C bond cleavage drives the unfavorable ET process to completion. Stern-Volmer quenching studies revealed that cyclobutylaniline **1a** quenches the photoexcited **3a** while alkynes **2a** and **2h** showed little quenching.

Cyclic Voltammograms of **1a** and **3a**

Cyclic voltammograms were recorded on a CH Instruments-Electrochemical Analyzer using a three-electrode cell at room temperature under an argon atmosphere. The reference electrode was a saturated calomel electrode (SCE), which was separated from the solution by a bridge compartment filled with the same supporting electrolyte solution used in the cell. A platinum disc (2.0 mm diameter) was used as the working electrode and a platinum wire as the auxiliary electrode. Tetrabutylammonium hexafluorophosphate (0.1 M in CH₃CN) was used as the supporting electrolyte. Voltammograms were taken in a solution of 4-*tert*-butyl-*N*-cyclobutylaniline (**1a**) in CH₃CN (c ~ 2.10-3 mol.L⁻¹). The peak potentials for the irreversible oxidation of **1a** and **3a** were measured as 0.8 V vs. SCE and 1.14 V vs. SCE respectively.

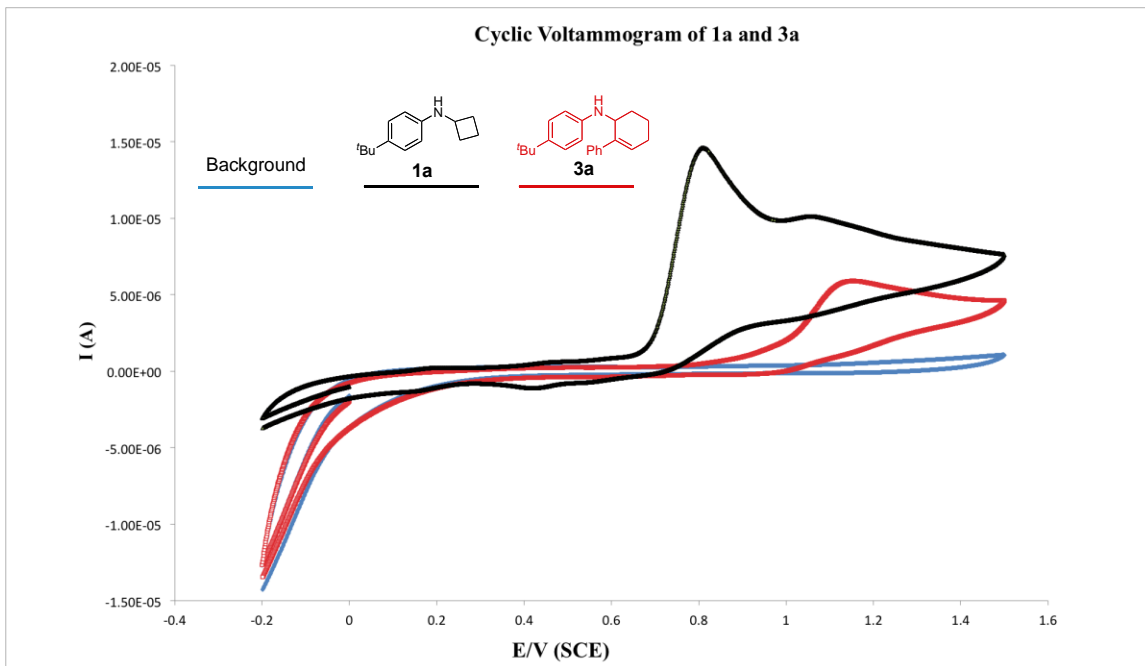


Chart 2.2 Cyclic Voltammograms of 1a and 3a.

Stern-Volmer Quenching study

Fluorescence quenching studies were conducted using a Photon Technology Fluorescence Spectrophotometer. In each experiment, a solution of 5.0×10^{-4} M $\text{Ir}(\text{ppy})_2(\text{dtbbpy})\text{PF}_6$ in MeOH was mixed with a MeOH solution of a quencher of various concentration in a screw-top 1.0 cm quartz cuvette. After degassing by sparging with argon for ten minutes, the resulting solution was irradiated at 460 nm, and fluorescence was measured at 575 nm. Plots were constructed according to the Stern-Volmer equation: $I_0/I = 1 + k_q\tau_0[Q]$.

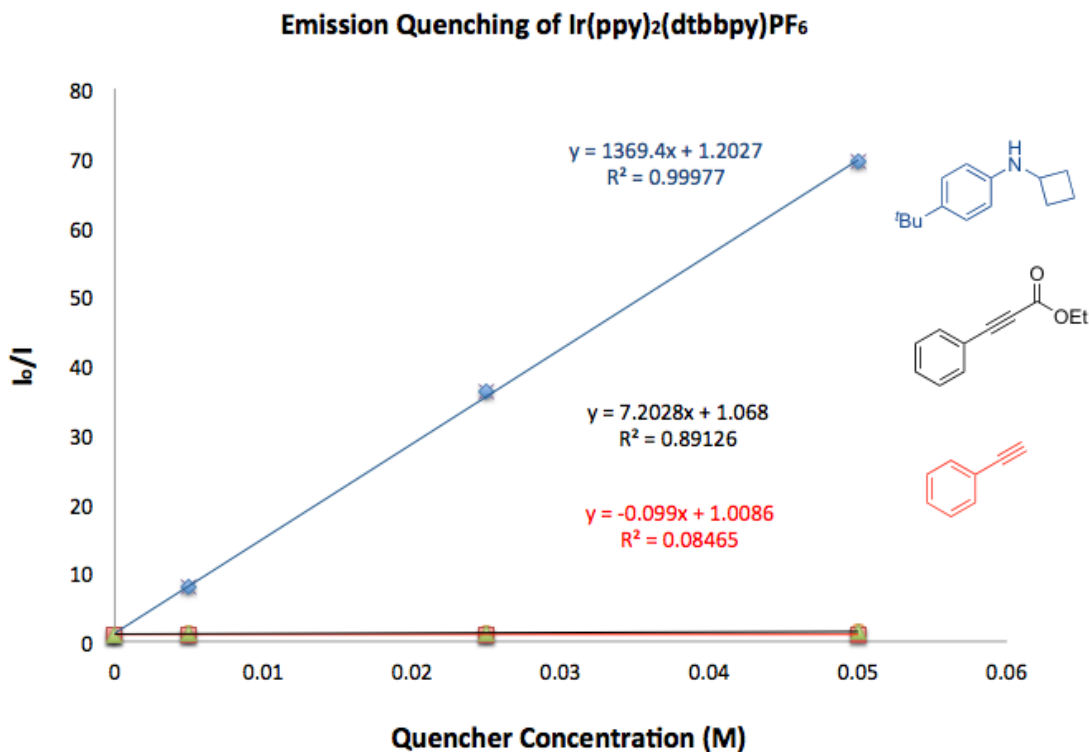


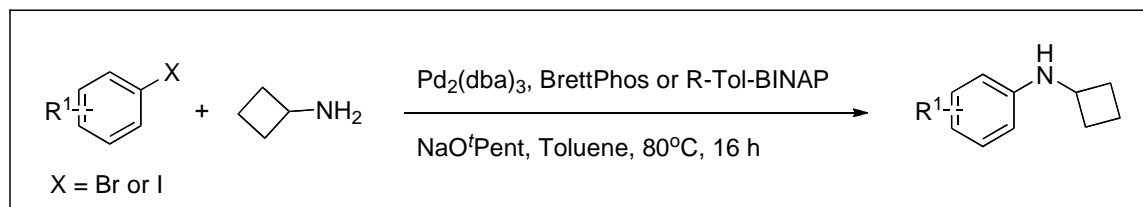
Chart 2.3 Fluorescence Quenching Studies.

2.2.4 Experimental Section

All reactions were carried out under a nitrogen atmosphere unless otherwise stated. Dry solvents were used as received except THF, CH_2Cl_2 , Et_2O , and toluene. They were rigorously purged with argon for 2 h and then further purified by passing through two packed columns of neutral alumina (for THF and Et_2O) or through neutral alumina and copper (II) oxide (for toluene and CH_2Cl_2) under argon from a solvent purification system. A standard workup protocol consisted of extraction with diethyl ether, washing with brine, drying over Na_2SO_4 , and removal of the solvent in vacuum. Column chromatography was carried out with silica gel (230-400 mesh). All new compounds were characterized by ^1H NMR, ^{13}C NMR, IR spectroscopy, high-resolution mass spectroscopy (HRMS), and melting point if solid. Nuclear magnetic resonance (NMR) spectra were obtained on a Bruker Avance DPX-300 and Bruker Avance DPX-400.

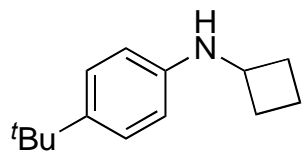
Chemical shifts (δ) were reported in parts per million (ppm) relative to residual proton signals in CDCl_3 (7.26 ppm, 77.23 ppm) or CD_2Cl_2 (5.32 ppm, 54 ppm) at room temperature. IR spectra were recorded (thin film on NaCl plates) on a PerkinElmer Spectrum 100 series instrument. High resolution mass spectra were recorded on a Bruker Ultraflex II TOF/TOF mass spectrometer. Gas chromatography/mass spectroscopy (GC/MS) analyses were performed on an Agilent 6890N Network GC System/5973 inert Mass Selective Detector. Gas chromatography analyses were performed using a Shimadzu GC-2010 Plus instrument. Melting points (m.p.) were recorded using Stuart SMP10 Melting Point Apparatus and were uncorrected.

General procedure 1 (GP1): Preparation of *N*-cyclobutylanilines



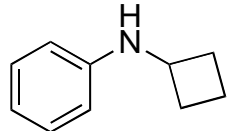
To an oven-dried schlenk tube equipped with a stir bar were added 0.02 mmol of $\text{Pd}_2(\text{dba})_3$ and 0.06 mmol of ligand ((R)-Tol-BINAP or BrettPhos). Glove box was used to add 3 mmol of NaO^tPent , followed by 2 mmol of aromatic halide, 2.2 mmol of cyclobutylamine, and 4 mL of toluene were then added to the reaction mixture and heated at 80°C for 16 h. After completion, the reaction mixture was cooled to room temperature, diluted with diethyl ether, filtered over a short pad of silica gel, and concentrated in vacuum. Purification by flash chromatography on silica gel afforded *N*-cyclobutylaniline.

4-*tert*-Butyl-*N*-cyclobutylaniline (1a). Following **GP1** with 4-*tert*-butyl-bromobenzene (0.87



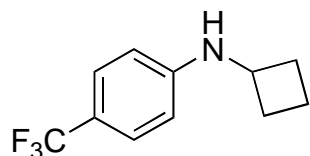
mL, 5 mmol) and BrettPhos (80.5 mg, 0.15 mmol, 3 mol%), the product was isolated after flash chromatography on silica gel (1: 30 EtOAc/hexanes) as yellow oil (1.01 g, 99%). IR ν_{max} (cm⁻¹) 3400, 3045, 2959, 2866, 1614, 1518, 1472, 1361, 1319, 1192, 820; ¹H NMR (400 MHz, Chloroform-*d*) δ 7.13 – 7.04 (m, 2H), 6.45 – 6.37 (m, 2H), 3.80 (tt, *J* = 8.1, 6.9 Hz, 1H), 3.61 (s, 1H), 2.36 – 2.23 (m, 2H), 1.79 – 1.60 (m, 4H), 1.17 (d, *J* = 0.7 Hz, 9H); ¹³C NMR (101 MHz, CDCl₃) δ 144.86, 140.04, 125.98, 112.67, 49.18, 33.83, 31.55, 31.37, 15.26; HRMS (ESI) m/z [M+H]⁺, calc'd for C₁₃H₁₉N 204.1747; found 204.1749.

***N*-cyclobutylaniline (1b).** Following **GP1** with iodobenzene (0.56 mL, 5



mmol) and BrettPhos (80.5 mg, 0.15 mmol, 3 mol%), the product was isolated after flash chromatography on silica gel (1: 50 EtOAc/hexanes) as colorless oil (570 mg, 78%). IR ν_{max} (cm⁻¹) 3400, 3050, 2934, 1603, 1504, 1315, 1270, 1167, 748; ¹H NMR (400 MHz, Chloroform-*d*) δ 7.13 – 7.05 (m, 2H), 6.63 (tt, *J* = 7.3, 1.1 Hz, 1H), 6.49 (dq, *J* = 7.5, 1.0 Hz, 2H), 3.91 – 3.72 (m, 2H), 2.43 – 2.24 (m, 2H), 1.84 – 1.62 (m, 4H); ¹³C NMR (101 MHz, CDCl₃) δ 147.19, 129.27, 117.40, 113.06, 49.04, 31.28, 15.30; HRMS (ESI) m/z [M+H]⁺, calc'd for C₁₀H₁₃N 148.1121; found 148.1126.

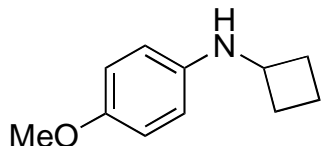
4-Trifluoromethyl-*N*-cyclobutylaniline (1c). **1c** is prepared according



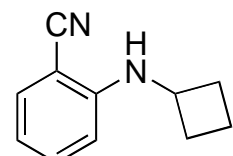
to Ma's procedure¹: An oven-dried schlenk tube was charged with CuI (48 mg, 0.25 mmol), K₂CO₃ (830 mg, 6 mmol), proline (69 mg, 0.6 mmol), cyclobutylamine (0.51 mL, 6 mmol), 4-iodobenzotrifluoride (0.74 mL, 5 mmol), DMSO (6 mL) and a stir bar. After purging with argon for a few seconds, the tube was sealed with a Teflon screw cap. The mixture was heated at 70 °C for 12 h. The reaction mixture was then

cooled to room temperature, quenched with brine and diluted with diethyl ether. The organic layer was separated and the aqueous layer was extracted with diethyl ether. The combined organic layers were dried over Na_2SO_4 , filtered, and concentrated under vacuum. Purification of the residual mass by silica gel flash chromatography (1:20 EtOAc/hexanes) afforded the product (1.01 g, 94%) as yellowish oil. IR ν_{max} (cm^{-1}) 3437, 3013, 2977, 2941, 1617, 1533, 1484, 1414, 1325, 1279, 1186, 1157, 1107, 1065, 825; ^1H NMR (400 MHz, Chloroform-*d*) δ 7.44 – 7.32 (m, 2H), 6.63 – 6.46 (m, 2H), 4.30 (s, 1H), 4.03 – 3.86 (m, 1H), 2.55 – 2.33 (m, 2H), 1.97 – 1.71 (m, 4H); ^{13}C NMR (101 MHz, CDCl_3) δ 149.61, 126.65, 125.26 (q, $J^1 = 270.3$ Hz), 118.86 (q, $J^2 = 32.5$ Hz), 111.99, 48.51, 30.99, 15.26; HRMS (ESI) m/z [M+H] $^+$, calc'd for $\text{C}_{11}\text{H}_{12}\text{F}_3\text{N}$ 216.0995; found 216.0986.

***N*-cyclobutyl-4-methoxyaniline (1d).** Following **GP1** with 1-bromo-

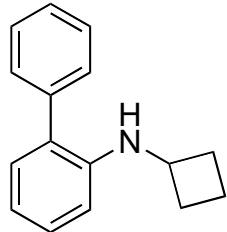


4-methoxybenzene (0.68 mL, 5 mmol) and BrettPhos (80.5 mg, 0.15 mmol, 3 mol%), the product was isolated after flash chromatography on silica gel (1: 20 EtOAc/hexanes) as brown oil (0.76 g, 86%). IR ν_{max} (cm^{-1}) 3375, 2935, 2831, 1511, 1464, 1235, 1037, 819; ^1H NMR (400 MHz, Chloroform-*d*) δ 6.71 – 6.66 (m, 2H), 6.48 – 6.43 (m, 2H), 3.81 – 3.73 (m, 1H), 3.66 (s, 3H), 2.37 – 2.26 (m, 2H), 1.77 – 1.63 (m, 4H); ^{13}C NMR (101 MHz, CDCl_3) δ 152.17, 141.34, 127.84, 114.90, 114.45, 55.81, 49.89, 31.28, 15.22; HRMS (ESI) m/z [M+H] $^+$, calc'd for $\text{C}_{11}\text{H}_{15}\text{NO}$ 178.1226; found 178.1221.

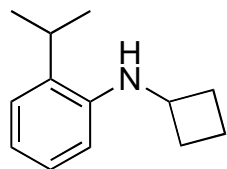


2-(cyclobutylamino)benzonitrile (1e). Following **GP1** with 2-bromobenzonitrile (0.364 g, 2 mmol) and (*R*)-Tol-BINAP (41 mg, 0.06 mmol, 3 mol%), the product was isolated after flash chromatography on silica gel (1:20 EtOAc/hexanes) as colorless oil (279 mg, 81%). IR ν_{max} (cm^{-1}) 3357, 2976, 2936, 2212, 1603, 1576, 1511, 1461, 1324, 1267, 1169, 749; ^1H NMR (400 MHz, Chloroform-*d*) δ 7.43 –

7.30 (m, 2H), 6.67 (dddd, $J = 7.8, 7.3, 1.0, 0.4$ Hz, 1H), 6.57 (ddt, $J = 8.4, 1.0, 0.5$ Hz, 1H), 3.97 (dq, $J = 7.9, 7.1$ Hz, 1H), 2.54 – 2.37 (m, 2H), 2.00 – 1.79 (m, 4H); ^{13}C NMR (101 MHz, CDCl_3) δ 149.23, 134.20, 132.75, 117.96, 116.49, 111.09, 95.48, 77.34, 48.33, 30.88, 15.28; HRMS (ESI) m/z [M+H] $^+$, calc'd for $\text{C}_{11}\text{H}_{12}\text{N}_2$ 173.1073; found 173.1077.



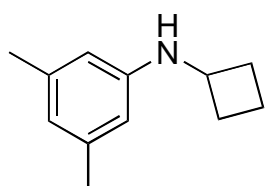
N-cyclobutyl-2-biphenylamine (1f). Following **GP1** with 2-bromobiphenyl (0.86 mL, 5 mmol) and (*R*)-Tol-BINAP (102 mg, 0.15 mmol, 3 mol%), the product was isolated after a flash chromatography on silica gel (1:30 EtOAc/hexanes) as colorless oil (1.01 g, 91%). IR ν_{max} (cm $^{-1}$) 3417, 3065, 2979, 2963, 2934, 2880, 1603, 1581, 1507, 1448, 1460, 1312, 1285, 1168, 747; ^1H NMR (400 MHz, Chloroform-*d*) δ 7.52 – 7.42 (m, 4H), 7.40 – 7.34 (m, 1H), 7.23 (ddd, $J = 8.1, 7.3, 1.7$ Hz, 1H), 7.10 (ddd, $J = 7.5, 1.6, 0.4$ Hz, 1H), 6.78 (td, $J = 7.4, 1.2$ Hz, 1H), 6.70 – 6.60 (m, 1H), 4.00 – 3.86 (m, 1H), 2.49 – 2.31 (m, 2H), 1.87 – 1.67 (m, 4H); ^{13}C NMR (75 MHz, CDCl_3) δ 144.16, 139.73, 130.47, 129.49, 129.08, 128.85, 127.61, 127.34, 117.18, 111.23, 49.18, 31.35, 15.44; HRMS (ESI) m/z [M+H] $^+$, calc'd for $\text{C}_{16}\text{H}_{17}\text{N}$ 224.1434; found 224.1444.



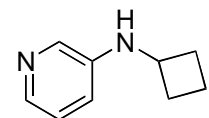
2-Isopropyl-N-cyclobutylaniline (1g). Following **GP1** with 1-bromo-2-isopropylbenzene (0.31 mL, 2 mmol) and (*R*)-Tol-BINAP (41 mg, 0.06 mmol, 3 mol%), the product was isolated after flash chromatography on silica gel (50:1 EtOAc/hexanes) as colorless oil (272 mg, 72%). IR ν_{max} (cm $^{-1}$) 3437, 3031, 2962, 2934, 2869, 1603, 1583, 1505, 1450, 1383, 1306, 1266, 1170, 1039, 743; ^1H NMR (400 MHz, Chloroform-*d*) δ 7.24 – 7.06 (m, 2H), 6.86 – 6.70 (m, 1H), 6.56 (d, $J = 8.1$ Hz, 1H), 4.11 – 3.93 (m, 1H), 3.83 (s, 1H), 2.89 (h, $J = 7.3, 6.8$ Hz, 1H), 2.62 – 2.38 (m, 2H), 1.99 – 1.74 (m, 4H), 1.34 – 1.24 (m, 6H); ^{13}C NMR (101 MHz, CDCl_3) δ 144.08, 132.27, 126.86,

125.13, 117.51, 111.36, 49.38, 31.63, 27.33, 22.56, 15.56; HRMS (ESI) m/z [M+H]⁺, calc'd for C₁₃H₁₉N 190.1590; found 190.1587.

3,5-Dimethyl-N-cyclobutylaniline (1h). Following **GP1** with 5-bromo-m-xylene (0.27 mL, 2

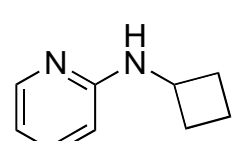


mmol) and BrettPhos (32.2 mg, 0.06 mmol, 3 mol%), the product was isolated after a flash chromatography on silica gel (1: 30 EtOAc/hexanes) as colorless oil (343 mg, 98%). IR ν_{max} (cm⁻¹) 3393, 3046, 2976, 2969, 2888, 1603, 1510, 1471, 1334, 1303, 1192, 821; ¹H NMR (300 MHz, Chloroform-*d*) δ 6.42 – 6.33 (m, 1H), 6.26 – 6.17 (m, 2H), 4.33 – 3.46 (m, 2H), 2.49 – 2.33 (m, 2H), 2.24 (s, 6H), 1.91 – 1.71 (m, 4H); ¹³C NMR (75 MHz, CDCl₃) δ 147.36, 139.09, 119.66, 111.23, 49.28, 31.54, 21.72, 15.45; HRMS (ESI) m/z [M+H]⁺, calc'd for C₁₂H₁₇N 176.1434; found 176.1426.



N-cyclobutyl-3-pyridinamine (1i). Following **GP1** with 3-bromopyridine (0.2 mL, 2 mmol) and BrettPhos (32.2 mg, 0.06 mmol, 3 mol%), the product was isolated after flash chromatography on silica gel (2:1 EtOAc/hexanes) as pale-yellow solid (238 mg, 80%). m.p. 51-52 °C; IR ν_{max} (cm⁻¹) 3266, 3093, 3037, 2976, 2936, 1587, 1519, 1482, 1415, 1313, 1246, 1161, 795; ¹H NMR (400 MHz, Chloroform-*d*) δ 8.15 – 7.84 (m, 2H), 7.06 (dd, *J* = 8.4, 4.5 Hz, 1H), 6.80 (dd, *J* = 8.1, 2.7 Hz, 1H), 3.90 (p, *J* = 7.9, 7.4 Hz, 2H), 2.44 (tdd, *J* = 9.0, 5.3, 2.2 Hz, 2H), 1.84 (pd, *J* = 7.2, 3.4 Hz, 4H); ¹³C NMR (101 MHz, CDCl₃) δ 143.39, 138.81, 136.21, 123.97, 118.99, 48.88, 31.19, 15.39; HRMS (ESI) m/z [M+H]⁺, calc'd for C₉H₁₂N₂ 149.1073; found 149.1061.

N-cyclobutyl-2-pyridinamine (1j). Following **GP1** with 2-bromopyridine (0.2 mL, 2 mmol)



and BrettPhos (32.2 mg, 0.06 mmol, 3 mol%), the product was isolated after flash chromatography on silica gel (2:1 EtOAc/hexanes) as pale-yellow solid (160 mg, 54%). m.p. 40-42 °C; IR ν_{max} (cm⁻¹) 3251, 3031, 3015, 2976, 2939,

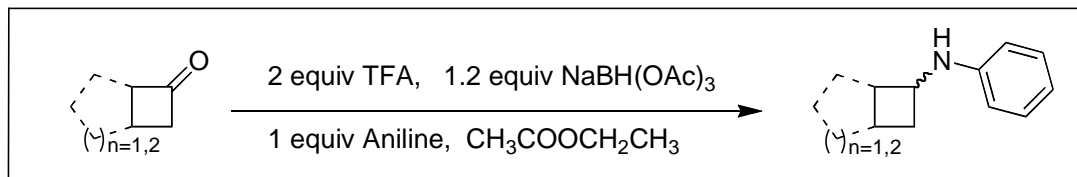
2854, 1609, 1573, 1446, 1336, 1291, 1155, 767; ^1H NMR (400 MHz, Chloroform-*d*) δ 8.06 (dt, *J* = 4.8, 1.4 Hz, 1H), 7.42 (ddd, *J* = 8.8, 7.2, 1.9 Hz, 1H), 6.56 (ddd, *J* = 7.1, 5.1, 1.0 Hz, 1H), 6.31 (d, *J* = 8.4 Hz, 1H), 4.83 (s, 1H), 4.12 (h, *J* = 7.5 Hz, 1H), 2.51 – 2.36 (m, 2H), 1.90 – 1.74 (m, 4H); ^{13}C NMR (101 MHz, CDCl_3) δ 158.02, 148.28, 137.81, 113.04, 106.51, 47.52, 31.50, 15.39; HRMS (ESI) m/z [M+H] $^+$, calc'd for $\text{C}_9\text{H}_{12}\text{N}_2$ 149.1073; found 149.1074.

N-cyclobutyl-4-fluoroaniline (1k). Following **GP1** with 1-bromo-4-fluorobenzene (0.22

mL, 2 mmol) and BrettPhos (32.2 mg, 0.06 mmol, 3 mol%), the product was isolated after flash chromatography on silica gel (1: 50 EtOAc/hexanes) as yellow oil (0.27 g, 83%). IR $\nu_{\text{max}}(\text{cm}^{-1})$ 3410, 2973, 2937, 1612, 1511, 1346, 1268, 1216, 1159, 820; ^1H NMR (400 MHz, Chloroform-*d*) δ 6.92 – 6.83 (m, 2H), 6.53 – 6.44 (m, 2H), 3.98 – 3.69 (m, 2H), 2.48 – 2.35 (m, 2H), 1.89 – 1.70 (m, 4H); ^{13}C NMR (101 MHz, CDCl_3) δ 156.06 (d, $^1J_{\text{CF}} = 234.7$ Hz), 143.65, 115.85 (d, $^2J_{\text{CF}} = 22.3$ Hz), 114.09 (d, $^3J_{\text{CF}} = 7.5$ Hz), 49.80, 31.34, 15.43; HRMS (ESI) m/z [M+H] $^+$, calc'd for $\text{C}_{10}\text{H}_{12}\text{FN}$ 166.1027; found 166.1020.

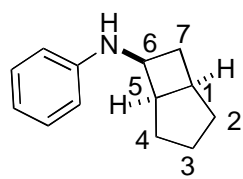
General procedure 2 (GP2): Synthesis of bicyclic cyclobutylaniline

Bicyclo[3.2.0]heptan-6-one and bicyclo[4.2.0]octan-7-one were prepared according to Mollet's procedure. Conversion of the bicyclic ketone to bicyclic cyclobutylaniline was accomplished via a reductive amination procedure developed by Davies.



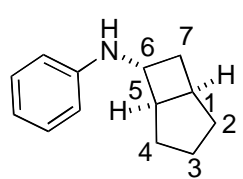
To a 25 mL round bottle flask equipped with a stir bar was added bicyclic ketone (3.6 mmol, 1.1 equiv.), aniline (3.27 mmol, 1 equiv.), trifluoroacetic acid (6.54 mmol, 2 equiv.) and ethyl acetate (6 mL). Sodium triacetoxyborohydride (3.9 mmol, 1.2 equiv.) was added to the mixture in one portion and the reaction temperature rose to 40 °C. The reaction mixture continued to stir for another 30 minutes, and was monitored by TLC. The reaction mixture was then added with 10% sodium hydroxide solution to adjust the pH to 8-9, followed by the extraction with diethyl ether. The organic layer was then washed with water and brine, dried over sodium sulfate and concentrate. Column chromatography was used to purify the crude product to yield the desired bicyclic cyclobutylaniline with a distereoselectivity of 1:1.

(1S,5S,6R)-N-phenylbicyclo[3.2.0]heptan-6-amine (1ba): Following **GP2** with



bicyclo[3.2.0]heptan-6-one (394 mg, 3.6 mmol), the product was isolated from two diastereomers (**1ba** and **1bb**, 1:1) after flash chromatography on silica gel (1: 30 EtOAc/hexanes) as a colorless oil (243 mg, 36%). IR ν_{max} (cm⁻¹) 3367, 2943, 2861, 1618, 1601, 1500, 1315, 749; ¹H NMR (400 MHz, Chloroform-*d*) δ 7.33 – 7.09 (m, 2H), 6.74 (q, *J* = 7.2, 6.7 Hz, 1H), 6.62 – 6.51 (m, 2H), 4.06 – 3.94 (m, 1H), 3.06 (qd, *J* = 7.9, 7.1, 2.5 Hz, 1H), 2.79 – 2.61 (m, 2H), 1.88 – 1.78 (m, 2H), 1.76 – 1.69 (m, 1H), 1.57 (dtd, *J* = 12.3, 6.0, 2.9 Hz, 2H), 1.45 (dddd, *J* = 12.4, 10.8, 6.0, 2.6 Hz, 1H), 1.38 – 1.29 (m, 1H); ¹³C NMR (101 MHz, CDCl₃) δ 129.23, 129.19, 117.18, 112.87, 46.45, 43.30, 33.77, 33.10, 33.07, 26.46, 25.97; HRMS (ESI) m/z [M+H]⁺, calc'd for C₁₃H₁₇N 188.1434; found 188.1439.

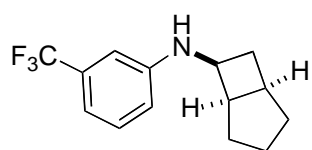
(1S,5S,6S)-N-phenylbicyclo[3.2.0]heptan-6-amine (1bb): Following **GP2** with



bicyclo[3.2.0]heptan-6-one (394 mg, 3.6 mmol), the product was isolated from two diastereomers (**6a** and **6b**, 1:1) after flash chromatography on silica gel (1: 30 EtOAc/hexanes) as a colorless oil (228 mg, 34%). IR ν_{max}

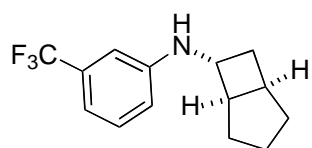
(cm⁻¹) 3398, 2942, 2852, 1602, 1503, 1314, 1269, 1177, 748; ¹H NMR (400 MHz, Methylene Chloride-*d*₂) δ 7.25 – 7.14 (m, 2H), 6.74 (tt, *J* = 7.3, 1.2 Hz, 1H), 6.58 – 6.48 (m, 2H), 3.41 (ddd, *J* = 7.0, 5.8, 3.6 Hz, 1H), 2.88 – 2.76 (m, 1H), 2.54 (td, *J* = 7.4, 3.6 Hz, 1H), 2.02 – 1.95 (m, 2H), 1.92 – 1.78 (m, 3H), 1.62 – 1.52 (m, 3H); ¹³C NMR (101 MHz, CDCl₃) δ 129.40, 117.67, 113.64, 113.63, 52.47, 46.72, 33.47, 33.39, 32.90, 32.31, 25.58; HRMS (ESI) m/z [M+H]⁺, calc'd for C₁₃H₁₇N 188.1434; found 188.1435.

(1S,5S,6R)-N-(4-iodophenyl)bicyclo[3.2.0]heptan-6-amine (1bc): Following **GP2** with



bicyclo[3.2.0]heptan-6-one (394 mg, 3.6 mmol) and 3-(trifluoromethyl)aniline (716 mg, 3.27 mmol), the product was isolated from two diastereomers (**1bc** and **1bc'**, 1:1) after flash chromatography on silica gel (1: 30 EtOAc/hexanes) as a colorless oil (287 mg, 28%). IR ν_{max} (cm⁻¹) 3401, 2941, 1590, 1491, 1314, 1179, 809; ¹H NMR (400 MHz, Methylene Chloride-*d*₂) δ 7.23 (t, *J* = 7.9 Hz, 1H), 6.88 (d, *J* = 7.7 Hz, 1H), 6.73 – 6.63 (m, 2H), 3.96 (q, *J* = 7.8, 7.2 Hz, 2H), 3.02 (q, *J* = 7.6 Hz, 1H), 2.74 – 2.56 (m, 2H), 1.75 (ddq, *J* = 24.1, 12.2, 5.8 Hz, 2H), 1.59 (dd, *J* = 13.6, 6.8 Hz, 1H), 1.53 – 1.46 (m, 2H), 1.43 – 1.37 (m, 1H), 1.36 – 1.24 (m, 1H); ¹³C NMR (101 MHz, CD₂Cl₂) δ 148.01, 131.71 (q, *J*² = 31.5 Hz), 129.57, 125.1 (q, *J*¹ = 272.2 Hz), 115.59, 112.94, 108.57, 46.13, 43.09, 33.83, 32.93, 32.71, 26.31, 25.83; HRMS (ESI) m/z [M+H]⁺, calc'd for C₁₃H₁₆IN 314.0400; found 314.0410.

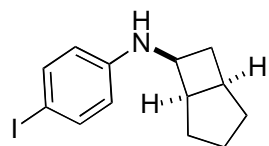
(1S,5S,6S)-N-(4-iodophenyl)bicyclo[3.2.0]heptan-6-amine (1bc'): Following **GP2 with**



bicyclo[3.2.0]heptan-6-one (394 mg, 3.6 mmol) and 3-(trifluoromethyl)aniline (716 mg, 3.27 mmol), the product was isolated from two diastereomers (**1bc** and **1bc'**, 1:1) after flash chromatography on silica gel (1: 30 EtOAc/hexanes) as a colorless oil (273 mg, 27%). IR ν_{max}

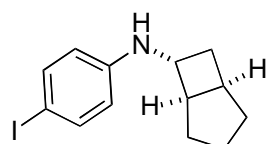
(cm⁻¹) 3369, 2930, 2857, 1589, 1490, 1179, 808; ¹H NMR (400 MHz, Methylene Chloride-*d*₂) δ 7.28 (t, *J* = 7.8 Hz, 1H), 6.97 – 6.90 (m, 1H), 6.75 – 6.63 (m, 2H), 4.29 – 4.15 (m, 1H), 3.41 (td, *J* = 5.9, 4.7, 2.5 Hz, 1H), 2.90 – 2.78 (m, 1H), 2.53 (td, *J* = 7.5, 3.6 Hz, 1H), 2.03 – 1.97 (m, 2H), 1.93 – 1.78 (m, 3H), 1.63 – 1.53 (m, 3H); ¹³C NMR (75 MHz, CD₂Cl₂) δ 147.58, 131.68 (q, *J*² = 31.4 Hz), 129.55, 125.08 (q, *J*¹ = 272.1 Hz), 116.19, 113.16, 109.03, 51.82, 46.47, 33.34, 32.86, 32.57, 31.99, 25.31; HRMS (ESI) m/z [M+H]⁺, calc'd for C₁₃H₁₆IN 314.0400; found 314.0399.

(1S,5S,6R)-N-(3-(trifluoromethyl)phenyl)bicyclo[3.2.0]heptan-6-amine (1bd):



amine (1bd): Following **GP2** with *bicyclo[3.2.0]heptan-6-one* (394 mg, 3.6 mmol) and *4-iodoaniline* (0.41 mL, 3.27 mmol), the product was isolated from two diastereomers (**1bd** and **1bd'**, 1:1) after flash chromatography on silica gel (1:50 EtOAc/hexanes) as a colorless oil (259 mg, 31%). IR ν_{max} (cm⁻¹) 3418, 2949, 2856, 1493, 1342, 1162, 1069, 767; ¹H NMR (400 MHz, Methylene Chloride-*d*₂) δ 7.46 – 7.31 (m, 2H), 6.38 – 6.24 (m, 2H), 3.95 – 3.82 (m, 1H), 2.98 (tdd, *J* = 8.6, 4.4, 1.6 Hz, 1H), 2.72 – 2.53 (m, 2H), 1.81 – 1.73 (m, 1H), 1.73 – 1.65 (m, 1H), 1.59 – 1.53 (m, 1H), 1.47 (ddd, *J* = 12.6, 6.3, 4.8 Hz, 2H), 1.41 – 1.33 (m, 1H), 1.31 – 1.24 (m, 1H); ¹³C NMR (101 MHz, CD₂Cl₂) δ 147.43, 137.61, 114.83, 76.89, 46.13, 43.16, 33.82, 32.96, 32.72, 26.34, 25.83; HRMS (ESI) m/z [M+H]⁺, calc'd for C₁₄H₁₆F₃N 256.1308; found 256.1313.

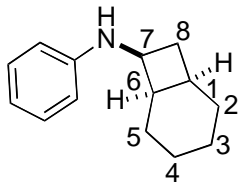
(1S,5S,6S)-N-(4-(trifluoromethyl)phenyl)bicyclo[3.2.0]heptan-6-amine (1bd'): Following



GP2 with *bicyclo[3.2.0]heptan-6-one* (394 mg, 3.6 mmol) and *4-iodoaniline* (0.41 mL, 3.27 mmol), the product was isolated from two diastereomers (**1bd** and **1bd'**, 1:1) after flash chromatography on silica gel (1:50 EtOAc/hexanes) as a colorless oil (218 mg, 26%). IR ν_{max} (cm⁻¹) 3421, 2947, 2856, 1616, 1515, 1342, 1123, 787; ¹H NMR (400 MHz, Methylene Chloride-*d*₂) δ 7.46 – 7.34 (m, 2H), 6.36

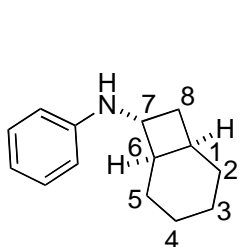
– 6.23 (m, 2H), 3.35 (td, J = 6.7, 3.6 Hz, 1H), 2.88 – 2.72 (m, 1H), 2.50 (td, J = 7.4, 3.6 Hz, 1H), 1.99 – 1.93 (m, 2H), 1.91 – 1.82 (m, 2H), 1.81 – 1.74 (m, 1H), 1.56 (tdd, J = 7.3, 5.0, 2.3 Hz, 3H); ^{13}C NMR (101 MHz, CD_2Cl_2) δ 147.00, 137.62, 115.32, 77.12, 51.85, 46.50, 33.35, 32.93, 32.58, 32.01, 25.29; HRMS (ESI) m/z [M+H] $^+$, calc'd for $\text{C}_{14}\text{H}_{16}\text{F}_3\text{N}$ 256.1308; found 256.1311.

(1S,6S,7R)-N-phenylbicyclo[4.2.0]octan-7-amine (1be): Following **GP2** with



bicyclo[4.2.0]octan-7-one (440 mg, 3.6 mmol), the product was isolated from two diastereomers (**1be** and **1bf**, 1:1) after flash chromatography on silica gel (1: 50 EtOAc/hexanes) as a colorless oil (217 mg, 33%). IR ν_{max} (cm^{-1}) 3382, 2928, 2858, 1602, 1499, 1314, 1176, 749; ^1H NMR (400 MHz, Chloroform-*d*) δ 7.13 – 7.06 (m, 2H), 6.60 (m, 1H), 6.56 – 6.52 (m, 2H), 4.00 – 3.83 (m, 1H), 3.74 (dt, J = 9.5, 6.7 Hz, 1H), 2.57 (dddd, J = 14.9, 12.0, 9.4, 6.4 Hz, 1H), 2.28 – 2.13 (m, 2H), 1.90 – 1.82 (m, 1H), 1.62 – 1.51 (m, 3H), 1.51 – 1.42 (m, 3H), 1.35 – 1.27 (m, 1H), 1.06 – 1.00 (m, 1H); ^{13}C NMR (101 MHz, CDCl_3) δ 148.47, 129.63, 117.27, 112.93, 48.48, 38.54, 31.25, 27.12, 26.44, 23.33, 22.45, 21.26; HRMS (ESI) m/z [M+H] $^+$, calc'd for $\text{C}_{14}\text{H}_{19}\text{N}$ 202.1590; found 202.1597.

(1S,6S,7S)-N-phenylbicyclo[4.2.0]octan-7-amine (1bf): Following **GP2** with



bicyclo[4.2.0]octan-7-one (440 mg, 3.6 mmol), the product was isolated from two diastereomers (**1be** and **1bf**, 1:1) after a flash chromatography on silica gel (1: 50 EtOAc/hexane) as a colorless oil (224 mg, 34%). IR ν_{max} (cm^{-1}) 3398, 2927, 2853, 1601, 1502, 1315, 1261, 748; ^1H NMR (400 MHz, Methylene Chloride-*d*₂) δ 7.14 – 6.99 (m, 2H), 6.60 (tt, J = 7.3, 1.1 Hz, 1H), 6.56 – 6.46 (m, 2H), 3.89 (q, J = 7.4 Hz, 1H), 2.19 – 2.08 (m, 2H), 2.06 – 2.00 (m, 1H), 1.93 – 1.84 (m, 1H), 1.70 – 1.51 (m, 4H), 1.43 (dddt, J = 15.5, 11.3, 6.6, 2.2 Hz, 2H), 1.35 – 1.23 (m, 1H), 1.15 – 1.03 (m,

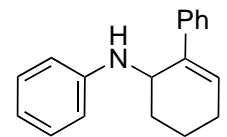
1H); ^{13}C NMR (101 MHz, CD_2Cl_2) δ 148.43, 129.68, 117.43, 113.26, 50.07, 42.81, 36.12, 30.42, 27.40, 25.9; HRMS (ESI) m/z [M+H] $^+$, calc'd for $\text{C}_{14}\text{H}_{19}\text{N}$ 202.1590; found 202.1593.

General Procedure 3 (GP3); Visible light catalyzed [4+2] annulation reaction

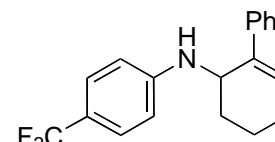
An oven-dried test tube equipped with a stir bar was charged with $\text{Ir}(\text{dtbbpy})(\text{ppy})_2\text{PF}_6$ (2 mol%) and cyclobutylaniline derivative (0.2 mmol), alkyne derivative (0.6 mmol) (phenylacetylene was used in 1 mmol scale), and MeOH (2 mL). The test tube was capped with a Teflon screw cap and followed by degassing using Freeze-Pump-Thaw sequence three times. The reaction mixture was then irradiated with two LED (18 watts) positioned 6 cm from the test tube. After the reaction was complete as monitored by TLC, the mixture was dilute with diethyl ether and filtered through a short pad of silica gel. The solution was concentrated and the residue was purified by silica gel flash chromatography to afford the corresponding annulation product.

4-tert-butyl-N-(2-phenylcyclohex-2-enyl)aniline (3a): Following GP3 with 1a (41 mg, 0.2 mmol) and phenylacetylene (2a) (0.12 mL, 1 mmol), the product was isolated after flash chromatography on silica gel (1: 30 EtOAc/hexanes) as brown oil (55 mg, 90%). IR ν_{max} (cm^{-1}) 3424, 3024, 2950, 2904, 2862, 1612, 1517, 1473, 1361, 1320, 1252, 1193, 818; ^1H NMR (400 MHz, Chloroform-d) δ 7.43 (d, J = 7.5 Hz, 2H), 7.30 – 7.22 (m, 2H), 7.22 – 7.17 (m, 3H), 6.61 (d, J = 8.2 Hz, 2H), 6.39 – 6.26 (m, 1H), 4.48 (d, J = 3.3 Hz, 1H), 2.38 – 2.10 (m, 3H), 1.65 (dd, J = 13.8, 10.0 Hz, 3H), 1.28 (s, 9H); ^{13}C NMR (75 MHz, CDCl_3) δ 144.51, 140.52, 139.90, 137.28, 129.07, 128.58, 127.13, 126.26, 125.73, 112.89, 48.41, 34.04, 31.77, 27.45, 26.20, 17.20; HRMS (ESI) m/z [M+H] $^+$, calc'd for $\text{C}_{22}\text{H}_{27}\text{N}$ 306.2216; found 306.2214.

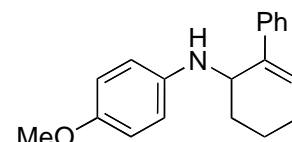
N-(2-phenylcyclohex-2-enyl)aniline (3ab): Following GP3 with 1b (30 mg, 0.2 mmol) and

 phenylacetylene (2a) (0.12 mL, 1 mmol), the product was isolated after flash chromatography on silica gel (1: 50 EtOAc/hexanes) as yellow oil (37 mg, 76%). IR ν_{max} (cm⁻¹) 3400, 3020, 2927, 2864, 1598, 1500, 1424, 1310, 1251, 1161, 750; ¹H NMR (400 MHz, Chloroform-d) δ 7.50 – 7.44 (m, 2H), 7.34 – 7.26 (m, 2H), 7.26 – 7.17 (m, 3H), 6.71 (tq, J = 7.3, 0.9 Hz, 1H), 6.68 – 6.61 (m, 2H), 6.38 (dd, J = 5.0, 3.0 Hz, 1H), 4.51 (d, J = 2.5 Hz, 1H), 3.84 (d, J = 20.8 Hz, 1H), 2.53 – 2.14 (m, 3H), 1.88 – 1.62 (m, 3H); ¹³C NMR (101 MHz, CDCl₃) δ 147.03, 140.20, 137.05, 129.35, 128.81, 128.44, 127.02, 125.47, 116.92, 112.84, 48.01, 27.46, 26.01, 17.09; HRMS (ESI) m/z [M+H]⁺, calc'd for C₁₉H₂₁N 250.1590; found 250.1594.

N-(2-phenylcyclohex-2-enyl)-4-(trifluoromethyl)aniline (3ac): Following GP3 with 1c (43 mg,

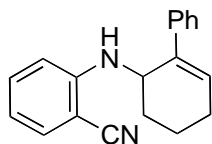
 0.2 mmol) and phenylacetylene (2a) (0.12 mL, 1 mmol), the product was isolated after flash chromatography on silica gel (1: 20 EtOAc/hexanes) as yellow solid (50 mg, 79%). m.p. 75-77 °C; IR ν_{max} (cm⁻¹) 3414, 3047, 2933, 2873, 1614, 1528, 1485, 1322, 1259, 1109, 1058, 823; ¹H NMR (400 MHz, Benzene-d₆) δ 7.35 – 7.27 (m, 4H), 7.15 – 7.09 (m, 2H), 7.09 – 7.03 (m, 1H), 6.12 (ddd, J = 4.8, 2.3, 1.5 Hz, 1H), 6.03 (d, J = 8.5 Hz, 2H), 4.22 – 4.12 (m, 1H), 3.56 (d, J = 7.3 Hz, 1H), 2.04 – 1.70 (m, 3H), 1.42 – 1.29 (m, 3H); ¹³C NMR (101 MHz, C₆D₆) δ 149.97, 140.42, 136.99, 129.25, 129.14, 127.89, 127.36 (q, J^3 = 3.8 Hz), 126.38 (q, J^1 = 270.1 Hz), 125.94, 119.03 (q, J^2 = 32.4 Hz), 112.47, 48.06, 27.85, 26.41, 17.59; HRMS (ESI) m/z [M+H]⁺, calc'd for C₁₉H₁₈F₃N 318.1464; found 318.1464.

4-methoxy-N-(2-phenylcyclohex-2-enyl)aniline (3ad): Following GP3 with 1d (36 mg, 0.2

 mmol) and phenylacetylene (2a) (0.12 mL, 1 mmol), the product was

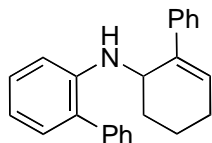
isolated after a flash chromatography on silica gel (1: 50 EtOAc/hexanes) as brown oil (16 mg, 28%). IR ν_{max} (cm⁻¹) 3405, 3026, 2931, 2859, 2830, 1608, 1510, 1442, 1402, 1237, 1174, 1036, 818; ¹H NMR (300 MHz, Chloroform-d) δ 7.55 – 7.41 (m, 2H), 7.34 – 7.20 (m, 3H), 6.88 – 6.74 (m, 2H), 6.69 – 6.56 (m, 2H), 6.41 – 6.28 (m, 1H), 4.48 – 4.35 (m, 1H), 3.76 (s, 3H), 2.41 – 2.06 (m, 3H), 1.69 (dd, J = 3.5, 1.7 Hz, 3H); ¹³C NMR (75 MHz, CDCl₃) δ 151.88, 141.14, 140.31, 137.20, 128.73, 128.41, 126.97, 125.51, 114.98, 114.34, 55.85, 49.12, 27.45, 26.01, 17.01; HRMS (ESI) m/z [M+H]⁺, calc'd for C₁₉H₂₁NO 280.1696; found 280.1701.

2-(2-phenylcyclohex-2-enylamino)benzonitrile (3ae): Following GP3 with 1e (35 mg, 0.2



mmol) and phenylacetylene (2a) (0.12 mL, 1 mmol), the product was isolated after a flash chromatography on silica gel (1: 20 EtOAc/hexanes) as brown oil (46 mg, 84%). IR ν_{max} (cm⁻¹) 3420, 3024, 2932, 2867, 2832, 2209, 1602, 1574, 1505, 1449, 1442, 1318, 1284, 1165, 1070, 751; ¹H NMR (400 MHz, Chloroform-d) δ 7.69 – 7.35 (m, 5H), 7.35 – 7.23 (m, 2H), 6.85 (d, J = 8.5 Hz, 1H), 6.68 (t, J = 7.5 Hz, 1H), 6.38 (dd, J = 4.9, 2.9 Hz, 1H), 4.63 (d, J = 21.9 Hz, 2H), 2.47 – 2.01 (m, 3H), 1.90 – 1.52 (m, 3H); ¹³C NMR (75 MHz, CDCl₃) δ 149.12, 139.94, 136.12, 134.27, 133.09, 129.99, 128.50, 127.25, 125.50, 117.77, 116.37, 110.79, 96.07, 48.09, 27.56, 25.79, 16.93. HRMS (ESI) m/z [M+H]⁺, calc'd for C₁₉H₁₈N₂ 275.1543; found 275.1524.

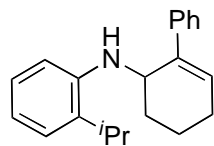
N-(2-phenylcyclohex-2-enyl)biphenyl-2-amine (3af): Following GP3 with 1f (45 mg, 0.2



mmol) and phenylacetylene (2a) (0.12 mL, 1 mmol), the product was isolated after a flash chromatography on silica gel (1: 50 EtOAc/hexanes) as white solid (54 mg, 83%). m.p. 125-128 °C; IR ν_{max} (cm⁻¹) 3419, 3053, 2921, 1595, 1504, 1486, 1434, 1310, 1282, 760; ¹H NMR (300 MHz, Chloroform-d) δ 7.36 – 7.21 (m, 9H), 7.09 – 6.97 (m, 3H), 6.88 (d, J = 8.2 Hz, 1H), 6.75 (t, J = 7.3 Hz, 1H), 6.17 (t, J = 3.9 Hz, 1H), 4.49 (t, J = 3.4 Hz,

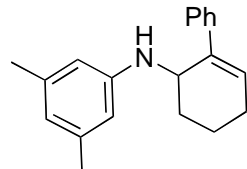
1H), 2.12 (ddd, $J = 14.1, 5.8, 2.8$ Hz, 3H), 1.82 – 1.42 (m, 3H); ^{13}C NMR (75 MHz, CDCl_3) δ 143.74, 140.67, 139.26, 137.41, 130.50, 129.14, 129.02, 128.78, 128.69, 128.39, 127.87, 127.00, 126.92, 125.94, 116.73, 110.47, 49.09, 28.06, 25.87, 17.44; HRMS (ESI) m/z [M+H] $^+$, calc'd for $\text{C}_{24}\text{H}_{23}\text{N}$ 326.1903; found 326.1907.

2-isopropyl-N-(2-phenylcyclohex-2-enyl)aniline (3ag): Following GP3 with 1g (38 mg, 0.2



mmol) and phenylacetylene (2a) (0.12 mL, 1 mmol), the product was isolated after a flash chromatography on silica gel (1: 30 EtOAc/hexanes) as yellow oil (44 mg, 76%). IR ν_{max} (cm $^{-1}$) 3441, 3029, 2958, 2932, 2865, 1602, 1582, 1503, 1448, 1358, 1306, 1253, 757; ^1H NMR (400 MHz, Chloroform-d) δ 7.47 – 7.42 (m, 2H), 7.30 – 7.24 (m, 2H), 7.23 – 7.18 (m, 1H), 7.18 – 7.11 (m, 2H), 6.82 (dt, $J = 8.0, 0.9$ Hz, 1H), 6.74 (td, $J = 7.5, 1.2$ Hz, 1H), 6.41 – 6.35 (m, 1H), 4.55 (d, $J = 3.7$ Hz, 1H), 2.66 (hept, $J = 6.8$ Hz, 1H), 2.40 – 2.15 (m, 3H), 1.79 – 1.67 (m, 3H), 1.22 (d, $J = 6.8$ Hz, 3H), 0.97 (d, $J = 6.8$ Hz, 3H); ^{13}C NMR (101 MHz, CDCl_3) δ 143.61, 140.28, 137.34, 131.96, 128.81, 128.42, 127.01, 126.75, 125.54, 125.10, 116.72, 110.03, 48.22, 27.57, 27.11, 26.06, 22.15, 17.39; HRMS (ESI) m/z [M+H] $^+$, calc'd for $\text{C}_{21}\text{H}_{25}\text{N}$ 292.2060; found 292.2065.

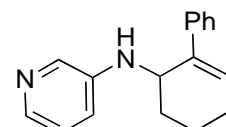
3,5-dimethyl-N-(2-phenylcyclohex-2-enyl)aniline (3ah): Following GP3 with **1h** (35 mg, 0.2



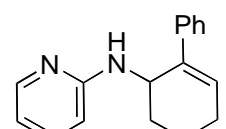
mmol) and phenylacetylene (2a) (0.12 mL, 1 mmol), the product was isolated after a flash chromatography on silica gel (1: 50 EtOAc/hexanes) as yellow oil (46 mg, 87%). IR ν_{max} (cm $^{-1}$) 3417, 3031, 2935, 2860, 1598, 1507, 1496, 1443, 1339, 1189, 819; ^1H NMR (400 MHz, Chloroform-d) δ 7.53 – 7.40 (m, 2H), 7.34 – 7.26 (m, 2H), 7.24 – 7.17 (m, 1H), 6.42 – 6.32 (m, 2H), 6.29 (s, 2H), 4.49 (t, $J = 3.0$ Hz, 1H), 2.43 – 2.09 (m, 9H), 1.81 – 1.57 (m, 3H); ^{13}C NMR (75 MHz, CDCl_3) δ

147.11, 140.42, 139.16, 137.23, 128.90, 128.59, 127.13, 125.63, 119.15, 110.92, 48.02, 27.61, 26.19, 21.75, 17.22; HRMS (ESI) m/z [M+H]⁺, calc'd for C₂₀H₂₃N 278.1903; found 278.1905.

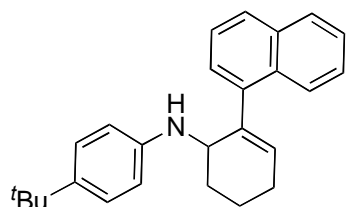
N-(2-phenylcyclohex-2-enyl)pyridin-3-amine (3ai): Following GP3 with **1i** (30 mg, 0.2 mmol)

 and phenylacetylene (**2a**) (0.12 mL, 1 mmol), the product was isolated after a flash chromatography on silica gel (1: 5 EtOAc/hexanes) as yellow solid (37 mg, 73%). m.p. 132-134 °C; IR ν_{max} (cm⁻¹) 3255, 3086, 3028, 2927, 2859, 2213, 1580, 1506, 1481, 1415, 1318, 1296, 786; ¹H NMR (400 MHz, Chloroform-d) δ 8.08 (d, J = 2.7 Hz, 1H), 7.88 (d, J = 5.0 Hz, 1H), 7.40 – 7.33 (m, 2H), 7.31 – 7.26 (m, 2H), 7.25 – 7.19 (m, 2H), 7.13 – 7.04 (m, 1H), 6.35 (dd, J = 5.0, 3.0 Hz, 1H), 4.47 (d, J = 10.0 Hz, 2H), 2.40 – 2.16 (m, 2H), 2.12 – 2.01 (m, 1H), 1.83 – 1.63 (m, 3H); ¹³C NMR (101 MHz, CDCl₃) δ 143.40, 140.08, 137.86, 136.77, 135.55, 129.59, 128.68, 127.40, 125.63, 124.16, 119.10, 48.10, 27.55, 26.08, 17.26; HRMS (ESI) m/z [M+H]⁺, calc'd for C₁₇H₁₈N₂ 251.1543; found 251.1542.

N-(2-phenylcyclohex-2-enyl)pyridin-2-amine (3aj): Following GP3 with **1j** (30 mg, 0.2 mmol)

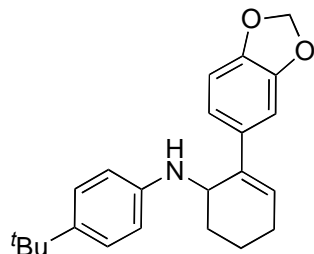
 and phenylacetylene (**2a**) (0.12 mL, 1 mmol), the product was isolated after a flash chromatography on silica gel (1: 5 EtOAc/hexanes) as yellow solid (39 mg, 78%). m.p. 83-84 °C; IR ν_{max} (cm⁻¹) 3425, 3020, 2931, 1600, 1570, 1484, 1442, 755; ¹H NMR (400 MHz, Chloroform-d) δ 8.00 (ddt, J = 5.1, 1.8, 0.8 Hz, 1H), 7.33 (ddt, J = 7.0, 1.3, 0.7 Hz, 2H), 7.30 – 7.23 (m, 1H), 7.21 – 7.14 (m, 2H), 7.13 – 7.05 (m, 1H), 6.44 (ddt, J = 7.0, 5.1, 0.9 Hz, 1H), 6.29 – 6.20 (m, 2H), 4.88 – 4.80 (m, 1H), 4.54 (d, J = 8.0 Hz, 1H), 2.27 – 2.07 (m, 2H), 2.07 – 1.97 (m, 1H), 1.76 – 1.67 (m, 1H), 1.63 (ttd, J = 10.6, 6.1, 5.3, 3.4 Hz, 2H); ¹³C NMR (101 MHz, CDCl₃) δ 157.51, 147.93, 140.12, 137.34, 137.13, 129.16, 128.37, 127.01, 125.61, 112.48, 107.56, 46.35, 28.55, 26.02, 17.44. HRMS (ESI) m/z [M+H]⁺, calc'd for C₁₇H₁₈N₂ 251.1543; found 251.1542. FTMS (ESI) m/z [M+H]⁺, calc'd for C₁₇H₁₈N₂ 251.1543; found 251.1542.

4-tert-butyl-N-(2-(naphthalen-1-yl)cyclohex-2-enyl)aniline (3ba): Following GP3 with **1a** (41



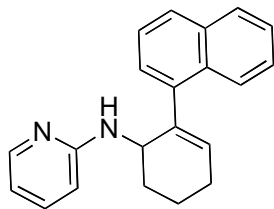
mg, 0.2 mmol) and 1-ethynylnaphthalene (**2b**) (91 mg, 0.6 mmol), the product was isolated after a flash chromatography on silica gel (1: 30 EtOAc/hexanes) as yellow oil (50, 71%). IR ν_{max} (cm⁻¹) 3395, 3043, 2926, 1603, 1514, 1463, 1391, 1296, 1248, 1191, 816, 774; ¹H NMR (400 MHz, Benzene-d₆) δ 8.16 (d, *J* = 8.4 Hz, 1H), 7.64 (d, *J* = 8.1 Hz, 1H), 7.52 (dd, *J* = 8.3, 1.3 Hz, 1H), 7.37 (ddt, *J* = 8.3, 6.8, 1.2 Hz, 1H), 7.34 – 7.24 (m, 2H), 7.20 (ddd, *J* = 8.1, 6.9, 1.0 Hz, 1H), 7.05 – 6.94 (m, 2H), 6.33 – 6.23 (m, 2H), 5.80 (t, *J* = 3.9 Hz, 1H), 4.37 (d, *J* = 4.4 Hz, 1H), 3.54 (s, 1H), 2.11 – 1.89 (m, 3H), 1.78 – 1.58 (m, 2H), 1.46 (ddt, *J* = 12.7, 6.1, 3.2 Hz, 1H), 1.21 (d, *J* = 1.0 Hz, 9H); ¹³C NMR (101 MHz, C₆D₆) δ 145.00, 140.43, 139.40, 138.12, 134.15, 132.39, 131.27, 128.62, 127.29, 125.76, 125.71, 125.45, 125.38, 125.22, 113.08, 51.74, 33.47, 31.40, 28.08, 25.43, 17.32; HRMS (ESI) m/z [M+H]⁺, calc'd for C₂₆H₂₉N 356.2373; found 356.2369.

N-(2-(benzo[d][1,3]dioxol-5-yl)cyclohex-2-enyl)-4-tert-butylaniline (3bb): Following GP3



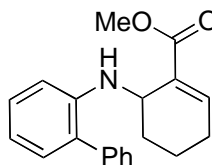
with **1a** (41 mg, 0.2 mmol) and 5-ethynylbenzo[d][1,3]dioxole (**2c**) (88 mg, 0.6 mmol), the product was isolated after a flash chromatography on silica gel (1: 30 EtOAc/hexanes) as brown oil (40 mg, 57%). IR ν_{max} (cm⁻¹) 3406, 2926, 2857, 1724, 1610, 1516, 1238, 1037, 801; ¹H NMR (400 MHz, Chloroform-d) δ 7.24 – 7.18 (m, 2H), 6.97 (d, *J* = 1.8 Hz, 1H), 6.93 (dd, *J* = 8.1, 1.9 Hz, 1H), 6.72 (d, *J* = 8.2 Hz, 1H), 6.62 – 6.55 (m, 2H), 6.19 (dd, *J* = 4.9, 3.0 Hz, 1H), 5.92 (q, *J* = 1.5 Hz, 2H), 4.43 – 4.32 (m, 1H), 2.31 – 2.12 (m, 3H), 1.65 (tdd, *J* = 13.1, 6.4, 3.2 Hz, 3H), 1.29 (s, 9H); ¹³C NMR (75 MHz, CDCl₃) δ 147.89, 146.77, 144.73, 139.78, 137.16, 135.26, 128.04, 126.28, 119.31, 112.71, 108.32, 106.47, 101.10, 48.53, 34.04, 31.79, 27.44, 26.15, 17.16; HRMS (ESI) m/z [M+H]⁺, calc'd for C₂₃H₂₇NO₂ 350.2115; found 350.2121.

N-(2-(naphthalen-1-yl)cyclohex-2-enyl)pyridin-2-amine (3bc): Following GP3 of the



annulation with **1j** (30 mg, 0.2 mmol) and 1-ethynynlnaphthalene (**2b**) (91 mg, 0.6 mmol), the product was isolated after a flash chromatography on silica gel (1: 5 EtOAc/hexanes) as yellow solid (43 mg, 72%). m.p. 99–102 °C; IR ν_{max} (cm⁻¹) 3289, 3026, 2862, 2852, 1596, 1569, 1484, 1442, 1394, 1326, 1282, 799; ¹H NMR (400 MHz, Chloroform-d) δ 8.05 (dd, J = 7.9, 1.8 Hz, 1H), 7.95 (dd, J = 4.8, 2.1 Hz, 1H), 7.84 (dd, J = 7.7, 1.9 Hz, 1H), 7.77 – 7.70 (m, 1H), 7.57 – 7.44 (m, 2H), 7.43 – 7.32 (m, 2H), 7.21 (ddd, J = 8.7, 7.1, 1.9 Hz, 1H), 6.42 (dd, J = 7.1, 5.0 Hz, 1H), 6.13 (d, J = 8.4 Hz, 1H), 6.01 (dd, J = 4.5, 3.0 Hz, 1H), 4.72 (s, 2H), 2.44 – 2.25 (m, 2H), 2.21 – 2.02 (m, 2H), 1.97 – 1.81 (m, 2H); ¹³C NMR (101 MHz, CD₂Cl₂) δ 157.82, 147.81, 140.23, 137.56, 136.87, 133.75, 132.13, 132.01, 128.29, 127.12, 125.85, 125.83, 125.55, 125.40, 125.16, 112.33, 106.92, 49.66, 28.85, 25.62, 17.80; HRMS (ESI) m/z [M+H]⁺, calc'd for C₂₁H₂₀N₂ 301.1700; found 301.1702.

Methyl 6-(biphenyl-2-ylamino)cyclohex-1-enecarboxylate (3bd): Following GP3 with **1f** (45



mg, 0.2 mmol) and methyl propiolate (**2d**) (51 mg, 0.6 mmol), the product was isolated after a flash chromatography on silica gel (1: 10 EtOAc/hexanes) as colorless oil (26 mg, 42%). IR ν_{max} (cm⁻¹) 3435, 3046, 2934, 2858, 1715, 1646, 1600, 1506, 1489, 1436, 1244, 1060, 753; ¹H NMR (400 MHz, Chloroform-d) δ 7.50 – 7.32 (m, 5H), 7.32 – 7.24 (m, 1H), 7.08 (ddd, J = 12.5, 6.2, 2.2 Hz, 2H), 6.98 (d, J = 8.1 Hz, 1H), 6.80 (td, J = 7.4, 1.2 Hz, 1H), 4.52 (d, J = 4.0 Hz, 1H), 3.74 (s, 3H), 2.31 – 2.18 (m, 1H), 2.18 – 2.04 (m, 2H), 1.69 – 1.56 (m, 1H), 1.45 (ddddd, J = 31.3, 13.4, 10.9, 4.8, 2.7 Hz, 2H); ¹³C NMR (75 MHz, CDCl₃) δ 167.45, 144.11, 143.22, 139.74, 131.12, 130.58, 129.47, 129.06, 128.89, 128.54, 127.33, 117.40, 112.01, 51.98, 46.36, 27.18, 25.87, 16.46; HRMS (ESI) m/z [M+H]⁺, calc'd for C₂₀H₂₁NO₂ 308.1645; found 308.1641.

4-tert-butyl-N-(2-(thiophen-3-yl)cyclohex-2-enyl)aniline (3be): Following GP3 with **1a** (41

mg, 0.2 mmol) and 3-ethynylthiophene (**2e**) (65 mg, 0.6 mmol), the product was isolated after a flash chromatography on silica gel (1: 30 EtOAc/hexanes) as yellow oil (41 mg, 66%). IR ν_{max} (cm⁻¹) 3424, 3026, 2946, 2934, 2860, 1611, 1516, 1360, 1299, 1252, 1193, 818; ¹H NMR (400 MHz, Chloroform-d) δ 7.17 – 7.11 (m, 4H), 7.09 (qd, J = 2.8, 1.2 Hz, 1H), 6.57 – 6.43 (m, 2H), 6.27 (ddd, J = 4.6, 3.2, 1.6 Hz, 1H), 4.27 (d, J = 3.3 Hz, 1H), 3.70 (s, 1H), 2.26 – 2.03 (m, 3H), 1.74 – 1.45 (m, 3H), 1.22 (s, 9H); ¹³C NMR (101 MHz, CDCl₃) δ 144.85, 142.04, 139.83, 132.87, 127.64, 126.37, 125.46, 125.30, 119.51, 112.53, 48.97, 34.05, 31.80, 27.52, 25.91, 17.21; HRMS (ESI) m/z [M+H]⁺, calc'd for C₂₀H₂₅NS 312.1780; found 312.1790.

4-tert-butyl-N-(3-methyl-2-phenylcyclohex-2-enyl)aniline (3bf): Following GP3 with **1a** (41

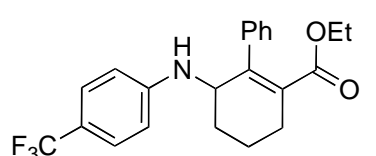
mg, 0.2 mmol) and prop-1-ynylbenzene (**2f**) (70 mg, 0.6 mmol), the product was isolated after a flash chromatography on silica gel (1: 30 EtOAc/hexanes) as yellow oil (39 mg, 61%). IR ν_{max} (cm⁻¹) 3415, 3031, 2950, 2864, 1613, 1517, 1470, 1441, 1301, 1259, 1193, 1033, 816; ¹H NMR (300 MHz, Chloroform-d) δ 7.44 – 7.30 (m, 2H), 7.29 – 7.13 (m, 5H), 6.55 (d, J = 8.2 Hz, 2H), 4.29 – 4.17 (m, 1H), 2.29 – 2.07 (m, 3H), 1.89 – 1.68 (m, 3H), 1.66 (s, 3H), 1.31 (d, J = 1.1 Hz, 9H); ¹³C NMR (75 MHz, CDCl₃) δ 145.15, 142.22, 139.46, 134.57, 133.49, 129.11, 128.22, 126.55, 126.08, 112.75, 52.10, 33.95, 31.92, 31.74, 27.81, 21.31, 18.02; HRMS (ESI) m/z [M+H]⁺, calc'd for C₂₃H₂₉N 320.2373; found 320.2374.

N-(3-butyl-2-(3-(trifluoromethyl)phenyl)cyclohex-2-enyl)-3,5-dimethylaniline (3bg):

Following GP3 with **1h** (35 mg, 0.2 mmol) and 1-(hex-1-ynyl)-3-(trifluoromethyl)benzene (**2g**) (136 mg, 0.6 mmol), the product was

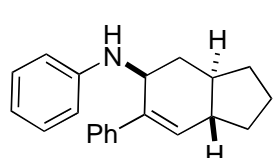
isolated after a flash chromatography on silica gel (1: 20 EtOAc/hexanes) as yellow oil (34 mg, 42%). IR ν_{max} (cm⁻¹) 3402, 3022, 2932, 2860, 1600, 1329, 1162, 1124, 1093, 1072; ¹H NMR (300 MHz, Benzene-d₆) δ 7.56 (s, 1H), 7.16 (s, 12H), 6.88 (t, *J* = 7.8 Hz, 1H), 6.32 (s, 1H), 6.07 (s, 2H), 4.07 (d, *J* = 4.2 Hz, 1H), 3.34 (s, 1H), 2.11 (s, 6H), 2.08 – 1.96 (m, 1H), 1.83 (ddt, *J* = 20.8, 7.4, 3.9 Hz, 4H), 1.58 – 1.42 (m, 3H), 1.31 – 1.18 (m, 2H), 1.15 – 0.99 (m, 2H), 0.75 (dd, *J* = 7.9, 6.4 Hz, 3H); ¹³C NMR (75 MHz, CD₂Cl₂) δ 147.74, 143.93, 140.36, 139.19, 133.22, 133.03, 130.41 (q, *J*² = 31.8 Hz), 128.96, 126.31 (q, *J*³ = 3.8 Hz), 124.96 (q, *J*¹ = 272.3 Hz), 123.57 (q, *J*³ = 3.8 Hz), 119.35, 111.44, 52.64, 34.52, 31.11, 29.41, 28.52, 23.05, 21.66, 18.51, 14.14; HRMS (ESI) m/z [M+H]⁺, calc'd for C₂₅H₃₀F₃N 402.2403; found 402.2399.

Ethyl 2-phenyl-3-(4-(trifluoromethyl)phenylamino)cyclohex-1-enecarboxylate (3bh):



Following GP3 with **1c** (43 mg, 0.2 mmol) and ethyl 3-phenylpropiolate (**2h**) (104 mg, 0.6 mmol), the product was isolated after a flash chromatography on silica gel (1: 10 EtOAc/hexanes) as yellow solid (72 mg, 92%). m.p. 145–148 °C; IR ν_{max} (cm⁻¹) 3396, 2938, 2921, 1700, 1612, 1529, 1318, 1266, 1109, 1063, 1052, 865; ¹H NMR (300 MHz, Chloroform-d) δ 7.38 – 7.30 (m, 2H), 7.25 (dtd, *J* = 7.9, 5.3, 3.5 Hz, 5H), 6.60 – 6.47 (m, 2H), 4.40 (d, *J* = 3.1 Hz, 1H), 3.92 (q, *J* = 7.1 Hz, 2H), 2.73 – 2.55 (m, 1H), 2.44 – 2.25 (m, 1H), 2.18 – 2.02 (m, 1H), 1.90 – 1.64 (m, 3H), 0.86 (t, *J* = 7.2 Hz, 3H); ¹³C NMR (75 MHz, CDCl₃) δ 170.01, 149.28, 141.67, 140.35, 133.28, 128.22, 127.70, 127.41, 126.74 (q, *J*³ = 3.8 Hz), 125.05 (q, *J*¹ = 270.3 Hz), 118.9 (q, *J*² = 32.6 Hz), 112.06, 60.61, 51.29, 27.41, 26.93, 17.03, 13.52; HRMS (ESI) m/z [M+H]⁺, calc'd for C₂₂H₂₂F₃NO₂ 390.1675; found 390.1682.

(3aS,5R,7aR)-N,6-diphenyl-2,3,3a,4,5,7a-hexahydro-1H-inden-5-amine (3ca) (major isomer):

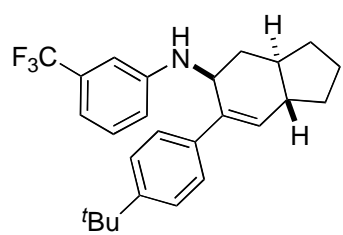


Following GP3 with **1ba** (38 mg, 0.2 mmol) and phenylacetylene (**2a**)

(0.07 mL, 0.6 mmol), the product was isolated after a flash chromatography on silica gel (1: 30 EtOAc/hexanes) as colorless oil (51 mg, 88%). IR ν_{max} (cm⁻¹) 3392, 2934, 2864, 1599, 1502, 1247, 747; ¹H NMR (400 MHz, Methylene Chloride-d₂) δ 7.40 – 7.34 (m, 2H), 7.33 – 7.27 (m, 2H), 7.27 – 7.20 (m, 1H), 7.18 – 7.12 (m, 2H), 6.66 (tt, J = 7.3, 1.1 Hz, 1H), 6.63 – 6.58 (m, 2H), 6.37 (t, J = 1.9 Hz, 1H), 4.81 (dddd, J = 9.0, 6.9, 3.6, 2.0 Hz, 1H), 2.82 (ddd, J = 12.4, 6.9, 2.5 Hz, 1H), 2.11 (ddddd, J = 12.3, 8.8, 7.0, 3.6, 1.9 Hz, 1H), 2.00 (ttd, J = 11.2, 5.9, 5.4, 2.8 Hz, 1H), 1.91 – 1.71 (m, 3H), 1.61 (dddt, J = 14.5, 10.5, 6.1, 2.4 Hz, 1H), 1.48 (td, J = 12.5, 9.3 Hz, 1H), 1.39 – 1.24 (m, 2H); ¹³C NMR (101 MHz, CD₂Cl₂) δ 148.08, 141.33, 140.02, 132.84, 129.69, 128.55, 127.34, 126.94, 117.40, 113.52, 53.43, 46.00, 44.19, 36.93, 30.32, 30.23, 22.68; HRMS (ESI) m/z [M+H]⁺, calc'd for C₂₁H₂₃N 290.1903; found 290.1908.

7a (major isomer) has also been obtained by following GP3 with 6b (38 mg, 0.2 mmol) and phenylacetylene (2a) (0.07 mL, 0.6 mmol), the product was isolated after a flash chromatography on silica gel (1: 30 EtOAc/hexanes) as colorless oil (52 mg, 90%).

(3aS,5R,7aR)-6-(4-tert-butylphenyl)-N-(3-(trifluoromethyl)phenyl)-2,3,3a,4,5,7a-



hexahydro-1H-inden-5-amine (3cb) (major isomer): Following GP3 with 1bc (51 mg, 0.2 mmol) and 1-tert-butyl-4-ethynylbenzene (2i) (95 mg, 0.6 mmol), the product was isolated after a flash chromatography on silica gel (1: 40 EtOAc/hexanes)

as colorless oil (70 mg, 85%). IR ν_{max} (cm⁻¹) 3407, 2953, 2866, 1612, 1593, 1341, 1119, 832; ¹H NMR (400 MHz, Methylene Chloride-d₂) δ 7.23 – 7.11 (m, 5H), 6.84 – 6.74 (m, 1H), 6.73 – 6.70 (m, 1H), 6.67 – 6.62 (m, 1H), 6.25 (t, J = 1.9 Hz, 1H), 4.71 (s, 1H), 3.79 (s, 1H), 2.69 (ddd, J = 12.4, 6.9, 2.4 Hz, 1H), 1.98 (ddddd, J = 12.2, 10.4, 7.0, 3.4, 1.9 Hz, 1H), 1.91 – 1.84 (m, 1H), 1.77 – 1.60 (m, 3H), 1.53 – 1.42 (m, 2H), 1.41 – 1.31 (m, 1H), 1.20 (d, J = 0.4 Hz, 10H); ¹³C

¹H NMR (101 MHz, CD₂Cl₂) δ 149.96, 147.84, 138.53, 137.40, 132.11, 131.15 (q, *J*² = 31.5 Hz), 129.60, 125.88, 125.00, 124.51 (q, *J*¹ = 272.3 Hz), 116.10, 112.94, 108.88, 52.63, 45.36, 43.52, 36.02, 34.30, 31.00, 29.73, 29.68, 22.10; HRMS (ESI) m/z [M+H]⁺, calc'd for C₂₆H₃₀F₃N 414.2403; found 414.2404.

Following GP3 with **1ba** (38 mg, 0.2 mmol) and ethyl 3-phenylpropiolate (**2h**) (104 mg, 0.6 mmol), the products (two isomers, **3cc** and **3cc'**) were isolated after a flash chromatography on silica gel (1: 30 EtOAc/hexanes).

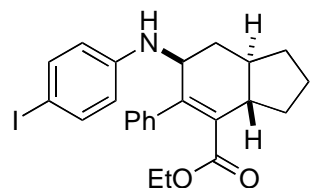
(3aR,6R,7aS)-ethyl 5-phenyl-6-(phenylamino)-2,3,3a,6,7,7a-hexahydro-1H-indene-4-carboxylate (3cc) major isomer, colorless oil (57 mg, 78%). IR ν_{max} (cm⁻¹) 3364, 2947, 2877, 1712, 1600, 1499, 1307, 1157, 752; ¹H NMR (400 MHz, Chloroform-d) δ 7.26 – 7.19 (m, 3H), 7.17 – 7.12 (m, 2H), 7.11 – 7.04 (m, 2H), 6.70 – 6.61 (m, 1H), 6.52 – 6.42 (m, 2H), 4.61 (ddd, *J* = 9.6, 6.9, 3.9 Hz, 1H), 3.92 (qd, *J* = 7.1, 4.6 Hz, 2H), 2.69 (ddd, *J* = 12.7, 6.8, 2.4 Hz, 1H), 2.43 (dddd, *J* = 12.4, 10.8, 6.8, 3.9 Hz, 1H), 2.00 (dtd, *J* = 11.4, 7.3, 3.5 Hz, 1H), 1.86 (dddd, *J* = 11.5, 8.8, 5.5, 3.2 Hz, 1H), 1.82 – 1.65 (m, 3H), 1.58 (td, *J* = 12.7, 9.9 Hz, 1H), 1.40 – 1.21 (m, 3H), 0.90 (t, *J* = 7.1 Hz, 3H); ¹³C NMR (101 MHz, CDCl₃) δ 169.31, 147.18, 142.69, 139.41, 135.55, 129.16, 128.15, 127.62, 127.50, 117.56, 113.65, 60.35, 56.35, 45.83, 43.22, 36.06, 29.98, 28.23, 21.88, 13.85; HRMS (ESI) m/z [M+H]⁺, calc'd for C₂₄H₂₇NO₂ 362.2115; found 362.2121.

(3aR,6R,7aR)-ethyl 5-phenyl-6-(phenylamino)-2,3,3a,6,7,7a-hexahydro-1H-indene-4-carboxylate (3cc') minor isomer, colorless oil (14 mg, 20%). IR ν_{max} (cm⁻¹) 3401, 2934, 2875, 1712, 1600, 1501, 1314, 1245, 747; ¹H NMR (400 MHz, Methylene Chloride-d₂) δ 7.37 – 7.31 (m, 2H), 7.31 – 7.24 (m, 2H), 7.16 – 7.08 (m, 2H), 6.65 (tt, *J* = 7.4, 1.1 Hz, 1H), 6.57 – 6.50 (m, 2H), 4.44 (s, 1H), 4.06 – 3.85

(m, 3H), 2.28 (dt, $J = 12.4, 1.6$ Hz, 1H), 2.19 (dddd, $J = 13.2, 11.5, 6.3, 2.9$ Hz, 1H), 2.02 – 1.91 (m, 1H), 1.89 – 1.78 (m, 4H), 1.76 – 1.66 (m, 2H), 1.57 – 1.43 (m, 1H), 1.38 – 1.26 (m, 2H), 0.98 (t, $J = 7.1$ Hz, 2H); ^{13}C NMR (101 MHz, CD_2Cl_2) δ 169.32, 147.32, 141.06, 140.83, 137.04, 129.73, 128.57, 128.42, 127.90, 117.74, 113.35, 60.75, 54.62, 46.82, 39.56, 33.58, 29.67, 28.53, 23.01, 14.17; HRMS (ESI) m/z [M+H] $^+$, calc'd for $\text{C}_{24}\text{H}_{27}\text{NO}_2$ 362.2115; found 362.2121.

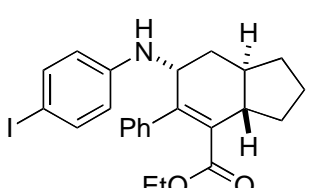
Following GP3 with **1bd** (63 mg, 0.2 mmol) and ethyl 3-phenylpropiolate (**2h**) (104 mg, 0.6 mmol), the products (two isomers **3cd** and **3cd'**) were isolated after a flash chromatography on silica gel (1: 20 EtOAc/hexanes).

(3aR,6R,7aS)-ethyl 6-(4-iodophenylamino)-5-phenyl-2,3,3a,6,7,7a-hexahydro-1H-indene-4-carboxylate (3cd) major isomer, colorless oil (70 mg, 71%). IR ν_{max}



(cm $^{-1}$) 3379, 2925, 2855, 1716, 1603, 1503, 1244, 1026, 750; ^1H NMR (400 MHz, Methylene Chloride- d_2) δ 7.35 – 7.26 (m, 2H), 7.26 – 7.17 (m, 3H), 7.17 – 7.07 (m, 2H), 6.30 – 6.19 (m, 2H), 4.59 (ddd, $J = 10.3, 7.0, 3.9$ Hz, 1H), 3.98 – 3.82 (m, 2H), 2.60 (ddd, $J = 12.7, 6.9, 2.5$ Hz, 1H), 2.38 (dddd, $J = 12.3, 10.8, 6.9, 3.9$ Hz, 1H), 2.04 – 1.91 (m, 1H), 1.85 (dddd, $J = 12.6, 8.2, 4.3, 2.5$ Hz, 1H), 1.74 (tddd, $J = 16.4, 12.9, 7.7, 3.5$ Hz, 3H), 1.52 (td, $J = 12.6, 9.9$ Hz, 1H), 1.35 – 1.22 (m, 3H), 0.92 (t, $J = 7.1$ Hz, 3H); ^{13}C NMR (101 MHz, CD_2Cl_2) δ 169.31, 147.45, 142.41, 140.02, 138.06, 136.25, 128.48, 128.01, 127.80, 115.87, 77.73, 60.67, 56.31, 46.18, 43.63, 36.06, 30.31, 28.65, 22.23, 14.14; HRMS (ESI) m/z [M+H] $^+$, calc'd for $\text{C}_{24}\text{H}_{26}\text{INO}_2$ 488.1081; found 488.1084.

(3aR,6R,7aR)-ethyl 6-(4-iodophenylamino)-5-phenyl-2,3,3a,6,7,7a-hexahydro-1H-indene-4-carboxylate (3cd') minor isomer, colorless oil (17 mg, 18%). IR ν_{max}

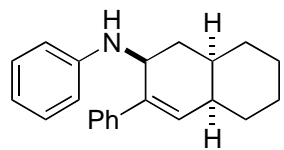


(cm $^{-1}$) 3412, 2926, 2863, 1694, 1582, 1483, 1308, 1231, 1170, 869; ^1H NMR (400 MHz, Methylene Chloride- d_2) δ 7.33 (dq, $J = 9.3, 2.6, 2.1$ Hz, 1H), 7.26 – 7.17 (m, 3H), 7.17 – 7.07 (m, 2H), 6.30 – 6.19 (m, 2H), 4.59 (ddd, $J = 10.3, 7.0, 3.9$ Hz, 1H), 3.98 – 3.82 (m, 2H), 2.60 (ddd, $J = 12.7, 6.9, 2.5$ Hz, 1H), 2.38 (dddd, $J = 12.3, 10.8, 6.9, 3.9$ Hz, 1H), 2.04 – 1.91 (m, 1H), 1.85 (dddd, $J = 12.6, 8.2, 4.3, 2.5$ Hz, 1H), 1.74 (tddd, $J = 16.4, 12.9, 7.7, 3.5$ Hz, 3H), 1.52 (td, $J = 12.6, 9.9$ Hz, 1H), 1.35 – 1.22 (m, 3H), 0.92 (t, $J = 7.1$ Hz, 3H); ^{13}C NMR (101 MHz, CD_2Cl_2) δ 169.31, 147.45, 142.41, 140.02, 138.06, 136.25, 128.48, 128.01, 127.80, 115.87, 77.73, 60.67, 56.31, 46.18, 43.63, 36.06, 30.31, 28.65, 22.23, 14.14; HRMS (ESI) m/z [M+H] $^+$, calc'd for $\text{C}_{24}\text{H}_{26}\text{INO}_2$ 488.1081; found 488.1084.

Hz, 2H), 7.30 – 7.17 (m, 5H), 6.34 – 6.27 (m, 2H), 4.39 – 4.29 (m, 1H), 4.03 (d, J = 8.4 Hz, 1H), 3.90 (q, J = 7.1 Hz, 2H), 2.21 (d, J = 1.5 Hz, 2H), 1.96 – 1.86 (m, 1H), 1.84 – 1.74 (m, 3H), 1.63 (ddd, J = 11.8, 9.8, 5.6 Hz, 2H), 1.51 – 1.38 (m, 1H), 1.33 – 1.24 (m, 1H), 0.93 (t, J = 7.1 Hz, 3H); ^{13}C NMR (101 MHz, CD_2Cl_2) δ 169.21, 146.96, 140.79, 140.32, 138.26, 137.29, 128.52, 128.49, 128.00, 115.61, 77.85, 60.79, 54.59, 46.76, 39.55, 33.51, 29.63, 28.48, 22.98, 14.16; HRMS (ESI) m/z [M+H]⁺, calc'd for $\text{C}_{24}\text{H}_{26}\text{INO}_2$ 488.1081; found 488.1092.

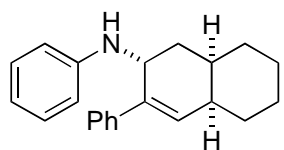
Following GP3 with **1be** (40 mg, 0.2 mmol) and phenylacetylene (**2a**) (0.07 mL, 0.6 mmol), the products (two isomers, **3ce** and **3ce'**) were isolated after a flash chromatography on silica gel (1:30 EtOAc/hexanes).

(2S,4aR,8aR)-N,3-diphenyl-1,2,4a,5,6,7,8,8a-octahydronaphthalen-2-amine (3ce) major



isomer, colorless oil (49 mg, 80%). IR ν_{max} (cm⁻¹) 3409, 2919, 2843, 1661, 1599, 1427, 1111, 1027, 743; ^1H NMR (400 MHz, Methylene Chloride-d₂) δ 7.33 – 7.28 (m, 2H), 7.28 – 7.22 (m, 2H), 7.21 – 7.16 (m, 1H), 7.14 – 7.05 (m, 2H), 6.61 (tt, J = 7.3, 1.1 Hz, 1H), 6.57 – 6.51 (m, 2H), 5.90 (t, J = 1.9 Hz, 1H), 4.72 (d, J = 7.1 Hz, 1H), 3.45 (s, 1H), 2.46 – 2.35 (m, 1H), 1.90 (dddd, J = 11.2, 5.8, 3.8, 2.2 Hz, 1H), 1.86 (tt, J = 3.3, 1.7 Hz, 1H), 1.79 (ddddd, J = 13.8, 11.0, 4.4, 2.9, 1.6 Hz, 2H), 1.68 (dq, J = 15.3, 2.8 Hz, 1H), 1.45 – 1.31 (m, 4H), 1.13 (tdq, J = 16.9, 8.9, 4.6, 4.0 Hz, 2H); ^{13}C NMR (101 MHz, CD_2Cl_2) δ 147.76, 140.41, 138.74, 134.97, 129.13, 127.92, 126.70, 126.44, 116.72, 112.83, 51.66, 42.90, 40.19, 38.41, 32.77, 32.76, 26.73, 26.39; HRMS (ESI) m/z [M+H]⁺, calc'd for $\text{C}_{22}\text{H}_{25}\text{N}$ 304.2060; found 304.2066.

(2R,4aR,8aR)-N,3-diphenyl-1,2,4a,5,6,7,8,8a-octahydronaphthalen-2-amine (3ce') minor

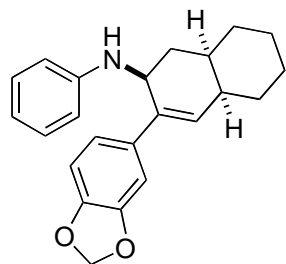


isomer, colorless oil (9 mg, 14%). IR ν_{max} (cm⁻¹) 3377, 2916, 2848, 1599, 1502, 1442, 1250, 1224, 747; ^1H NMR (400 MHz, Methylene Chloride-

d_2) δ 7.45 – 7.40 (m, 2H), 7.30 – 7.24 (m, 2H), 7.22 – 7.17 (m, 1H), 7.16 – 7.10 (m, 2H), 6.63 (tt, J = 7.3, 1.1 Hz, 1H), 6.61 – 6.56 (m, 2H), 6.17 – 6.08 (m, 1H), 4.52 (d, J = 4.5 Hz, 1H), 3.82 (s, 1H), 2.01 (dt, J = 13.0, 2.0 Hz, 1H), 1.88 (dtd, J = 12.9, 3.4, 1.7 Hz, 1H), 1.82 – 1.76 (m, 3H), 1.63 – 1.57 (m, 1H), 1.52 – 1.45 (m, 1H), 1.37 (dddd, J = 24.3, 12.3, 6.2, 2.9 Hz, 3H), 1.22 – 1.10 (m, 2H). ^{13}C NMR (101 MHz, CD_2Cl_2) δ 147.64, 140.61, 136.91, 136.89, 134.74, 129.80, 128.86, 127.55, 126.21, 117.27, 113.01, 111.07, 48.98, 43.85, 36.01, 35.72, 33.40, 33.34, 27.51, 27.25; HRMS (ESI) m/z [M+H] $^+$, calc'd for $\text{C}_{22}\text{H}_{25}\text{N}$ 304.2060; found 304.2061.

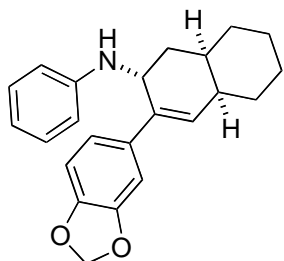
Following GP3 with **1bf** (40 mg, 0.2 mmol) and 5-ethynylbenzo[d][1,3]dioxole (**2c**) (88 mg, 0.6 mmol), the products (two isomers, **3cf** and **3cf'**) were isolated after a flash chromatography on silica gel (1: 30 EtOAc/hexanes).

(2S,4aR,8aR)-3-(benzo[d][1,3]dioxol-5-yl)-N-phenyl-1,2,4a,5,6,7,8,8a-octahydronaphthalen-2-amine (3cf) major isomer, colorless oil (51 mg, 73%). IR ν_{max} (cm^{-1})



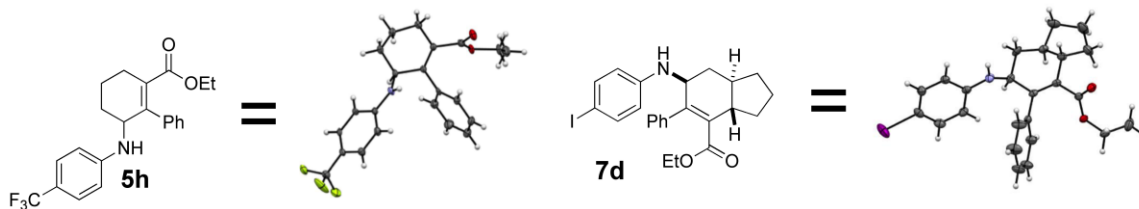
2-amine (3cf) major isomer, colorless oil (51 mg, 73%). IR ν_{max} (cm^{-1}) 3407, 2917, 2856, 1600, 1435, 1245, 1039, 752; ^1H NMR (400 MHz, Methylene Chloride- d_2) δ 7.18 – 7.10 (m, 2H), 6.86 – 6.78 (m, 2H), 6.74 (d, J = 7.9 Hz, 1H), 6.65 (tt, J = 7.3, 1.1 Hz, 1H), 6.61 – 6.54 (m, 2H), 5.97 – 5.91 (m, 2H), 5.84 (t, J = 1.9 Hz, 1H), 4.64 (dq, J = 9.9, 4.4, 3.3 Hz, 1H), 3.50 (s, 1H), 2.47 – 2.37 (m, 1H), 1.96 – 1.89 (m, 1H), 1.87 (dt, J = 3.2, 1.6 Hz, 1H), 1.86 – 1.78 (m, 2H), 1.73 – 1.66 (m, 1H), 1.47 – 1.33 (m, 4H), 1.21 – 1.06 (m, 2H); ^{13}C NMR (101 MHz, CD_2Cl_2) δ 148.30, 147.97, 147.04, 138.94, 135.26, 134.70, 129.70, 120.37, 117.32, 113.45, 108.24, 107.57, 101.63, 52.45, 43.37, 40.71, 39.02, 33.36, 33.32, 27.30, 26.97; HRMS (ESI) m/z [M+H] $^+$, calc'd for $\text{C}_{23}\text{H}_{25}\text{NO}_2$ 348.1958; found 348.1958.

(2R,4aR,8aR)-3-(benzo[d][1,3]dioxol-5-yl)-N-phenyl-1,2,4a,5,6,7,8,8a-



octahydronaphthalen-2-amine (3cf') minor isomer, colorless oil (10 mg, 16%). IR ν_{max} (cm⁻¹) 3409, 3081, 2918, 2849, 1599, 1501, 1444, 1104, 1029, 745; ¹H NMR (400 MHz, Methylene Chloride-d₂) δ 7.20 – 7.07 (m, 2H), 6.98 – 6.85 (m, 2H), 6.71 (d, J = 8.1 Hz, 1H), 6.63 (tt, J = 7.3, 1.1 Hz, 1H), 6.59 (m, 2H), 6.03 – 5.94 (m, 1H), 5.94 – 5.88 (m, 2H), 4.41 (s, 1H), 3.79 (s, 1H), 2.03 – 1.93 (m, 1H), 1.90 – 1.86 (m, 1H), 1.84 (dq, J = 4.8, 2.4, 1.9 Hz, 1H), 1.81 – 1.75 (m, 2H), 1.63 – 1.56 (m, 1H), 1.52 – 1.42 (m, 1H), 1.39 – 1.27 (m, 3H), 1.14 (ddt, J = 15.6, 9.4, 3.5 Hz, 2H); ¹³C NMR (101 MHz, CD₂Cl₂) δ 148.36, 147.63, 147.28, 136.65, 135.19, 133.84, 129.82, 119.71, 117.31, 113.03, 108.47, 106.78, 101.71, 49.40, 43.80, 36.00, 35.74, 33.37, 27.48, 27.25; HRMS (ESI) m/z [M+H]⁺, calc'd for C₂₃H₂₅NO₂ 348.1958; found 348.1954.

Crystal data for (3bh) and (3cd):



For the X-ray data collection, structure solution and Refinement:

The crystal was mounted on a glass fiber and transferred to a Bruker Kappa APEX II CCD diffractometer. The APEX2 software program was used for determination of the unit cell parameters and data collection. The data were collected at 100 K using an Oxford Cryostream Plus system. The raw frame data were processed using APEX2 program. The absorption

correction was applied using the program SADABS. Subsequent calculations were carried out using the SHELXTL program.

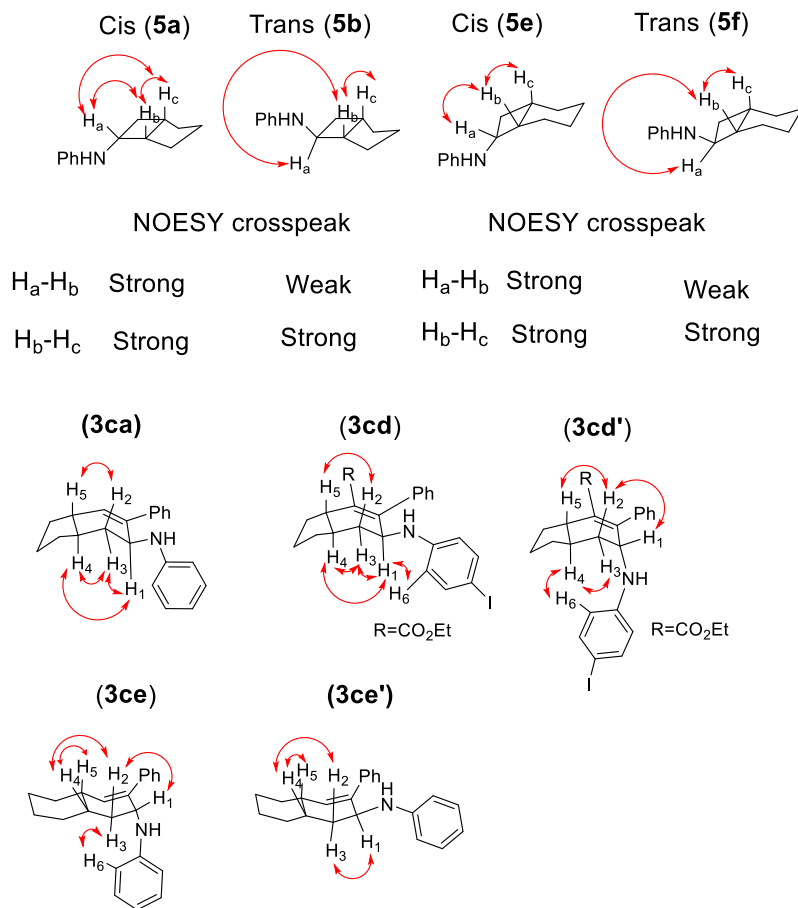


Chart 2.4 Diastereomer Identification.

2.2.5 Summary

In conclusion, we have accomplished the first example of cleaving C-C bonds of cyclobutylanilines enabled by visible light photoredox catalysis. Monocyclic and bicyclic cyclobutylanilines undergo the [4+2] annulation with terminal and internal alkynes to produce amine-substituted six-membered carbocycles. Good to excellent diastereoselectivity is observed for the latter class of the compounds, yielding new hydrindan and decalin derivatives. Finally,

the approach we have developed to overcome cyclobutylanilines' less propensity for ring cleavage can be potentially applied to open rings larger than three- and four-membered with suitable built-in ring strain.

2.3. [4+2] Annulation of *N*-Cyclobutylanilines with *pi* bonds under Continuous Flow

Synthetic chemists have been striving to improve chemical reactions' efficiency from multiple fronts, including exploring new and innovative technologies²⁶. Recently, continuous flow has emerged as a preferred technology to drive reactions' efficiency and has shown to greatly impact many reactions²⁷, including photochemistry. Because of the use of photons, photochemistry suffers some inherent limitations associated with how efficiently photons are transmitted through solutions. Governing by the Lambert-Beer's law, light penetration is impeded in large volumes, which is the root cause for the scale up issue commonly found in batch photochemistry²⁸. Flow reactor's small volume, high surface-to-volume ratio, and precise control of irradiation time allow for maximum and uniform irradiation of solution, thereby circumventing the limitations in batch chemistry while reaping the benefits of shorter reaction time, less byproducts, and higher yields²⁹. Published results generally support that continuous flow is superior to batch particularly on a large scale. However, there are isolated examples in which both modes perform comparably in both yields and productivities³⁰.

We recently developed a [4+2] annulation of cyclobutylanilines with alkynes under visible-light photoredox catalysis³¹. A tandem ring opening, promoted by photooxidation of the parent amine, and subsequent annulation sequence were proposed for the construction of amine-

substituted six-membered carbocycles. The annulation reactions were reported in moderate to excellent yields. However, long reaction time (12 to 24 h) was typically required for the reaction to complete. Additionally, we encountered the scale-up issues often found in batch photochemistry. We questioned whether the continuous flow technique could address the above issues. Herein, we report our investigation of the [4+2] annulation of cyclobutylanilines with alkenes, alkynes, and diynes in continuous flow. It is worth mentioning that we have not reported the [4+2] annulation of cyclobutylanilines with alkenes and diynes previously. Comparing against the previously reported annulation with alkynes in batch, similar and improved yields with significantly shorter reaction time are observed in continuous flow. Lastly, one example of the annulation with alkynes is successfully demonstrated on a gram scale.

2.3.1. Results and Discussion

Cyclobutylaniline **1a** and phenylacetylene **2a** were chosen as the standard substrates to optimize the catalyst system for the [4+2] annulation in flow (Table 2.3.1). Similar to the annulation in batch, the use of $\text{Ir(dtbbpy)(ppy)}_2(\text{PF}_6)$ **4a** as catalyst in methanol showed the highest reactivity (Table 2.3.1, entry 1) when comparing to other catalysts in flow (entries 2-5). The desired product **3a** was obtained in 99% GC yield (93% isolated yield) after 6 h irradiation. The reaction time was cut in half from the batch while maintaining the yield. Control studies showed that both light and catalyst were crucial to the annulation. When the reaction was conducted without either $\text{Ir(dtbbpy)(ppy)}_2(\text{PF}_6)$ (entry 6) or light irradiation (entry 7), product **3a** was not observed. Another control experiment showed that air (oxygen in air) was detrimental to

the formation of **3a** (entry 8). Not surprisingly, the results from these control studies were fully consistent with those obtained in batch.

Table 2.3.1. Optimization of [4+2] annulation under flow

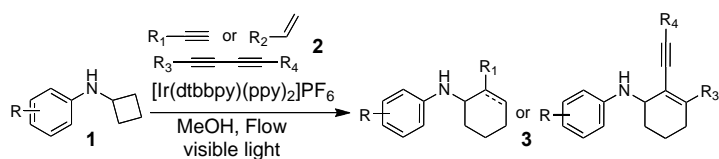
Entry ^[a]	Catalyst	Solvent	Yield of 3a ^[b]
1	Ir(dtbbpy)(ppy) ₂ (PF ₆) (4a)	MeOH	99%
2 ^[c]	Ru(bpz) ₃ (PF ₆) ₂ (4b)	MeOH + MeCN	51%
3 ^[c]	Ir(ppy) ₃ (4c)	MeOH + MeCN	43%
4	Ir[dFCF ₃ ppy] ₂ (bpy)PF ₆ (4d)	MeOH	54%
5	Ru(bpy) ₃ (PF ₆) ₂ (4e)	MeOH	81%
6 ^[d]	None	MeOH	<1%
7 ^[e]	Ir(dtbbpy)(ppy) ₂ (PF ₆) (4a)	MeOH	<1%
8 ^[f]	Ir(dtbbpy)(ppy) ₂ (PF ₆) (4a)	MeOH	65%

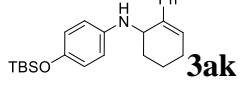
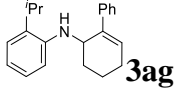
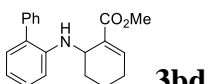
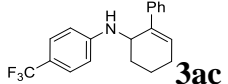
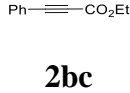
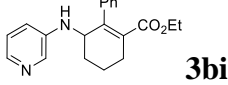
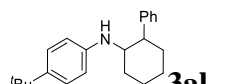
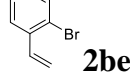
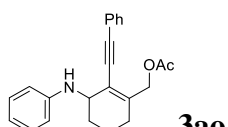
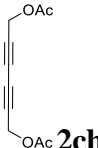
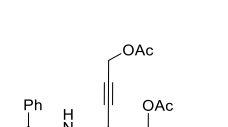
[a] Reaction conditions: **1a** (0.2 mmol, 0.1 M in degassed solvent), **2a** (0.6 mmol), **4** (2 mol%) flow Royal blue LED. [b] Yields determined by GC analysis using dodecane as an internal standard unless noted. [c] A co-solvent of MeOH and CH₃CN (1:1) used due to the solubility issue of the catalyst. [d] Reaction conducted in the absent of catalyst. [e] Reaction conducted in dark. [f] Reaction conducted in the presence of air.

To examine the scope of the annulation in continuous flow, cyclobutylanilines with variable electronic and steric characters were subjected to the optimized conditions (entry 1, Table 2.3.2) with alkynes, alkenes, or diynes. The results are summarized in Table 2.3.2. Substrate **1k** with an electron-donating substituent (OTBS) was problematic in batch, and

product **3ak** was formed in only 8% yield after 24 h. Using continuous flow, the yield was improved to 32% (entry 1). On the other hand, substrate **1c** with an electron-withdrawing substituent (CF_3) that performed much better in batch (79% yield after 24 h), also improved using continuous flow to afford product **3ac** in the same yield with half of the time (entry 4). Steric hindrance was well tolerated in batch as well as in continuous flow. Using flow was found to shorten the reaction time (**1g**, entry 2) or shorten the reaction time and also improve the yield (**1f**, entry 3). *N*-(3-pyridyl)cyclobutylamine **1i**, which had not been studied in the annulation with alkyne **2c** in batch, underwent the annulation in flow uneventfully, providing pyridine-containing product **3bi** in a modest yield (entry 5). In our previously reported [3+2] annulation³², alkenes are the most reactive class of π -bonds, and poor diasteroselectivity is usually observed when monocyclic cyclopropylanilines are used. Using continuous flow, three alkenes (**2bd-bf**) were examined in the [4+2] annulation (entries 6-8). It took 6 to 8 h for the reaction to be complete. Modest to excellent yields were achieved but with poor diastereoselectivity. Diynes generally show poor reactivity in the [3+2] annulation³³. The use of flow allowed the [4+2] annulation with diarynes to be complete within a reasonable amount of time (12 to 14 h, entries 9 and 10). The annulation products (**3ao** and **3ap**) were obtained in good yields with 100% regioselectivity. The complete regiocontrol was also observed in the [3+2] annulation. This common phenomenon shared by the two types of annulation reactions suggests that both probably proceed through similar pathways involving distonic iminium ions.

Table 2.3.2 [4+2] Annulation with various π bonds.

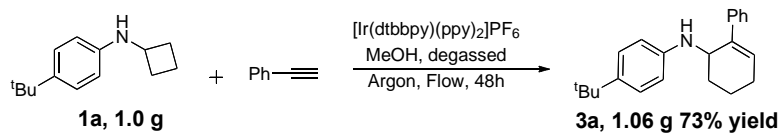


Entry ^a	Substrate	Olefin	Product	t(h)	Yield (%) ^b
1	1k , R = 4-OTBS	2a		22	32
2	1g , R = 2- <i>i</i> Pr	2a		12	70
3	1f , R = 2-phenyl			9	73
4	1c , R = 4-CF ₃	2a		12	79
5				12	55
6 ^c	1a			6	90
7 ^{d,f}	1f			8	53
8 ^e	1c			8	69
9				14	60
10	1f			12	85

[a] Reaction condition: substrate (0.2 mmol, 0.1 M in degassed MeOH), 2 (1 mmol), **4a** (2 mol%), flow LED. [b] Isolated yields. [c] d.r. = 3:2, [d] d.r. = 2:1 and [e] d.r. = 1:1 as determined by ¹H NMR spectroscopy of crude products. [f] DMSO used as solvent.

2.3.2. Gram Scale Synthesis

To fully take advantage of continuous flow, we decided to investigate one of the annulation reactions on a gram scale using conditions slightly modified from the optimal conditions (entry 1, Table 2.3.1). Cyclobutylaniline **1a** (1 g, 4.8 mmol), phenylacetylene **2a** (1.46 g, 14.4 mmol), and [Ir(dtbbpy)(ppy)₂](PF₆) (21 mg, 0.024 mmol, 0.5 mol%) were mixed with MeOH (30 mL). The resulting solution was sparged with argon for 30 min and then flowed through the photoreactor (Scheme 2.3.1). Even with a much lower catalyst loading (0.5 mol% vs. 2 mol%), the reaction was completed, albeit longer time (48 h vs. 6 h). Product **3a** was isolated in a somewhat lower yield (1.06g, 73% vs. 93%).



Scheme 2.3.1 Gram Scale Reaction.

2.3.3 Experimental Section

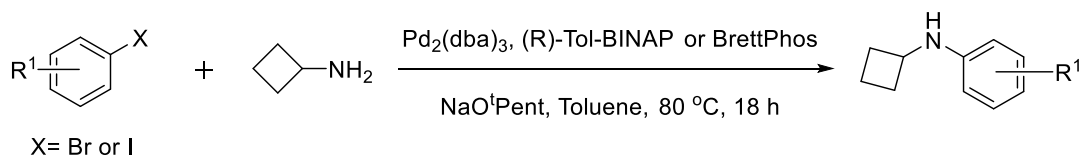
General Considerations

All reactions were carried out under argon atmosphere, unless stated otherwise. Anhydrous methanol (CH₃OH, AcroSeal) was purchased from Acros Organics and dimethylsulfoxide (DMSO) was pre-dried over molecular sieves. Toluene was collected under argon from a solvent purification system. Phenylacetylene **2a**, Ethyl phenylpropiolate **2bc**, Styrene **2bd**, and Acrylonitrile **2bf** were purchased from Sigma-Aldrich. Methyl propiolate **2b**

and 2-Bromostyrene **2be** were purchased from Matrix Scientific. Diynes **2eg** and **2eh** were prepared as described in the literature. Column chromatography was performed using silica gel (230-400 mesh). All new compounds were characterized by ¹H NMR, ¹³C NMR, IR spectroscopy, high-resolution mass spectroscopy (HRMS), and melting point if solid. Nuclear magnetic resonance (NMR) spectra were obtained on a Bruker Avance DPX-300 and a Bruker Avance DPX-400.

Chemical shifts (δ) were reported in parts per million (ppm) relative to residual proton signals in CDCl₃ (7.26 ppm, 77.23 ppm) or CD₂Cl₂ (5.32 ppm, 54.00 ppm) at room temperature. IR spectra were recorded on a Shimadzu IRAffinity-1S instrument. High-resolution mass spectra were recorded on an Agilent 6210 TOF mass spectrometer. Gas chromatography/mass spectroscopy (GC/MS) analyses were performed on an Agilent 6890N Network GC System/5973 inert Mass Selective Detector. Gas chromatography analyses were performed using a Shimadzu GC-2010 Plus instrument. Melting points (m.p.) were recorded using a Stuart SMP10 Melting Point Apparatus and were uncorrected.

General Procedure 1 (GP1): Preparation of *N*-cyclobutylanilines

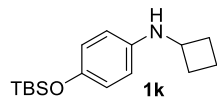


(R)-Tol-BINAP = (R)-(+)-2,2'-Bis(di-p-tolylphosphino)-1,1'-binaphthyl
 BrettPhos = 2-(Dicyclohexylphosphino)3,6-dimethoxy-2',4',6'-triisopropyl-1,1'-biphenyl

To an oven-dried test tube equipped with a stir bar were added 0.01 mmol of Pd₂(dba)₃ and 0.03 mmol of ligand ((*R*)-Tol-BINAP or BrettPhos). Glove box was used to add 1.5 mmol of NaO^tPent and the tube was sealed with a Teflon screw cap. Aryl halide (1 mmol), cyclobutylamine (1.6 mmol), and toluene (2 mL) were then added to the reaction mixture and heated at 80 °C for 18 h. After completion, the reaction mixture was cooled to room

temperature, diluted with diethyl ether, filtered over a short pad of silica gel, and concentrated in vacuum. Purification by flash chromatography on silica gel afforded *N*-cyclobutylaniline.

4-*tert*-Butyldimethylsilyl ether-*N*-cyclobutylaniline (1k). Following the above procedure with



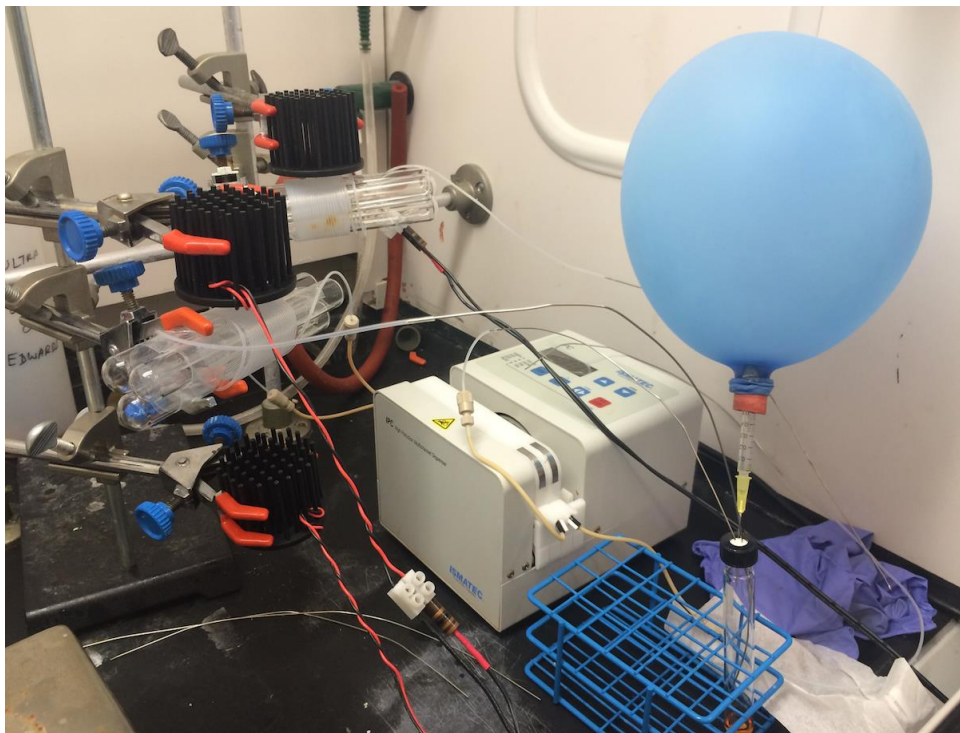
(4-bromophenoxy)-*tert*-butyldimethylsilane (1.23 mL, 5 mmol, 1 equiv) and BrettPhos (80.5 mg, 0.15 mmol, 3 mol %), the product was isolated after flash chromatography on silica gel (5:1 hexane/ EtOAc) as a colorless oil (1.22 g, 88%); IR ν_{max} (cm⁻¹) 3403, 3062, 2956, 2931, 2889, 2857, 1509, 1471, 1463, 1247, 1163, 922, 908, 839; ¹H NMR (400 MHz, Chloroform-*d*) δ 6.70 – 6.60 (m, 2H), 6.48 – 6.39 (m, 2H), 3.86 – 3.75 (m, 1H), 2.43 – 2.29 (m, 2H), 1.90 – 1.67 (m, 4H), 0.94 (d, *J* = 0.6 Hz, 9H), 0.13 (d, *J* = 0.6 Hz, 6H); ¹³C NMR (101 MHz, CDCl₃) δ 147.73, 141.74, 120.84, 114.48, 80.56, 50.11, 31.49, 25.97, 18.39, 15.43, -4.26; HRMS (ESI) *m/z* [M+H]⁺, calc'd for C₁₆H₂₇NOSi 278.1935; found 278.1927.

Preparation and characterization of cyclobutylanilines **1a**, **1c**, **1f**, **1g**, **1h**, **1i**, **1k** correspond to those described in the literature.²³

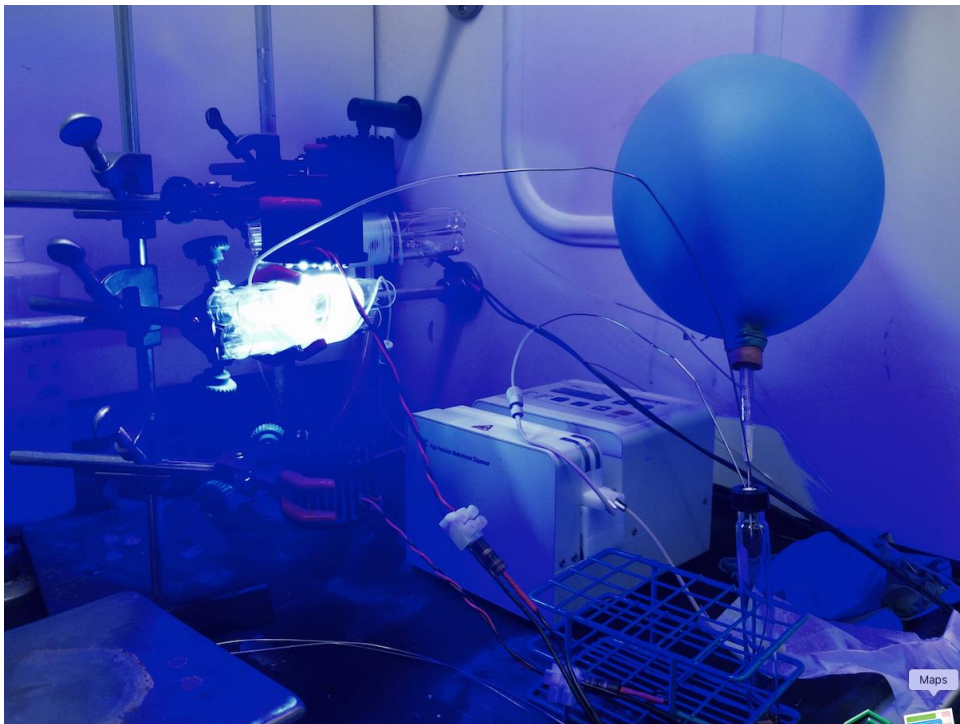
The continuous flow setup

The continuous flow setup was adopted from Professor Stephenson and coworkers' method. Seven prearranged Luxeon Rebel high power LEDs (royal blue color, $\lambda_{\text{max}} = 447.5$ nm) were used as the light source. PFA Tubing (IDEX Health and Science, Part # 1514L) was wrapped around three borosilicate glass test tubes, supported on both ends by small pieces of cardboards. A total volume of 1.34 mL was placed inside the test tubes. The tubing was then connected to the peristaltic pump tubing (IDEX Health and Science, Part # SC0717) with a conical adapter (IDEX Health and Science, Part # P-797). The distance between the light and the tubing was 3 cm.

Light Off:



Light On:

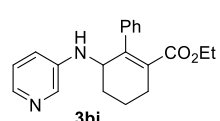


General Procedure 2 (GP2): [4+2] Annulation. An oven-dried test tube equipped with a stir bar was charged with Ir(dtbbpy)(ppy)₂PF₆ (2 mol%), cyclobutylaniline derivative (0.2 mmol), alkyne, olefin, or diyne derivative (1 mmol), and dry MeOH (2 mL). The test tube was capped with a Teflon screw cap, degassed by Freeze-Pump-Thaw (3-5 cycles), and then backfilled with argon. The reaction mixture was next pumped through a flow photoreactor in a closed loop system at a flow rate of 75 μ L min⁻¹ under the protection of an argon balloon. After the reaction was complete, monitored by TLC, the solution was collected in a flask and concentrated in vacuum. Purification by silica gel flash chromatography afforded the corresponding annulation products.

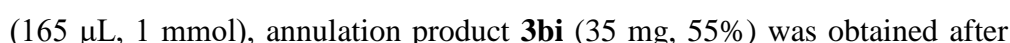
Characterization of annulation products **3a**, **3ag**, **3bd**, and **3ac** were described in the literature.³

Following **GP2** with cyclobutylaniline **1k** (55 mg, 0.2 mmol) and phenylacetylene **2a** (110 μ L, 1 mmol), annulation product **3ak** (24 mg, 32%) was obtained after silica gel column chromatography (30:1 hexane/ EtOAc) as colorless oil; IR ν max (cm⁻¹) 3417, 3022, 2950, 2930, 2903, 1507, 1471, 1250, 1229, 1112, 838; ¹H NMR (400 MHz, Chloroform-*d*) δ 7.54 – 7.39 (m, 2H), 7.33 – 7.26 (m, 2H), 7.26 – 7.20 (m, 1H), 6.76 – 6.63 (m, 2H), 6.59 – 6.47 (m, 2H), 6.39 – 6.27 (m, 1H), 4.40 (d, *J* = 2.5 Hz, 1H), 3.49 (s, 1H), 2.40 – 2.08 (m, 3H), 1.78 – 1.61 (m, 3H), 1.00 (s, *J* = 0.7 Hz, 9H), 0.19 (s, *J* = 0.7 Hz, 6H); ¹³C NMR (101 MHz, CDCl₃) δ 147.29, 141.97, 140.58, 137.67, 128.70, 128.57, 127.14, 125.74, 120.84, 114.31, 49.32, 27.86, 26.23, 25.98, 18.38, 17.25, -4.24; HRMS (ESI) *m/z* [M+H]⁺, calc'd for C₂₄H₃₃NOSi 380.2404; found 380.2414.

Following **GP2** with cyclobutylaniline **1i** (30 mg, 0.2 mmol) and Ethyl phenylpropiolate **2bc** (165 μ L, 1 mmol), annulation product **3bi** (35 mg, 55%) was obtained after



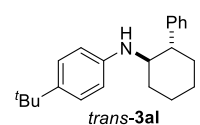
(165 μ L, 1 mmol), annulation product **3bi** (35 mg, 55%) was obtained after



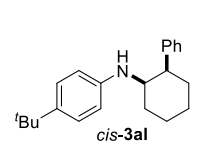
silica gel column chromatography (20:1 hexane/ EtOAc then 1:2 hexane/ EtOAc) as a green gray solid, m.p. 151–153 °C; IR ν_{max} (cm^{−1}) 3261, 2941, 1689, 1585, 1417, 1269, 1236, 1049, 790, 756, 696; ¹H NMR (400 MHz, Chloroform-*d*) δ 7.93 – 7.83 (m, 2H), 7.24 – 7.20 (m, 3H), 7.20 – 7.15 (m, 2H), 7.01 – 6.92 (m, 1H), 6.74 (ddd, *J* = 8.3, 3.0, 1.4 Hz, 1H), 4.35 – 4.25 (m, 1H), 3.90 – 3.83 (m, 2H), 3.73 (d, *J* = 8.0 Hz, 1H), 2.67 – 2.54 (m, 1H), 2.36 – 2.22 (m, 1H), 2.13 – 1.99 (m, 1H), 1.83 – 1.64 (m, 3H), 0.82 (td, *J* = 7.2, 0.4 Hz, 3H); ¹³C NMR (101 MHz, CDCl₃) δ 170.14, 143.08, 142.16, 140.56, 139.02, 136.56, 133.28, 128.39, 127.87, 127.65, 123.82, 118.96, 60.76, 51.75, 27.71, 27.11, 17.27, 13.72; HRMS (ESI/APCL) *m/z* [M+H]⁺, calc'd for C₂₀H₂₂N₂O₂ 323.1754; found 323.175.

Following **GP2** with cyclobutylaniline **1a** (41 mg, 0.2 mmol) and styrene **2d** (115 μ L, 1 mmol), annulation product **3al** (55 mg, 90 %) was obtained after silica gel column chromatography (30:1 hexane/ EtOAc) as a 3:2 mixture of two diastereoisomers.

Data for **trans-3al**: red-brown oil; IR ν_{max} (cm $^{-1}$) 2926, 2854, 1614, 1516, 1448, 1259, 1193,



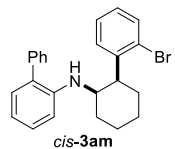
¹H NMR (400 MHz, Methylene Chloride-*d*₂) δ 7.36 – 7.24 (m, 4H), 7.24 – 7.17 (m, 1H), 7.16 – 7.06 (m, 2H), 6.48 – 6.40 (m, 2H), 3.48 (td, *J* = 10.7, 3.8 Hz, 1H), 3.35 (s, 1H), 2.55 (ddd, *J* = 11.8, 10.4, 3.7 Hz, 1H), 2.44 (dtd, *J* = 10.6, 3.7, 2.0 Hz, 1H), 1.99 (dddd, *J* = 13.2, 6.2, 3.6, 2.3 Hz, 1H), 1.92 – 1.81 (m, 2H), 1.71 – 1.37 (m, 4H), 1.29 – 1.23 (m, 9H); ¹³C NMR (101 MHz, CD₂Cl₂) δ 145.77, 145.30, 140.00, 128.97, 127.99, 126.84, 126.36, 113.05, 56.76, 51.76, 36.46, 34.32, 34.16, 31.83, 27.07, 25.83; HRMS (ESI/APCL) *m/z* [M+H]⁺, calc'd for C₂₂H₂₉N 308.2373; found 308.2381.



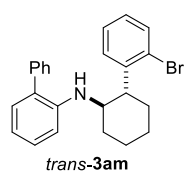
Data for **cis-3al**: colorless oil; IR ν_{max} (cm^{-1}) 2920, 2854, 1614, 1517, 1323, 1192, 817, 748, 696, 542; ^1H NMR (400 MHz, Methylene Chloride- d_2) δ 7.38 – 7.16 (ddt, J = 6.6, 5.9, 2.6 Hz, 1H), 7.09 – 7.01 (m, 2H), 6.40 – 6.32 (m, 2H), 3.79

(q, $J = 3.2$ Hz, 1H), 3.63 (s, 1H), 3.00 (dt, $J = 12.5, 3.8$ Hz, 1H), 2.16 – 2.02 (m, 1H), 1.96 – 1.80 (m, 3H), 1.60 – 1.50 (m, 4H), 1.20 (s, 9H); ^{13}C NMR (101 MHz, CD_2Cl_2) δ 146.02, 144.89, 139.97, 128.68, 128.02, 126.63, 126.30, 113.22, 54.19, 46.76, 34.13, 31.80, 30.71, 26.60, 26.03, 20.75; HRMS (ESI/APCL) m/z [M+H] $^+$, calc'd for $\text{C}_{22}\text{H}_{29}\text{N}$ 308.2373; found 308.2382.

Following **GP2** with cyclobutylaniline **1f** (45 mg, 0.2 mmol) and 2-Bromostyrene **2be** (125 μL , 1 mmol) in DMSO (2 mL), annulation product **3am** (43 mg, 53%) was obtained after silica gel column chromatography (100 % hexane then 100:1 hexane/ EtOAc) as a 2:1 mixture of two diastereoisomers.



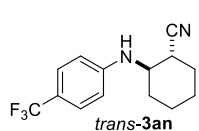
Data for *cis*-**3am**: colorless oil, IR ν_{max} (cm^{-1}) 2926, 2854, 1577, 1508, 1467, 1435, 1317, 1022, 1008, 736, 702; ^1H NMR (400 MHz, Methylene Chloride- d_2) δ 7.55 – 7.47 (m, 3H), 7.46 – 7.39 (m, 1H), 7.34 – 7.28 (m, 2H), 7.13 – 7.06 (m, 1H), 7.05 – 6.97 (m, 2H), 6.94 (ddd, $J = 7.5, 1.7, 0.4$ Hz, 1H), 6.79 (dd, $J = 7.7, 1.8$ Hz, 1H), 6.57 (td, $J = 7.4, 1.1$ Hz, 1H), 6.36 – 6.28 (m, 1H), 4.09 (d, $J = 7.8$ Hz, 1H), 3.98 (dq, $J = 6.7, 3.1$ Hz, 1H), 3.31 (ddd, $J = 11.3, 5.5, 3.2$ Hz, 1H), 2.08 – 1.99 (m, 1H), 1.82 – 1.72 (m, 1H), 1.67 – 1.57 (m, 1H), 1.54 (dd, $J = 8.4, 3.3$ Hz, 2H), 1.46 – 1.35 (m, 1H), 1.34 – 1.19 (m, 2H); ^{13}C NMR (101 MHz, CD_2Cl_2) δ 144.98, 143.02, 140.10, 133.27, 130.17, 130.06, 129.35, 129.32, 129.04, 128.27, 128.18, 127.82, 127.62, 125.11, 116.53, 110.79, 51.08, 46.51, 30.42, 26.69, 26.03, 20.68; HRMS (ESI/APCL) m/z [M+H] $^+$, calc'd for $\text{C}_{24}\text{H}_{24}\text{BrN}$ 406.1165; found 406.1160.



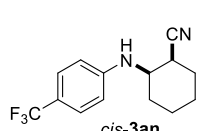
Data for *trans*-**3am**: colorless oil; IR ν_{max} (cm^{-1}) 2927, 2852, 1577, 1508, 1435, 1317, 1022, 744, 734, 702; ^1H NMR (400 MHz, Methylene Chloride- d_2) δ 7.56 – 7.50 (m, 1H), 7.27 (dddd, $J = 4.9, 3.0, 1.9, 0.8$ Hz, 5H), 7.16 – 7.09 (m, 1H), 7.09 – 7.03 (m, 1H), 6.90 (ddd, $J = 7.4, 1.7, 0.4$ Hz, 1H), 6.88 – 6.80 (m, 2H), 6.68 – 6.56 (m, 2H), 3.71 (d, $J = 7.0$ Hz, 1H), 3.46 (s, 1H), 3.04 (td, $J = 11.2, 3.6$ Hz, 1H), 2.37 (dddd, $J = 12.0$,

5.1, 3.5, 1.6 Hz, 1H), 1.95 – 1.85 (m, 1H), 1.85 – 1.71 (m, 2H), 1.53 – 1.31 (m, 3H), 1.19 – 1.07 (m, 1H); ^{13}C NMR (75 MHz, CD_2Cl_2) δ 144.74, 143.88, 139.72, 133.20, 130.68, 129.49, 129.41, 129.01, 128.40, 128.31, 128.07, 127.79, 127.43, 125.85, 116.59, 110.42, 57.17, 49.45, 34.90, 34.15, 26.81, 25.70; HRMS (ESI/APCL) m/z [M+H] $^+$, calc'd for $\text{C}_{24}\text{H}_{24}\text{BrN}$ 406.1165; found 406.1159.

Following **GP2** with cyclobutylaniline **1c** (43 mg, 0.2 mmol) and acrylonitrile **2bf** (65 μL , 1 mmol), annulation product **3an** (37 mg, 69%) was obtained after silica gel column chromatography (5:1 hexane/ EtOAc) as a 1:1 mixture of two diastereoisomers.



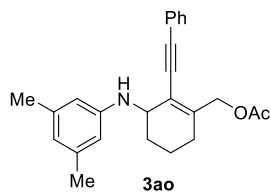
Data for *trans*-**3an**: white solid, m.p. 117-119 °C; IR ν_{max} (cm $^{-1}$) 3338, 2951, 2247, 1614, 1541, 1315, 1095, 1062, 831, 503; ^1H NMR (400 MHz, Methylene Chloride- d_2) δ 7.44 (d, J = 8.4 Hz, 2H), 6.67 (d, J = 8.4 Hz, 2H), 4.31 (d, J = 8.8 Hz, 1H), 3.52 (ddt, J = 12.5, 8.5, 4.0 Hz, 1H), 3.36 (p, J = 3.3 Hz, 1H), 2.08 (dp, J = 12.4, 2.9 Hz, 1H), 2.04 – 1.95 (m, 1H), 1.95 – 1.86 (m, 1H), 1.77 – 1.69 (m, 1H), 1.68 – 1.60 (m, 2H), 1.60 – 1.53 (m, 1H), 1.44 (qt, J = 12.7, 3.8 Hz, 1H); ^{13}C NMR (75 MHz, CD_2Cl_2) δ 149.21, 127.29 (q, J = 3.7 Hz), 126.28 (q, J = 268.6 Hz), 120.06, 119.70 (q, J = 32.6 Hz), 113.00, 52.07, 34.01, 29.95, 28.02, 25.17, 22.04; HRMS (ESI/APCL) m/z [M+H] $^+$, calc'd for $\text{C}_{14}\text{H}_{15}\text{F}_3\text{N}_2$ 269.1260; found 269.1247.



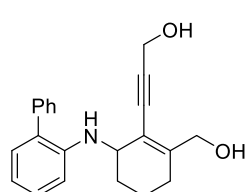
Data for *cis*-**3an**: yellow solid, m.p. 97-100 °C; IR ν_{max} (cm $^{-1}$) 3358, 2954, 2241, 1614, 1533, 1317, 1093, 1062, 827, 590; ^1H NMR (300 MHz, Methylene Chloride- d_2) δ 7.40 (dd, J = 13.6, 8.5 Hz, 2H), 6.71 (dd, J = 8.8, 2.6 Hz, 2H), 4.13 – 3.99 (m, 1H), 3.62 (qd, J = 9.1, 3.9 Hz, 1H), 2.56 (ddd, J = 10.0, 9.1, 3.9 Hz, 1H), 2.24 – 2.04 (m, 1H), 1.76 (dddd, J = 14.0, 10.8, 6.3, 3.2 Hz, 2H), 1.56 – 1.42 (m, 1H), 1.41 – 1.33 (m, 1H), 1.32 – 1.19 (m, 2H); ^{13}C NMR (75 MHz, CD_2Cl_2) δ 149.78, 127.18 (q, J = 3.8 Hz), 126.12 (q, J = 268.8

Hz), 121.66, 119.65 (q, $J = 32.6$ Hz), 114.53, 113.04, 53.48, 35.58, 32.41, 29.23, 24.35, 24.07; HRMS (ESI/APCL) m/z [M+H]⁺, calc'd for C₁₄H₁₅F₃N₂ 269.1260; found 269.1257.

Following **GP2** with cyclobutylaniline **1h** (35 mg, 0.2 mmol) and diyne **2cg** (198 mg, 1 mmol),

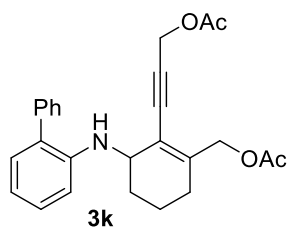


annulation product **3ao** (45 mg, 60%) was obtained after silica gel column chromatography (30:1 hexane/ EtOAc) as yellow brown oil; IR ν_{max} (cm⁻¹) 3360, 2939, 2864, 1724, 1597, 1369, 1242, 1182, 1024, 756, 690; ¹H NMR (400 MHz, Methylene Chloride-*d*₂) δ 7.39 – 7.15 (m, 5H), 6.44 – 6.25 (m, 3H), 5.01 – 4.85 (m, 2H), 4.27 – 4.07 (m, 1H), 2.28 – 2.19 (m, 7H), 2.12 – 2.04 (m, 3H), 1.90 – 1.64 (m, 5H); ¹³C NMR (101 MHz, CD₂Cl₂) δ 171.23, 148.38, 143.05, 139.31, 131.89, 128.79, 128.71, 123.67, 121.90, 119.73, 111.72, 94.60, 87.52, 66.56, 51.93, 29.01, 27.61, 21.78, 21.22, 18.71; HRMS (ESI/APCL) m/z [M+H]⁺, calc'd for C₂₅H₂₇NO₂ 374.2115; found 374.2130.



Following **GP2** with cyclobutylaniline **1f** (45 mg, 0.2 mmol) and diyne **2ch** (120 mg, 1 mmol), annulation product **3ap** (71 mg, 85%) was obtained after silica gel column chromatography (30:1 hexane/ EtOAc to elute excess diyne, then 10:1 hexane/ EtOAc) as brown oil; IR ν_{max} (cm⁻¹) 2933, 2864, 1739, 1735, 1508, 1436, 1217, 1024, 908, 731, 704; ¹H NMR (400 MHz, Chloroform-*d*) δ 7.52 – 7.43 (m, 4H), 7.43 – 7.36 (m, 1H), 7.32 – 7.27 (m, 1H), 7.15 (dd, $J = 7.5, 1.6$ Hz, 1H), 7.00 (d, $J = 8.2$ Hz, 1H), 6.89 (t, $J = 7.4$ Hz, 1H), 4.85 – 4.72 (m, 2H), 4.70 (s, 2H), 4.06 (d, $J = 5.0$ Hz, 1H), 2.18 – 2.10 (m, 2H), 2.09 (d, $J = 0.6$ Hz, 3H), 2.08 (d, $J = 0.7$ Hz, 3H), 1.88 (ddt, $J = 16.3, 7.6, 4.0$ Hz, 1H), 1.82 – 1.72 (m, 1H), 1.66 – 1.50 (m, 2H); ¹³C NMR (101 MHz, CDCl₃) δ 170.96, 170.32, 144.30, 144.04, 139.65, 130.71, 129.56, 129.03, 128.72, 128.05, 127.30, 120.05, 117.15, 111.13, 88.31, 83.79, 66.10, 52.87, 51.64, 28.26, 27.00, 20.97, 20.88, 18.16; HRMS (ESI/APCL) m/z [M+H]⁺, calc'd for C₂₆H₂₇NO₄ 418.2040; found 418.2035.

The diol was formed by cleavage of the two acetate groups of **3ap**. It was used to further confirm



3ap's structure. Yellow oil; IR ν_{max} (cm⁻¹) 3313, 2926, 2858, 1577, 1508, 1309, 1166, 1012, 742, 702; ¹H NMR (400 MHz, Methylene Chloride-*d*₂) δ 7.50 – 7.38 (m, 3H), 7.38 – 7.29 (m, 1H), 7.24 – 7.15 (m, 1H), 7.09 – 6.98 (m, 1H), 6.80 (dd, *J* = 8.5, 1.1 Hz, 1H), 6.72 (td, *J* = 7.4, 1.1 Hz, 1H), 4.22 (s, 4H), 4.09 – 4.01 (m, 1H), 2.20 – 2.11 (m, 2H), 1.80 – 1.68 (m, 3H), 1.66 – 1.49 (m, 4H); ¹³C NMR (101 MHz, CD₂Cl₂) δ 148.64, 145.12, 140.13, 130.99, 129.90, 129.47, 129.06, 128.46, 127.72, 118.43, 117.37, 111.68, 92.56, 83.49, 65.19, 52.17, 51.83, 28.97, 27.47, 18.92; HRMS (ESI/APCL) *m/z* [M+H]⁺, calc'd for C₂₂H₂₃NO₂ 334.1802; found 334.1809.

2.3.4 Summary

In summary, we have successfully applied the continuous flow technique to the [4+2] annulation of cyclobutylanilines with alkynes developed in our lab. Noticeable benefits, such as shorter reaction time and/or higher yields, are achieved with the substrates examined. We have also successfully extended the [4+2] annulation to include alkenes and diynes that have not been reported. Finally, we were able to demonstrate one of the annulation reactions on a gram scale using a much lower catalyst loading.

2.4. [4+2] Annulation under Heterogeneous Ti³⁺@TiO₂ Catalysis

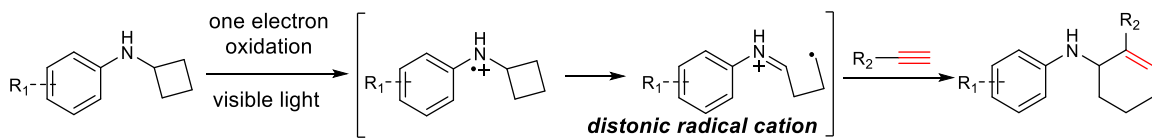
Since Fujishima and Honda's landmark work on discovering TiO₂'s ability as a photochemical water-splitting catalyst in 1971,³⁴ TiO₂ has been developed into a major class of photocatalysts for a variety of applications ranged from water splitting to detoxification of water.³⁵ The popularity of TiO₂ as photocatalysts is driven by some of its exceptional features,

such as earth abundance, stability, and non-toxicity. Unfortunately, since pure TiO₂ (anatase phase) has a band gap of 3.2 eV, its photoactivation can be achieved only by ultraviolet (UV) light. This shortcoming has certainly limited pure TiO₂'s applications, particularly in catalysis, as functional group compatibility and chemoselectivity under UV light is generally worse than lower-energy visible light.³⁶ A number of methods have been developed to narrow the band gap to the level that can be overcome by visible light.³⁷ Among them, doping proves very effective for narrowing the band gap by producing extra energy states within the band gap.³⁸ Compared to doping by addition of a foreign metal or nonmetal element to TiO₂, self-doping by partial reduction of TiO₂ to generate Ti³⁺ ion or the oxygen vacancy, provides an alternative and potentially better approach for conversion of TiO₂ to a visible light photocatalyst.³⁹ Professor Pingyun Feng at the University of California, Riverside, one of the authors in this work, has developed a simple, economical, and one-step method for self-doped Ti³⁺@TiO₂.⁴⁰ High-quality, uniform self-doped Ti³⁺@TiO₂ with tunable concentration of Ti³⁺ ion or the oxygen vacancy can be easily obtained using this method. Since the Ti³⁺ ion is buried inside TiO₂, it is stable upon exposure to air and water under light irradiation. The self-doped Ti³⁺@TiO₂ has also been shown highly thermo- and photo-stable. These features are all critically important for catalysis applications. Not surprisingly, the Feng group recently used the catalyst to successfully catalyze water splitting⁴¹ and CO₂ reduction⁴² under visible light irradiation.

Encouraged by the initial success of self-doped Ti³⁺@TiO₂ as visible light photocatalysts, we started to investigate its use to catalyze organic reactions. TiO₂, which is arguably the most studied semiconductor photocatalyst, is also appealing to synthetic chemists for the same reasons (earth-abundant, stable, and non-toxic) that others find TiO₂ attractive. Equally importantly, TiO₂ is used as a heterogeneous catalyst, which makes its recycle trivial. Moreover, since TiO₂-

catalyzed reactions occur at the semiconductor/liquid interface, ample evidence from the literature suggests different reactivity and/or pathways between homogeneous and heterogeneous reactions can occur for the same substrates. Despite all the advantages possessed by TiO₂, its use as photocatalyst in organic synthesis has remained limited. Early work on TiO₂'s synthetic applications mostly focused on UV light irradiation. Unfortunately, this work was often plagued by overoxidation and poor chemoselectivity, and thus later refocused on wastewater treatment.⁴⁴ Now armed with better understanding about how TiO₂ works in photocatalysis⁴⁵ and availability of a large number of visible-light-active TiO₂⁴⁶, we strongly felt that it might be time to revisit the topic of using TiO₂ to catalyze organic reactions particularly from the angle of visible light photocatalysis.⁴⁷

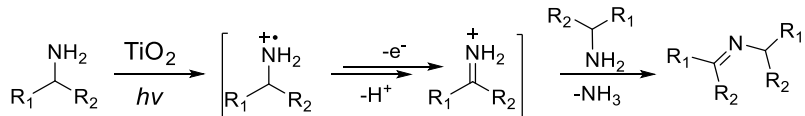
The [4+2] annulation reaction of cyclobutylanilines with alkynes was chosen as the first model reaction to examine self-doped Ti³⁺@TiO₂'s potential as visible light photocatalyst. We developed the homogeneous variant of this reaction in which an iridium complex was used as photocatalyst in 2015 (Scheme 2.4.1).^{31,48} To the best of our knowledge, this is the first reported example of this type of reaction. With a relatively unactivated cyclobutane ring, we were able to successfully apply one-electron photooxidation of cyclobutylanilines to the amine radical cations to open the ring, producing reactive distonic radical cations that underwent the annulation with alkynes. This one-electron oxidation strategy proved to be fruitful and quite general, as a variety of aniline-substituted cyclobutanes successfully underwent the desired opening and thereby broadened the use of cyclobutanes as synthetic building blocks.



Scheme 2.4.1. [4+2] Annulation of Cyclobutylanilines with Alkynes.

We questioned whether the iridium complex could be replaced by self-doped $\text{Ti}^{3+}@\text{TiO}_2$ in the [4+2] annulation reaction. In 1986, the Fox group reported that upon UV irradiation, primary amines were converted to imines on bare TiO_2 powder suspended in oxygenated CH_3CN (Scheme 2.4.2).⁴⁹ The reaction was proposed to proceed through two one-electron oxidation steps via amine radical cations. The proposed pathway was corroborated by cyclic voltammetry, which revealed two irreversible oxidation waves presumably corresponding to the two oxidations. The necessity of oxygen in the reaction suggested that it played a critical role. In this role, oxygen was believed to act as an electron acceptor and thereby minimize unproductive back electron transfer in which amine radical cations were reduced to the starting amines. O_2 was presumably reduced to superoxide, which is one of reactive oxygen species (ROS). Since O_2 is commonly used as a terminal oxidant in photooxidation by semiconductors⁵⁰ and ROS plays a significant role in biology, medicine, and atmospheric chemistry, photogeneration of ROS on the semiconductor surface has been studied quite extensively. In addition to superoxide, ${}^1\text{O}_2$ is another ROS that is often suggested to be produced by semiconductor photocatalysis.⁵¹ However, detection of ${}^1\text{O}_2$ in suspension poses various issues.⁵² Two main pathways have been proposed for the formation of ${}^1\text{O}_2$. One is energy transfer between photoexcited semiconductors and oxygen;⁵³ the other is hole oxidation of superoxide.⁵⁴ Although both pathways have been supported by experimental evidence, it remains debatable about which pathway is dominated. Additionally, ${}^1\text{O}_2$ has been shown to directly oxidize amines, leading to various types of products.^{55,56} This poses an interesting and significant question in our proposed studies, whether

cyclobutylanilines are oxidized by the hole or ${}^1\text{O}_2$. Furthermore, how self-doped $\text{Ti}^{3+}@\text{TiO}_2$ excited by visible light affects the pathways arises as another significant question. Herein we report our findings on the [4+2] annulation of cyclobutylanilines with alkynes catalyzed by self-doped $\text{Ti}^{3+}@\text{TiO}_2$ including the viability of $\text{Ti}^{3+}@\text{TiO}_2$ as visible light photocatalyst and the involvement of ${}^1\text{O}_2$ in the reaction.



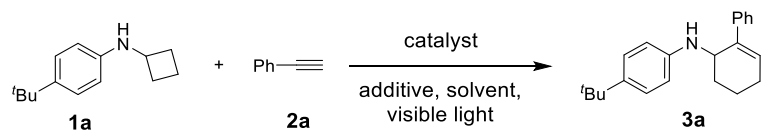
Scheme 2.4.2. Oxidation of Primary Amines to Imines on UV-irradiated TiO_2 .

2.4.1. Results and Discussion

We chose Cyclobutylaniline **1a** and phenylacetylene **2a** as representative substrates as well as self-doped $\text{Ti}^{3+}@\text{TiO}_2$ with 16.7 $\mu\text{mol/g}$ of Ti^{3+} (referred to as “**T3**”) as the photocatalyst initially to optimize the catalyst system. Using the conditions optimized for the homogeneous annulation except the photocatalyst and air rather than a nitrogen atmosphere, a negligible amount (3%) of product **3a** was detected (Table 2.4.1, entry 1). This was not surprising, since oxidation of MeOH on the TiO_2 surface was known to be facile⁵⁷ and thereby might compromise the desired annulation reaction. Examination of other solvents revealed that DMSO and ${}^3\text{BuOH}$ were the two best, although the latter was slightly better (entries 2-5). The reason why ${}^3\text{BuOH}$ was superior to MeOH was probably because that it lacks hydrogen at the carbon alpha to the oxygen atom, which makes the resulting alkoxy radical inert towards TiO_2 .⁵⁸ Air or oxygen in the air was found to be essential as the reaction barely proceeded under degassing conditions (entry 6). On the other hand, under an oxygen atmosphere, the [4+2] annulation reaction was completely suppressed, and a new product, endoperoxide was produced instead (entry 7).⁵⁹ Control studies showed that both light and the catalyst were required for the annulation reaction

to occur. Very little reaction was observed in the dark (entry 8). In comparison, without the catalyst, although the majority of cyclobutylaniline **1a** was consumed (72% conversion), product **3a** was detected in 9% yield (entry 9).

Table 2.4.1. Optimization of $\text{Ti}^{3+}@\text{TiO}_2$ catalyzed [4+2] annulation



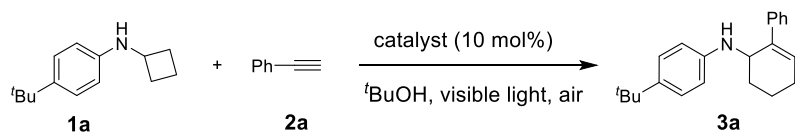
Entry ^[a]	Condition	Solvent	t [h]	Conversion 1a [%] ^[b]	Yield 3a [%] ^[b]
1	$\text{Ti}^{3+}@\text{TiO}_2$	MeOH	14	40	3
2	$\text{Ti}^{3+}@\text{TiO}_2$	CH_3NO_2	14	28	2
3	$\text{Ti}^{3+}@\text{TiO}_2$	DMF	14	18	14
4	$\text{Ti}^{3+}@\text{TiO}_2$	DMSO	14	97	78
5	$\text{Ti}^{3+}@\text{TiO}_2$	$^t\text{BuOH}$	14	100	83
6 ^[c]	$\text{Ti}^{3+}@\text{TiO}_2$	$^t\text{BuOH}$	14	16	8
7 ^[d]	$\text{Ti}^{3+}@\text{TiO}_2$, dark	$^t\text{BuOH}$	14	100	0 ^[e]
8	$\text{Ti}^{3+}@\text{TiO}_2$, dark	$^t\text{BuOH}$	14	5	0
9	No catalyst	$^t\text{BuOH}$	14	72	9

[a] Reaction conditions: **1a** (0.2 mmol, 0.1 M in solvent), **2a** (0.6 mmol), **4a** (2 mg), irradiation with two 18 W LED light bulb at room temperature. [b] Measured by GC using dodecane as an internal standard. [c] Degassed and refilled with N_2 . [d] Degassed and refilled with O_2 . [e] Endoperoxide was isolated in 57% yield.

We anticipated that Ti^{3+} 's concentration in self-doped $\text{Ti}^{3+}@\text{TiO}_2$ would greatly affect TiO_2 's photoactivity as it was shown to enhance visible light absorption while reduce the band

gap. However, in controlling the Ti^{3+} 's concentration, other parameters of the forming TiO_2 crystals such as phase, size, crystallinity, BET surface areas, and defect were also affected. All these factors were intertwined, and would collectively determine TiO_2 's photocatalytic activity, which unfortunately made it difficult for us to choose a specific TiO_2 to catalyze the targeted reaction. We previously studied water splitting catalyzed by self-doped $\text{Ti}^{3+}@\text{TiO}_2$ with various concentrations of Ti^{3+} , and the optimal TiO_2 didn't have the highest concentration of Ti^{3+} . Coincidentally, the optimal catalyst for water splitting turned out to be also the best for the annulation reaction (entry 3, Table 2.4.2). It has been suggested that better crystallinity and less defect favor water splitting, while surface area is generally more important than crystallinity for photodecomposition of organic pollutants. Our screening results of self-doped $\text{Ti}^{3+}@\text{TiO}_2$ with various concentrations of Ti^{3+} suggested that adsorption of the substrates was not as important as we anticipated and thus supported that ${}^1\text{O}_2$ rather than the hole oxidized cyclobutylanilines. However, more mechanistic studies will be required to establish this thesis. For comparison, we examined commercially available TiO_2 (P25) in the annulation reaction (entry 5). It was inferior to all self-doped $\text{Ti}^{3+}@\text{TiO}_2$ examined, which strengthened our argument for studying self-doped $\text{Ti}^{3+}@\text{TiO}_2$ to catalyze organic reactions.

Table 2.4.2. Evaluation of Ti^{3+} influence in $\text{Ti}^{3+}@\text{TiO}_2$.



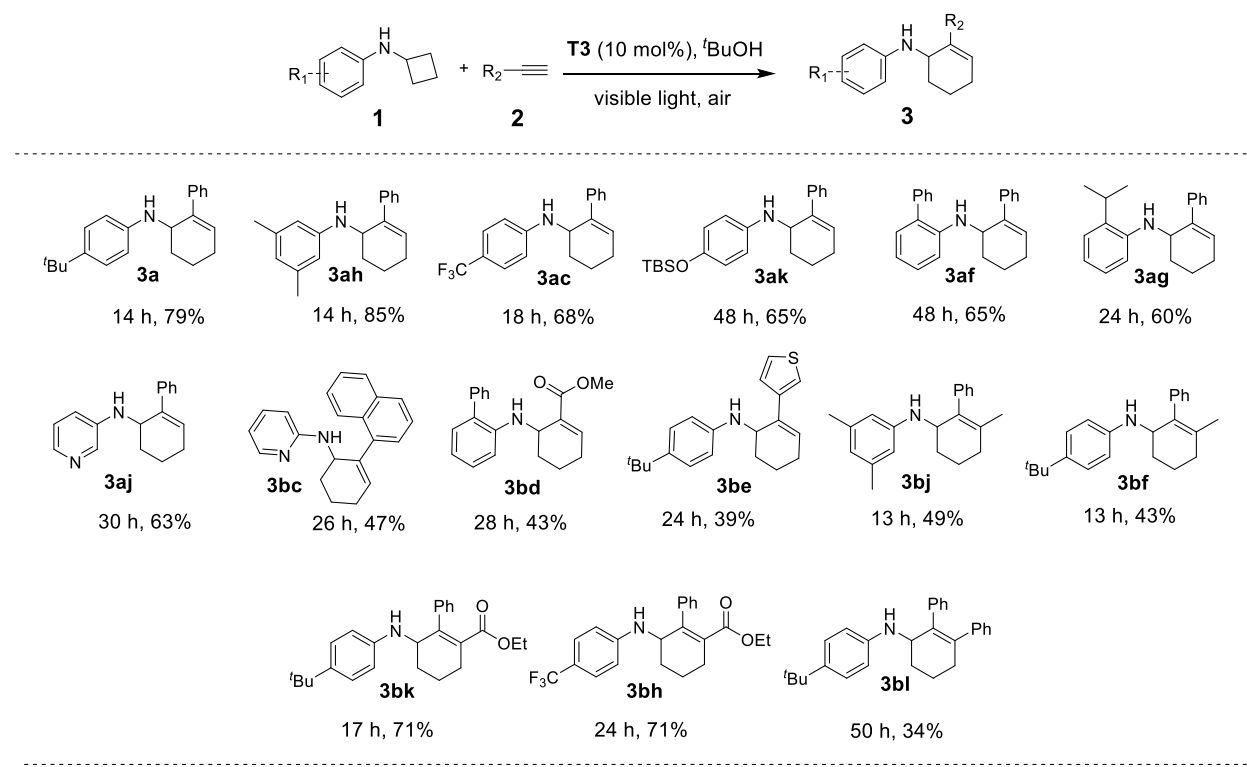
Entry ^[a]	Catalyst [4]	Concentration of Ti^{3+} ($\mu\text{mol/g}$)	t [h]	Conversion 1a [%] ^[b]	Yield 3a [%] ^[b]
1	$\text{Ti}^{3+}@\text{TiO}_2$ (T1)	0.3	14	70	21
2	$\text{Ti}^{3+}@\text{TiO}_2$ (T2)	4.5	14	83	39
3	$\text{Ti}^{3+}@\text{TiO}_2$ (4a) (T3)	16.7	14	100	82
4	$\text{Ti}^{3+}@\text{TiO}_2$ (T4)	25.5	14	82	45
5	TiO_2 (P25)	0	14	72	20

[a] Reaction conditions: **1a** (0.2 mmol, 0.1 M in $^t\text{BuOH}$), **2a** (0.6 mmol), **4** (2 mg) irriadiation with two 18 W LED lightbulb at room temperature. [b] Measured by GC using dodecane as an internal standard.

2.4.2 Substrate Scope.

Using the optimized conditions (entry 5, scheme 2.4.3), we examined the scope of cyclobutylanilines and alkynes (scheme 2.4.3). The annulation catalyzed by **T3** displayed the scope similar to the homogeneous variant catalyzed by $\text{Ir}(\text{ppy})_2(\text{dtbbpy})\text{PF}_6$, although somewhat lower yields (34-85%) than the latter (42-93%) were generally observed. Also similar to the homogeneous variant, the substituents on the *N*-aryl group were well tolerated. Electron donating groups (e.g., *p*- ^tBu **3a**, *p*-OTBS **3ak**, and *o*-Ph **3af**), electron withdrawing substituents (e.g., *p*- CF_3 **3ac**), and bulky groups (e.g., *o*- ^iPr **3ag**) were all amenable to the annulation, as were

heterocycles such as pyridine (**3aj** and **3bc**). For the other annulation partner, alkynes, the confinement was that they had to bear with at least one substituent capable of stabilizing radicals (e.g., Ph or CO₂Me). The reactivity pattern displayed by alkynes was consistent with intermolecular addition of alkyl radicals to alkynes, one of the key steps in what we proposed for the Ir-catalyzed [4+2] annulation as well as the one catalyzed by **T3** (see scheme 2.4.4). However, diphenylacetylene, which was not reactive in the Ir-catalyzed annulation, surprisingly participated in the annulation catalyzed by self-doped Ti³⁺@TiO₂, providing product **3bl** in modest yield. This result highlighted the difference of reactivity between homogeneous photocatalysis and semiconductor photocatalysis, as we discussed in the introduction.

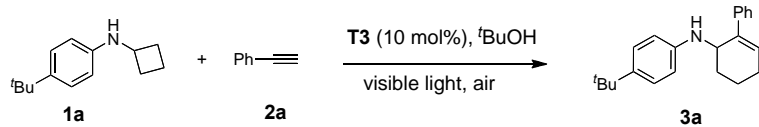


[a] Reaction condition: substrate **1** (0.2 mmol, 0.1 M in *t*-BuOH), **2** (0.6 mmol), **T3** (2 mg, 10 mol%), irradiation with two 18 W white LED light bulbs. [b] Isolated yield after silica gel chromatograph.

Scheme 2.4.3. Substrate Scope of the [4+2] Annulation Catalyzed by Self-doped Ti³⁺@TiO₂^{a,b}

2.4.3 Catalyst Reuse.

Facile separation and repeated use of catalysts are two of the significant strengths that heterogeneous catalysis holds over homogeneous catalysis. To exploit these two strengths in our self doped $Ti^{3+}@\text{TiO}_2$ system, we performed the annulation of cyclobutylaniline **1a** and phenylacetylene **2a** catalyzed by the same batch of **T3** for 5 cycles. A representative procedure of recycling **T3** for each run was as follows: after 14 h of irradiation, the reaction tube was centrifuged for 5 min; the clear liquid was removed for determination of GC yield of product **3a**; the solid residue was washed with $t\text{BuOH}$ (0.5 mL) three times and then used for the next cycle. The GC yield of **3a** for each cycle was held steady (Figure 2.4.1), suggesting that there was no appreciable loss of activity for **T3** over 5 cycles. To support this thesis, we took TEM images of **T3** before and after the five cycles. The size, shape, and morphology of **T3** changed very little after the five uses (Figures 2.4.2 and 2.4.3), further confirming the stability of **T3** as photocatalyst.



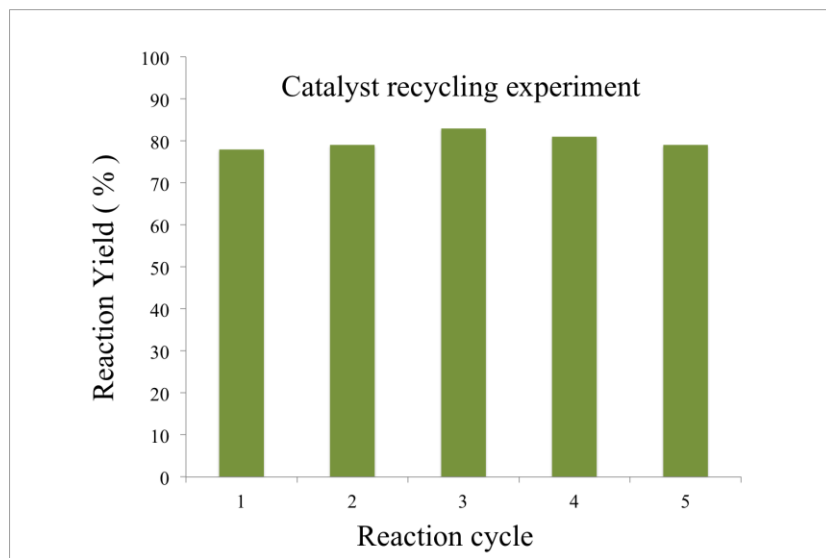


Figure 2.4.1. Catalyst Recycle.

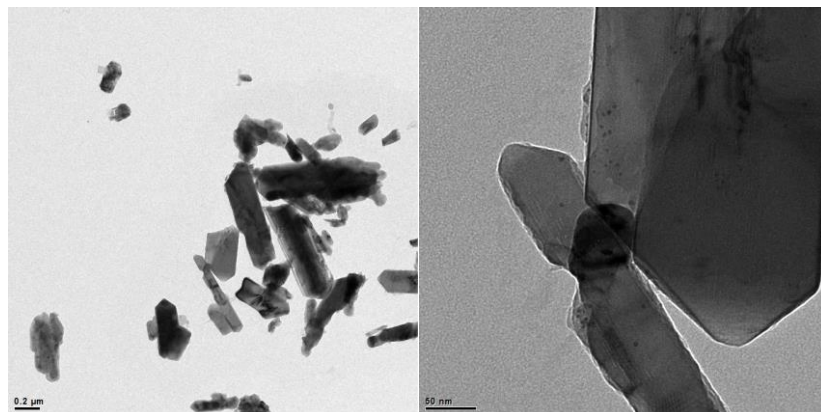


Figure 2.4.2. TEM Images of Self-doped $\text{Ti}^{3+}@\text{TiO}_2$ before Reactions.

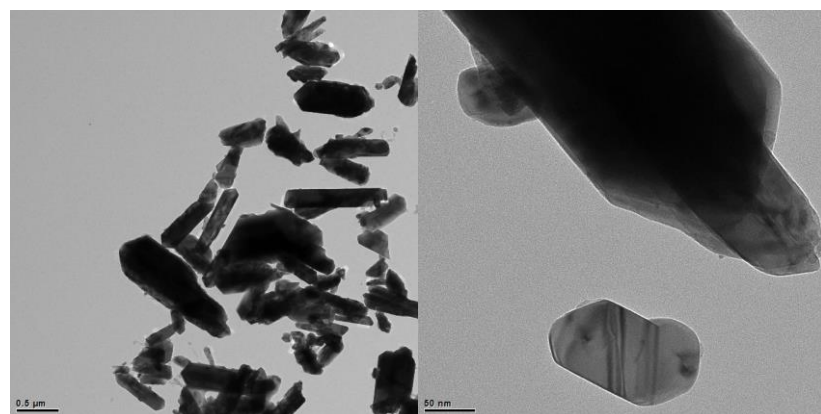
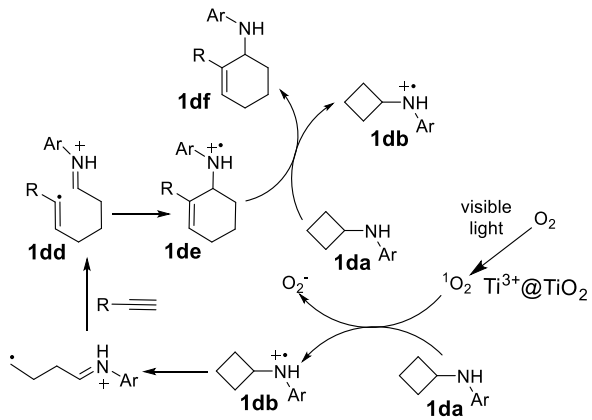


Figure 2.4.3. TEM Images of Self-doped $\text{Ti}^{3+}@\text{TiO}_2$ after 5 Runs.

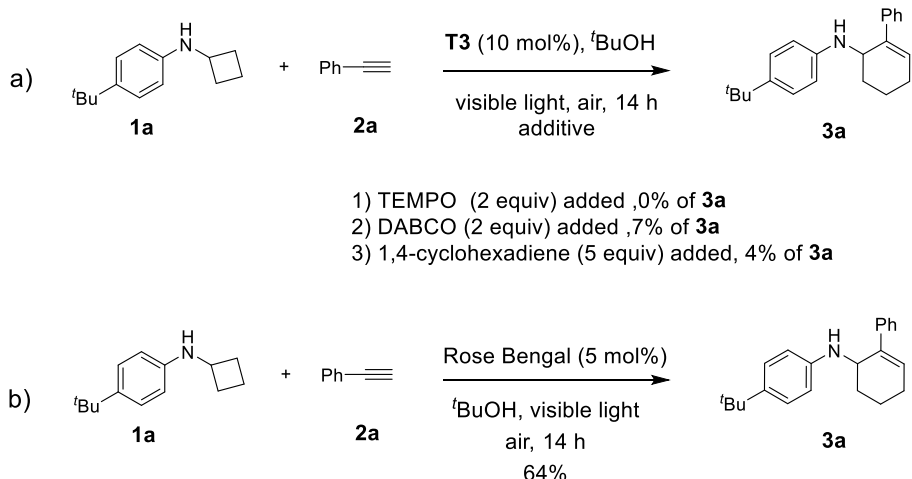
2.4.4 Mechanistic Studies.

Our working model for the [4+2] annulation catalyzed by self-doped $\text{Ti}^{3+}@\text{TiO}_2$ was similar to the one we previously proposed for the Ir-catalyzed annulation (Scheme 2.4.4).³² The noticeable changes between the two catalytic cycles were ascribed to the role of O_2 played in the reaction. Singlet oxygen, generated by visible light irradiation in the presence of a photosensitizer such as Rose Bengal or porphyrin derivatives, was shown to oxidize amines to the corresponding amine radical cations, which were subsequently converted to synthetically useful intermediates such as iminium ions or alpha-amino radicals. We anticipated that upon visible light irradiation, self-doped $\text{Ti}^{3+}@\text{TiO}_2$ sensitizes triplet oxygen to singlet oxygen, which affects the initial oxidation of cyclobutylaniline **1da** to amine radical cation **1db** in the place of the photoexcited Ir complex. Following the oxidation step, the two cycles shared the same elementary steps, such as ring opening of amine radical cation **1db** to distonic radical cation **1dc**, intermolecular addition of distonic radical cation **1dd** to alkyne, and intramolecular addition of vinyl radical **1de** to the iminium ion to form the cyclohexenyl ring. To close the catalytic cycle, we proposed a chain process in which the product radical cation **1de** is reduced to the product **1df** with concomitant oxidation of cyclobutylaniline **1da** to the amine radical cation **1db**. However, other pathways such as reduction of the product radical cation **1de** by superoxide or the electron in the conduction band of TiO_2 might also operate to close the catalytic cycle.



Scheme 2.4.4. Proposed Catalytic Cycle for the [4+2] Annulation Catalyzed by Self-doped $\text{Ti}^{3+}@\text{TiO}_2$.

A series of radical intermediates were proposed in the catalytic cycle. In order to lend indirect support of their existence, we decided to chemically perturb them. TEMPO, a radical scavenger shut down the reaction (Scheme 2.4.5). So did 1,4-cyclohexadiene, a good hydrogen donor (Scheme 2.4.5). Both data supported the involvement of radical intermediates. Since $^1\text{O}_2$ was proposed to be the actual oxidant oxidizing cyclobutylanilines and triggering the serial radical events, we envisioned that self-doped $\text{Ti}^{3+}@\text{TiO}_2$ could be replaced by another $^1\text{O}_2$ photosensitizer, such as Rose Bengal. Indeed, Rose Bengal catalyzed the annulation rather efficiently under visible light irradiation, and afforded product **3a** in 64% yield (Scheme 2.5.4). On the other hand, DABCO, a $^1\text{O}_2$ quencher,⁶⁰ almost completely inhibited the annulation reaction (Scheme 2.4.5). These two results were consistent with our proposed catalytic cycle involving $^1\text{O}_2$.



Scheme 2.4.5. Chemical Probes for the Involvement of $^1\text{O}_2$ and Radical Intermediates.

Although we obtained rather strong evidence to indirectly support the involvement of $^1\text{O}_2$, the important roles played by $^1\text{O}_2$ in a variety of fields and complexity of its detection particularly on the semiconductor surface prompted us to further investigate the formation of $^1\text{O}_2$. We focused on spectroscopic methods that permit us to detect $^1\text{O}_2$. Two methods, EPR and SOSG⁶¹, were chosen because of their robustness, sensitivity, and especially capability for differentiation of ROS. 2,2,6,6-Tetramethylpiperidine (TEMP), a spin trap specifically for detection of $^1\text{O}_2$, was used in our EPR studies. Two sets of data over a period of 10 min were collected. In the first set, a suspension of **T3** and TEMP in $^1\text{BuOH}$ was irradiated by a 8 W LED, and EPR spectra were then recorded after 0 min, 1 min, 5 min, and 10 min. The signals corresponding to 2,2,6,6-tetramethyl-1-piperidinyloxy (TEMPO), the product of $^1\text{O}_2$ and TEMP, increased as the time progressed (Figure 2.4.4). In the second set, cyclobutylaniline **1a** was added in addition to **T3** and TEMP in $^1\text{BuOH}$. EPR spectra were recorded after 0 min, 1 min, 5 min, and 10 min irradiation by the 8 W LED. The signals of TEMPO initially grew and then depleted (Figure 2.4.5). This observation could be rationalized by the following: the concentration of $^1\text{O}_2$ grew upon more irradiation and then began to deplete when it started to

react with **1a** and/or TEMPO reacted with the radical intermediates in the proposed catalytic cycle (Scheme 2.4.4). We also performed a control study in which TEMP in *t*BuOH without **T3** was irradiated. A lower level of TEMPO was detected, and more importantly, the intensity of the signals changed very little over the time (Figure 2.4.6). Thus the TEMPO signals likely resulted from the background. Overall, the EPR data provided another strong evidence to support the involvement of $^1\text{O}_2$.

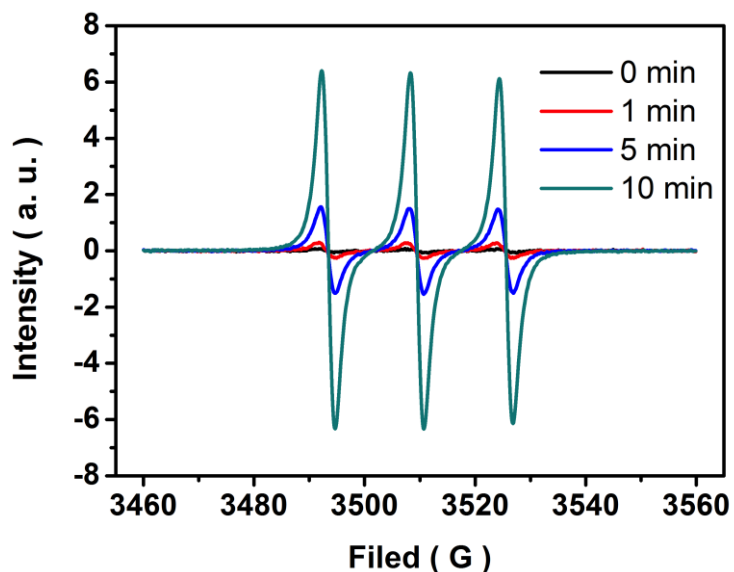


Figure 2.4.4. Trapping of $^1\text{O}_2$ by TEMP without cyclobutylaniline **1a**.

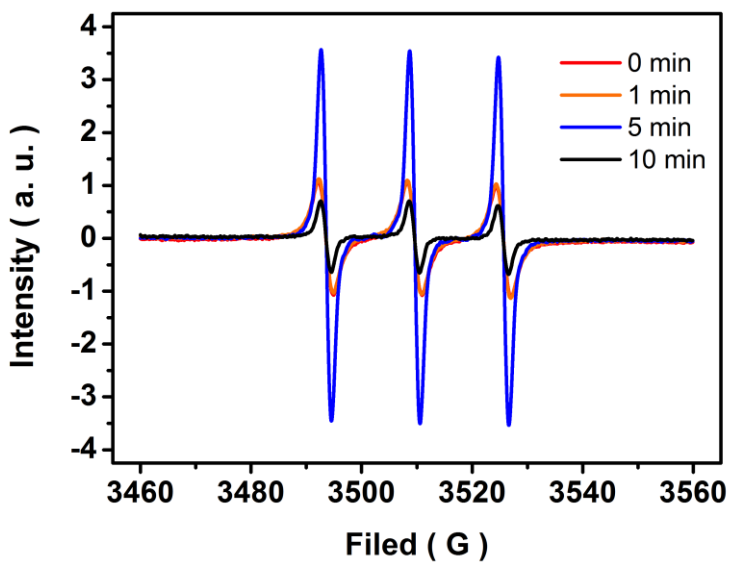


Figure 2.4.5. Trapping of $^1\text{O}_2$ by TEMP with cyclobutylaniline **1a**.

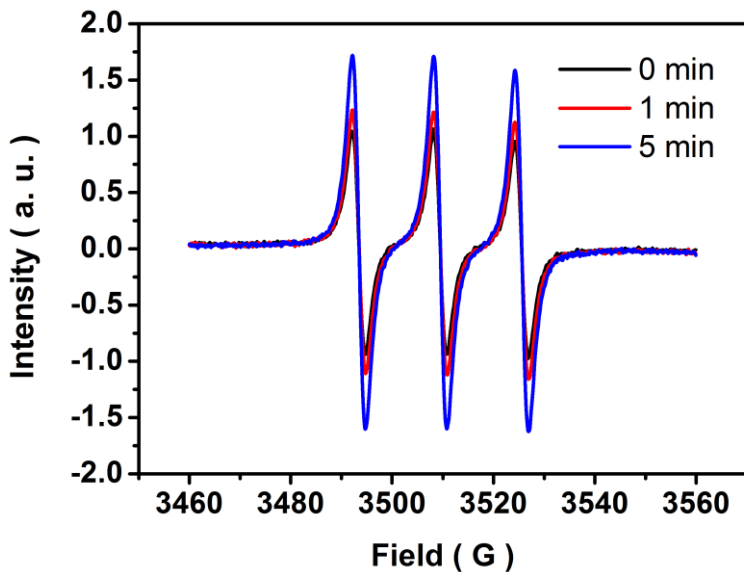


Figure 2.4.6. Control: Trapping of $^1\text{O}_2$ Generated by Visible Light Irradiation without $\text{Ti}^{3+}@\text{TiO}_2$.

The commercially available Singlet Oxygen Sensor Green (SOSG),⁶¹ which is popularized by biochemists for detection of $^1\text{O}_2$ in plants and other biological systems,⁶² is a highly specific molecular probe for $^1\text{O}_2$ and does not show any noticeable response towards

hydroxyl radical or superoxide. Recently, it was applied to detect ${}^1\text{O}_2$ generated on photoirradiated surface of surfaced-modified TiO_2 nanoparticles and metal nanoparticles.⁶³ We selected SOSG to qualitatively measure the efficiency of ${}^1\text{O}_2$ generation by self-doped $\text{Ti}^{3+}@\text{TiO}_2$ with various concentrations of $\text{Ti}(3+)$. Four self-doped TiO_2 samples (**T1**, **T2**, **T3**, and **T4**) were mixed with SOSG separately in 1:1 ${}^3\text{BuOH} : \text{D}_2\text{O}$. The resulting suspensions were irradiated by a 18 W white LED. As expected, strong fluorescence ($\lambda_{\text{em}} = 535 \text{ nm}$) was observed for the four TiO_2 samples (Figure 2.4.7). But unfortunately, they all produced fluorescence in similar intensity that could not be differentiated by the fluorometer. We also performed two control studies: one was **T3** with SOSG in the dark, while the other was SOSG without the self-doped TiO_2 . The ${}^1\text{O}_2$ generation was negligible in both studies. Again, although the SOSG studies didn't meet our goal to differentiate the TiO_2 samples' efficiency in generating ${}^1\text{O}_2$, they nevertheless unequivocally supported its formation.

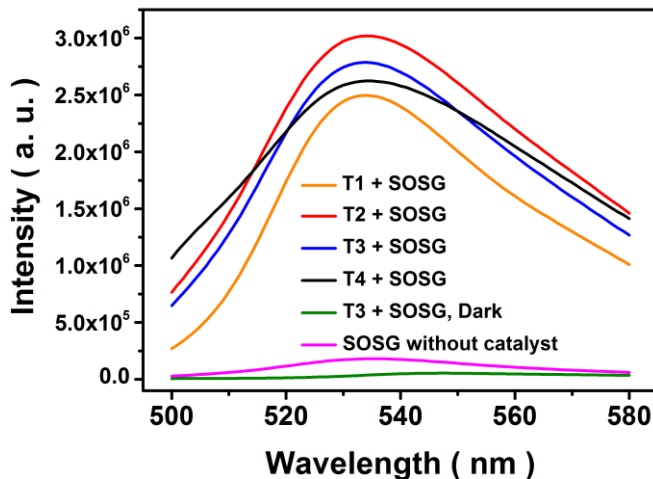
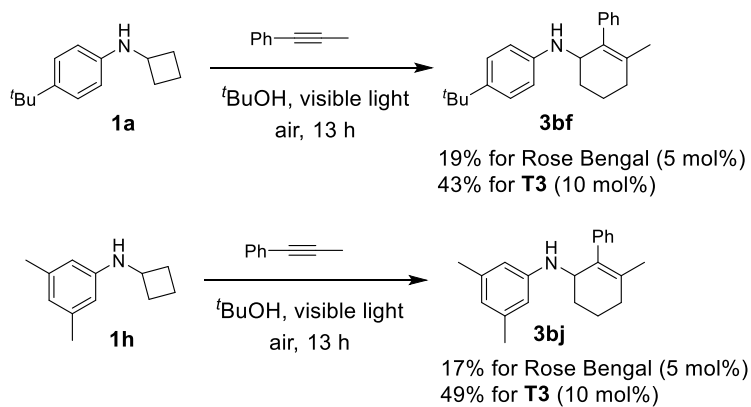


Figure 2.4.7. Fluorescence Spectra of SOSG in the Presence of Self-Doped $\text{Ti}^{3+}@\text{TiO}_2$ with light, without light, or in the Absence of Self-Doped $\text{Ti}^{3+}@\text{TiO}_2$.

Comparison with Rose Bengal.

In our mechanistic studies (vide supra), Rose Bengal was shown to catalyze the [4+2] annulation reaction in the place of self-doped $\text{Ti}^{3+}@\text{TiO}_2$ (**T3**), affording product **3a** in slightly lower yield. Since Rose Bengal is one of the widely used photosensitizers for ${}^1\text{O}_2$ generation, to demonstrate that **T3** is a more efficient and recyclable alternative to Rose Bengal, we decided to benchmark **T3** against the latter in the [4+2] annulation reaction. We performed two annulation reactions, and in both cases, **T3** gave the products in higher yields (Scheme 2.4.6).



Scheme 2.4.6. Comparison of Self-doped $\text{Ti}^{3+}@\text{TiO}_2$ against Rose Bengal.

2.3.5. Experimental Section

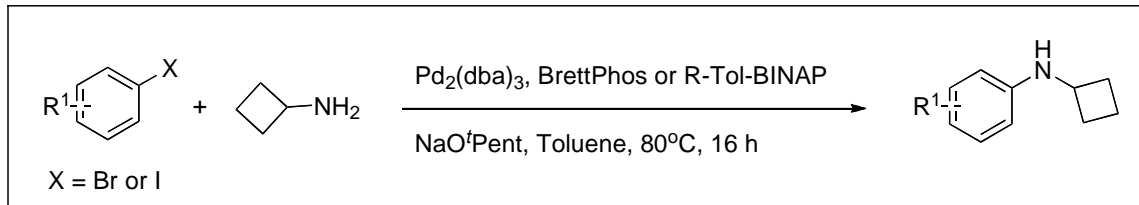
General Considerations

All reactions were carried out under a nitrogen atmosphere unless otherwise stated. Dry solvents were used as received from chemical supplies except THF, CH_2Cl_2 , Et_2O , and toluene. They were rigorously purged with argon for 2 h and then further purified by passing through two

packed columns of neutral alumina (for THF and Et₂O) or through neutral alumina and copper(II) oxide (for toluene and CH₂Cl₂) under argon from a solvent purification system. Column chromatography was carried out with silica gel (230-400 mesh). All new compounds were characterized by ¹H NMR, ¹³C NMR, IR spectroscopy, high-resolution mass spectroscopy (HRMS). Nuclear magnetic resonance (NMR) spectra were obtained on a Bruker Avance DPX-300 and Bruker Avance DPX-400. Chemical shifts (δ) were reported in parts per million (ppm) relative to residual proton signals in CDCl₃ (7.27 ppm, 77.23 ppm) at room temperature. IR spectra were recorded (thin film on NaCl plates) on a PerkinElmer Spectrum 100 series instrument. High resolution mass spectra were recorded on a Bruker Ultraflex II TOF/TOF Mass Spectrometer or IonSpec Ultima Fourier Transform Mass Spectrometer. Gas chromatography/mass spectroscopy (GC/MS) analyses were performed on an Agilent 6890N Network GC System/5973 inert Mass Selective Detector. Gas chromatography analyses were performed using a Shimadzu GC-2010 Plus instrument.

2.3.5 Experimental Procedures and Spectroscopic Data

General procedure 1 (GP1): Preparation of N-Cyclobutylanilines

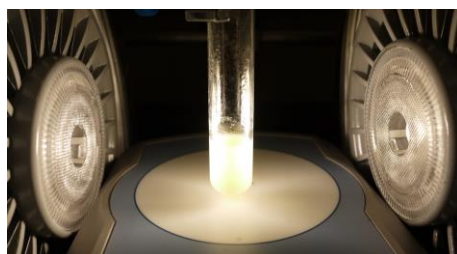


To an oven-dried test tube equipped with a stir bar were added 0.01 mmol of Pd₂(dba)₃ and 0.03 mmol of ligand ((R)-Tol-BINAP or BrettPhos). Glove box was used to add 1.5 mmol of NaO^tPent and the tube was sealed with a Teflon screw cap. Aryl halide (1 mmol),

cyclobutylamine (1.6 mmol), and toluene (2 mL) were then added to the reaction mixture and heated at 80 °C for 16 h. After completion, the reaction mixture was cooled to room temperature, diluted with diethyl ether, filtered over a short pad of silica gel, and concentrated in vacuum. Purification by flash chromatography on silica gel afforded *N*-cyclobutylaniline.

For the detailed preparation and characterization of *N*-cyclobutylanilines **1a**, **1ac**, **1ah**, **1ak**, **1af**, **1ag**, **1aj**, **1ai**, correspond to those described in the literatures.³¹

General Procedure 2 (GP2); Visible light catalyzed [4+2] annulation reaction



An oven-dried test tube equipped with a stir bar was charged with $\text{Ti}^{3+}@\text{TiO}_2$ (2 mg) and *N*-cyclobutylaniline derivative (0.2 mmol), alkyne derivative (0.6 mmol), and $^3\text{BuOH}$ (2 mL). The test tube was capped with a Teflon screw cap and the reaction mixture was sonicated for 3 minutes followed by irradiation with two LED (18 watts) positioned 6 cm from the test tube. After the reaction was complete, monitored by TLC, the mixture was diluted with diethyl ether and filtered through a short pad of silica gel. The solution was concentrated and the residue was purified by silica gel flash chromatography to afford the corresponding annulation products.

Light Source Information:

The 18-Watt White LED light bulb used in the experiments was manufactured by Sylvania. Its model number was: Sylvania 78495 18-Watt Ultra LED for PAR38 Narrow

Floodlight. We purchased the LED light bulbs from a local store of Lowe's Home Improvement. The spectral flux graph of the LED light bulb shown below was provided by Sylvania.

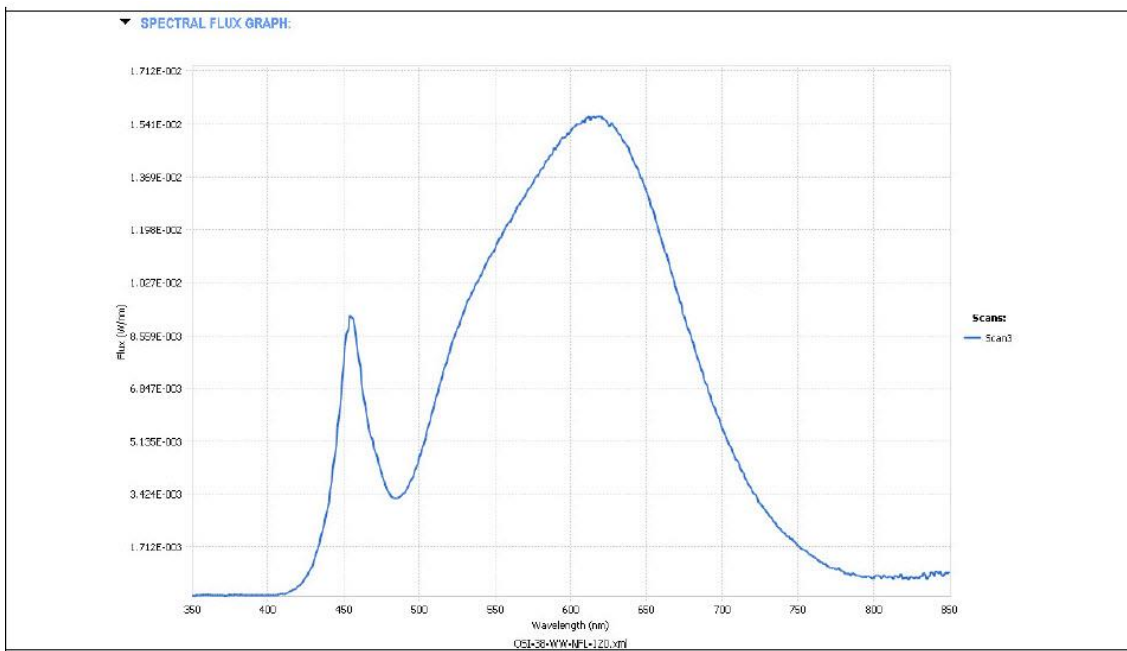


Figure 2.4.8. Light source flux graph.

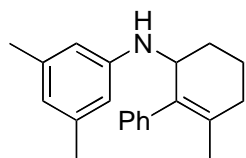
Catalysts Preparation:

A series of $\text{Ti}^{3+}@\text{TiO}_2$ that differs in the concentration of Ti^{3+} were prepared using two methods reported by the Feng group. **T3** was prepared by mixing titanium powder (0.3 g) and hydrochloric acid (10 mL, 2 M), the mixture was then hydrothermally treated under 220 °C for 12 h.³ **T1**, **T2**, and **T4** were prepared by the addition of titanium (IV) isopropoxide (2.0 g) dropwise to a mixture of ethanol (10.0 g), 2-ethylimidazole (0.1-2.5 g) and hydrochloric acid (2.5 g, 37.1%), followed by combustion of the mixture in a 500 °C oven for 5 h.⁴ The concentration of Ti^{3+} in the $\text{Ti}^{3+}@\text{TiO}_2$ was determined by EPR with the absolute accuracy of approximate $\pm 20\%$.

Compounds Characterization:

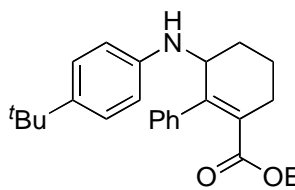
Characterization of annulation products **3a**, **3ah**, **3ac**, **3ak**, **3af**, **3ag**, **3aj**, **3bc**, **3bd**, **3be**, **3bf** and **3bh** were described in the literature.³²

3,5-dimethyl-N-(3-methyl-2-phenylcyclohex-2-enyl)aniline (3bj): Following **GP2**, the product



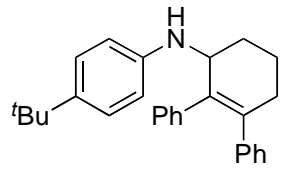
was isolated after a flash chromatography on silica gel (1: 30 EtOAc/hexanes). Yellow oil (29 mg, 49%); IR ν_{max} (cm⁻¹) 3401, 3022, 2924, 2857, 1599, 1491, 1441, 1336, 1185, 1117, 824; ¹H NMR (400 MHz, CDCl₃) δ 7.32 – 7.25 (m, 2H), 7.23 – 7.17 (m, 3H), 6.28 (s, 1H), 6.17 (d, *J* = 1.5 Hz, 2H), 4.17 (d, *J* = 3.4 Hz, 1H), 2.19 (q, *J* = 0.6 Hz, 6H), 2.17 – 2.02 (m, 3H), 1.79 – 1.63 (m, 3H), 1.60 (dd, *J* = 1.4, 0.7 Hz, 3H). ¹³C NMR (75 MHz, CDCl₃) δ 147.27, 141.99, 138.78, 134.42, 133.25, 128.89, 128.03, 126.35, 118.71, 110.88, 51.79, 31.71, 27.69, 21.49, 21.13, 17.82. HRMS (ESI) m/z [M+H]⁺, calc'd for C₂₁H₂₅N 292.2060; found 292.2057.

Ethyl 3-(4-*tert*-butylphenylamino)-2-phenylcyclohex-1-enecarboxylate (3bk): Following



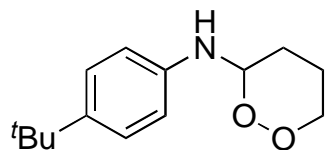
GP2, the product was isolated after a flash chromatography on silica gel (1: 5 EtOAc/hexanes). Yellow oil (54 mg, 71%); IR ν_{max} (cm⁻¹) 3405, 2952, 1706, 1613, 1510, 1369, 1270, 1242, 1194, 1051, 819, 758; ¹H NMR (400 MHz, CDCl₃) δ 7.36 – 7.23 (m, 5H), 7.23 – 7.14 (m, 2H), 6.55 (d, *J* = 8.1 Hz, 2H), 4.36 (d, *J* = 4.4 Hz, 1H), 3.93 (q, *J* = 7.1 Hz, 2H), 2.65 (dt, *J* = 18.5, 3.9 Hz, 1H), 2.43 – 2.16 (m, 2H), 1.87 – 1.68 (m, 3H), 1.28 (s, 9H), 0.88 (t, *J* = 7.1 Hz, 3H). ¹³C NMR (75 MHz, CDCl₃) δ 170.25, 144.41, 142.67, 140.90, 140.00, 132.74, 128.10, 127.53, 127.47, 126.00, 112.76, 60.48, 51.58, 33.83, 31.55, 27.20, 27.04, 16.90, 13.56. HRMS (ESI) m/z [M+H]⁺, calc'd for C₂₅H₃₁NO₂ 378.2428; found 378.2425.

4-*tert*-butyl-N-(2,3-diphenylcyclohex-2-enyl)aniline (3bl): Following **GP2**, the product was



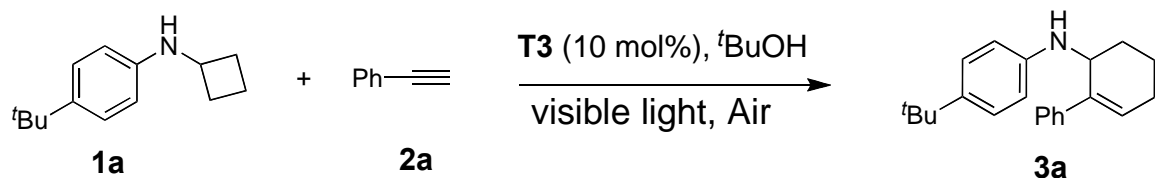
isolated after a flash chromatography on silica gel (1: 50 EtOAc/hexanes). colorless oil (26 mg, 34%); IR ν_{max} (cm⁻¹) 3401, 3051, 3021, 2944, 2862, 1612, 1516, 1442, 1361, 1301, 1260, 1193; ¹H NMR (400 MHz, CD₂Cl₂) δ 7.20 – 6.97 (m, 14H), 6.56 – 6.45 (m, 2H), 4.41 (m, 1H), 2.66 – 2.54 (m, 1H), 2.42 – 2.25 (m, 1H), 2.24 – 2.13 (m, 1H), 1.93 – 1.72 (m, 3H), 1.24 (d, J = 1.2 Hz, 9H). ¹³C NMR (101 MHz, CD₂Cl₂) δ 145.46, 143.84, 142.43, 140.27, 140.14, 136.18, 130.08, 129.57, 128.18, 128.10, 126.65, 126.57, 126.44, 112.93, 52.44, 34.18, 32.99, 31.81, 28.25, 18.60. FTMS (ESI) m/z [M+H]⁺, calc'd for C₂₈H₃₁N 382.2529; found 382.2531.

N-(4-*tert*-butylphenyl)-1,2-dioxan-3-amine: Following **GP2** with an oxygen balloon on top of



the reaction tube, the product was isolated after a flash chromatography on silica gel (1: 10 EtOAc/hexanes) as yellow solid (27 mg, 57%). m.p. 110-112 °C; IR ν_{max} (cm⁻¹) 3365, 2949, 2843, 1612, 1519, 1369, 1301, 1263, 1190, 1074, 1026, 954; ¹H NMR (300 MHz, CDCl₃) δ 7.28 – 7.19 (m, 2H), 6.82 – 6.69 (m, 2H), 5.45 – 5.31 (m, 1H), 4.32 (s, 1H), 4.18 – 4.09 (m, 2H), 2.17 – 1.99 (m, 2H), 1.92 (ddq, J = 10.8, 5.4, 2.8 Hz, 1H), 1.63 (tdd, J = 12.7, 9.7, 5.1 Hz, 1H), 1.28 (s, 9H). ¹³C NMR (75 MHz, CDCl₃) δ 142.66, 142.01, 126.27, 114.07, 85.96, 71.79, 34.16, 31.69, 29.55, 24.89. FTMS (ESI) m/z [M+H]⁺, calc'd for C₁₄H₂₁NO₂ 236.1645; found 236.1644.

Catalyst recycling experiment



An oven-dried test tube equipped with a stir bar was charged with **T3** (2 mg, 10 mol%) and *N*-cyclobutylaniline **1a** (0.041g, 0.2 mmol), phenylacetylene **2a** (0.072 mL, 0.6 mmol), and *t*BuOH (2 mL). The test tube was capped with a Teflon screw cap and the reaction mixture was sonicated for 3 min followed by irradiation with two LED (18 watts) positioned 6 cm from the test tube for 14 h. The test tube was centrifuged for 5 min and **T3** completely precipitated at the bottom of the tube. The reaction solution was then taken out for determination of GC yield with *n*-dodecane as internal standard. **T3** in the test tube was washed with 0.5 mL *t*BuOH three times for the next reaction cycle. The same reaction was repeated for 4 times. The reaction yields were determined to be 78%, 79%, 83%, 81% and 79% respectively for the five reaction cycles.

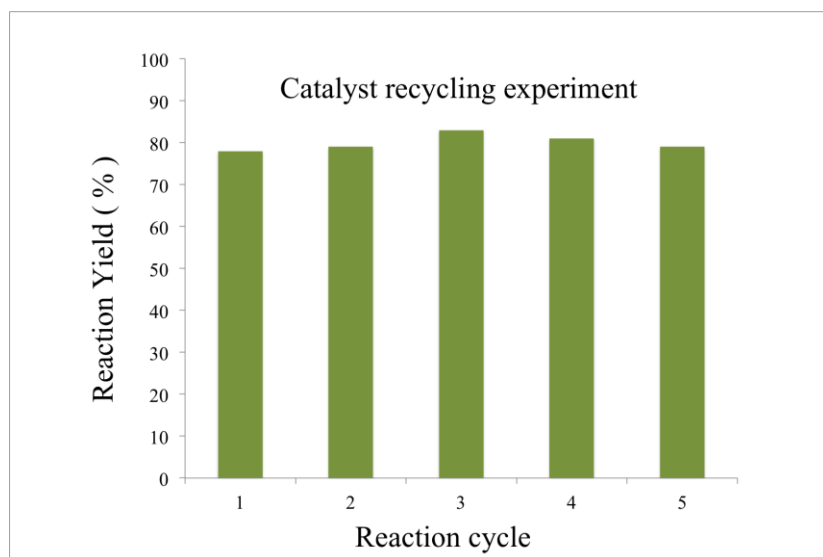


Figure 2.4.9. Catalyst recycling experiment.

We also conducted the catalyst recycling experiment for 6 h. The catalyst, **T3**, was recovered using the same method as for 14 h, and 5 cycles were completed. The conversion of **1a** and the GC yield of **3a** for each cycle were listed in the following table.

Reaction cycle	1	2	3	4	5
Conversion of 1a (%)	64	60	59	66	62
Yield of 3a (%)	53	52	49	54	52

EPR study:

EPR spectra were recorded on a Bruker E500 spectrometer with 2,2,6,6-tetramethylpiperidine (TEMP) as singlet oxygen ($^1\text{O}_2$) trap at room temperature. In order to detect $^1\text{O}_2$ generated by $\text{Ti}^{3+}@\text{TiO}_2$ (**T3**), 2 mg of **T3** was mixed with 4 mL of $^3\text{BuOH}$, the mixture was sonicated for 3 min for fully suspension to make mixture **A**. 100 μL of mixture **A** was transferred to a Bruker Aquax liquid sample cell, followed by the addition of 3 μL TEMP. The sample cell was then irradiated by 8 W LED for specific time (0 min, 1 min, 5 min and 10 min) prior to measurement with the EPR spectrometer. As shown in **Figure 2.4.10a**, a time dependent increase in $^1\text{O}_2$ production was observed as the detection of the formation of 2,2,6,6-tetramethylpiperidine-1-oxyl (TEMPO) by EPR spectrometer. Control reaction showed that without **T3**, there was little change in the formation of TEMPO with the increase of irradiation time (**Figure 2.4.10b**). We further tested the effect of *N*-cyclobutylaniline **1a** on the generation of $^1\text{O}_2$ by adding 0.2 mmol (0.041 g) of **1a** to 4 mL of $^3\text{BuOH}$ and 2 mg of **T3**. The mixture was then sonicated for 3 min to make mixture **B**. 100 μL of mixture **B** was transferred to a Bruker Aquax liquid sample cell, followed by the addition of 3 μL TEMP, and then the resulting

mixture was irradiated under 8 W LED. The amount of ${}^1\text{O}_2$, which was detected via the formation of TEMPO, grew during the first 5 min and then interestingly decreased afterwards (Figure 2.4.10c). One possible explanation for this phenomenon was that TEMPO reacted with the ring opening intermediate (the distonic radical ion) of *N*-cyclobutylaniline **1a**.

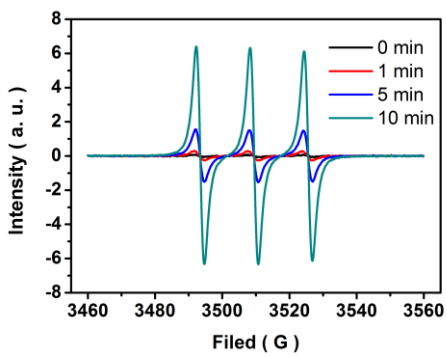


Figure 2.4.10a. ${}^1\text{O}_2$ from T3 trapped by TEMPO...

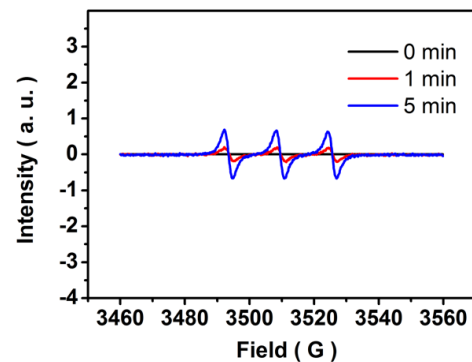


Figure 2.4.10b. ${}^1\text{O}_2$ trapped without T3

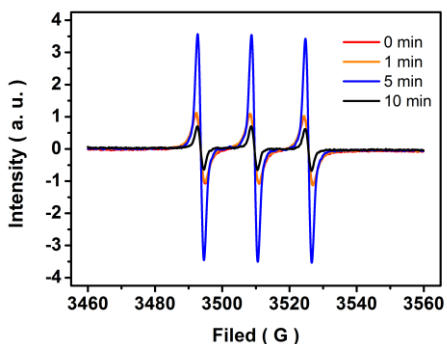


Figure 2.4.10c. Control experiment of addition of **1a**

Trapping $^1\text{O}_2$ by SOSG:

The trapping study was conducted using a Photon Technology Fluorescence Spectrophotometer. A stock solution of Singlet Oxygen Sensor Green (SOSG, molecular probe) was prepared by dissolving 100 μg of SOSG in methanol (33 μL) to make a concentration of 5 mM in dark. Taken from the stock solution, 0.1 mM of SOSG was added into a $\text{D}_2\text{O}/\text{BuOH}$ (1:1) mixture containing $\text{Ti}^{3+}@\text{TiO}_2$ (1 mg in 0.165 mL of $\text{D}_2\text{O}/\text{BuOH}$ (1:1), pre-sonication of the mixture for 10 min to fully suspend $\text{Ti}^{3+}@\text{TiO}_2$ in solvent). The mixture was then irradiated for 1 min using a 18 W LED light bulb, followed by recording the fluorescence emission of the product at 535 nm with the use of an excitation wavelength of 382 nm. A series of $\text{Ti}^{3+}@\text{TiO}_2$ with various Ti^{3+} concentration were examined, and they all generated $^1\text{O}_2$ as shown in **Figure 2.4.11**. However, there was no significant correlation between the concentration of Ti^{3+} in $\text{Ti}^{3+}@\text{TiO}_2$ and the amount of $^1\text{O}_2$ generated. Control experiments showed that without $\text{Ti}^{3+}@\text{TiO}_2$ or light, the amount of $^1\text{O}_2$ generated was almost negligible compared to that of $^1\text{O}_2$ generated by $\text{Ti}^{3+}@\text{TiO}_2$ in the presence of light.

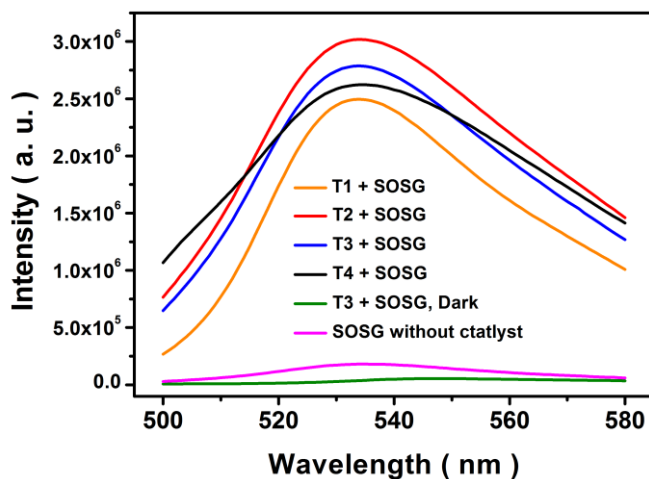


Figure 2.4.11. Fluorescence spectra of SOSG in the presence of $\text{Ti}^{3+}@\text{TiO}_2$, or in the absence of $\text{Ti}^{3+}@\text{TiO}_2$

Since D₂O was reported to greatly increase the lifetime of ¹O₂, a co-solvent of D₂O and ¹BuOH (1:1) was then used in the experiment of trapping ¹O₂ by SOSG, as is shown above. A control experiment of our standard [4+2] annulation reaction of **1a** and **2a** was also conducted using **GP2** in the co-solvent of D₂O and ¹BuOH (1:1, 2 mL). A GC yield of 64% of **3a** was obtained in comparision with the optimized reaction condition (83%, Figure 1, entry 5).

UV-visible absorption of Ti³⁺@TiO₂:

A series of UV-Vis diffuse reflectance experiments were carried out in order to support that our [4+2] annulation reactions are mediated by visible light (Figure 2.4.12). We first measured the spectrum of **T3** only, and found that the catalyst has an absorption in the visible light region between 400 and 500 nm. We then measured the UV-Vis diffuse reflectance spectra of **T3** complexed with either *N*-cyclobutylaniline **1a** or phenylacetylene **2a**. The surface complex showed slight redshift. Compared against the spectrum flux graph of the LED light bulb, **T3** or the surface complex of **T3** with either **1a** or **2a** was capable of absorbing the light.

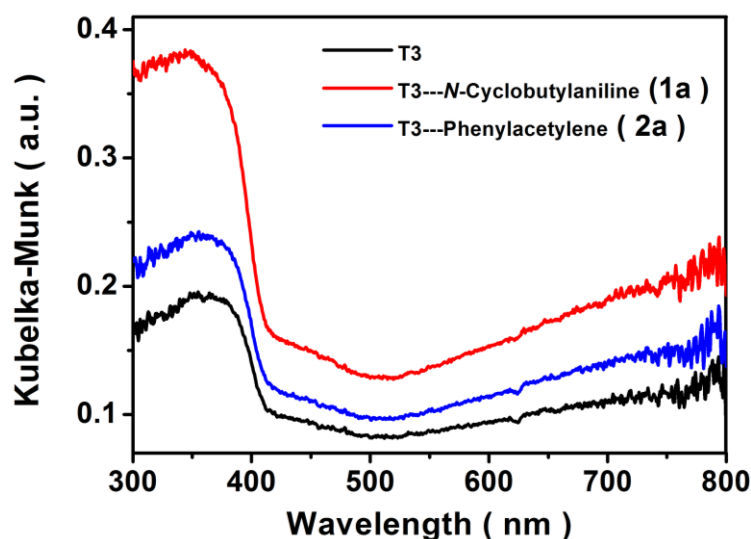


Figure 2.4.12. Absorption spectra of Ti³⁺@TiO₂, *N*-cyclobutylaniline adsorbed onto Ti³⁺@TiO₂ surface and phenylacetylene adsorbed onto the Ti³⁺@TiO₂ surface.

Preparation of **T3** absorbed with *N*-cyclobutylaniline **1a** or phenylacetylene **2a**: 20 mg of $\text{Ti}^{3+}@\text{TiO}_2$ (**T3**) was added into 2 mL $^t\text{BuOH}$ solution containing 0.6 mmol of *N*-cyclobutylaniline **1a** or 0.6 mmol of phenylacetylene **2a**, followed by stirring for 12 h under room temperature. The surface complex was then collected by centrifuge and washed with 2 mL of $^t\text{BuOH}$ for 3 times, followed by drying under room temperature. The obtained sample was denoted as **T3-N**-cyclobutylaniline (**1a**) or **T3-Phenylacetylene** (**2a**). The UV-Vis diffuse reflectance spectra were recorded on a Shimadzu UV-3101PC UV-Vis-NIR spectrophotometer operating in the diffuse mode based on the Kubelka-Munk equation.

2.3.6 Summary

We have successfully developed a heterogeneous [4+2] annulation of cyclobutylanilines with alkynes catalyzed by self-doped $\text{Ti}^{3+}@\text{TiO}_2$. The substrate scope is comparable to that of the homogeneous variant catalyzed by a far more expensive iridium complex. Self-doped $\text{Ti}^{3+}@\text{TiO}_2$ has shown excellent stability under the conditions of the annulation reaction. No appreciable loss of activity has been observed after it was reused to catalyze the annulation for 5 consecutive times. Recycling the TiO_2 is trivial. The catalyst is collected by centrifuge, washed by fresh solvent three times, and then used directly in the next reaction. Mechanistically, we have conducted a series of experiments to probe [4+2] annulation. All the data support that upon visible light irradiation, self-doped $\text{Ti}^{3+}@\text{TiO}_2$ sensitizes triplet O_2 to singlet O_2 , which then oxidizes cyclobutylanilines to the amine radical cations and initializes the serial radical events en route to the annulation product. Interestingly, the most active self-doped TiO_2 doesn't have the highest concentration of Ti^{3+} . Other parameters of the catalyst such as phase composition (anatase vs. rutile), surface area, crystallinity, and defect all contribute to the TiO_2 's overall

catalytic performance. Self-doped TiO₂ has been compared favorably against Rose Bengal as ¹O₂ photosensitizer in terms of efficiency and recyclability. More studies on improving self-doped TiO₂'s catalytic activity and developing new reactions are ongoing.

2.6 Reference:

1. (a) Trost, B. M., Strain and reactivity: Partners for selective synthesis. In *Small Ring Compounds in Organic Synthesis I*, de Meijere, A., Ed. Springer Berlin Heidelberg: Berlin, Heidelberg, 1986; pp 3-82. (b) Rybtchinski, B.; Milstein, D., Metal Insertion into C–C Bonds in Solution. *Angewandte Chemie International Edition* **1999**, *38* (7), 870-883. (c) Rybtchinski, B.; Milstein, D., Metallinsertion in C-C-Bindungen in Lösung. *Angewandte Chemie* **1999**, *111* (7), 918-932. (d) Walczak, M. A. A.; Krainz, T.; Wipf, P., Ring-Strain-Enabled Reaction Discovery: New Heterocycles from Bicyclo[1.1.0]butanes. *Accounts of Chemical Research* **2015**, *48* (4), 1149-1158.
2. (a) Reissig, H.-U.; Zimmer, R., Donor–Acceptor-Substituted Cyclopropane Derivatives and Their Application in Organic Synthesis. *Chemical Reviews* **2003**, *103* (4), 1151-1196. (b) Yu, M.; Pagenkopf, B. L., Recent advances in donor–acceptor (DA) cyclopropanes. *Tetrahedron* **2005**, *61* (2), 321-347. (c) Carson, C. A.; Kerr, M. A., Heterocycles from cyclopropanes: applications in natural product synthesis. *Chemical Society Reviews* **2009**, *38* (11), 3051-3060.
3. (a) Maity, S.; Zhu, M.; Shinaberger, R. S.; Zheng, N., Intermolecular [3+2] Cycloaddition of Cyclopropylamines with Olefins by Visible-Light Photocatalysis. *Angewandte Chemie International Edition* **2012**, *51* (1), 222-226. (b) Nguyen, T. H.; Maity, S.; Zheng, N., Visible light mediated intermolecular [3 + 2] annulation of cyclopropylanilines with alkynes. *Beilstein Journal of Organic Chemistry* **2014**, *10*, 975-980. (c) Nguyen, T. H.; Morris, S. A.; Zheng, N., Intermolecular [3+2] Annulation of Cyclopropylanilines with Alkynes, Enynes, and Diynes via Visible Light Photocatalysis. *Advanced Synthesis & Catalysis* **2014**, *356* (13), 2831-2837.
4. The oxidation peak potential of 4-*tert*-butyl-*N*-cyclobutylaniline was measured to be +0.8 V vs. SCE in comparison with +0.83 V vs. SCE for *N*-cyclopropylaniline.
5. (a) Wiberg, K. B., Cyclobutane—Physical Properties and Theoretical Studies. In *The Chemistry of Cyclobutanes*, John Wiley & Sons, Ltd: 2006; pp 1-15. (b) Khoury, P. R.; Goddard, J. D.; Tam, W., Ring strain energies: substituted rings, norbornanes, norbornenes and norbornadienes. *Tetrahedron* **2004**, *60* (37), 8103-8112.
6. (a) Bach, R. D.; Dmitrenko, O., Strain Energy of Small Ring Hydrocarbons. Influence of C–H Bond Dissociation Energies. *Journal of the American Chemical Society* **2004**, *126* (13), 4444-4452. (b) Wu, W.; Ma, B.; I-Chia Wu, J.; Schleyer, P. v. R.; Mo, Y., Is Cyclopropane Really the σ-Aromatic Paradigm? *Chemistry – A European Journal* **2009**, *15* (38), 9730-9736.

7. (a) Musa, O. M.; Horner, J. H.; Shahin, H.; Newcomb, M., A Kinetic Scale for Dialkylaminyl Radical Reactions. *Journal of the American Chemical Society* **1996**, *118* (16), 3862-3868. (b) Jin, J.; Newcomb, M., Rate Constants and Arrhenius Functions for Ring Opening of a Cyclobutylcarbiny Radical Clock and for Hydrogen Atom Transfer From the Et₃B-MeOH Complex. *The Journal of Organic Chemistry* **2008**, *73* (12), 4740-4742.
8. Maeda, Y.; Ingold, K. U., Kinetic applications of electron paramagnetic resonance spectroscopy. 35. The search for a dialkylaminyl rearrangement. Ring opening of N-cyclobutyl-N-n-propylaminyl. *Journal of the American Chemical Society* **1980**, *102* (1), 328-331.
9. Horner, J. H.; Martinez, F. N.; Musa, O. M.; Newcomb, M.; Shahin, H. E., Kinetics of Dialkylaminium Cation Radical Reactions: Radical Clocks, Solvent Effects, Acidity Constants, and Rate Constants for Reactions with Hydrogen Atom Donors. *Journal of the American Chemical Society* **1995**, *117* (45), 11124-11133.
10. (a) Namyslo, J. C.; Kaufmann, D. E., The Application of Cyclobutane Derivatives in Organic Synthesis. *Chemical Reviews* **2003**, *103* (4), 1485-1538. (b) Seiser, T.; Saget, T.; Tran, D. N.; Cramer, N., Cyclobutanes in Catalysis. *Angewandte Chemie International Edition* **2011**, *50* (34), 7740-7752.
11. (a) Matsuo, J.-i.; Sasaki, S.; Tanaka, H.; Ishibashi, H., Lewis Acid-Catalyzed Intermolecular [4 + 2] Cycloaddition of 3-Alkoxyyclobutanones to Aldehydes and Ketones. *Journal of the American Chemical Society* **2008**, *130* (35), 11600-11601. (b) Matsuo, J.-i.; Negishi, S.; Ishibashi, H., Formal [4+2] cycloaddition between 3-ethoxycyclobutanones and silyl enol ethers. *Tetrahedron Letters* **2009**, *50* (42), 5831-5833. (c) Kawano, M.; Kiuchi, T.; Negishi, S.; Tanaka, H.; Hoshikawa, T.; Matsuo, J.-i.; Ishibashi, H., Regioselective Inter- and Intramolecular Formal [4+2] Cycloaddition of Cyclobutanones with Indoles and Total Synthesis of (\pm)-Aspidospermidine. *Angewandte Chemie International Edition* **2013**, *52* (3), 906-910. (d) Parsons, A. T.; Johnson, J. S., Formal [4 + 2] Cycloaddition of Donor-Acceptor Cyclobutanes and Aldehydes: Stereoselective Access to Substituted Tetrahydropyrans. *Journal of the American Chemical Society* **2009**, *131* (40), 14202-14203. (e) Moustafa, M. M. A. R.; Stevens, A. C.; Machin, B. P.; Pagenkopf, B. L., Formal [4 + 2] Cycloaddition of Alkoxy-Substituted Donor-Acceptor Cyclobutanes and Aldehydes Catalyzed by Yb(OTf)₃. *Organic Letters* **2010**, *12* (21), 4736-4738. (f) Stevens, A. C.; Palmer, C.; Pagenkopf, B. L., The Formal [4+3] Cycloaddition between Donor-Acceptor Cyclobutanes and Nitrones. *Organic Letters* **2011**, *13* (6), 1528-1531. (g) Perrotta, D.; Racine, S.; Vuilleumier, J.; de Nanteuil, F.; Waser, J., [4 + 2]-Annulations of Aminocyclobutanes. *Organic Letters* **2015**, *17* (4), 1030-1033.
12. (a) Souillart, L.; Cramer, N., Exploitation of Rh(i)-Rh(iii) cycles in enantioselective C-C bond cleavages: access to [small beta]-tetalones and benzobicyclo[2.2.2]octanones. *Chemical Science* **2014**, *5* (2), 837-840. (b) Murakami, M.; Ashida, S.; Matsuda, T., Nickel-Catalyzed Intermolecular Alkyne Insertion into Cyclobutanones. *Journal of the American Chemical Society* **2005**, *127* (19), 6932-6933. (c) Xu, T.; Ko, H. M.; Savage,

N. A.; Dong, G., Highly Enantioselective Rh-Catalyzed Carboacylation of Olefins: Efficient Syntheses of Chiral Poly-Fused Rings. *Journal of the American Chemical Society* **2012**, *134* (49), 20005-20008. (d) Xu, T.; Dong, G., Rhodium-Catalyzed Regioselective Carboacylation of Olefins: A C \square C Bond Activation Approach for Accessing Fused-Ring Systems. *Angewandte Chemie International Edition* **2012**, *51* (30), 7567-7571.

13. (a) Xuan, J.; Lu, L.-Q.; Chen, J.-R.; Xiao, W.-J., Visible-Light-Driven Photoredox Catalysis in the Construction of Carbocyclic and Heterocyclic Ring Systems. *European Journal of Organic Chemistry* **2013**, *2013* (30), 6755-6770. (b) Prier, C. K.; Rankic, D. A.; MacMillan, D. W. C., Visible Light Photoredox Catalysis with Transition Metal Complexes: Applications in Organic Synthesis. *Chemical Reviews* **2013**, *113* (7), 5322-5363.

14. (a) Surry, D. S.; Buchwald, S. L., Dialkylbiaryl phosphines in Pd-catalyzed amination: a user's guide. *Chemical Science* **2011**, *2* (1), 27-50. (b) Hartwig, J. F., Evolution of a Fourth Generation Catalyst for the Amination and Thioetherification of Aryl Halides. *Accounts of Chemical Research* **2008**, *41* (11), 1534-1544.

15. (a) Wille, U., Radical Cascades Initiated by Intermolecular Radical Addition to Alkynes and Related Triple Bond Systems. *Chemical Reviews* **2013**, *113* (1), 813-853. (b) Giese, B.; Lachhein, S., Addition of Alkyl Radicals to Alkynes: Distinction between Radical and Ionic Nucleophiles. *Angewandte Chemie International Edition in English* **1982**, *21* (10), 768-775.

16. Upon irradiation of cyclobutylaniline **1k** and **2d** in the presence of **4a** (2 mol%) under degassed condition, a 1,4- addition reaction product of **1k** to **2d** was formed with a yield of 38%.

FC1=CC=C(N2CCCC2)C=C1 + CC(=O)OCC $\xrightarrow{[\text{Ir}(\text{dtbbpy})(\text{ppy})_2]\text{PF}_6}$
 MeOH, visible light 36%

17. CCDC 1060321 (**3bh**) contains the supplementary crystallographic data for this paper. These data can be obtained free of charge from The Cambridge Crystallographic data Center via www.ccdc.cam.ac.uk/data_request/cif

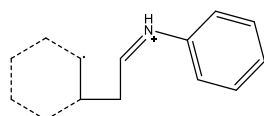
18. (a) Takao, K.-i.; Munakata, R.; Tadano, K.-i., Recent Advances in Natural Product Synthesis by Using Intramolecular Diels–Alder Reactions. *Chemical Reviews* **2005**, *105* (12), 4779-4807. (b) Nicolaou, K. C.; Snyder, S. A.; Montagnon, T.; Vassilikogiannakis, G., The Diels–Alder Reaction in Total Synthesis. *Angewandte Chemie International Edition* **2002**, *41* (10), 1668-1698.

19. (a) Jung, M. E., A review of annulation. *Tetrahedron* **1976**, 32 (1), 3-31. (b) Gawley, R. E., The Robinson Annulation and Related Reactions. *Synthesis* **1976**, 1976 (12), 777-794.

20. Ghosez, L.; Montaigne, R.; Roussel, A.; Vanlierde, H.; Mollet, P., Cycloadditions of dichloroketene to olefins and dienes. *Tetrahedron* **1971**, 27 (3), 615-633.

21. McLaughlin, M.; Palucki, M.; Davies, I. W., Efficient Access to Azaindoles and Indoles. *Organic Letters* **2006**, 8 (15), 3307-3310.

22. Proposed distonic radical iminium ion 1dc:



23. The third isomer from the annulation of **1be** and **2a** could not be detected by ¹H NMR or GC analysis of the crude product. The diastereomer ratio for the three isomers (**3ce** : **3ce'** : the third isomer) from the annulation of **1bf** and **2c** was measured by GC to be 13 : 3 : 1.

24. CCDC 1060320 (**3cd**) contains the supplementary crystallographic data for this paper. These data can be obtained free of charge from The Cambridge Crystallographic data Center via www.ccdc.cam.ac.uk/data_request/cif.

25. (a) Yasu, Y.; Koike, T.; Akita, M., Visible Light-Induced Selective Generation of Radicals from Organoborates by Photoredox Catalysis. *Advanced Synthesis & Catalysis* **2012**, 354 (18), 3414-3420. (b) Primer, D. N.; Karakaya, I.; Tellis, J. C.; Molander, G. A., Single-Electron Transmetalation: An Enabling Technology for Secondary Alkylboron Cross-Coupling. *Journal of the American Chemical Society* **2015**, 137 (6), 2195-2198.

26. (a) Ley, S. V.; Fitzpatrick, D. E.; Myers, R. M.; Battilocchio, C.; Ingham, R. J., Machine-Assisted Organic Synthesis. *Angew. Chem., Int. Ed.* **2015**, 54 (35), 10122-10136; (b) Han, X.; Poliakoff, M., Continuous reactions in supercritical carbon dioxide: problems, solutions and possible ways forward. *Chem. Soc. Rev.* **2012**, 41 (4), 1428-1436; (c) Cravotto, G.; Cintas, P., Power ultrasound in organic synthesis: moving cavitation chemistry from academia to innovative and large-scale applications. *Chem. Soc. Rev.* **2006**, 35 (2), 180-196.

27. (a) Webb, D.; Jamison, T. F., Continuous flow multi-step organic synthesis. *Chem. Sci.* **2010**, 1 (6), 675-680; (b) Kirschning, A.; Solodenko, W.; Mennecke, K., Combining enabling techniques in organic synthesis: continuous flow processes with heterogenized catalysts. *Chem. - Eur. J.* **2006**, 12 (23), 5972-5990; (c) Zhao, D.; Ding, K., Recent Advances in Asymmetric Catalysis in Flow. *ACS Catal.* **2013**, 3 (5), 928-944; (d)

Wegner, J.; Ceylan, S.; Kirschning, A., Flow Chemistry - A Key Enabling Technology for (Multistep) Organic Synthesis. *Adv. Synth. Catal.* **2012**, *354* (1), 17-57; (e) Wiles, C.; Watts, P., Continuous flow reactors: a perspective. *Green Chem.* **2012**, *14* (1), 38-54.

28. Braun, A. M.; Jakob, L.; Oliveros, E.; Oller do Nascimento, C. A., Up-scaling photochemical reactions. *Adv. Photochem.* **1993**, *18*, 235-313.

29. (a) Su, Y.; Straathof, N. J. W.; Hessel, V.; Noel, T., Photochemical transformations accelerated in continuous-flow reactors: Basic concepts and applications. *Chem. - Eur. J.* **2014**, *20* (34), (b) 10562-10589; Wegner, J.; Ceylan, S.; Kirschning, A., Ten key issues in modern flow chemistry. *Chem. Commun. (Cambridge, U. K.)* **2011**, *47* (16), 4583-4592.

30. Elliott, L. D.; Knowles, J. P.; Koovits, P. J.; Maskill, K. G.; Ralph, M. J.; Lejeune, G.; Edwards, L. J.; Robinson, R. I.; Clemens, I. R.; Cox, B.; Pascoe, D. D.; Koch, G.; Eberle, M.; Berry, M. B.; Booker-Milburn, K. I., Batch versus Flow Photochemistry: A Revealing Comparison of Yield and Productivity. *Chemistry – A European Journal* **2014**, *20* (46), 15226-15232.

31. Wang, J.; Zheng, N., The cleavage of a C-C Bond in cyclobutylanilines by visible-light photoredox catalysis: Development of a [4+2] annulation method. *Angew. Chem., Int. Ed.* **2015**, *54* (39), 11424-11427.

32. Maity, S.; Zhu, M.; Shinabery, R. S.; Zheng, N., Intermolecular [3+2] Cycloaddition of Cyclopropylamines with Olefins by Visible-Light Photocatalysis. *Angew. Chem., Int. Ed.* **2012**, *51* (1), 222-226.

33. Nguyen, T. H.; Morris, S. A.; Zheng, N., Intermolecular [3+2] Annulation of Cyclopropylanilines with Alkynes, Enynes, and Diynes via Visible Light Photocatalysis. *Adv. Synth. Catal.* **2014**, *356* (13), 2831-2837.

34. Fujishima, A.; Honda, K., Electrochemical Photolysis of Water at a Semiconductor Electrode. *Nature* **1972**, *238* (5358), 37-38.

35. Hakki, A.; Schneider, J.; Bahnemann, D., CHAPTER 2 Understanding the Chemistry of Photocatalytic Processes. In *Photocatalysis: Fundamentals and Perspectives*, The Royal Society of Chemistry: 2016; pp 29-50.

36. (a) Lang, X.; Ma, W.; Chen, C.; Ji, H.; Zhao, J., Selective Aerobic Oxidation Mediated by TiO₂ Photocatalysis. *Accounts of Chemical Research* **2014**, *47* (2), 355-363. (b) Lang, X.; Chen, X.; Zhao, J., Heterogeneous visible light photocatalysis for selective organic transformations. *Chemical Society Reviews* **2014**, *43* (1), 473-486. (c) Friedmann, D.; Hakki, A.; Kim, H.; Choi, W.; Bahnemann, D., Heterogeneous photocatalytic organic synthesis: state-of-the-art and future perspectives. *Green Chemistry* **2016**, *18* (20), 5391-5411.

37. Kisch, H., Semiconductor Photocatalysis—Mechanistic and Synthetic Aspects. *Angewandte Chemie International Edition* **2013**, *52* (3), 812-847.

38. (a) Anpo, M.; Takeuchi, M., The design and development of highly reactive titanium oxide photocatalysts operating under visible light irradiation. *Journal of Catalysis* **2003**, *216* (1), 505-516. (b) Dahl, M.; Liu, Y.; Yin, Y., Composite Titanium Dioxide Nanomaterials. *Chemical Reviews* **2014**, *114* (19), 9853-9889. (c) Asahi, R.; Morikawa, T.; Irie, H.; Ohwaki, T., Nitrogen-Doped Titanium Dioxide as Visible-Light-Sensitive Photocatalyst: Designs, Developments, and Prospects. *Chemical Reviews* **2014**, *114* (19), 9824-9852.

39. Liu, L.; Chen, X., Titanium Dioxide Nanomaterials: Self-Structural Modifications. *Chemical Reviews* **2014**, *114* (19), 9890-9918.

40. (a) Zuo, F.; Wang, L.; Wu, T.; Zhang, Z.; Borchardt, D.; Feng, P., Self-Doped Ti³⁺ Enhanced Photocatalyst for Hydrogen Production under Visible Light. *Journal of the American Chemical Society* **2010**, *132* (34), 11856-11857. (b) Zuo, F.; Bozhilov, K.; Dillon, R. J.; Wang, L.; Smith, P.; Zhao, X.; Bardeen, C.; Feng, P., Active Facets on Titanium(III)-Doped TiO₂: An Effective Strategy to Improve the Visible-Light Photocatalytic Activity. *Angewandte Chemie International Edition* **2012**, *51* (25), 6223-6226.

41. Zuo, F.; Wang, L.; Feng, P., Self-doped Ti³⁺@TiO₂ visible light photocatalyst: Influence of synthetic parameters on the H₂ production activity. *International Journal of Hydrogen Energy* **2014**, *39* (2), 711-717.

42. Sasan, K.; Zuo, F.; Wang, Y.; Feng, P., Self-doped Ti³⁺-TiO₂ as a photocatalyst for the reduction of CO₂ into a hydrocarbon fuel under visible light irradiation. *Nanoscale* **2015**, *7* (32), 13369-13372.

43. Conner, W. C.; Falconer, J. L., Spillover in Heterogeneous Catalysis. *Chemical Reviews* **1995**, *95* (3), 759-788.

44. Fox, M. A.; Dulay, M. T., Heterogeneous photocatalysis. *Chemical Reviews* **1993**, *93* (1), 341-357.

45. Chen, C.; Ma, W.; Zhao, J., Semiconductor-mediated photodegradation of pollutants under visible-light irradiation. *Chemical Society Reviews* **2010**, *39* (11), 4206-4219.

46. Wang, Z.; Wen, B.; Hao, Q.; Liu, L.-M.; Zhou, C.; Mao, X.; Lang, X.; Yin, W.-J.; Dai, D.; Selloni, A.; Yang, X., Localized Excitation of Ti³⁺ Ions in the Photoabsorption and Photocatalytic Activity of Reduced Rutile TiO₂. *Journal of the American Chemical Society* **2015**, *137* (28), 9146-9152.

47. Gratzel, M., Photoelectrochemical cells. *Nature* **2001**, *414* (6861), 338-344.

48. Wang, J.; Nguyen, T. H.; Zheng, N., Photoredox-catalyzed [4+2] annulation of cyclobutylanilines with alkenes, alkynes, and diynes in continuous flow. *Science China Chemistry* **2016**, *59* (2), 180-183.

49. Fox, M. A.; Younathan, J. N., Radical cation intermediates in the formation of schiff bases on irradiated semiconductor powders. *Tetrahedron* **1986**, *42* (22), 6285-6291.

50. Lang, X.; Ma, W.; Zhao, Y.; Chen, C.; Ji, H.; Zhao, J., Visible-Light-Induced Selective Photocatalytic Aerobic Oxidation of Amines into Imines on TiO₂. *Chemistry – A European Journal* **2012**, *18* (9), 2624-2631.

51. Hayyan, M.; Hashim, M. A.; AlNashef, I. M., Superoxide Ion: Generation and Chemical Implications. *Chemical Reviews* **2016**, *116* (5), 3029-3085.

52. (a) Rajendran, V.; Lehnig, M.; Niemeyer, C. M., Photocatalytic activity of colloidal CdS nanoparticles with different capping ligands. *Journal of Materials Chemistry* **2009**, *19* (35), 6348-6353. (b) Li, Y.; Zhang, W.; Niu, J.; Chen, Y., Mechanism of Photogenerated Reactive Oxygen Species and Correlation with the Antibacterial Properties of Engineered Metal-Oxide Nanoparticles. *ACS Nano* **2012**, *6* (6), 5164-5173.

53. Daimon, T.; Nosaka, Y., Formation and Behavior of Singlet Molecular Oxygen in TiO₂ Photocatalysis Studied by Detection of Near-Infrared Phosphorescence. *The Journal of Physical Chemistry C* **2007**, *111* (11), 4420-4424.

54. Jańczyk, A.; Krakowska, E.; Stochel, G.; Macyk, W., Singlet Oxygen Photogeneration at Surface Modified Titanium Dioxide. *Journal of the American Chemical Society* **2006**, *128* (49), 15574-15575.

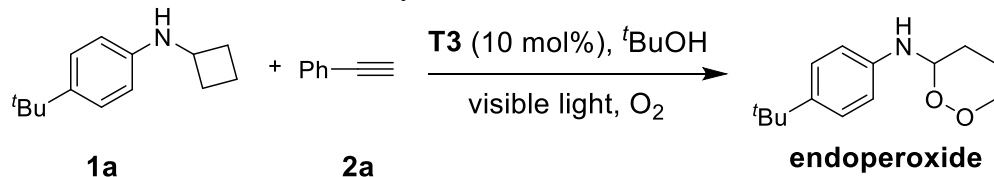
55. (a) Nosaka, Y.; Daimon, T.; Nosaka, A. Y.; Murakami, Y., Singlet oxygen formation in photocatalytic TiO_2 aqueous suspension. *Physical Chemistry Chemical Physics* **2004**, *6* (11), 2917-2918. (b) Saito, H.; Nosaka, Y., Mechanism of Singlet Oxygen Generation in Visible-Light-Induced Photocatalysis of Gold-Nanoparticle-Deposited Titanium Dioxide. *The Journal of Physical Chemistry C* **2014**, *118* (29), 15656-15663.

56. Baciocchi, E.; Del Giacco, T.; Lapi, A., Oxygenation of Benzylidimethylamine by Singlet Oxygen. Products and Mechanism. *Organic Letters* **2004**, *6* (25), 4791-4794.

57. Kaise, M.; Nagai, H.; Tokuhashi, K.; Kondo, S.; Nimura, S.; Kikuchi, O., Electron Spin Resonance Studies of Photocatalytic Interface Reactions of Suspended M/ TiO_2 (M = Pt, Pd, Ir, Rh, Os, or Ru) with Alcohol and Acetic Acid in Aqueous Media. *Langmuir* **1994**, *10* (5), 1345-1347.

58. Tamaki, Y.; Furube, A.; Murai, M.; Hara, K.; Katoh, R.; Tachiya, M., Direct Observation of Reactive Trapped Holes in TiO_2 Undergoing Photocatalytic Oxidation of Adsorbed Alcohols: Evaluation of the Reaction Rates and Yields. *Journal of the American Chemical Society* **2006**, *128* (2), 416-417.

59. Upon irradiation of **1a** and **2a** in the presence of **T3** (2 mg) under oxygen balloon, an endoperoxide was formed with 57% yield.



60. Ouannes, C.; Wilson, T., Quenching of singlet oxygen by tertiary aliphatic amines. Effect of DABCO (1,4-diazabicyclo[2.2.2]octane). *Journal of the American Chemical Society* **1968**, *90* (23), 6527-6528.
61. SOSG, the acronym name of Singlet Oxygen Sensor Green, is a highly selective detection reagent for singlet oxygen and marketed by ThermoFisher Scientific.
62. Ragas, X.; Jimenez-Banzo, A.; Sanchez-Garcia, D.; Batllori, X.; Nonell, S., Singlet oxygen photosensitisation by the fluorescent probe Singlet Oxygen Sensor Green[registered sign]. *Chemical Communications* **2009**, (20), 2920-2922.
63. Vankayala, R.; Sagadevan, A.; Vijayaraghavan, P.; Kuo, C.-L.; Hwang, K. C., Metal Nanoparticles Sensitize the Formation of Singlet Oxygen. *Angewandte Chemie International Edition* **2011**, *50* (45), 10640-10644.

Chapter 3: Difunctionalization of *N*-Cyclobutylanilines under Photoredox Catalysis

3.1 Introduction

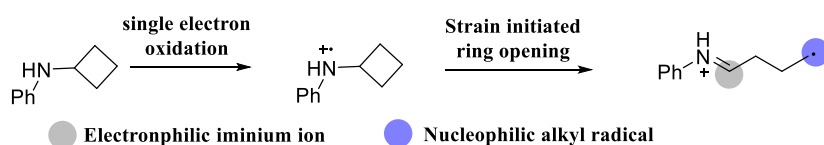
Distonic radical cations are defined as intermediates that possess a cation and a radical within the same molecule but separated by two or more atoms.¹ First discovered in mass spectrometry, they have been extensively studied in gas phase.² In contrast, their reactivity in solution phase has been seldom investigated.³ Bearing two orthogonal reactive sites, the distonic radical cations are highly reactive both towards ionic reactions and radical reactions.⁴ Hence, those reactive organic intermediates are highly desired in synthetic organic chemistry field and worth exceptional efforts for further investigation of their utilities for the development of synthetically useful methodologies. Current methods that utilizing distonic radical cations as reactive intermediates are all based on the sequential intramolecular cyclization reactions⁴, and thus greatly limited the use of the two reactive sites on the distonic radical cation. The limited methods for the generation of distonic radical cations which typically involve strong oxidants or UV-irradiation^{5,6} also downshifted their investigation in organic synthesis.

Recently, we have successfully established a series of annulation reactions for the construction of amine substituted five and six membered carbon cycles through single electron oxidative cleavage of *N*-cyclopropylanilines and *N*-cyclobutylanilines under photoredox catalysis.^{4b} All of those transformations are built upon our proposed ring opening reactive intermediates, distonic radical cations, and their sequential cyclization with various *Pi* bonds. Compared to the rather fast ring opening rate of *N*-cyclopropylaniline under room temperature, the sluggish ring opening rate derived from *N*-cyclobutylaniline forced us to conduct the reaction with a much higher reaction temperature (60°C) and more photon flux input to enable the success [4+2] annulation to occur. We questioned whether a nucleophile can be included to react with the

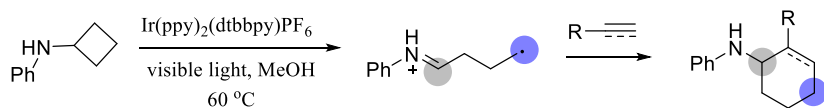
generated distonic radical cation intermediates of *N*-cyclobutylanilines under photoredox catalysis through a nucleophilic addition fashion to further assist the rather sluggish ring opening process. Presumably, with the nucleophilic addition of a nucleophile to the iminium ion site of the distonic radical ion, the four carbon alkyl radical chain from *N*-cyclobutylaniline would be released, a further remote functionalization on the four membered carbon chain would be ideal and a new C_{sp^3} -C bond⁷ or C_{sp^3} -X bond⁸ could be constructed depending on the alkyl radical acceptors. Herein, we report a catalytic method for the difunctionalization of *N*-cyclobutylanilines and *N*-cyclopropylanilines through the involvement of a nucleophile and a radical acceptor.

Taking the well-developed Strecker synthesis into consideration,⁹ we decided to use cyanide as our initial nucleophile source. While allylsulfone as a well-documented radical acceptor, especially towards the superior reactivity with alkyl radicals¹⁰, we think it would be ideal for the further construction of a C_{sp^3} -C bond with our four membered alkyl radicals.

Distonic Radical Cation:



Previous Work: Sequential Quench of The Two Reactive Sites with various Pi bonds



This Work: Difunctionalization of Distonic Radical Cation

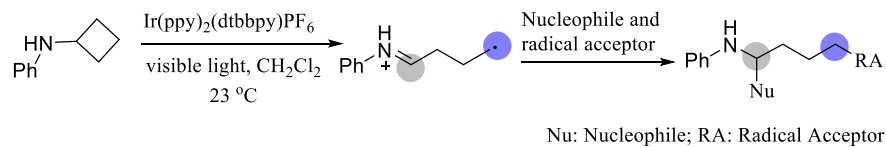


Figure 3.1. The distonic radical cation: generation and reactivity.

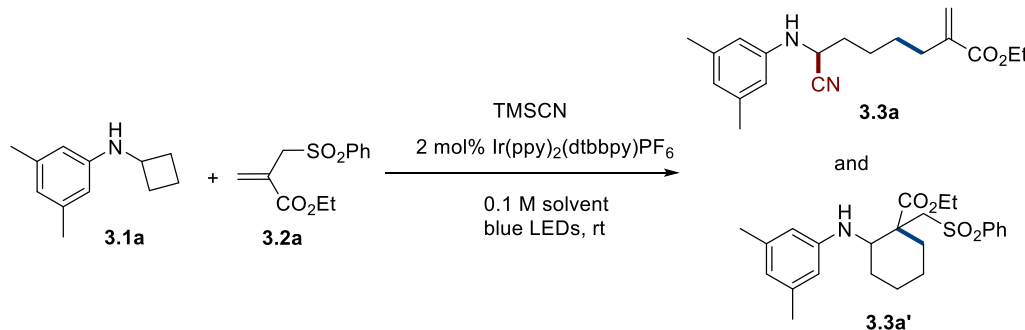
3.2 Results and Discussion

3.2.1 Reaction Optimization.

We chose *N*-cyclobutylaniline **3.1a**, allylsulfone **3.2a** and TMSCN as the standard substrates to optimize the difunctionalization reaction. Using $\text{Ir}(\text{ppy})_2(\text{dtbbpy})\text{PF}_6$ as the photoredox catalyst, methanol as the solvent, the desired product **3.3a** was formed with a modest yield of 36% along with a [4+2] annulation byproduct **3.3a'** of **3.1a** and **3.2a**. Switching of solvent to CH_3NO_2 , however, completely suppressed the reaction and **3.3a** was barely formed. The use of a less polar solvent, such as DMF, has significantly improved the reaction yield and selectivity towards **3.3a**. Further screening of none polar solvents revealed that the use of dichloromethane as the reaction solvent is optimal, a yield of 90% of **3.3a** was obtained while the byproduct **3.3a'** was completely suppressed. We hypothesized that the use of a nonpolar solvent would greatly slow down radical nucleophilic addition of alkyl radical to allylsulfone¹¹ and hence provide a better selectivity towards the cyanide nucleophilic addition for further formation of the desired product **3.3a**. Other photoredox catalysts, such as $\text{Ru}(\text{bpy})_3\text{BArF}$ or $\text{Ir}(\text{dF}(\text{CF}_3)\text{ppy})_2(\text{dtbbpy})\text{PF}_6$, was not as efficient as the $\text{Ir}(\text{ppy})_2(\text{dtbbpy})\text{PF}_6$. The use of other cyanide source such as KCN instead of TMSCN also greatly decreased the formation of **3.3a**. Control experiments showed that omitting either the photoredox catalyst or light would results no product formation. Conducting the reaction in the presence of air led to a significant decrease in the yield. Contradictory to our previous observation in the [4+2] annulation reaction of *N*-cyclobutylanilines with alkynes¹² which has been shown to require an inert temperature (60°C) to facilitate the rather sluggish ring opening rate of *N*-cyclobutylanilines, all the screening of the difunctionalization of *N*-cyclobutylaniline were conducted at room temperature (23 °C). Thus,

the reaction optimization data has further supported our argument on the role of cyanide to assist the sluggish cyclobutylaniline ring opening process.

Table 3.1. Difunctionalization Reaction Optimization.

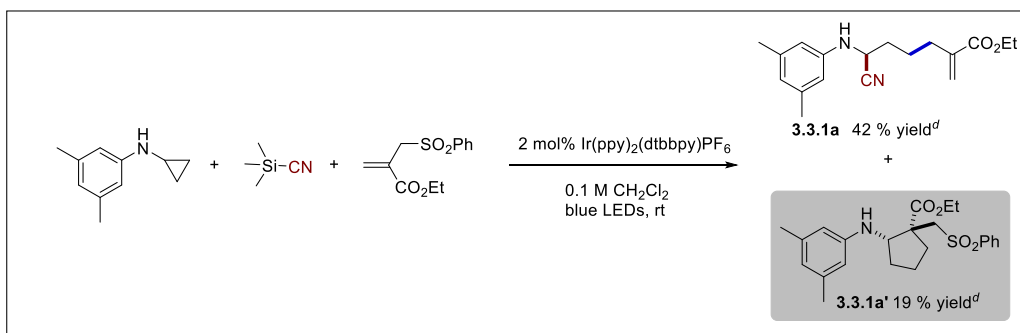
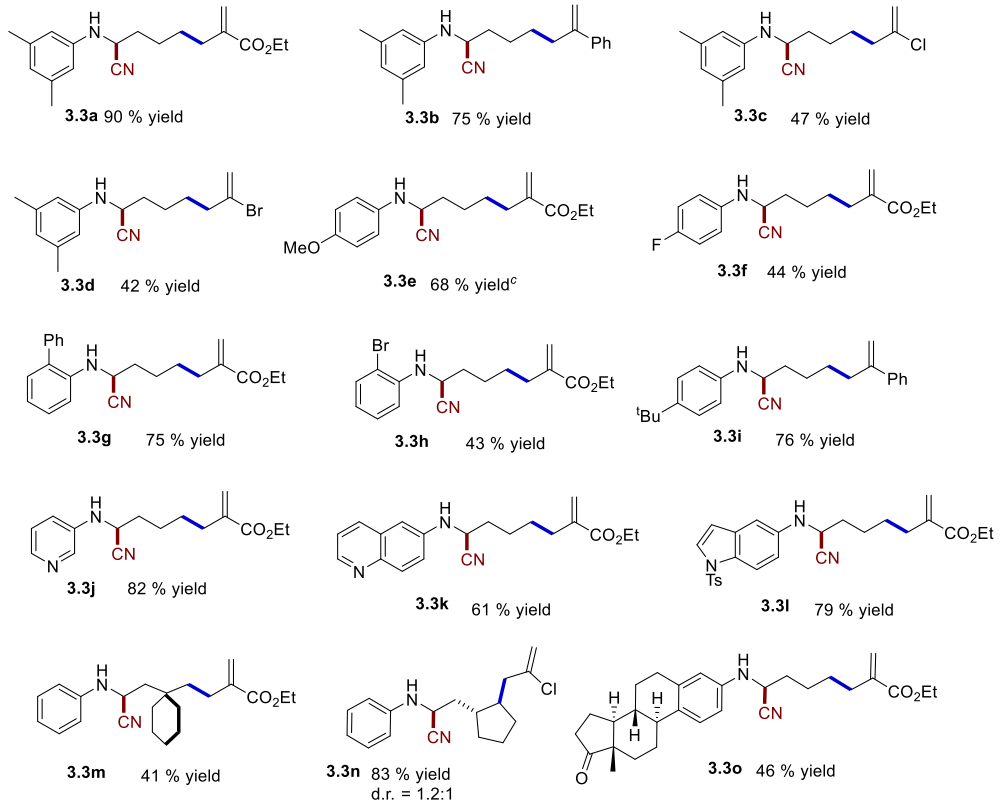
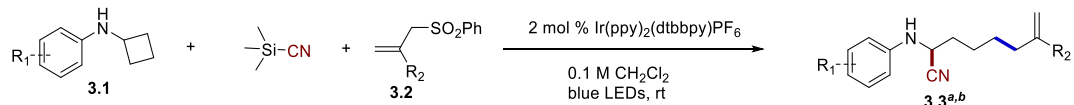


Entry ^[a]	Photocatalyst	Solvent	Yield of 3	Yield of 3'
			[%] ^[b]	[%] ^[b]
1	Ir(ppy) ₂ (dtbbpy)PF ₆	MeOH	36	8
2	Ir(ppy) ₂ (dtbbpy)PF ₆	CH ₃ NO ₂	5	<1
3	Ir(ppy) ₂ (dtbbpy)PF ₆	DMF	62	5
4	Ir(ppy) ₂ (dtbbpy)PF ₆	CH ₂ Cl ₂	90	0
5	Ru(bpy) ₃ BArF	CH ₂ Cl ₂	9	<1
6	Ir(dF(CF ₃)ppy) ₂ (dtbbpy)PF ₆	CH ₂ Cl ₂	29	<1
7 ^[c]	Ir(ppy) ₂ (dtbbpy)PF ₆	CH ₂ Cl ₂	5	<1
8	Without catalyst	CH ₂ Cl ₂	0	0
9	Ir(ppy) ₂ (dtbbpy)PF ₆ , dark	CH ₂ Cl ₂	0	0
10	Ir(ppy) ₂ (dtbbpy)PF ₆ , air	CH ₂ Cl ₂	31	<1

[a] Reaction Condition: 1 a (0.2 mmol, 0.1 M in degassed solvent), 2 a (0.6 mmol), TMSCN (0.6 mmol), irradiation with 6 W blue LED Strip at 23 °C for 8 h. [b] Yields were determined by ¹H NMR analysis of the crude reaction mixtures using CH₂Br₂ as internal standard. [c] 3 equiv. of KCN was added instead of TMSCN.

3.2.2 Reaction Substrate Scope.

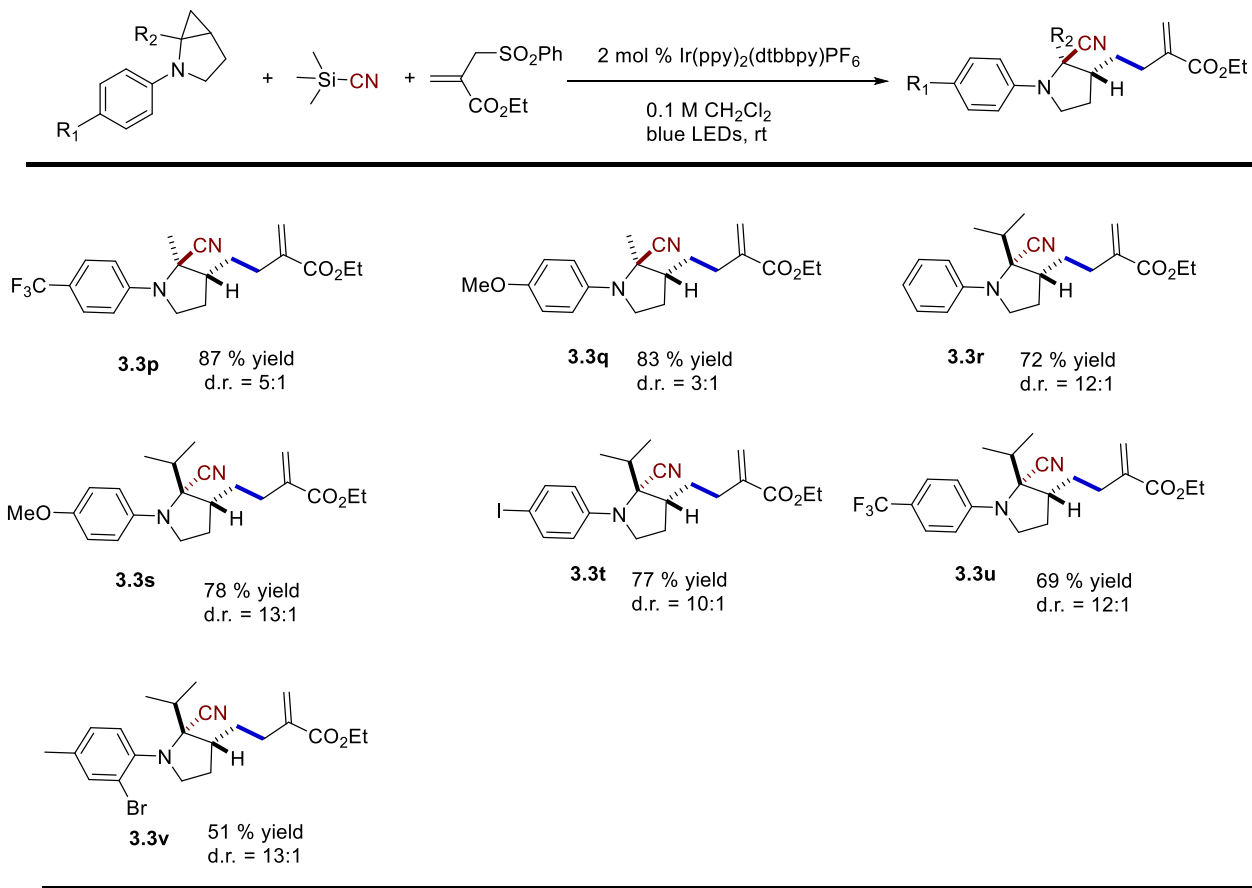
With the optimized condition in hands, we next examined the scope of cyclobutylaniline derivatives with various allylsulfones in the presence of TMSCN. Cyclobutylanilines were readily prepared through Buchwald-Hartwig amination of cyclobutylamine with aryl halides.¹³ Different substituents on allylsulfone were studies initially as alkyl radical acceptors. We found that electron withdrawing substituents (e.g., CO₂Et, Cl and Br) or phenyl substituent on allylsulfones were necessary for the radical allylation reaction to occur, albeit slightly lower reaction yields were obtained when using halides substituents. Unsubstituted or alkyl-substituted allylsulfones were not compatible and no products were observed (SI), likely due to the thermodynamically disfavored formation of the secondary or tertiary radical addition intermediates. We further turned our attention on the substituents on the *N*-cyclobutylanilines. The difunctionalization reaction generally tolerated both electron withdrawing (e.g., F and Br) and electron donating substituents (e.g. OMe, Ph and alkyl) on the aryl ring. Higher reaction temperature and longer irradiation time were required to facilitate the ring opening of 4-methoxyl-*N*-cyclobutylaniline due to the highly stable amine radical cation intermediate. The reaction was further proved to tolerate the steric hindrance quite well, as the *ortho*-substituents showed little effect on the reaction. We also conducted the reaction in the presence of heterocycles, such as (pyridyl, quinolone and indole), and the reaction were procedded uneventfully, modest to good yields were obtained. Furthermore, spirocyclobutylaniline and [5,4] fused cyclobutylaniline were also tested and good yield were obtained in both cases albeit the a low diastereoselecticvity was obtained in the latter case. Finally, a late stage functionalization example was also demonstrated by using estrone as substituent on cyclobutylamine. A synthetically useful yield was obtained after a 16 h irradiation which highlighted the utility of this method.



[a] Reaction Condition: 1 (0.2 mmol, 0.1 M in degassed solvent), 2 (0.6 mmol), TMSCN (0.6 mmol), irradiation with 6 W blue LED Strip at 23 °C for 8-16 h. [b] Yield of isolated product. [c] Reaction irradiated with 4 strip blue LEDs (50°C) for 24 h. [d] Reaction irradiated for 2.5 h.

Scheme 3.1 Difunctionalization of Monocyclic Substrates.

We have shown in our previous studies that the ring opening rate of *N*-cyclopropylpyrrolaniline is faster than *N*-cyclobutylpyrrolaniline, which promoted us to investigate the possibility of applying this method to the three membered carbon cycle. 3,5-dimethyl-*N*-cyclopropylpyrrolaniline was chosen as our example along with **2a** and TMSCN. Without surprise, the reaction was completed in 2.5 hours under standard irradiation conditions. A mixture of difunctionalized product (**3.3.1a**) and [3+2] annulation product (**3.3.1a'**) with a ratio of 2.2:1 was obtained. Presumably, without the aid of cyanide, the ring opening rate of cyclopropylpyrrolaniline was fast enough to generate the untrapped distonic radical cation, which was responsible for the formation of the undesired cyclic byproduct. In order to support our hypothesis, we were further intrigued by using the trisubstituted cyclopropylpyrrolanilines which was proposed to have a slower ring opening rate than those disubstituted cyclopropylpyrrolanilines. We were pleased to find that the [3+2] annulation byproducts were completely suppressed in those fused cyclopropylpyrrolanilines and only difunctionalized products were obtained with good to excellent reaction yields as well as distereoselectivities. Various novel α -cyano pyrrolidine structures were obtained as the final products along with the generation of a new quaternary carbon center on α position of those pyrrolidines.

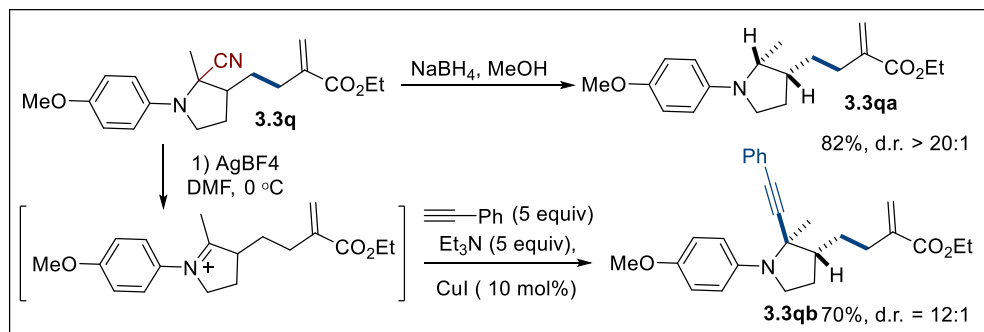


Scheme 3.2 Difunctionalization of Bicyclic cyclopropylaniline Substrates.

3.2.3. Product derivatization.

Cyano functional group, especially those α -cyano pyrrolidines could potentially serve as good leaving group to form iminium ion on the pyrrolidine ring and hence is ideal pre-functional group to illustrate the utility of those 1,2 disubstituted pyrrolidine products as valuable building blocks for further organic synthesis. To this end, we explored two derivatization reactions, each of which was performed with only minimal optimization (Table 4). We used NaBH_4 to reduce the cyano functional group of **3.3q**, and a new 1,2 disubstituted pyrrolidine (**3.3qa**) was formed with a 82% yield and a high diastereoselectivity (d.r. > 20:1). Alternatively, the α -cyano of **3.3q** can also be reduced by AgBF_4 in DMF and regenerate the iminium ion. Phenylacetylene then

was used as a nucleophile to react with the iminium ion intermediate for further construction of a new C-C bond on the α position of **3.3qb** with high yield and excellent diastereoselectivity.

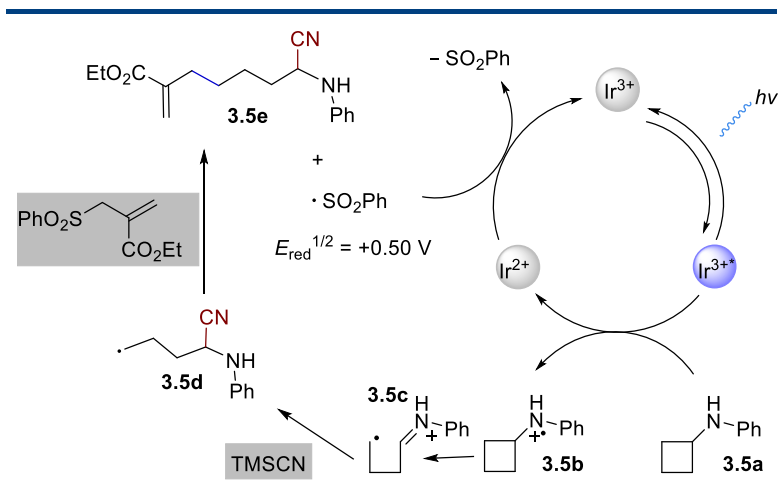


Scheme 3.3 Derivatization of **3.3q**.

3.2.4 Proposed Reaction Mechanism.

A proposed catalytic cycle for the difunctionalization of *N*-cyclobutylanilines and *N*-cyclopropylanilines is shown in **Scheme 2.2**. Exposure of $\text{Ir}(\text{ppy})_2(\text{dtbbpy})\text{PF}_6$ to a 6 W two strip blue LED produces the photoexcited $\text{Ir}(\text{ppy})_2(\text{dtbbpy})^{1+*}$, which is reductively quenched by cyclobutylaniline **3.5a** to generate $\text{Ir}(\text{ppy})_2(\text{dtbbpy})$ with the concomitant formation of amine radical cation **3.5b**. Subsequent ring opening generates distonic radical iminium ion **3.5c**, which is further reacted immediately with TMSCN at the iminium ion site to further release the alkyl radical intermediate. Allylsulfone is then used to trap the alkyl radical intermediate **3.5d** through a radical allylation reaction to yield the desired product **3.5e**. The in situ generated sulfonyl radical ($E_{\text{red}}^{1/2} = +0.50$ V) can accept an electron from the reduced photoredox catalyst, and thus close the catalytic cycle. The proposed reaction mechanism is further supported by our fluorescence quenching studies as only *N*-cyclobutylaniline **3.1a** can quench the excited photoredox catalyst $\text{Ir}(\text{ppy})_2(\text{dtbbpy})^{1+*}$. Other two reaction components, trimethylsilyl cyanide and allylsulfone **3.2a** all revealed to not quenching the excited $\text{Ir}(\text{ppy})_2(\text{dtbbpy})^{1+*}$ efficiently.

We also measured the overall reaction quantum yield of the difunctionalization of *N*-cyclobutylaniline **3.1a** and allylsulfone **3.2a**. Using potassium ferrioxalate as an actinometer and a 300 W Xenon lamp (50% of light intensity, 439±5 nm bandpass filter high transmittance), we determined the quantum yield of the reaction after 2 h irradiation. The quantum yield was calculated to be 0.214 which indicate a none radical chain process of the difunctionalization reaction. The low quantum yield can be attributed to the low oxidation potential of the sulfonyl radical which could not oxidize the *N*-cyclobutylaniline that possesses a +0.8 V oxidation peak potential.



Scheme 3.4 Proposed Reaction Mechanism.

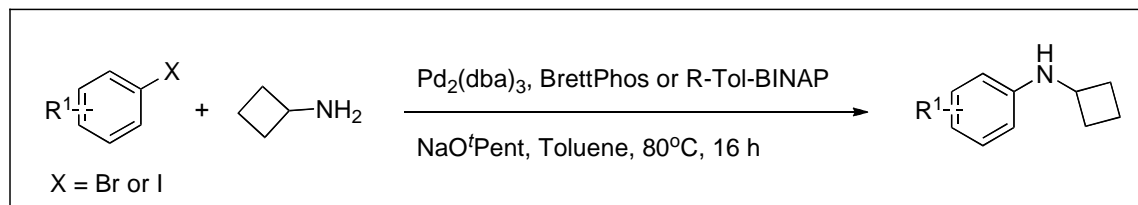
3.2.5 Experimental section.

All reactions were carried out under a nitrogen atmosphere unless otherwise stated. Dry solvents were used as received except THF, CH₂Cl₂, Et₂O, and toluene. They were rigorously purged with argon for 2 h and then further purified by passing through two packed columns of neutral alumina (for THF and Et₂O) or through neutral alumina and copper (II) oxide (for toluene

and CH_2Cl_2) under argon from a solvent purification system. A standard workup protocol consisted of extraction with diethyl ether, washing with brine, drying over Na_2SO_4 , and removal of the solvent in vacuum. Column chromatography was carried out with silica gel (230-400 mesh). All new compounds were characterized by ^1H NMR, ^{13}C NMR, IR spectroscopy, high-resolution mass spectroscopy (HRMS), and melting point if solid. Nuclear magnetic resonance (NMR) spectra were obtained on a Bruker Avance DPX-300 and Bruker Avance DPX-400. Chemical shifts (δ) were reported in parts per million (ppm) relative to residual proton signals in CDCl_3 (7.26 ppm, 77.23 ppm) or CD_2Cl_2 (5.32 ppm, 54 ppm) at room temperature. IR spectra were recorded (thin film on NaCl plates) on a PerkinElmer Spectrum 100 series instrument. High resolution mass spectra were recorded on a Bruker Ultraflex II TOF/TOF mass spectrometer. Gas chromatography/mass spectroscopy (GC/MS) analyses were performed on an Agilent 6890N Network GC System/5973 inert Mass Selective Detector. Gas chromatography analyses were performed using a Shimadzu GC-2010 Plus instrument. Melting points (m.p.) were recorded using Stuart SMP10 Melting Point Apparatus and were uncorrected.

3.2.5.1 Experimental Procedures and Spectroscopic Data

General procedure 1 (GP1): Preparation of N-Cyclobutylanilines

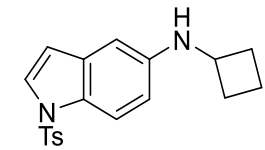


To an oven-dried test tube equipped with a stir bar were added 0.02 mmol of $\text{Pd}_2(\text{dba})_3$ and 0.06 mmol of ligand ((R)-Tol-BINAP or BrettPhos). Glove box was used to add 3 mmol of NaO'Pent and the tube was sealed with a Teflon screw cap. Aryl halide (2 mmol), cyclobutylamine (2.2 mmol), and toluene (4 mL) were then added to the reaction mixture and heated at 80 °C for 16 h. After completion, the reaction mixture was cooled to room temperature, diluted with diethyl ether, filtered over a short pad of silica gel, and concentrated in vacuum. Purification by flash chromatography on silica gel afforded *N*-cyclobutylaniline.

For the detailed preparation and characterization of *N*-cyclobutylanilines **3.1a**, **3.1e**, **3.1f**, **3.1g**, **3.1h**, **3.1i**, **3.1j** correspond to those described in the literatures.¹²

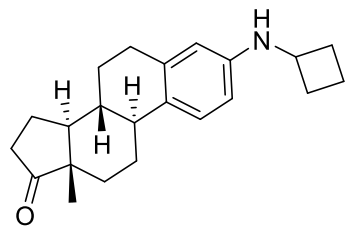
N-cyclobutylquinolin-6-amine (3.1k). Following **GP1** with 6-bromoquinoline (0.27 mL, 2 mmol) and BrettPhos (32.2 mg, 0.06 mmol, 3 mol%), the product was isolated after a flash chromatography on silica gel (1: 2 EtOAc/hexanes) as light yellow oil (367 mg, 93%). IR $\nu_{\text{max}}(\text{cm}^{-1})$: 3397, 2920, 2347, 1647, 1507, 1386, 1251, 1101; IR $\nu_{\text{max}}(\text{cm}^{-1})$: ¹H NMR (400 MHz, Chloroform-*d*) δ 8.61 (dd, *J* = 4.2, 1.7 Hz, 1H), 7.97 – 7.77 (m, 2H), 7.28 – 7.19 (m, 1H), 7.05 (dd, *J* = 9.0, 2.6 Hz, 1H), 6.61 (d, *J* = 2.5 Hz, 1H), 4.15 (d, *J* = 10.7 Hz, 1H), 4.03 (q, *J* = 8.7, 7.9 Hz, 1H), 2.60 – 2.42 (m, 2H), 1.98 – 1.72 (m, 4H). ¹³C NMR (101 MHz, CDCl_3) δ 146.33, 145.21, 143.40, 133.94, 130.52, 130.32, 121.52, 121.48, 103.62, 49.11, 31.27, 15.61. HRMS (ESI) m/z [M+H]⁺, calc'd for $\text{C}_{13}\text{H}_{14}\text{N}_2$ 199.1230; found 199.1225.

N-cyclobutyl-1-tosyl-1*H*-indol-5-amine (3.1l). **3.1l** is prepared according to following procedure: An oven-dried schlenk tube was charged with $\text{Pd}(\text{OAc})_2$ (13.5 mg, 0.06 mmol, 3 mol%), Cs_2CO_3 (1.3 g, 4 mmol, 2 equiv), (R)-Tol-BINAP (54 mg, 0.08 mmol, 4 mol%),



cyclobutylamine (0.18 mL, 2.4 mmol), 5-bromo-1-tosylindole (700 mg, 2 mmol), Toluene (4 mL) and a stir bar. After purging with argon for a 5 min, the tube was sealed with a Teflon screw cap. The mixture was heated at 100 °C for 72 h. The reaction mixture was then cooled to room temperature, diluted with diethyl ether, filtered over a short pad of silica gel, and concentrated in vacuum. Product was purified by flash chromatography on silica gel (1:2 EtOAc/hexanes) as colorless oil (279 mg, 41%). IR $\nu_{\text{max}}(\text{cm}^{-1})$: 3330, 2944, 2838, 1652, 1456, 1362, 1125, 1012; ^1H NMR (400 MHz, Chloroform-*d*) δ 7.78 (s, 1H), 7.72 (d, J = 8.0 Hz, 2H), 7.45 (d, J = 3.7 Hz, 1H), 7.17 (d, J = 8.0 Hz, 2H), 6.60 (d, J = 9.0 Hz, 2H), 6.50 (d, J = 3.7 Hz, 1H), 4.02 – 3.70 (m, 2H), 2.42 (dq, J = 9.0, 5.3, 3.8 Hz, 2H), 2.31 (s, 3H), 1.80 (dt, J = 10.7, 6.1 Hz, 4H). ^{13}C NMR (101 MHz, CDCl_3) δ 144.69, 144.09, 135.45, 132.26, 129.83, 128.24, 126.81, 126.77, 114.51, 113.16, 109.36, 102.97, 49.58, 31.34, 21.62, 15.42. HRMS (ESI) m/z [M+H] $^+$, calc'd for $\text{C}_{19}\text{H}_{20}\text{N}_2\text{O}_2\text{S}$ 341.1318; found 341.1318.

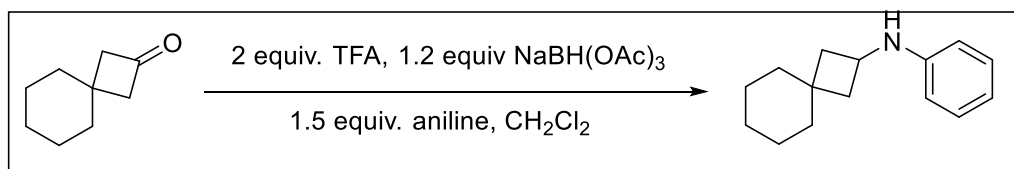
(8*R*,9*S*,13*S*,14*S*)-3-(cyclobutylamino)-13-methyl-7,8,9,11,12,13,15,16-octahydro-6*H*-



cyclopenta[*a*]phenanthren-17(14*H*)-one (3.1o). **3.1o** is prepared according to following procedure: An oven-dried schlenk tube was charged with $\text{Pd}(\text{OAc})_2$ (45 mg, 0.2 mmol, 10 mol%), Cs_2CO_3 (782 mg, 2.4 mmol, 1.2 equiv), XPhos (95 mg, 0.2 mmol, 10 mol%), cyclobutylamine (0.18 mL, 2.4 mmol), estrone triflate (804 mg, 2 mmol), Toluene (6 mL) and a stir bar. After purging with argon for a 5 min, the tube was sealed with a Teflon screw cap. The mixture was heated at 120 °C for 16 h. The reaction mixture was then cooled to room temperature, diluted with diethyl ether, filtered over a short pad of silica gel, and concentrated in vacuum. Product was purified by flash chromatography on silica gel (1:5 EtOAc/hexanes) as

yellow solid (503 mg, 78%). IR $\nu_{\text{max}}(\text{cm}^{-1})$: 3340, 2939, 2843, 1734, 1512, 1367, 1222, 1019; ^1H NMR (400 MHz, Chloroform-*d*) δ 7.10 (dd, *J* = 8.5, 1.1 Hz, 1H), 6.41 (dd, *J* = 8.4, 2.6 Hz, 1H), 6.32 (d, *J* = 2.5 Hz, 1H), 3.91 (tt, *J* = 8.1, 5.7 Hz, 1H), 3.71 (s, 1H), 2.86 (td, *J* = 8.0, 7.1, 4.1 Hz, 2H), 2.58 – 2.47 (m, 1H), 2.46 – 2.31 (m, 3H), 2.23 (ddd, *J* = 17.8, 9.2, 3.9 Hz, 1H), 2.18 – 2.07 (m, 1H), 2.07 – 1.90 (m, 3H), 1.90 – 1.70 (m, 4H), 1.67 – 1.37 (m, 6H), 0.91 (s, 3H). ^{13}C NMR (101 MHz, CDCl_3) δ 221.27, 145.40, 137.43, 128.99, 126.32, 113.23, 111.32, 50.60, 49.27, 48.26, 44.18, 38.75, 36.08, 31.80, 31.54, 29.91, 26.88, 26.12, 21.78, 15.43, 14.07. HRMS (ESI) m/z [M+H]⁺, calc'd for $\text{C}_{22}\text{H}_{29}\text{NO}$ 324.2322; found 324.2321.

N-phenylspiro[3.5]nonan-2-amine (3.1m). **3.1m** is prepared according to the procedure below:



Spiro [3,5] nonan-2-one was prepared according to Gu and Reusch's procedure.¹⁴ Conversion of the spirocyclic ketone to spirocyclic cyclobutylaniline was accomplished via a reductive amination procedure developed by Davies.¹⁵ To a 25 mL round bottle flask equipped with a stir

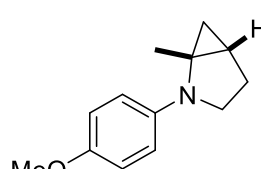
bar was added spiro [3.5] nonan-2-one (276 mg, 2 mmol, 1 equiv), aniline (0.28 mL, 3 mmol, 1.5 equiv), sodium triacetoxyborohydride (509 mg, 2.4 mmol, 1.2 equiv) and CH_2Cl_2 (6 mL). trifluoroacetic acid (0.31 mL, 4 mmol, 2 equiv) was added to the mixture at room temperature. The reaction mixture continued to stir for 6 h, and was monitored by TLC. The reaction mixture was then added with 10% sodium hydroxide solution to adjust the pH to 8-9, followed by the extraction with diethyl ether. The organic layer was then washed with water and brine, dried over sodium sulfate and concentrate. Product was purified by flash chromatography on silica gel (1:50 EtOAc/hexanes) as light yellow liquid (256 mg, 64%). IR $\nu_{\text{max}}(\text{cm}^{-1})$: 3335, 3007, 2915, 1732, 1427, 1367, 1215, 1019;

¹H NMR (400 MHz, Chloroform-*d*) δ 7.23 – 7.11 (m, 2H), 6.71 (tt, J = 7.3, 1.2 Hz, 1H), 6.62 – 6.48 (m, 2H), 3.87 (p, J = 7.5 Hz, 1H), 3.80 – 3.67 (m, 1H), 2.38 – 2.26 (m, 2H), 1.60 – 1.43 (m, 8H), 1.38 (dt, J = 6.0, 3.0 Hz, 4H). ¹³C NMR (101 MHz, CDCl₃) δ 147.65, 129.39, 117.44, 113.23, 44.05, 41.68, 41.09, 37.87, 34.43, 26.17, 23.31, 23.04. HRMS (ESI) m/z [M+H]⁺, calc'd for C₁₅H₂₁N 216.1747; found 216.1741.

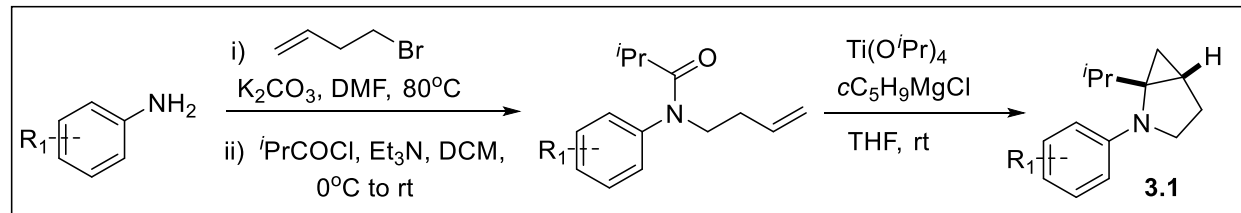
General procedure 2 (GP2): Preparation of [3. 1. 0] bicyclic cyclopropylanilines

For the preparation and characterization of compound **3.1p**: see Maity, S.; Zhu, M.; Shinabery, R. S.; Zheng, M. *Angew. Chem. Int. Ed.* **2012**, *51*, 222-226. **3.1q** is also prepared based on the same procedure.

(1*R*,5*S*)-2-(4-methoxyphenyl)-1-methyl-2-azabicyclo[3.1.0]hexane (3.1q). The compound was

 isolated after a flash chromatography on silica gel (1: 50 EtOAc/hexanes) as brown oil (290 mg, 71%). IR $\nu_{\text{max}}(\text{cm}^{-1})$: 3330, 2949, 2838, 1570, 1509, 1447, 1244, 1022; ¹H NMR (400 MHz, Chloroform-*d*) δ 6.99 – 6.88 (m, 2H), 6.87 – 6.79 (m, 2H), 3.85 (td, J = 9.6, 1.9 Hz, 1H), 3.78 (t, J = 0.8 Hz, 3H), 2.66 (td, J = 9.9, 8.1 Hz, 1H), 2.34 – 2.20 (m, 1H), 1.96 – 1.84 (m, 1H), 1.50 (s, 3H), 1.30 (dd, J = 8.7, 4.9 Hz, 1H), 0.81 (t, J = 5.1 Hz, 1H), 0.77 – 0.67 (m, 1H). ¹³C NMR (101 MHz, CDCl₃) δ 153.27, 144.39, 119.54, 114.50, 55.83, 53.69, 43.34, 26.42, 24.09, 20.15, 15.27. HRMS (ESI) m/z [M+H]⁺, calc'd for C₁₃H₁₇NO 204.1383; found 204.1382.

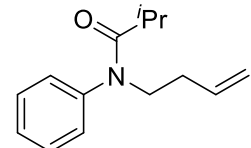
The following sequence was applied for the preparation of bicyclic cyclopropylanilines **3.1r-v**.



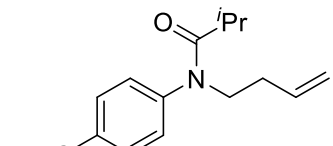
4-Bromo-1-butene (0.3 mL, 3 mmol, 1 equiv) was added to a mixture of aniline (3.6 mmol, 1.2 equiv) and potassium carbonate (830 mg, 6 mmol, 2 equiv) in dimethylformamide (5 mL). After heating at 80°C for 12 h, the reaction mixture was cooled to room temperature, diluted with CH₂Cl₂ (10 mL), and then washed with 1 N HCl aqueous solution (2 x 10 mL) to remove excess aniline. The organic layer was washed with 1 N NaOH aqueous solution (10 mL), dried over sodium sulfate, concentrated under vacuum. The alkylated intermediates were directly used in the acylation reaction without further purification.

A solution of isobutyryl chloride (0.23 mL, 2.2 mmol, 1 equiv) in CH₂Cl₂ (3 mL) was added dropwise at 0°C to a mixture of the above alkylaniline (2.2 mol, 1 equiv) and triethylamine (0.37 mL, 2.64 mmol, 1.2 equiv) in CH₂Cl₂ (3 mL). The resulting mixture was stirred overnight at room temperature. The solvents were removed under vacuum and the crude product was purified by silica gel column chromatography to give corresponding alkyl isobutyramide as listed below.

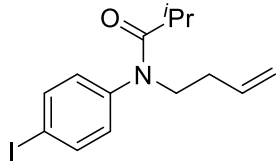
Following **GP2**, the compound was isolated after a flash chromatography

 on silica gel (1: 20 EtOAc/hexanes) as colorless oil (349 mg, 73%). IR $\nu_{\text{max}}(\text{cm}^{-1})$: ¹H NMR (400 MHz, Chloroform-*d*) δ 7.43 – 7.37 (m, 2H), 7.36 – 7.30 (m, 1H), 7.20 – 7.09 (m, 2H), 5.74 (ddt, *J* = 17.0, 10.2, 6.7 Hz, 1H), 5.09 – 4.93 (m, 2H), 3.80 – 3.68 (m, 2H), 2.39 (hept, *J* = 6.7 Hz, 1H), 2.29 – 2.20 (m, 2H), 0.98 (d, *J* = 6.8 Hz, 6H). ¹³C NMR (101 MHz, CDCl₃) δ 177.28, 142.87, 135.59, 129.80, 128.55, 127.99, 116.66, 48.54, 32.38, 31.48, 19.86.

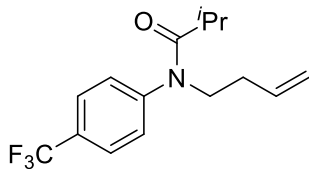
Following **GP2**, the compound was isolated after a flash

 chromatography on silica gel (1: 10 EtOAc/hexanes) as colorless oil (365 mg, 67%). IR $\nu_{\text{max}}(\text{cm}^{-1})$: ¹H NMR (400 MHz, Chloroform-*d*) δ 7.14 – 7.05 (m, 2H), 6.97 – 6.87 (m, 2H), 5.77 (ddt, *J* = 17.0, 10.2, 6.7 Hz, 1H), 5.11 – 4.97 (m,

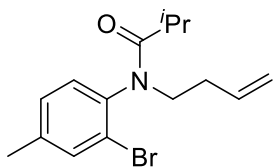
2H), 3.84 (s, 3H), 3.76 – 3.67 (m, 2H), 2.42 (p, J = 6.7 Hz, 1H), 2.32 – 2.21 (m, 2H), 1.00 (d, J = 6.7 Hz, 6H). ^{13}C NMR (101 MHz, CDCl_3) δ 177.71, 159.08, 135.70, 135.49, 129.56, 116.63, 114.88, 55.66, 48.58, 32.37, 31.35, 19.85



Following **GP2**, the compound was isolated after a flash chromatography on silica gel (1: 10 EtOAc/hexanes) as colorless oil (545 mg, 72%). IR $\nu_{\text{max}}(\text{cm}^{-1})$: ^1H NMR (400 MHz, Chloroform-*d*) δ 7.75 (d, J = 8.1 Hz, 2H), 7.00 – 6.80 (m, 2H), 5.74 (ddt, J = 17.0, 10.1, 6.7 Hz, 1H), 5.11 – 4.96 (m, 2H), 3.72 (t, J = 7.4 Hz, 2H), 2.39 (hept, J = 6.7 Hz, 1H), 2.30 – 2.17 (m, 2H), 1.00 (d, J = 6.7 Hz, 6H). ^{13}C NMR (101 MHz, CDCl_3) δ 177.05, 142.65, 139.07, 135.40, 130.57, 116.93, 93.21, 48.44, 32.37, 31.56, 19.86.



Following **GP2**, the compound was isolated after a flash chromatography on silica gel (1: 5 EtOAc/hexanes) as colorless oil (516 mg, 82%). IR $\nu_{\text{max}}(\text{cm}^{-1})$: ^1H NMR (400 MHz, Chloroform-*d*) δ 7.69 (d, J = 8.2 Hz, 2H), 7.31 (d, J = 8.1 Hz, 2H), 5.74 (ddt, J = 17.0, 10.2, 6.8 Hz, 1H), 5.12 – 4.96 (m, 2H), 3.83 – 3.70 (m, 2H), 2.35 (tt, J = 12.2, 7.7 Hz, 1H), 2.26 (tdd, J = 8.4, 6.2, 1.4 Hz, 2H), 1.02 (d, J = 6.7 Hz, 6H). ^{13}C NMR (101 MHz, CDCl_3) δ 176.89, 146.15, 135.21, 130.10 (q , J^2 = 35.1 Hz), 128.95, 126.90 (q , J^3 = 3.6 Hz), 123.84 (q , J^1 = 272.3 Hz), 116.99, 48.61, 32.36, 31.65, 19.76.



Following **GP2**, the compound was isolated after a flash chromatography on silica gel (1: 10 EtOAc/hexanes) as colorless oil (441 mg, 65%). IR $\nu_{\text{max}}(\text{cm}^{-1})$: ^1H NMR (300 MHz, Chloroform-*d*) δ 7.52 (d, J = 2.0 Hz, 1H), 7.24 – 7.05 (m, 2H), 5.89 – 5.66 (m, 1H), 5.16 – 4.96 (m, 2H), 4.19 (dt, J = 13.2, 7.8 Hz, 1H), 3.28 – 3.09 (m, 1H), 2.39 (d, J = 5.0 Hz, 3H), 2.35 – 2.16 (m, 3H),

1.08 (t, $J = 5.3$ Hz, 3H), 0.99 (t, $J = 5.3$ Hz, 3H). ^{13}C NMR (75 MHz, CDCl_3) δ 177.38, 139.99, 138.71, 135.51, 134.31, 130.48, 129.15, 123.78, 116.48, 47.41, 32.15, 31.79, 20.79, 20.06, 19.25.

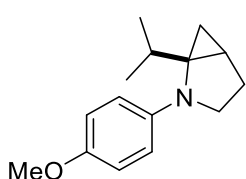
To a magnetically stirred solution of alkyl isobutyramide (2 mmol, 1 equiv) in THF (20 mL) was added titanium (IV) iso-propoxide (1 mL, 3.4 mmol, 1.7 equiv) followed by addition of cyclopentylmagnesium chloride (2 M in Et_2O) (4.4 mL, 8.8 mmol, 4.4 equiv) dropwise at room temperature. After 1 h, water (2 mL) was added at 0 °C and stirring was continued until the color dissipated. Et_2O was then added. The organic layer was separated, and the aqueous phase was extracted with Et_2O (30 mL x 2). The combined organic layers were dried over sodium sulfate and concentrated under reduced pressure. Purification of the crude compounds by column chromatography on silica gel afforded the corresponding fused cyclopropylaniline compounds as listed below.

(1S,5S)-1-isopropyl-2-phenyl-2-azabicyclo[3.1.0]hexane (3.1r). Following **GP2**, the

compound was isolated after a flash chromatography on neutral alumina gel (pure hexanes) as yellow oil (305 mg, 75%). IR $\nu_{\text{max}}(\text{cm}^{-1})$: 3340, 2944, 1739, 1437, 1367, 1215, 1022; ^1H NMR (300 MHz, Chloroform-*d*) δ 7.20 – 7.08 (m, 2H), 6.75 – 6.59 (m, 3H), 3.86 (tdd, $J = 9.7, 4.2, 1.4$ Hz, 1H), 2.90 (dddd, $J = 10.2, 8.8, 7.4, 1.4$ Hz, 1H), 2.40 (h, $J = 6.7$ Hz, 1H), 2.21 – 2.04 (m, 1H), 1.86 (dddt, $J = 12.8, 8.9, 4.4, 1.2$ Hz, 1H), 1.36 – 1.23 (m, 1H), 1.05 (ddt, $J = 9.1, 5.4, 1.0$ Hz, 1H), 0.91 (dd, $J = 6.5, 1.7$ Hz, 3H), 0.64 (dd, $J = 7.1, 1.5$ Hz, 3H), 0.48 (td, $J = 5.3, 1.5$ Hz, 1H). ^{13}C NMR (75 MHz, CDCl_3) δ 149.94, 128.86, 117.44, 116.37, 53.95, 52.92, 27.24, 26.28, 20.65, 18.73, 18.66, 17.87. HRMS (ESI) m/z [M+H]⁺, calc'd for $\text{C}_{14}\text{H}_{19}\text{N}$ 202.1590; found 202.1585.

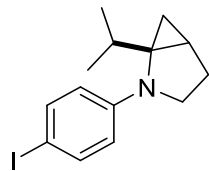
(1S,5S)-1-isopropyl-2-(4-methoxyphenyl)-2-azabicyclo[3.1.0]hexane (3.1s). Following **GP2**,

the compound was isolated after a flash chromatography on neutral



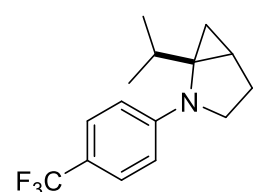
alumina gel (1: 50 EtOAc/hexanes) as brown oil (317 mg, 68%). IR $\nu_{\text{max}}(\text{cm}^{-1})$: 3530, 2964, 2371, 1720, 1565, 1507, 1239, 1034; ^1H NMR (400 MHz, Chloroform-*d*) δ 6.95 – 6.69 (m, 4H), 3.89 (td, *J* = 9.5, 2.9 Hz, 1H), 3.78 (s, 3H), 2.79 (dt, *J* = 9.7, 8.7 Hz, 1H), 2.47 – 2.34 (m, 1H), 2.24 – 2.13 (m, 1H), 1.96 (dddt, *J* = 12.3, 8.4, 2.9, 0.9 Hz, 1H), 1.35 (dt, *J* = 8.7, 5.4 Hz, 1H), 1.06 – 1.00 (m, 1H), 1.00 (d, *J* = 6.5 Hz, 3H), 0.73 (d, *J* = 7.0 Hz, 3H), 0.60 (t, *J* = 5.3 Hz, 1H). ^{13}C NMR (101 MHz, CDCl_3) δ 152.49, 144.60, 118.30, 114.53, 55.91, 53.81, 52.84, 27.11, 26.43, 20.62, 18.84, 18.41, 14.95. HRMS (ESI) m/z [M+H] $^+$, calc'd for $\text{C}_{15}\text{H}_{21}\text{NO}$ 232.1696; found 232.1690.

(1*S*,5*S*)-2-(4-iodophenyl)-1-isopropyl-2-azabicyclo[3.1.0]hexane (3.1t). Following **GP2**, the



compound was isolated after a flash chromatography on neutral alumina gel (pure hexanes) as brown oil (402 mg, 61%). IR $\nu_{\text{max}}(\text{cm}^{-1})$: 3325, 2954, 2829, 2043, 1582, 1488, 1367, 1111, 1019; ^1H NMR (400 MHz, Chloroform-*d*) δ 7.52 – 7.41 (m, 2H), 6.59 – 6.49 (m, 2H), 3.94 (qd, *J* = 9.9, 5.1 Hz, 1H), 3.00 (dddt, *J* = 9.9, 8.8, 7.1, 5.6 Hz, 1H), 2.48 – 2.36 (m, 1H), 2.29 – 2.15 (m, 1H), 1.96 (dddt, *J* = 12.7, 8.8, 4.7, 1.1 Hz, 1H), 1.42 (dtt, *J* = 7.9, 5.3, 0.8 Hz, 1H), 1.21 – 1.11 (m, 1H), 0.98 (dd, *J* = 8.3, 6.5 Hz, 3H), 0.72 (d, *J* = 6.9 Hz, 3H), 0.53 (t, *J* = 5.3 Hz, 1H). ^{13}C NMR (101 MHz, CDCl_3) δ 149.31, 137.50, 118.43, 116.39, 54.20, 53.07, 27.32, 26.23, 20.58, 18.98, 18.70, 18.61. ^{13}C NMR (101 MHz, CDCl_3) δ 149.31, 137.50, 118.43, 116.39, 54.20, 53.07, 27.32, 26.23, 20.58, 18.98, 18.70, 18.61. HRMS (ESI) m/z [M+H] $^+$, calc'd for $\text{C}_{14}\text{H}_{18}\text{IN}$ 328.0557; found 328.0555.

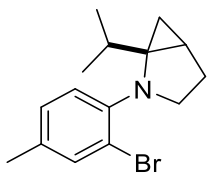
(1*S*,5*S*)-1-isopropyl-2-(4-(trifluoromethyl)phenyl)-2-azabicyclo[3.1.0]hexane (3.1u).



Following **GP2**, the compound was isolated after a flash chromatography on neutral alumina gel (1: 100 EtOAc/hexanes) as colorless oil (397 mg, 74%). IR $\nu_{\text{max}}(\text{cm}^{-1})$: 3340, 2968, 1611, 1526, 1328, 1109, 1012; ^1H NMR

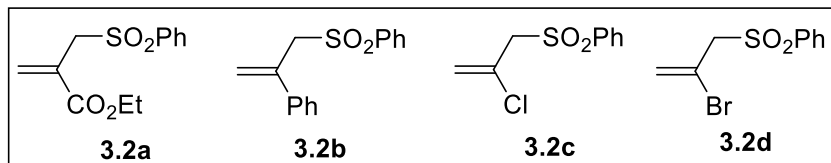
(400 MHz, Chloroform-*d*) δ 7.53 – 7.37 (m, 2H), 6.84 – 6.68 (m, 2H), 3.98 (td, J = 9.8, 5.7 Hz, 1H), 3.18 (ddd, J = 10.0, 8.9, 5.8 Hz, 1H), 2.49 (hept, J = 6.8 Hz, 1H), 2.28 (ddt, J = 12.4, 9.5, 6.1 Hz, 1H), 1.96 (dddt, J = 12.9, 9.0, 5.7, 1.2 Hz, 1H), 1.52 – 1.41 (m, 1H), 1.27 (dd, J = 9.0, 5.2 Hz, 1H), 0.98 (d, J = 6.5 Hz, 3H), 0.74 (d, J = 7.0 Hz, 3H), 0.55 (t, J = 5.3 Hz, 1H). ^{13}C NMR (101 MHz, CDCl₃) δ 151.68, 126.12 (q , J^3 = 3.8 Hz), 125.13 (q , J^1 = 270.3 Hz), 118.52 (q , J^2 = 32.5 Hz), 114.80, 54.54, 53.35, 27.45, 26.22, 20.59, 20.55, 19.15, 18.49. HRMS (ESI) m/z [M+H]⁺, calc'd for C₁₅H₁₈F₃N 270.1464; found 270.1467.

(1*S*,5*S*)-2-(2-bromo-4-methylphenyl)-1-isopropyl-2-azabicyclo[3.1.0]hexane (3.1v).



Following **GP2**, the compound was isolated after a flash chromatography on neutral alumina gel (pure hexanes) as brown oil (302 mg, 51%). IR ν_{max} (cm⁻¹): 3330, 2939, 2833, 1739, 1490, 1367, 1220, 1022; ^1H NMR (400 MHz, Chloroform-*d*) δ 7.35 (dd, J = 2.0, 0.9 Hz, 1H), 7.25 (d, J = 1.8 Hz, 1H), 7.01 (ddd, J = 8.3, 2.0, 0.8 Hz, 1H), 4.07 (ddd, J = 9.8, 8.8, 1.2 Hz, 1H), 2.32 – 2.19 (m, 4H), 2.11 – 1.96 (m, 2H), 1.89 (ddt, J = 12.2, 7.5, 1.2 Hz, 1H), 1.24 (dt, J = 9.3, 4.8 Hz, 1H), 0.99 (t, J = 5.2 Hz, 1H), 0.94 (d, J = 6.6 Hz, 3H), 0.85 (dd, J = 8.7, 5.6 Hz, 1H), 0.69 (d, J = 7.0 Hz, 3H). HRMS (ESI) m/z [M+H]⁺, calc'd for C₁₅H₂₀BrN 294.0852, 296.0832; found 294.0852, 296.0832.

Allylsulfone **3.2a**, **3.2b**, **3.2c** and **3.2d** were prepared according to those reported procedures.



General Procedure 3 (GP3): Visible light catalyzed difunctionalization of N-cyclobutylanilines and N-cyclopropylanilines



An oven-dried test tube equipped with a stir bar was charged with $\text{Ir}(\text{dtbbpy})(\text{ppy})_2\text{PF}_6$ (2 mol%), cyclopropylaniline or cyclobutylaniline derivative (0.2 mmol, 1 equiv), trimethylsilyl cyanide (75 μL , 0.6 mmol, 3 equiv), allylsulfone (0.6 mmol, 3 equiv) and CH_2Cl_2 (2 mL). The test tube was capped with a Teflon screw cap and followed by degassing using Freeze-Pump-Thaw sequence three times. The reaction mixture was then irradiated with a 6 W two strip blue LEDs circled 2 cm from the test tube. After the reaction was complete as monitored by TLC, the mixture was diluted with diethyl ether and filtered through a short pad of silica gel. The solution was concentrated and the residue was purified by silica gel flash chromatography to afford the corresponding annulation product.

Substrates Scope of *N*-cyclobutylaniline:

ethyl 7-cyano-7-(3,5-dimethylphenylamino)-2-methyleneheptanoate (3.3a). Following GP3

with **3.1a** (35 mg, 0.2 mmol) and allylsulfone **3.2a** (152 mg, 0.6 mmol), the product was isolated after flash chromatography on silica gel (1: 10 EtOAc/hexanes) as light yellow oil (56 mg, 90%). IR $\nu_{\text{max}}(\text{cm}^{-1})$: 3340, 2944, 2833, 1732, 1645, 1454, 1212, 1113, 1017; ^1H NMR (400 MHz, Chloroform-*d*) δ 6.56 – 6.50 (m, 1H), 6.42 – 6.30 (m, 2H), 6.18 (d, J = 1.4 Hz, 1H), 5.56 (q, J = 1.3 Hz, 1H), 4.23 (q, J = 7.1 Hz, 2H), 2.41 – 2.31 (m, 2H), 2.28 – 2.25 (m, 8H), 2.00 – 1.91 (m, 2H), 1.61 (dd, J = 15.8, 11.8, 6.7, 2.4 Hz, 4H), 1.32 (t, J = 7.1 Hz, 3H). ^{13}C NMR (101 MHz, CDCl_3) δ 167.32, 145.13, 140.50,

139.47, 125.14, 122.19, 119.87, 112.21, 60.91, 46.07, 33.54, 31.80, 28.04, 25.35, 21.67, 14.43. HRMS (ESI) m/z [M+Na]⁺, calc'd for C₁₉H₂₆N₂O₂ 337.1886; found 337.1884.

2-(3,5-dimethylphenylamino)-7-phenyloct-7-enenitrile (3.3b). Following **GP3** with **3.1a** (35

mg, 0.2 mmol) and allylsulfone **3.2b** (155 mg, 0.6 mmol), the product was isolated after flash chromatography on silica gel (1: 10 EtOAc/hexanes) as light yellow oil (48 mg, 75%). IR $\nu_{\text{max}}(\text{cm}^{-1})$: 3321, 2939, 2841, 1726, 1632, 1460, 1112, 1015; ¹H NMR (400 MHz, Chloroform-*d*) δ 7.43 – 7.39 (m, 2H), 7.38 – 7.33 (m, 2H), 7.32 – 7.28 (m, 1H), 6.54 (dd, *J* = 1.9, 1.1 Hz, 1H), 6.38 – 6.28 (m, 2H), 5.30 (d, *J* = 1.4 Hz, 1H), 5.09 (q, *J* = 1.3 Hz, 1H), 4.15 (d, *J* = 5.0 Hz, 1H), 3.59 (s, 1H), 2.63 – 2.52 (m, 2H), 2.28 (s, 6H), 1.96 – 1.87 (m, 2H), 1.68 – 1.51 (m, 5H). ¹³C NMR (101 MHz, CDCl₃) δ 148.11, 145.11, 141.15, 139.46, 128.57, 127.67, 126.33, 122.20, 119.88, 113.01, 112.22, 46.09, 35.21, 33.61, 27.62, 25.36, 21.67. HRMS (ESI) m/z [M+H]⁺, calc'd for C₂₂H₂₆N₂ 319.2169; found 319.2174.

7-chloro-2-(3,5-dimethylphenylamino)oct-7-enenitrile (3.3c). Following **GP3** with **3.1a** (35

mg, 0.2 mmol) and allylsulfone **3.2c** (130 mg, 0.6 mmol), the product was isolated after flash chromatography on silica gel (1: 10 EtOAc/hexanes) as light yellow oil (26 mg, 47%). IR $\nu_{\text{max}}(\text{cm}^{-1})$: 3315, 2944, 2833, 2033, 1645, 1454, 1118, 1024; ¹H NMR (400 MHz, Chloroform-*d*) δ 6.55 (s, 1H), 6.36 (s, 2H), 5.20 (d, *J* = 1.2 Hz, 1H), 5.17 (d, *J* = 1.4 Hz, 1H), 4.30 – 4.13 (m, 1H), 3.63 (d, *J* = 9.4 Hz, 1H), 2.41 (h, *J* = 8.5, 7.8 Hz, 2H), 2.29 (s, 6H), 1.95 (ttd, *J* = 12.3, 8.9, 7.9, 3.5 Hz, 2H), 1.71 – 1.56 (m, 6H). ¹³C NMR (101 MHz, CDCl₃) δ 145.08, 142.29, 139.48, 122.28,

119.80, 112.84, 112.27, 46.10, 38.94, 33.56, 26.64, 24.74, 21.66. HRMS (ESI) m/z [M+H]⁺, calc'd for C₁₆H₂₁ClN₂ 277.1466; found 277.1469.

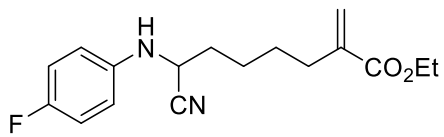
7-bromo-2-(3,5-dimethylphenylamino)oct-7-enenitrile (3.3d). Following **GP3** with **3.1a** (35

mg, 0.2 mmol) and allylsulfone **3.2d** (157 mg, 0.6 mmol), the product was isolated after flash chromatography on silica gel (1: 10 EtOAc/hexanes) as light yellow oil (27 mg, 42%). IR ν_{max} (cm⁻¹): 3320, 2935, 2829, 1659, 1451, 1406, 1116, 1022; ¹H NMR (400 MHz, Benzene-*d*₆) δ 6.58 (s, 1H), 6.27 (s, 2H), 5.38 (d, *J* = 1.7 Hz, 1H), 5.30 (q, *J* = 1.3 Hz, 1H), 3.75 – 3.61 (m, 1H), 3.08 (t, *J* = 9.2 Hz, 1H), 2.28 (s, 6H), 2.19 – 2.12 (m, 2H), 1.33 (dq, *J* = 14.6, 7.3, 6.9 Hz, 4H), 1.21 – 1.10 (m, 2H). ¹³C NMR (101 MHz, C₆D₆) δ 145.29, 138.89, 134.20, 122.00, 119.39, 116.73, 112.32, 45.47, 40.86, 33.04, 27.13, 24.25, 21.35. HRMS (ESI) m/z [M+H]⁺, calc'd for C₁₆H₂₁BrN₂ 321.0961, 323.0941; found 321.0965, 323.0944.

ethyl 7-cyano-7-(4-methoxyphenylamino)-2-methyleneheptanoate (3.3e). Following **GP3**

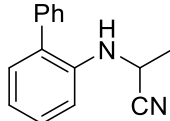
with **3.1e** (36 mg, 0.2 mmol), allylsulfone **3.2a** (152 mg, 0.6 mmol) under the irradiation of a 6 W 4 strip blue LED, the product was isolated after flash chromatography on silica gel (1: 10 EtOAc/hexanes) as light yellow oil (43 mg, 68%). IR ν_{max} (cm⁻¹): 3320, 2949, 2824, 1654, 1449, 1106, 1014; ¹H NMR (400 MHz, Chloroform-*d*) δ 6.92 – 6.80 (m, 2H), 6.76 – 6.63 (m, 2H), 6.17 (d, *J* = 1.4 Hz, 1H), 5.62 – 5.49 (m, 1H), 4.22 (q, *J* = 7.1 Hz, 2H), 4.15 – 4.07 (m, 1H), 3.77 (s, 3H), 3.51 (d, *J* = 9.8 Hz, 1H), 2.36 (t, *J* = 7.1 Hz, 2H), 1.96 (q, *J* = 7.3 Hz, 2H), 1.68 – 1.53 (m, 4H), 1.31 (t, *J* = 7.1 Hz, 3H). ¹³C NMR (101 MHz, CDCl₃) δ 167.32, 154.19, 140.51, 138.97, 125.11, 119.99, 116.37, 115.20, 60.90, 55.86, 47.49, 33.52, 31.80, 28.05, 25.37, 14.42. HRMS (ESI) m/z [M+H]⁺, calc'd for C₁₈H₂₄N₂O₃ 317.1860; found 317.1860.

ethyl 7-cyano-7-(4-fluorophenylamino)-2-methylenheptanoate (3.3f). Following **GP3** with



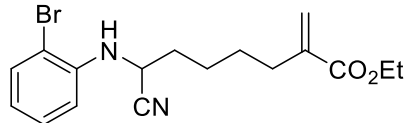
3.1f (33 mg, 0.2 mmol) and allylsulfone **3.2a** (152 mg, 0.6 mmol), the product was isolated after flash chromatography on silica gel (1: 10 EtOAc/hexanes) as light yellow oil (27 mg, 44%). IR $\nu_{\text{max}}(\text{cm}^{-1})$: 3320, 2960, 2873, 1680, 1466, 1131, 1018; ^1H NMR (400 MHz, Methylene Chloride-*d*₂) δ 7.06 – 6.93 (m, 2H), 6.73 (ddd, *J* = 6.6, 5.2, 3.0 Hz, 2H), 6.15 (d, *J* = 1.5 Hz, 1H), 5.57 (q, *J* = 1.3 Hz, 1H), 4.27 – 4.14 (m, 3H), 3.80 (dd, *J* = 8.3, 5.4 Hz, 1H), 2.43 – 2.29 (m, 2H), 2.05 – 1.93 (m, 2H), 1.68 – 1.56 (m, 4H), 1.30 (t, *J* = 7.1 Hz, 3H). ^{13}C NMR (101 MHz, CD₂Cl₂) δ 167.50, 158.81, 156.44, 142.12, 141.17, 124.98, 120.04, 116.58, 115.83, 61.16, 47.12, 33.68, 32.07, 28.37, 25.69, 14.55. HRMS (ESI) m/z [M+H]⁺, calc'd for C₁₇H₂₁FN₂O₂ 305.1660; found 305.1663.

ethyl 7-(biphenyl-2-ylamino)-7-cyano-2-methylenheptanoate (3.3g). Following **GP3** with



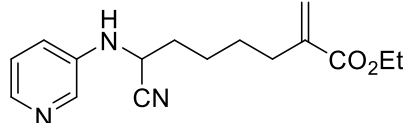
3.1g (45 mg, 0.2 mmol) and allylsulfone **3.2a** (152 mg, 0.6 mmol), the product was isolated after flash chromatography on silica gel (1: 10 EtOAc/hexanes) as light yellow oil (55 mg, 75%). IR $\nu_{\text{max}}(\text{cm}^{-1})$: 3325, 2964, 2853, 1650, 1452, 1120, 1020; ^1H NMR (400 MHz, Methylene Chloride-*d*₂) δ 7.51 – 7.44 (m, 2H), 7.42 – 7.35 (m, 3H), 7.32 (td, *J* = 7.8, 1.7 Hz, 1H), 7.17 (dd, *J* = 7.6, 1.6 Hz, 1H), 6.94 (td, *J* = 7.5, 1.1 Hz, 1H), 6.85 (d, *J* = 8.2 Hz, 1H), 6.12 (d, *J* = 1.5 Hz, 1H), 5.64 – 5.43 (m, 1H), 4.24 (dt, *J* = 9.2, 7.1 Hz, 1H), 4.17 (q, *J* = 7.1 Hz, 2H), 4.00 (d, *J* = 9.1 Hz, 1H), 2.29 (d, *J* = 6.8 Hz, 2H), 1.93 – 1.76 (m, 2H), 1.51 (td, *J* = 6.5, 3.4 Hz, 4H), 1.28 (t, *J* = 7.1 Hz, 3H). ^{13}C NMR (101 MHz, CD₂Cl₂) δ 167.42, 142.58, 141.11, 139.07, 131.19, 129.84, 129.82, 129.61, 129.31, 128.17, 124.92, 120.15, 120.13, 112.71, 61.13, 46.39, 33.54, 32.07, 28.20, 25.64, 14.56. HRMS (ESI) m/z [M+Na]⁺, calc'd for C₂₃H₂₆N₂O₂ 385.1886; found 385.1890.

ethyl 7-(2-bromophenylamino)-7-cyano-2-methyleneheptanoate (3.3h). Following **GP3** with



3.1h (45 mg, 0.2 mmol) and allylsulfone **3.2a** (152 mg, 0.6 mmol), the product was isolated after flash chromatography on silica gel (1: 10 EtOAc/hexanes) as light yellow oil (31 mg, 43%). IR $\nu_{\text{max}}(\text{cm}^{-1})$: 3335, 2944, 2833, 1652, 1459, 1106, 1017; ^1H NMR (400 MHz, Chloroform-*d*) δ 7.50 (dd, J = 7.8, 1.4 Hz, 1H), 7.36 – 7.21 (m, 1H), 6.87 – 6.68 (m, 2H), 6.14 (d, J = 1.4 Hz, 1H), 5.55 (s, 1H), 4.47 (d, J = 8.5 Hz, 1H), 4.27 (q, J = 7.6 Hz, 1H), 4.18 (q, J = 7.1 Hz, 2H), 2.36 (t, J = 7.3 Hz, 2H), 2.05 (dd, J = 11.1, 5.1 Hz, 2H), 1.62 (tdd, J = 12.5, 7.1, 4.7 Hz, 4H), 1.28 (d, J = 7.1 Hz, 3H). ^{13}C NMR (101 MHz, CDCl_3) δ 167.48, 142.76, 141.19, 133.39, 129.31, 124.98, 120.92, 119.57, 113.20, 111.12, 61.17, 46.13, 33.60, 32.12, 28.36, 25.71, 14.59. HRMS (ESI) m/z [M+Na] $^+$, calc'd for $\text{C}_{17}\text{H}_{21}\text{BrN}_2\text{O}_2$ 387.0679, 389.0659; found 387.0681, 389.0660.

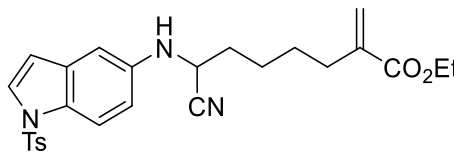
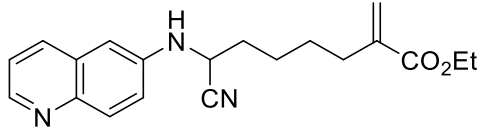
ethyl 7-cyano-2-methylene-7-(pyridin-3-ylamino)heptanoate (3.3j). Following **GP3** with **3.1j**



(30 mg, 0.2 mmol) and allylsulfone **3.2a** (152 mg, 0.6 mmol), the product was isolated after flash chromatography on silica gel (1: 1 EtOAc/hexanes) as yellow oil (47 mg, 82%). IR $\nu_{\text{max}}(\text{cm}^{-1})$: 3311, 2944, 2833, 2043, 1654, 1449, 1017; ^1H NMR (400 MHz, Chloroform-*d*) δ 8.15 (dd, J = 5.4, 3.5 Hz, 2H), 7.20 (dd, J = 8.3, 4.7 Hz, 1H), 7.04 (ddd, J = 8.3, 2.8, 1.3 Hz, 1H), 6.18 (d, J = 1.4 Hz, 1H), 5.57 (q, J = 1.4 Hz, 1H), 4.22 (q, J = 7.1 Hz, 3H), 3.99 (d, J = 9.1 Hz, 1H), 2.37 (t, J = 7.0 Hz, 2H), 2.09 – 1.95 (m, 2H), 1.70 – 1.55 (m, 4H), 1.32 (t, J = 7.1 Hz, 3H). ^{13}C NMR (101 MHz, CDCl_3) δ 167.31, 141.55, 140.96, 140.34, 137.10, 125.22, 124.09, 120.00, 119.14, 60.89, 45.46, 33.04, 31.63, 27.94, 25.23, 14.34. HRMS (ESI) m/z [M+H] $^+$, calc'd for $\text{C}_{16}\text{H}_{21}\text{N}_3\text{O}_2$ 288.1707; found 288.1705.

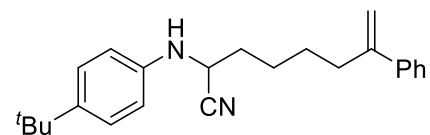
ethyl 7-cyano-2-methylene-7-(quinolin-6-ylamino)heptanoate (3.3k). Following **GP3** with **3.1k** (40 mg, 0.2 mmol) and allylsulfone **3.2a** (152 mg, 0.6 mmol), the product was isolated after flash chromatography on silica gel (1: 1 EtOAc/hexanes) as yellow oil (41 mg, 61%). IR $\nu_{\text{max}}(\text{cm}^{-1})$: 3311, 2939, 2824, 1736, 1447, 1362, 1217, 1027; ^1H NMR (400 MHz, Methylene Chloride-*d*₂) δ 8.67 (dd, *J* = 4.2, 1.7 Hz, 1H), 8.12 – 7.95 (m, 1H), 7.93 (d, *J* = 9.0 Hz, 1H), 7.33 (dd, *J* = 8.3, 4.2 Hz, 1H), 7.18 (dd, *J* = 9.0, 2.7 Hz, 1H), 6.93 (d, *J* = 2.7 Hz, 1H), 6.14 (d, *J* = 1.4 Hz, 1H), 5.56 (q, *J* = 1.4 Hz, 1H), 4.37 (dt, *J* = 8.8, 7.0 Hz, 1H), 4.27 (d, *J* = 8.9 Hz, 1H), 4.18 (q, *J* = 7.1 Hz, 2H), 2.41 – 2.30 (m, 2H), 2.13 – 2.01 (m, 2H), 1.65 (ddq, *J* = 29.0, 12.4, 5.3, 2.8 Hz, 4H), 1.34 – 1.21 (m, 3H). ^{13}C NMR (101 MHz, CD₂Cl₂) δ 167.53, 147.97, 144.59, 143.64, 141.16, 134.71, 131.34, 130.14, 125.05, 122.24, 121.65, 119.77, 105.99, 61.19, 46.17, 33.55, 32.06, 28.40, 25.72, 14.56. HRMS (ESI) m/z [M+H]⁺, calc'd for C₂₀H₂₃N₃O₂ 338.1863; found 338.1861.

ethyl 7-cyano-2-methylene-7-(1-tosyl-1*H*-indol-5-ylamino)heptanoate (3.3l). Following **GP3** with **3.1l** (68 mg, 0.2 mmol) and allylsulfone **3.2a** (152 mg, 0.6 mmol), the product was isolated after flash chromatography on silica gel (1: 5 EtOAc/hexanes) as light yellow oil (76 mg, 79%). IR $\nu_{\text{max}}(\text{cm}^{-1})$: 3320, 2944, 2824, 2033, 1703, 1461, 1121, 1019; ^1H NMR (400 MHz, Chloroform-*d*) δ 7.84 (d, *J* = 8.8 Hz, 1H), 7.77 – 7.67 (m, 2H), 7.49 (d, *J* = 3.6 Hz, 1H), 7.20 (d, *J* = 8.1 Hz, 2H), 6.81 (d, *J* = 2.3 Hz, 1H), 6.71 (dd, *J* = 8.9, 2.4 Hz, 1H), 6.54 (dd, *J* = 3.6, 0.8 Hz, 1H), 6.16 (d, *J* = 1.5 Hz, 1H), 5.54 (q, *J* = 1.4 Hz, 1H), 4.28 – 4.10 (m, 3H), 3.83 (d, *J* = 8.7 Hz, 1H), 2.33 (d, *J* = 7.8 Hz, 5H), 1.96 (q, *J* = 7.1 Hz, 2H), 1.60 (dd, *J* = 15.5, 13.1, 7.9, 5.5 Hz, 4H), 1.30 (t, *J* = 7.1 Hz, 3H). ^{13}C NMR (101 MHz, CDCl₃) δ 167.27,



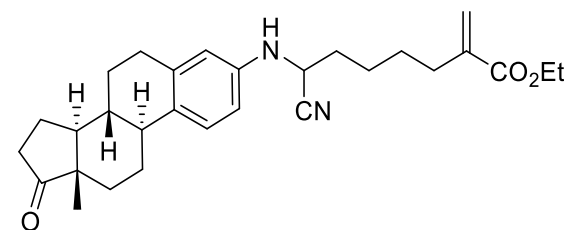
145.00, 141.65, 140.43, 135.32, 132.15, 129.99, 129.65, 127.27, 126.84, 125.09, 119.85, 114.76, 113.94, 109.25, 104.89, 60.85, 46.67, 33.33, 31.70, 27.96, 25.31, 21.68, 14.36. HRMS (ESI) m/z [M+H]⁺, calc'd for C₂₆H₂₉N₃O₄S 480.1952; found 480.1957.

2-(4-*tert*-butylphenylamino)-7-phenyloct-7-enenitrile (3.3i). Following **GP3** with **3.1i** (41 mg,



0.2 mmol) and allylsulfone **3.2b** (155 mg, 0.6 mmol), the product was isolated after flash chromatography on silica gel (1: 10 EtOAc/hexanes) as colorless oil (52 mg, 75%). IR ν_{max} (cm⁻¹): 3320, 2939, 2833, 2057, 1654, 1461, 1106, 1017; ¹H NMR (400 MHz, Chloroform-*d*) δ 7.44 – 7.39 (m, 2H), 7.39 – 7.32 (m, 2H), 7.29 (dd, *J* = 7.9, 6.1 Hz, 3H), 6.75 – 6.57 (m, 2H), 5.36 – 5.26 (m, 1H), 5.09 (d, *J* = 1.7 Hz, 1H), 4.14 (dt, *J* = 9.3, 7.0 Hz, 1H), 3.63 (d, *J* = 9.5 Hz, 1H), 2.57 (t, *J* = 7.3 Hz, 2H), 1.92 (ddd, *J* = 9.1, 7.1, 4.0 Hz, 2H), 1.71 – 1.47 (m, 4H), 1.31 (s, 9H). ¹³C NMR (101 MHz, CDCl₃) δ 148.08, 143.00, 142.62, 141.13, 128.54, 127.63, 126.49, 126.30, 119.93, 114.04, 112.96, 46.26, 35.17, 34.19, 33.53, 31.65, 27.61, 25.34. HRMS (ESI) m/z [M+H]⁺, calc'd for C₂₄H₃₀N₂ 347.2482; found 347.2481.

ethyl 7-cyano-7-((8*R*,9*S*,13*S*,14*S*)-13-methyl-17-oxo-7,8,9,11,12,13,14,15,16,17-decahydro-

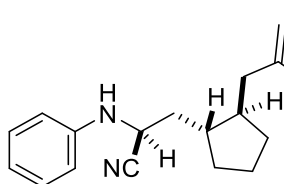


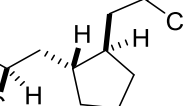
6*H*-cyclopenta[*a*]phenanthren-3-ylamino)-2-methyleneheptanoate (3.3o). Following **GP3** with **3.1o** (64 mg, 0.2 mmol) and allylsulfone **3.2a** (152 mg, 0.6 mmol), the product was isolated after flash chromatography on silica gel (1: 5 EtOAc/hexanes) as light yellow oil (42 mg, 45%). IR ν_{max} (cm⁻¹): 3311, 2944, 2843, 2014, 1657, 1444, 1116, 1017; ¹H NMR (400 MHz, Chloroform-*d*) δ 7.18 (d, *J* = 8.4 Hz, 1H), 6.55 (dd, *J* = 8.4, 2.6 Hz, 1H), 6.47 (d, *J* = 2.6 Hz, 1H), 6.17 (d, *J* = 1.4 Hz, 1H), 5.55 (q, *J* = 1.3 Hz, 1H), 4.32 – 4.14 (m, 3H), 3.66 (dt, *J* = 9.5, 4.9 Hz, 1H), 2.88 (dt, *J* =

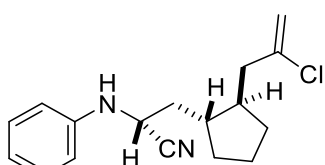
6.4, 3.5 Hz, 2H), 2.51 (dd, J = 18.8, 8.6 Hz, 1H), 2.37 (q, J = 6.8 Hz, 3H), 2.24 (dt, J = 10.1, 6.2 Hz, 1H), 2.14 (dd, J = 18.7, 9.0 Hz, 1H), 2.08 – 1.90 (m, 4H), 1.70 – 1.44 (m, 9 H), 1.32 (t, J = 7.1 Hz, 3H), 0.92 (s, 3H). ^{13}C NMR (101 MHz, CDCl_3) δ 221.06, 167.23, 142.98, 140.43, 137.86, 131.75, 126.60, 125.04, 119.80, 114.42, 112.31, 60.83, 50.54, 48.16, 46.17, 44.10, 38.52, 38.50, 36.01, 33.43, 31.72, 29.77, 27.97, 26.68, 26.00, 25.29, 21.71, 14.36, 14.00. HRMS (ESI) m/z [M+Na] $^+$, calc'd for $\text{C}_{29}\text{H}_{38}\text{N}_2\text{O}_3$ 485.2775; found 485.2778.

Following **GP3** with **3.1n** (38 mg, 0.2 mmol) and allylsulfone **3.2c** (130 mg, 0.6 mmol), the products (two isomers, **3.3n-cis** and **3.3n-trans**, d.r. = 1:1) were isolated after flash chromatography on silica gel (1: 10 EtOAc/hexanes) as light yellow oil (49 mg, 89%).

(S)-3-((1*R*,2*R*)-2-(2-chloroallyl)cyclopentyl)-2-(phenylamino)propanenitrile (3.3n-trans),



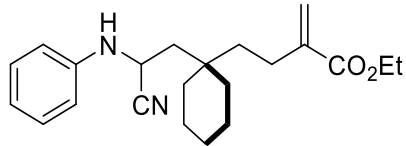

 colorless oil, (25 mg, 45%). IR $\nu_{\text{max}}(\text{cm}^{-1})$: 3320, 2939, 2833, 2043, 1729, 1454, 1019; ^1H NMR (400 MHz, Methylene Chloride- d_2) δ 7.30 – 7.23 (m, 2H), 6.87 (tt, J = 7.4, 1.1 Hz, 1H), 6.74 (ddd, J = 8.5, 2.5, 1.5 Hz, 2H), 5.21 (dq, J = 2.1, 1.2 Hz, 1H), 5.17 (d, J = 1.3 Hz, 1H), 4.25 (td, J = 9.5, 5.5 Hz, 1H), 3.87 (d, J = 9.4 Hz, 1H), 2.55 – 2.43 (m, 1H), 2.35 – 2.23 (m, 1H), 2.20 – 2.11 (m, 1H), 2.07 – 1.97 (m, 1H), 1.95 – 1.85 (m, 2H), 1.82 (tdd, J = 8.9, 5.9, 2.9 Hz, 2H), 1.72 – 1.58 (m, 2H), 1.32 (dddd, J = 14.8, 10.2, 7.6, 2.0 Hz, 2H). ^{13}C NMR (101 MHz, CD₂Cl₂) δ 145.60, 142.48, 130.01, 120.34, 120.03, 114.50, 113.70, 46.02, 45.10, 43.44, 42.41, 39.35, 32.87, 32.10, 24.38. HRMS (ESI) m/z [M+H]⁺, calc'd for C₁₇H₂₁ClN₂ 289.1466; found 289.1467.



(R)-3-((1*R*,2*R*)-2-(2-chloroallyl)cyclopentyl)-2-(phenylamino)propanenitrile (3.3n-cis), colorless oil, (24 mg, 44%). IR ν_{max} (cm⁻¹): 3328, 2976, 2856, 2019, 1772, 1503, 1020; ¹H NMR (400 MHz, Chloroform-*d*) δ 7.35 – 7.22 (m, 2H), 6.89 (tt, *J* =

7.3, 1.1 Hz, 1H), 6.77 – 6.65 (m, 2H), 4.31 – 4.18 (m, 1H), 3.68 (d, J = 9.6 Hz, 1H), 2.52 – 2.39 (m, 1H), 2.35 – 2.24 (m, 1H), 2.20 – 2.08 (m, 1H), 2.03 – 1.73 (m, 5H), 1.64 (dddt, J = 16.3, 13.1, 11.2, 6.8 Hz, 2H), 1.42 – 1.21 (m, 2H). ^{13}C NMR (101 MHz, CDCl_3) δ 145.46, 142.38, 130.12, 120.63, 120.44, 114.63, 114.01, 45.51, 45.46, 43.41, 41.81, 40.06, 33.09, 32.37, 24.50. HRMS (ESI) m/z [M+H] $^+$, calc'd for $\text{C}_{17}\text{H}_{21}\text{ClN}_2$ 289.1466; found 289.1467.

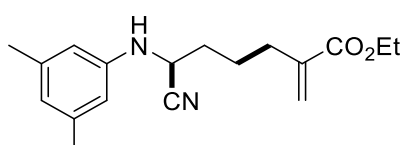
ethyl 4-(1-(2-cyano-2-(phenylamino)ethyl)cyclohexyl)-2-methylenebutanoate (3.3m).



Following **GP3** with **3.1m** (43 mg, 0.2 mmol) and allylsulfone **3.2a** (152 mg, 0.6 mmol), the product was isolated after flash chromatography on silica gel (1: 10 EtOAc/hexanes) as colorless oil (29 mg, 41%). IR $\nu_{\text{max}}(\text{cm}^{-1})$: 3315, 2949, 2829, 2033, 1642, 1456, 1014; ^1H NMR (300 MHz, Chloroform-*d*) δ 7.32 – 7.23 (m, 2H), 6.86 (t, J = 7.3 Hz, 1H), 6.78 (d, J = 8.0 Hz, 2H), 6.15 (d, J = 1.4 Hz, 1H), 5.60 (s, 1H), 4.42 (dt, J = 9.6, 6.8 Hz, 1H), 4.25 (q, J = 7.1 Hz, 2H), 4.04 (d, J = 10.0 Hz, 1H), 2.24 (tt, J = 13.0, 6.1 Hz, 2H), 2.04 (qd, J = 14.8, 6.7 Hz, 2H), 1.66 (ddd, J = 13.9, 12.0, 4.9 Hz, 1H), 1.54 – 1.39 (m, 11H), 1.33 (t, J = 7.1 Hz, 3H). ^{13}C NMR (75 MHz, CDCl_3) δ 167.42, 145.10, 140.97, 129.67, 125.29, 120.82, 119.96, 114.36, 61.06, 41.97, 36.44, 35.85, 35.59, 26.40, 26.25, 21.71, 21.67, 14.46. HRMS (ESI) m/z [M+Na] $^+$, calc'd for $\text{C}_{22}\text{H}_{30}\text{N}_2\text{O}_2$ 377.2199; found 377.2200.

Substrate Scope of *N*-cyclopropylaniline:

ethyl 6-cyano-6-(3,5-dimethylphenylamino)-2-methylenhexanoate (3.3.1a). Following **GP3**



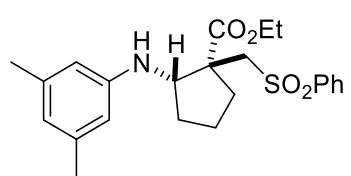
with **3.1.1a** (32 mg, 0.2 mmol) and allylsulfone **3.2a** (152 mg, 0.6 mmol), the product was isolated after flash chromatography on silica gel (1: 10 EtOAc/hexanes) as light yellow oil (25 mg, 42%). ^1H NMR (400 MHz, Chloroform-*d*) δ 6.54 (s, 1H), 6.35 (s, 2H), 6.21 (d, J = 1.3 Hz, 1H),

5.59 (q, $J = 1.4$ Hz, 1H), 4.23 (q, $J = 7.1$ Hz, 3H), 3.66 (d, $J = 9.5$ Hz, 1H), 2.46 – 2.36 (m, 2H), 2.28 (s, 6H), 2.01 – 1.91 (m, 2H), 1.80 (tdd, $J = 10.9, 7.0, 5.4$ Hz, 2H), 1.32 (t, $J = 7.1$ Hz, 3H).

^{13}C NMR (101 MHz, CDCl_3) δ 167.11, 145.09, 139.91, 139.45, 125.54, 122.24, 119.78, 112.25,

61.01, 46.00, 33.24, 31.35, 24.78, 21.65, 14.40. HRMS (ESI) m/z [M+H] $^+$, calc'd for

(1*S*,2*S*)-ethyl 2-(3,5-dimethylphenylamino)-1-



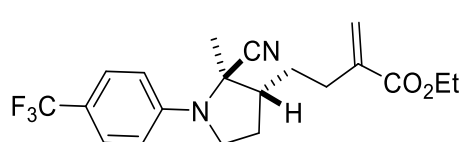
(phenylsulfonylmethyl)cyclopentanecarboxylate (3.3.1a').

Following **GP3** with **3.1.1a** (32 mg, 0.2 mmol) and allylsulfone **3.2a** (152 mg, 0.6 mmol), the product was isolated after flash chromatography on silica gel (1: 5 EtOAc/hexanes) as light yellow oil (16 mg, 19%). ^1H NMR (400 MHz, Chloroform-*d*) δ 7.96 – 7.84 (m, 2H), 7.70 – 7.60 (m, 1H), 7.55 (tt, $J = 6.8, 1.5$ Hz, 2H), 6.35 (d, $J = 2.5$ Hz, 1H), 6.20 (d, $J = 1.5$ Hz, 2H), 4.18 (q, $J = 7.1$ Hz, 2H), 4.07 (d, $J = 14.1$ Hz, 1H), 3.72 (dd, $J = 10.0, 6.8$ Hz, 1H), 3.18 (d, $J = 14.1$ Hz, 1H), 2.68 (tt, $J = 8.8, 4.3$ Hz, 1H), 2.26 (t, $J = 6.4$ Hz, 1H), 2.21 (s, 6H), 2.08 – 1.90 (m, 2H), 1.87 – 1.72 (m, 1H), 1.44 – 1.34 (m, 1H), 1.30 (t, $J = 7.1$ Hz, 3H), 1.27 (d, $J = 1.6$ Hz, 1H). ^{13}C NMR (101 MHz, CDCl_3) δ 172.61, 147.08, 141.02, 139.21, 133.86, 129.41, 127.99, 119.82, 111.13, 63.58, 63.11, 61.90, 54.04, 30.83, 30.12, 21.65, 20.58, 14.30. HRMS (ESI) m/z [M+H] $^+$, calc'd for

Substrate Scope of Fused cyclopropylaniline:

Following **GP3** with **3.1p** (48 mg, 0.2 mmol) and allylsulfone **3.2a** (152 mg, 0.6 mmol), major product (two isomers, d.r. = 5:1) was isolated after flash chromatography on neutral alumina gel (1: 30 EtOAc/hexanes).

ethyl 4-((2*R*,3*R*)-2-cyano-2-methyl-1-(4-(trifluoromethyl)phenyl)pyrrolidin-3-yl)-2-

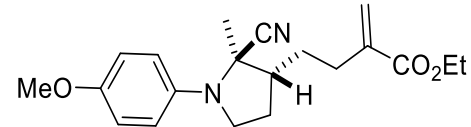


methylenebutanoate (3.3p), light yellow oil, (66 mg,

87%). IR $\nu_{\text{max}}(\text{cm}^{-1})$: 3325, 2949, 2838, 1654, 1447, 1116, 1022; ^1H NMR (400 MHz, Methylene Chloride- d_2) δ 7.65 – 7.55 (m, 2H), 7.46 – 7.37 (m, 2H), 6.23 (d, J = 1.5 Hz, 1H), 5.57 (q, J = 1.3 Hz, 1H), 4.24 – 4.17 (m, 2H), 3.27 (td, J = 12.2, 2.6 Hz, 1H), 3.07 (ddd, J = 12.2, 4.3, 2.6 Hz, 1H), 2.32 (dt, J = 7.0, 1.3 Hz, 2H), 2.11 – 1.99 (m, 2H), 1.82 (ddd, J = 13.0, 3.7, 2.3 Hz, 1H), 1.42 – 1.35 (m, 2H), 1.34 – 1.28 (m, 6H). ^{13}C NMR (101 MHz, CD_2Cl_2) δ 167.36, 152.66, 138.83, 128.22 (q , J^2 = 32.5 Hz), 127.73, 126.79, 126.47 (q , J^3 = 3.8 Hz), 123.42 (q , J^1 = 271.7), 120.39, 61.28, 57.63, 52.48, 45.48, 38.87, 33.35, 32.52, 27.51, 14.54. HRMS (ESI) m/z [M+H] $^+$, calc'd for $\text{C}_{20}\text{H}_{23}\text{F}_3\text{N}_2\text{O}_2$ 381.1784; found 381.1787.

Following **GP3** with **3.1q** (41 mg, 0.2 mmol) and allylsulfone **3.2a** (152 mg, 0.6 mmol), the products (two isomers, **3.3q** and **3.3q'**, d.r. = 3:1) were isolated after flash chromatography on neutral alumina gel (1: 15 EtOAc/hexanes).

ethyl **4-((2*R*,3*R*)-2-cyano-1-(4-methoxyphenyl)-2-methylpyrrolidin-3-yl)-2-methylenbutanoate (3.3q)**, colorless oil, (42 mg, 62%).



IR $\nu_{\text{max}}(\text{cm}^{-1})$: 3383, 2944, 2351, 1712, 1509, 1449, 1249, 1191, 1034; ^1H NMR (400 MHz, Benzene- d_6) δ 7.33 – 7.21 (m, 2H), 7.16 (d, J = 2.0 Hz, 1H), 6.74 – 6.64 (m, 2H), 6.24 (d, J = 1.7 Hz, 1H), 5.21 (d, J = 1.7 Hz, 1H), 4.03 (qd, J = 7.2, 3.8 Hz, 2H), 3.30 (s, 3H), 3.20 (dd, J = 12.2, 2.6 Hz, 1H), 2.78 (ddd, J = 12.3, 4.3, 2.4 Hz, 1H), 2.26 – 2.06 (m, 3H), 1.76 (dt, J = 13.7, 2.5 Hz, 1H), 1.51 (dt, J = 13.2, 2.6 Hz, 1H), 1.11 (ddt, J = 21.4, 12.6, 3.4 Hz, 2H), 1.02 (t, J = 7.3 Hz, 3H), 1.00 (s, 3H). ^{13}C NMR (101 MHz, C_6D_6) δ 167.07, 158.90, 142.29, 139.29, 127.69, 126.31, 120.86, 114.72, 61.10, 58.27, 55.27, 52.48, 45.56, 39.04, 33.54, 32.80, 27.51, 14.59. HRMS (ESI) m/z [M+Na] $^+$, calc'd for $\text{C}_{20}\text{H}_{26}\text{N}_2\text{O}_3$ 365.1836; found 365.1838.

ethyl

4-((2*S*,3*R*)-2-cyano-1-(4-methoxyphenyl)-2-methylpyrrolidin-3-yl)-2-methylenebutanoate (3.3q'), colorless oil, (14 mg, 21%).

IR $\nu_{\text{max}}(\text{cm}^{-1})$: 3325, 2949, 2838, 1654, 1447, 1116, 1022; ^1H NMR (400 MHz, Benzene- d_6) δ 7.07 – 6.96 (m, 2H), 6.87 – 6.74 (m, 2H), 6.19 (s, 1H), 5.34 – 5.23 (m, 1H), 4.02 (q, J = 7.0 Hz, 2H), 3.37 (s, 3H), 3.10 – 2.92 (m, 1H), 2.34 (ddd, J = 15.1, 9.9, 5.2 Hz, 1H), 2.18 (td, J = 13.3, 11.3, 6.3 Hz, 1H), 1.79 (dddd, J = 17.5, 13.1, 7.0, 4.0 Hz, 2H), 1.62 (dddd, J = 16.7, 10.7, 6.1, 3.5 Hz, 2H), 1.36 (td, J = 16.9, 16.2, 7.7 Hz, 2H), 1.24 (s, 3H), 1.01 – 0.96 (m, 3H). ^{13}C NMR (101 MHz, C_6D_6) δ 166.95, 155.28, 141.05, 139.34, 124.97, 120.64, 120.18, 115.14, 63.01, 61.01, 55.46, 51.64, 50.55, 30.83, 30.33, 28.63, 23.04, 14.57. HRMS (ESI) m/z [M+Na] $^+$, calc'd for $\text{C}_{20}\text{H}_{26}\text{N}_2\text{O}_3$ 365.1836; found 365.1838.

Following **GP3** with **3.1r** (41 mg, 0.2 mmol) and allylsulfone **2a** (152 mg, 0.6 mmol), major product **3.3r** (two isomers, d.r. = 12:1) was isolated after flash chromatography on neutral alumina gel (1: 50 EtOAc/hexanes).

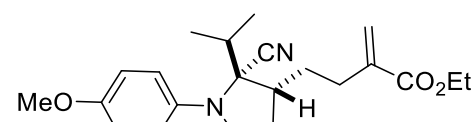
ethyl 4-((2*S*,3*R*)-2-cyano-2-isopropyl-1-phenylpyrrolidin-3-yl)-2-methylenebutanoate (3.3r),

colorless oil, (49 mg, 72%). IR $\nu_{\text{max}}(\text{cm}^{-1})$: 3354, 2978, 2361, 1710, 1604, 1507, 1326, 1188, 1147, 1022; ^1H NMR (400 MHz, Methylene Chloride- d_2) δ 7.51 – 7.40 (m, 2H), 7.33 (dd, J = 8.7, 6.9 Hz, 2H), 7.23 – 7.16 (m, 1H), 6.22 (d, J = 1.6 Hz, 1H), 5.57 (d, J = 1.6 Hz, 1H), 4.21 (qd, J = 7.1, 1.6 Hz, 2H), 3.19 (td, J = 12.3, 2.7 Hz, 1H), 3.08 – 3.02 (m, 1H), 2.37 (dd, J = 13.8, 6.4 Hz, 1H), 2.31 – 2.23 (m, 1H), 1.99 (ddt, J = 27.1, 13.6, 6.9 Hz, 2H), 1.84 – 1.69 (m, 2H), 1.38 – 1.22 (m, 5H), 1.02 (d, J = 7.0 Hz, 3H), 0.88 (d, J = 6.7 Hz, 3H). ^{13}C NMR (101 MHz, CD_2Cl_2) δ

167.49, 149.92, 139.06, 129.65, 129.61, 127.52, 126.57, 121.45, 65.23, 61.27, 54.73, 39.22, 35.12, 32.77, 32.62, 32.20, 18.38, 15.52, 14.59. HRMS (ESI) m/z [M+Na]⁺, calc'd for C₂₁H₂₈N₂O₂ 363.2043; found 363.2043.

Following **GP3** with **3.1s** (46 mg, 0.2 mmol) and allylsulfone **2a** (152 mg, 0.6 mmol), major product **3.3s** (two isomers, d.r. = 13:1) was isolated after flash chromatography on neutral alumina gel (1: 20 EtOAc/hexanes).

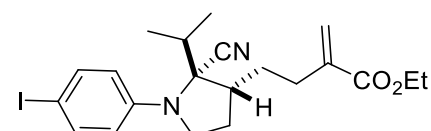
ethyl 4-((2S,3R)-2-cyano-2-isopropyl-1-(4-methoxyphenyl)pyrrolidin-3-yl)-2-methylenbutanoate (3.3s), colorless oil (58 mg, 78%).



IR $\nu_{\text{max}}(\text{cm}^{-1})$: 3417, 2939, 1710, 1628, 1514, 1459, 1287, 1241, 1181, 1159; ¹H NMR (400 MHz, Methylene Chloride-*d*₂) δ 7.44 – 7.31 (m, 2H), 6.89 – 6.79 (m, 2H), 6.21 (d, *J* = 1.6 Hz, 1H), 5.57 (q, *J* = 1.2 Hz, 1H), 4.21 (qd, *J* = 7.1, 1.5 Hz, 2H), 3.77 (s, 3H), 3.16 (dd, *J* = 12.3, 2.7 Hz, 1H), 2.98 (ddd, *J* = 12.3, 4.5, 2.5 Hz, 1H), 2.43 – 2.32 (m, 1H), 2.27 (ddd, *J* = 13.9, 7.4, 1.1 Hz, 1H), 2.11 – 1.94 (m, 1H), 1.88 (h, *J* = 6.8 Hz, 1H), 1.83 – 1.68 (m, 2H), 1.38 – 1.22 (m, 5H), 1.01 (d, *J* = 6.9 Hz, 3H), 0.90 (d, *J* = 6.7 Hz, 3H). ¹³C NMR (101 MHz, CD₂Cl₂) δ 167.49, 158.32, 142.56, 139.10, 128.47, 126.51, 121.48, 114.65, 65.83, 61.25, 55.86, 54.57, 39.23, 35.09, 32.78, 32.64, 32.30, 18.40, 15.57, 14.58. HRMS (ESI) m/z [M+H]⁺, calc'd for C₂₂H₃₀N₂O₃ 393.2149; found 393.2151.

Following **GP3** with **3.1t** (66 mg, 0.2 mmol) and allylsulfone **2a** (152 mg, 0.6 mmol), major product **3.3t** (two isomers, d.r. = 10:1) was isolated after flash chromatography on neutral alumina gel (1: 20 EtOAc/hexanes).

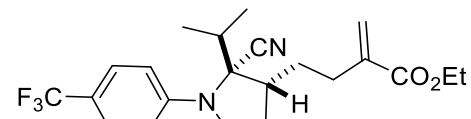
ethyl 4-((2S,3R)-2-cyano-1-(4-iodophenyl)-2-isopropylpyrrolidin-3-yl)-2-methylenbutanoate (3.3t), colorless oil (71 mg, 77%). IR



$\nu_{\text{max}}(\text{cm}^{-1})$: 3431, 2978, 2351, 1707, 1594, 1480, 1367, 1212, 1188, 1140; ^1H NMR (400 MHz, Methylene Chloride- d_2) δ 7.72 – 7.58 (m, 2H), 7.25 – 7.15 (m, 2H), 6.21 (d, J = 1.6 Hz, 1H), 5.60 – 5.52 (m, 1H), 4.20 (qd, J = 7.2, 1.6 Hz, 2H), 3.20 – 3.09 (m, 1H), 3.03 (ddd, J = 12.5, 4.6, 2.6 Hz, 1H), 2.36 (dd, J = 13.8, 6.4 Hz, 1H), 2.29 – 2.20 (m, 1H), 2.05 – 1.88 (m, 2H), 1.77 (dd, J = 30.4, 12.9, 3.5, 2.1 Hz, 2H), 1.36 – 1.20 (m, 5H), 1.02 (d, J = 6.9 Hz, 3H), 0.86 (dd, J = 8.7, 6.9 Hz, 3H). ^{13}C NMR (101 MHz, CD₂Cl₂) δ 167.45, 149.74, 138.97, 138.79, 129.73, 127.52, 126.62, 121.16, 91.08, 65.04, 61.28, 54.68, 39.16, 34.98, 32.70, 32.49, 32.22, 18.33, 15.46, 14.59. HRMS (ESI) m/z [M+Na]⁺, calc'd for C₂₁H₂₇IN₂O₂ 489.1009; found 489.1012.

Following **GP3** with **3.1u** (54 mg, 0.2 mmol) and allylsulfone **2a** (152 mg, 0.6 mmol), major product **3.3u** (two isomers, d.r. = 12:1) was isolated after flash chromatography on neutral alumina gel (1: 20 EtOAc/hexanes).

ethyl **4-((2S,3R)-2-cyano-2-isopropyl-1-(4-(trifluoromethyl)phenyl)pyrrolidin-3-yl)-2-methylenbutanoate (3.3u)**, colorless oil (56 mg, 69%).



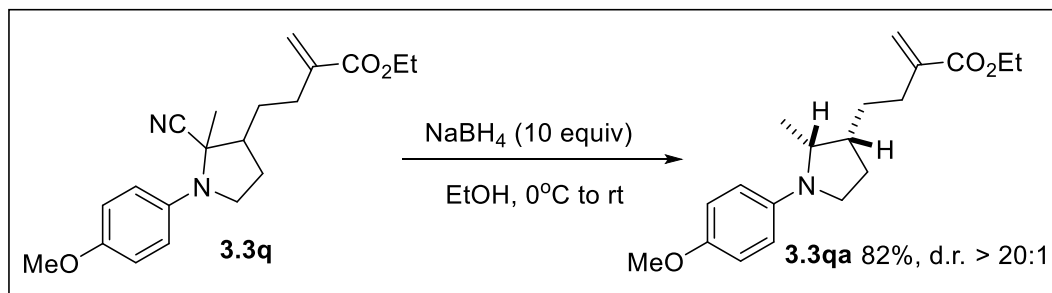
IR $\nu_{\text{max}}(\text{cm}^{-1})$: 3393, 2988, 2539, 1707, 1627, 1541, 1321, 1159, 1101; ^1H NMR (400 MHz, Methylene Chloride- d_2) δ 7.58 (q, J = 8.6 Hz, 4H), 6.23 (d, J = 1.6 Hz, 1H), 5.58 (d, J = 1.6 Hz, 1H), 4.21 (qd, J = 7.1, 1.6 Hz, 2H), 3.27 – 2.99 (m, 2H), 2.45 – 2.19 (m, 2H), 2.04 (dtd, J = 13.4, 7.7, 6.7, 3.8 Hz, 2H), 1.89 – 1.70 (m, 2H), 1.42 – 1.19 (m, 5H), 1.05 (d, J = 6.9 Hz, 3H), 0.85 (d, J = 6.7 Hz, 3H). ^{13}C NMR (101 MHz, CD₂Cl₂) δ 167.43, 153.35, 138.93, 128.09 ($q, J^2 = 32.5$ Hz), 127.82, 126.76 ($q, J^3 = 3.8$ Hz), 126.67, 124.77 ($q, J^1 = 271.9$ Hz), 121.09, 64.74, 61.30, 54.87, 39.14, 34.97, 32.68, 32.45, 32.16, 18.29, 15.38, 14.58. HRMS (ESI) m/z [M+Na]⁺, calc'd for C₂₂H₂₇F₃N₂O₂ 431.1917; found 431.1918.

Following **GP3** with **3.1v** (60 mg, 0.2 mmol) and allylsulfone **2a** (152 mg, 0.6 mmol), major product **3.3v** (two isomers, d.r. = 13:1) was isolated after flash chromatography on neutral alumina gel (1: 20 EtOAc/hexanes).

ethyl 4-((2S,3R)-1-(2-bromo-4-methylphenyl)-2-cyano-2-isopropylpyrrolidin-3-yl)-2-methylenbutanoate (3.3v), colorless oil, (45 mg, 51%)

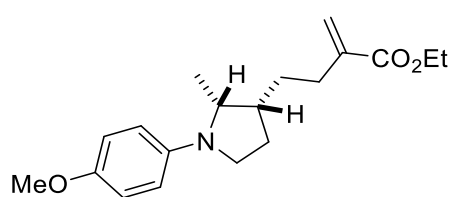
 IR $\nu_{\text{max}}(\text{cm}^{-1})$: 3397, 2949, 2833, 1700, 1637, 1490, 1309, 1191, 1154, 1019; ^1H NMR (400 MHz, Methylene Chloride- d_2) δ 7.68 (d, J = 8.1 Hz, 1H), 7.53 – 7.36 (m, 1H), 7.18 – 7.05 (m, 1H), 6.22 (d, J = 1.6 Hz, 1H), 5.57 (q, J = 1.2 Hz, 1H), 4.27 – 4.15 (m, 2H), 3.06 (ddd, J = 12.6, 4.6, 2.5 Hz, 1H), 2.92 (td, J = 12.3, 2.6 Hz, 1H), 2.38 (ddd, J = 13.9, 6.4, 1.1 Hz, 1H), 2.29 (s, 4H), 2.23 – 2.10 (m, 1H), 2.03 (dddd, J = 19.3, 12.1, 9.0, 5.7 Hz, 1H), 1.82 (ddd, J = 13.0, 3.5, 2.1 Hz, 1H), 1.77 – 1.66 (m, 1H), 1.49 – 1.36 (m, 1H), 1.31 (td, J = 7.2, 4.6 Hz, 4H), 1.06 (d, J = 6.9 Hz, 3H), 0.72 (d, J = 6.7 Hz, 3H). ^{13}C NMR (101 MHz, CD₂Cl₂) δ 167.47, 144.17, 139.05, 137.55, 134.85, 129.16, 126.61, 125.77, 124.36, 121.75, 64.21, 61.27, 53.52, 39.31, 35.23, 32.85, 32.11, 32.05, 20.82, 18.41, 15.08, 14.60. HRMS (ESI) m/z [M+Na]⁺, calc'd for C₂₂H₂₉BrN₂O₂ 455.1305, 457.1285; found 455.1308, 457.1288.

Derivatization of Product **3.3q**:

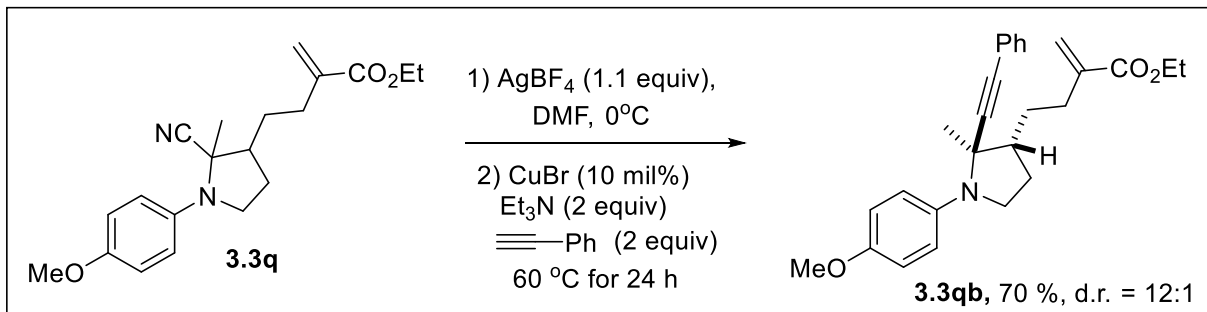


To a 25 mL round bottle flask equipped with a stir bar was added **3.3q** (51 mg, 0.15 mmol, 1 equiv), 10 mL of EtOH and cooled to 0 °C. NaBH₄ (57 mg, 1.5 mmol, 10 equiv) was added, and the reaction was allowed to slowly warm to room temperature. After 16 h, the reaction was quenched with 1 N NaOH (10 mL) and extracted with CH₂Cl₂, and the combined organic extracts were dried over sodium sulfate, filtered, concentrated and purified by flash column chromatography (1: 10 EtOAc/hexanes).

ethyl 4-((2*R*,3*R*)-1-(4-methoxyphenyl)-2-methylpyrrolidin-3-yl)-2-methylenecbutanoate

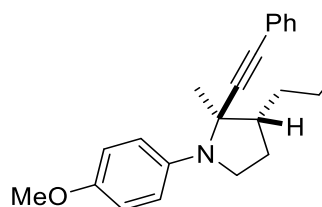


(3.3qa). Major product **3.3qa** was isolated as colorless oil, (39 mg, 82%). IR $\nu_{\text{max}}(\text{cm}^{-1})$: 3390, 2996, 2821, 1710, 1482, 1360, 1191, 1026; ¹H NMR (400 MHz, Methylene Chloride-*d*₂) δ 7.16 – 6.96 (m, 2H), 6.90 – 6.70 (m, 2H), 6.16 (d, *J* = 1.7 Hz, 1H), 5.57 – 5.48 (m, 1H), 4.18 (q, *J* = 7.1 Hz, 2H), 3.76 (s, 3H), 3.01 (dt, *J* = 11.6, 3.4 Hz, 1H), 2.64 (td, *J* = 11.9, 2.4 Hz, 1H), 2.27 (d, *J* = 6.6 Hz, 2H), 1.69 (tdt, *J* = 21.7, 11.8, 3.5 Hz, 4H), 1.35 – 1.22 (m, 4H), 1.01 (q, *J* = 11.9 Hz, 1H), 0.82 (d, *J* = 6.1 Hz, 3H). ¹³C NMR (101 MHz, CD₂Cl₂) δ 167.67, 157.09, 146.61, 139.75, 126.84, 126.04, 114.37, 61.09, 57.97, 56.13, 55.85, 42.21, 39.92, 35.92, 33.66, 30.27, 21.87, 14.57. FTMS (ESI) m/z [M+H]⁺, calc'd for C₁₉H₂₇NO₃ 318.2064; found 318.2064.



To a 25 mL round bottle flask equipped with a stir bar was added **3.3q** (51 mg, 0.15 mmol, 1 equiv), 5mL of DMF and cooled to 0 °C. AgBF₄ (33 mg, 0.17 mmol, 1.1 equiv) was added, and the reaction was monitored by TLC until all the **3.3q** is reacted. Triethylamine (42 µL, 0.3 mmol, 2 equiv), phenylacetylene (33 µL, 0.3 mmol, 2 equiv) and CuBr (3 mg, 0.015 mmol, 0.1 equiv) were then added to the round bottle flask and the resulting reaction mixtures were heated at 60 °C for 24 h. The solution was then filtered through a short pad of Celite, concentrated and purified by flash column chromatography (1: 20 EtOAc/hexanes).

ethyl 4-((2*R*,3*R*)-1-(4-methoxyphenyl)-2-methyl-2-(phenylethynyl)pyrrolidin-3-yl)-2-methylenbutanoate (3.3qb). Major product **3.3qb** (two



isomers, d.r. = 12:1) was isolated as colorless oil, (43 mg, 70%). IR $\nu_{\text{max}}(\text{cm}^{-1})$: 3407, 2920, 2356, 1712, 1502, 1379, 1246, 1186, 1027; ¹H NMR (400 MHz, Chloroform-*d*) δ 7.47 – 7.37 (m, 2H), 7.35 – 7.27 (m, 5H), 6.84 – 6.75 (m, 2H), 6.20 (d, *J* = 1.6 Hz, 1H), 5.56 – 5.50 (m, 1H), 4.19 (qd, *J* = 7.1, 1.2 Hz, 2H), 3.77 (s, 3H), 3.41 (td, *J* = 12.1, 2.6 Hz, 1H), 2.86 (ddd, *J* = 11.8, 4.3, 2.5 Hz, 1H), 2.35 – 2.26 (m, 2H), 2.18 (dtt, *J* = 15.2, 6.9, 3.4 Hz, 1H), 1.99 – 1.88 (m, 1H), 1.81 – 1.70 (m, 1H), 1.39 – 1.29 (m, 2H), 1.28 – 1.19 (m, 5H). ¹³C NMR (101 MHz, CDCl₃) δ 167.57, 157.30, 143.54, 139.15, 131.77, 128.62, 128.43, 127.98, 126.07, 123.82, 113.50, 91.66, 86.32, 60.84, 56.19, 55.55, 51.53, 47.41, 39.05, 33.25, 32.75, 30.03, 14.41. HRMS (ESI) m/z [M+H]⁺, calc'd for C₂₇H₃₁NO₃ 418.2377; found 418.2380.

Stern-Volmer Quenching study

Fluorescence quenching studies were conducted using a Photon Technology Fluorescence Spectrophotometer. In each experiment, a solution of 5.0 x 10⁻⁴ M Ir(ppy)₂(dtbbpy)PF₆ in CH₂Cl₂ was mixed with a CH₂Cl₂ solution of a quencher of various concentration in a screw-top

1.0 cm quartz cuvette. After degassing by sparging with argon for ten minutes, the resulting solution was irradiated at 460 nm, and fluorescence was measured at 575 nm. Plots were constructed according to the Stern-Volmer equation: $I_0/I = 1 + k_q\tau_0[Q]$.

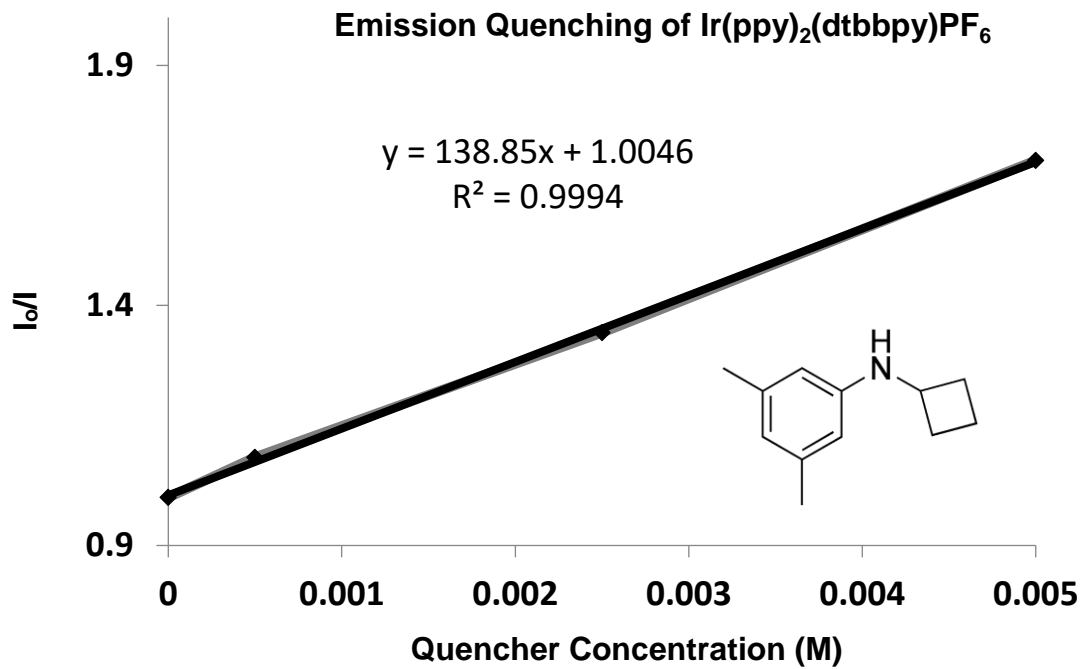


Chart 3.1a Using *N*-cyclobutylaniline to quench $\text{Ir}(\text{ppy})_2(\text{dtbbpy})\text{PF}_6$.

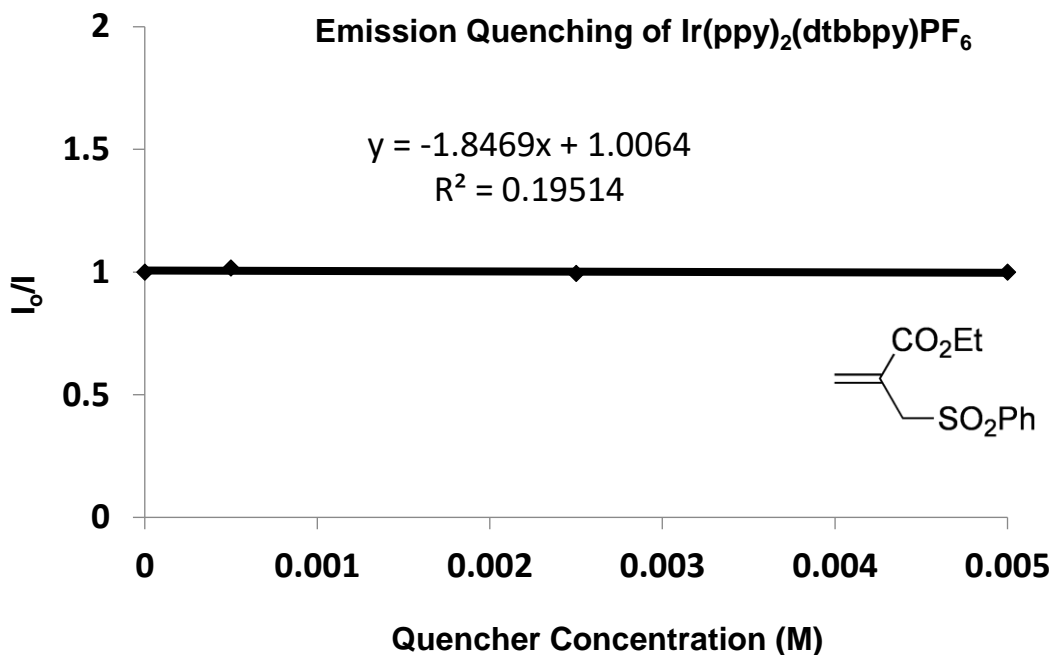


Chart 3.1b Using allylsulfone to quench $\text{Ir(ppy)}_2(\text{dtbbpy})\text{PF}_6$

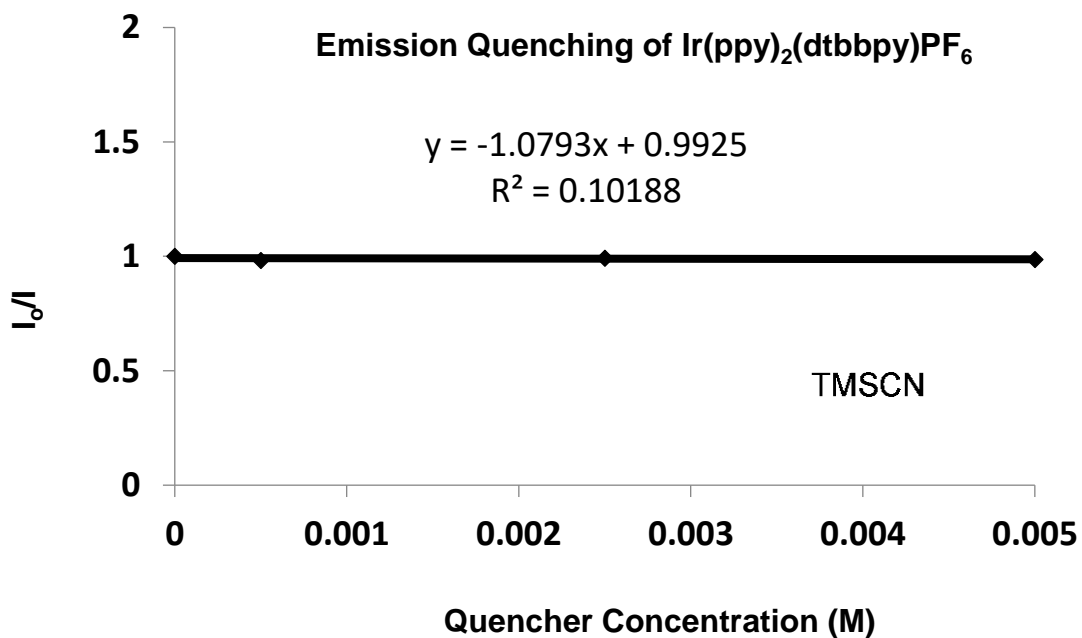


Chart 3.1c Using TMSCN to quench $\text{Ir(ppy)}_2(\text{dtbbpy})\text{PF}_6$

Quantum Yield measurement:

The quantum yield was measured according to the published procedures with modifications. A 300 W Xenon lamp (50% of light intensity, 439 ± 5 nm bandpass filter high transmittance). Standard ferrioxalate actinometry was used to determine the light intensity at 439 nm.

All the solutions were prepared and stored in the dark for immediate use:

1. Potassium ferrioxalate solution (0.15 M): 1.105 g of potassium ferrioxalate hydrate was dissolved in 15 mL of 0.05 M H_2SO_4 .
2. Buffered solution of phenanthroline: 50 mg of phenanthroline and 11.25 g of sodium acetate were dissolved in 50 mL of 0.5 M H_2SO_4 .

I) Measurement of light intensity at 439 nm:

To a quartz cuvette ($l = 1.000$ cm) was added 2 mL of the ferrioxalate solution. The actinometry solution (placed in a fixed position 7 cm away from lamp) was irradiated with a 300 W Xenon lamp (50% of light intensity, 439 ± 5 nm bandpass filter high transmittance) for specific time intervals (5s, 10s, 20s, 30s). After irradiation, 0.35 mL of the phenanthroline solution was added to the cuvette. The solution was then kept in dark for 1 hour to allow the complete coordination of the ferrous ions to phenanthroline. UV-Vis absorbance of the actinometry solution was measured at 510 nm. A non-irradiated sample was also prepared (in dark) and the absorbance was measured at 510 nm.

The formation of Fe^{2+} was calculated using equation 1.

$$\text{mol } \text{Fe}^{2+} = \frac{V \times \Delta A}{l \times \epsilon} \quad (1)$$

Where V is the total volume (0.00235 L) of the solution after the complete coordination; ΔA is the optical difference (510 nm) in absorbance between the irradiated and the non-irradiated

solutions; l is the path length; ε is the molar absorptivity of $\text{Fe}(\text{phen})_3^{2+}$ at 510 nm (11100 L mol $^{-1}$ cm $^{-1}$).

The photon flux was calculated using equation 2.

$$\text{photon flux} = \frac{d(\text{mol Fe}^{2+})/dt}{\Phi \times f} \quad (2)$$

where Φ is the quantum yield for the ferrioxalate actinometer (10.1 for a 0.15 M solution at $\lambda = 436$ nm)²; f is the fraction of light absorbed at $\lambda = 439$ nm (0.99814, *vide infra*).

The calculation data is listed below:

Table 3.2. The absorbance of the actinometry at 510 nm.

t/s	5	10	20	30
$\Delta A/\text{a.u.}$	1.1644	1.80965	2.6481	3.16903

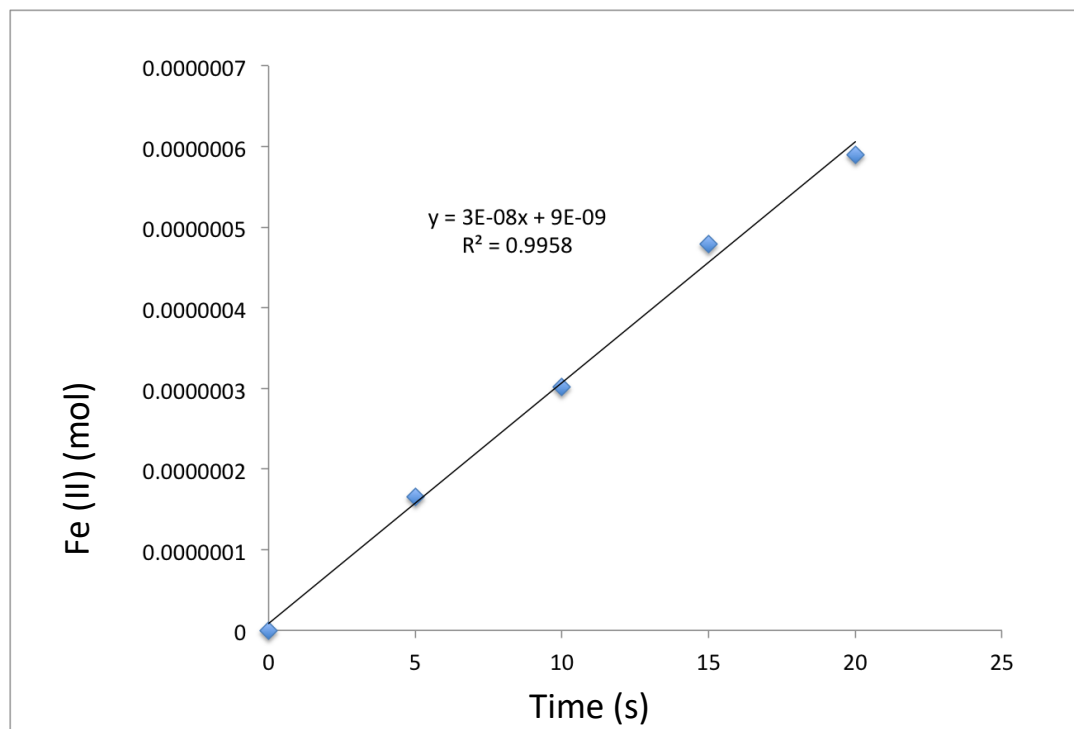


Chart 3.2 The moles of Fe^{2+} as a function of time (t)

According to equation 2,

$$\text{photon flux} = \frac{3 \times 10^{-8}}{1.01 \times 0.99814} = 2.98 \times 10^{-8} \text{ einstein} \square \text{s}^{-1}$$

II) Measurement of fraction of light absorbed at 439 nm for the ferrioxalate solution:

The absorbance of the ferrioxalate solution (A) at 439 nm was measured to be 2.72940. Hence, the fraction of light absorbed (f) by the solution was calculated using eq 3.

$$f = 1 - 10^{-A} \quad (3)$$

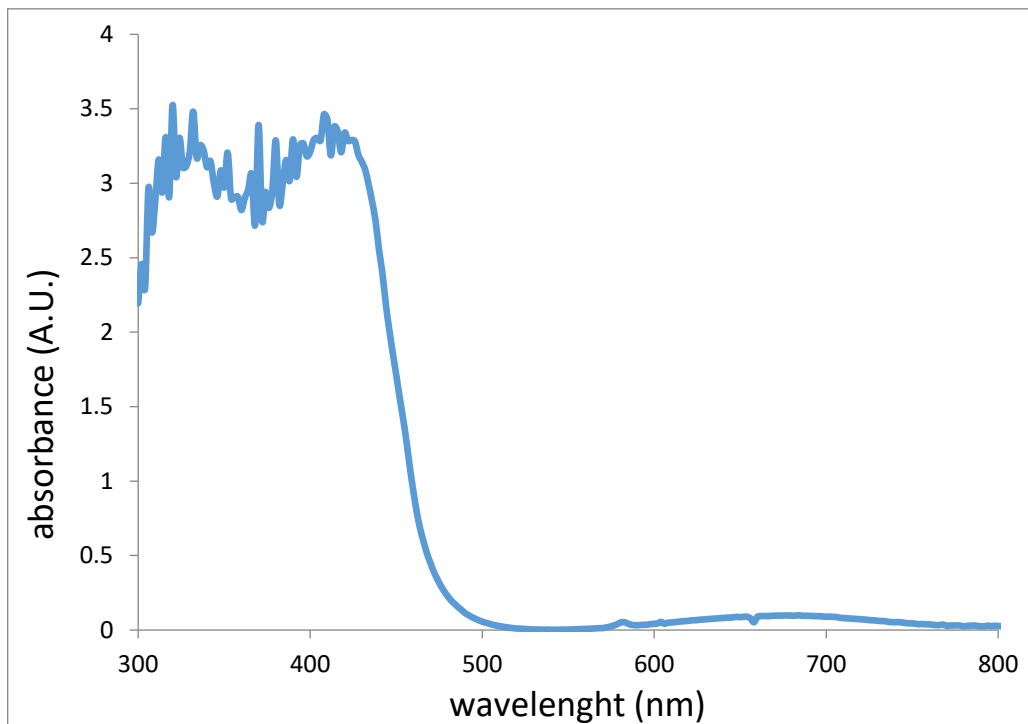
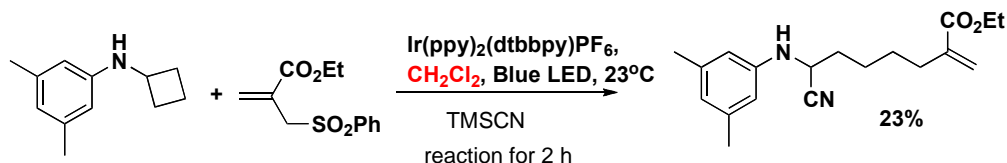


Chart 3.3. Absorbance of the ferrioxalate actinometer solution

III) Measurement of the quantum yield:



General procedure for the quantum yield measurement: To a dried 2.0 mL cuvette (with a PTFE screw cap) equipped with a stir bar was charged with $\text{Ir}(\text{ppy})_2(\text{dtbbpy})\text{PF}_6$ (2 mol%), 3,5-

dimethylcyclopropylaniline **3.1a** (33 mg, 0.2 mmol, 1 equiv), trimethylsilyl cyanide (75 μ L, 0.6 mmol, 3 equiv), allylsulfone **3.2a** (0.6 mmol, 3 equiv) and CH_2Cl_2 (2 mL). The cuvette was then degassed by bubbling nitrogen to the solution for 5 min. The sample (placed in a fixed position 7 cm away from lamp) was stirred and irradiated with a 300 W Xenon lamp (50% of light intensity, 439 ± 5 nm bandpass filter high transmittance) for fixed time, concentrated, and measured the NMR yield of the product. CH_2Br_2 (14 μ L, 0.2 mmol) was used as internal standard for NMR yield measurement. The quantum yield was determined using equation 4. The absorbance of the reaction solution (A) at 439 nm was measured to be 3.72513 ($f=1$, vide infra).

$$\phi = \frac{\text{mole of the product}}{\text{flux} \times t \times f} \quad (4)$$

Experiment 1: 33 mg (0.2 mmol) of **3.1a**, 153 mg (0.6 mmol) of **3.2a**, 75 μ L (0.6 mmol) of trimethylsilyl cyanide, 3.9 mg of $\text{Ir}(\text{ppy})_2(\text{dtbbpy})\text{PF}_6$ in 2 mL of CH_2Cl_2 after irradiation under a wavelength of 439 ± 5 nm. The yield of product **3.3a** was calculated to be 23%. $\Phi=1.44$.

$$\frac{0.46 \times 10^{-4} \text{ mol}}{2.98 \times 10^{-8} \text{ einstein s}^{-1} \times 7200 \text{ s} \times 1.00} = 0.214$$

Experiment 1(repeat): 34 mg (0.2 mmol) of **3.1a**, 155 mg (0.6 mmol) of **3.2a**, 75 μ L (0.6 mmol) of trimethylsilyl cyanide, 4 mg of $\text{Ir}(\text{ppy})_2(\text{dtbbpy})\text{PF}_6$ in 2 mL of CH_2Cl_2 after irradiation under a wavelength of 439 ± 5 nm. The yield of product **3.3a** was calculated to be 23%. $\Phi=1.44$.

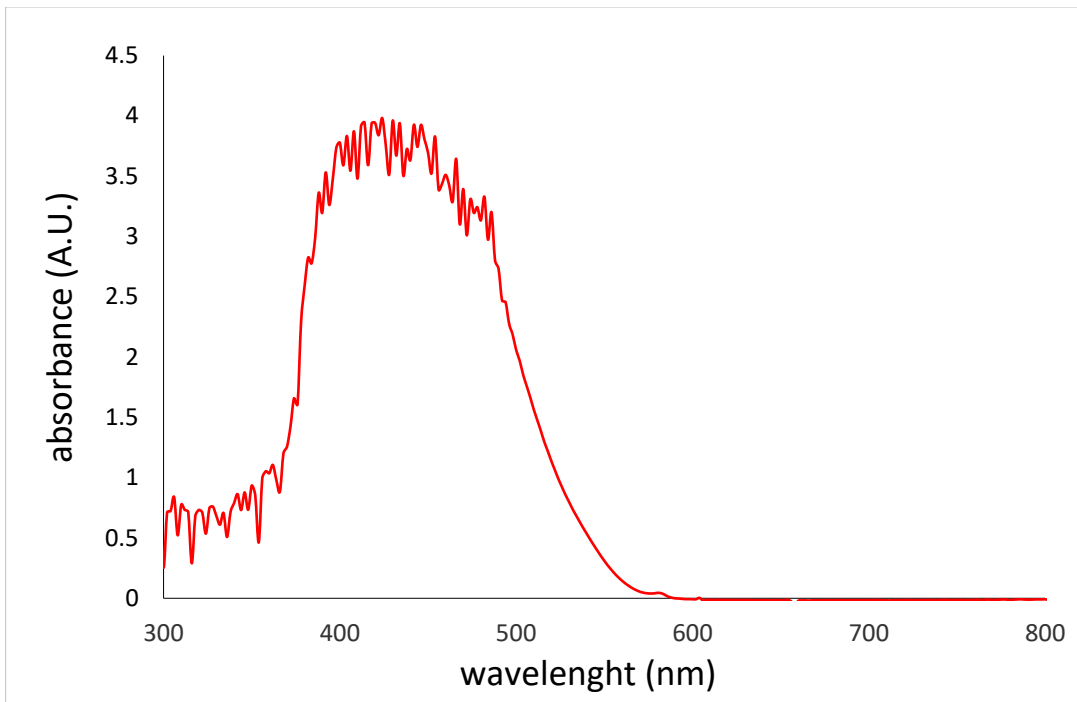


Chart 3.4 Absorbance of catalyst.

3.3 Summary

We have successfully developed a difunctionalization reaction of *N*-cyclobutylanilines and *N*-cyclopopylanilines. The reaction was conducted under an extremely mild reaction condition under visible light irradiation and room temperature. This method was used to synthesis a broad scope of α -cyano anilines. The method was further expanded to the success difunctionalization of fused cyclopropylanilines. Structurally important α -cyano pyrrolidines were synthesized with the generation of a quaternary carbon center on the α positin of pyrrolidines. Derivatization of those α -cyano pyrrolidine products provided further handle by the construction of new carbon-carbon bond at the α positin of pyrrolidine which successfully highlighted the versatility of this powerful method. Continuous work based on a similar transformation for remote construction of carbon-heteroatom bonds and carbon-carbon bonds are

now under investigated in our lab. On the other hand, different nucleophiles for assisting the ring opening of N-cyclobutylanilines are also under investigation in our lab.

3.4 References.

1. (a) Stirk, K. M.; Kiminkinen, L. K. M.; Kenttamaa, H. I., ION MOLECULE REACTIONS OF DISTONIC RADICAL CATIONS. *Chemical Reviews* **1992**, *92* (7), 1649-1665. (b) Hammerum, S., DISTONIC RADICAL CATIONS IN GASEOUS AND CONDENSED PHASE. *Mass Spectrometry Reviews* **1988**, *7* (2), 123-202.
2. (a) Zeller, L.; Farrell, J.; Vainiotalo, P.; Kenttamaa, H. I., LONG-LIVED RADICAL CATIONS OF SIMPLE ORGANOPHOSPHATES ISOMERIZE SPONTANEOUSLY TO DISTONIC STRUCTURES IN THE GAS-PHASE. *Journal of the American Chemical Society* **1992**, *114* (4), 1205-1214. (b) Stirk, K. M.; Orlowski, J. C.; Leek, D. T.; Kenttamaa, H. I., THE IDENTIFICATION OF DISTONIC RADICAL CATIONS ON THE BASIS OF A REACTION WITH DIMETHYL DISULFIDE. *Journal of the American Chemical Society* **1992**, *114* (22), 8604-8606. (c) Schaftenaar, G.; Postma, R.; Ruttink, P. J. A.; Burgers, P. C.; McGibbon, G. A.; Terlouw, J. K., THE GAS-PHASE CHEMISTRY OF THE METHYL CARBAMATE RADICAL CATION H₂NCOOCH₃⁺. - ISOMERIZATION INTO DISTONIC IONS, HYDROGEN-BRIDGED RADICAL CATIONS AND ION-DIPOLE COMPLEXES. *International Journal of Mass Spectrometry* **1990**, *100*, 521-544. (d) Kenttamaa, H. I., LONG-LIVED DISTONIC RADICAL CATIONS. *Organic Mass Spectrometry* **1994**, *29* (1), 1-10. (e) Gronert, S., Mass spectrometric studies of organic ion/molecule reactions. *Chemical Reviews* **2001**, *101* (2), 329-360. (f) Gauld, J. W.; Radom, L., Effects of neutral bases on the isomerization of conventional radical cations CH₃X center dot⁺ to their distonic isomers (CH₂X+H)-C-center dot (X = F, OH, NH₂): Proton-transport catalysis and other mechanisms. *Journal of the American Chemical Society* **1997**, *119* (41), 9831-9839.
3. (a) Chen, X. H.; Syrstad, E. A.; Nguyen, M. T.; Gerbaux, P.; Turek, F., Distonic isomers and tautomers of the adenine cation radical in the gas phase and aqueous solution. *Journal of Physical Chemistry A* **2004**, *108* (42), 9283-9293. (b) Rios, L. A.; Dolbier, W. R.; Paredes, R.; Lusztyk, J.; Ingold, K. U.; Jonsson, M., Generation and study of the reactivity of alpha-ammonium distonic radical cations in solution. *Journal of the American Chemical Society* **1996**, *118* (45), 11313-11314. (c) Widjaja, F.; Jin, Z. C.; Nash, J. J.; Kenttamaa, H. I., Direct Comparison of Solution and Gas-Phase Reactions of the Three Distonic Isomers of the Pyridine Radical Cation with Methanol. *Journal of the American Chemical Society* **2012**, *134* (4), 2085-2093. (d) Widjaja, F.; Jin, Z. C.; Nash, J. J.; Kenttamaa, H. I., Comparison of the Reactivity of the Three Distonic Isomers of the Pyridine Radical Cation Toward Tetrahydrofuran in Solution and in the Gas Phase. *Journal of the American Society for Mass Spectrometry* **2013**, *24* (4), 469-480.

4. (a) Hu, J.; Wang, J.; Nguyen, T. H.; Zheng, N., The chemistry of amine radical cations produced by visible light photoredox catalysis. *Beilstein Journal of Organic Chemistry* **2013**, 9, 1977-2001. (b) Morris, S. A.; Wang, J.; Zheng, N., The Prowess of Photogenerated Amine Radical Cations in Cascade Reactions: From Carbocycles to Heterocycles. *Accounts of Chemical Research* **2016**, 49 (9), 1957-1968.
5. Born, M.; Ingemann, S.; Nibbering, N. M. M., Formation and chemistry of radical anions in the gas phase. *Mass Spectrometry Reviews* **1997**, 16 (4), 181-200.
6. Rios, L. A.; Dolbier, W. R.; Paredes, R.; Lusztyk, J.; Ingold, K. U.; Jonsson, M., Generation and Study of the Reactivity of α -Ammonium Distonic Radical Cations in Solution. *Journal of the American Chemical Society* **1996**, 118 (45), 11313-11314.
7. (a) Wang, S.; Guo, L. N.; Wang, H.; Duan, X.-H., Alkynylation of Tertiary Cycloalkanols via Radical C–C Bond Cleavage: A Route to Distal Alkynylated Ketones. *Organic Letters* **2015**, 17 (19), 4798-4801. (b) Li, Y.; Ye, Z.; Bellman, T. M.; Chi, T.; Dai, M., Efficient Synthesis of β -CF₃/SCF₃-Substituted Carbonyls via Copper-Catalyzed Electrophilic Ring-Opening Cross-Coupling of Cyclopropanols. *Organic Letters* **2015**, 17 (9), 2186-2189. (c) Ye, Z.; Gettys, K. E.; Shen, X.; Dai, M., Copper-Catalyzed Cyclopropanol Ring Opening Csp₃–Csp₃ Cross-Couplings with (Fluoro)Alkyl Halides. *Organic Letters* **2015**, 17 (24), 6074-6077.
8. (a) Wang, D.; Ren, R.; Zhu, C., Manganese-Promoted Ring-Opening Hydrazination of Cyclobutanols: Synthesis of Alkyl Hydrazines. *The Journal of Organic Chemistry* **2016**, 81 (17), 8043-8049. (b) Ren, R.; Zhao, H.; Huan, L.; Zhu, C., Manganese-Catalyzed Oxidative Azidation of Cyclobutanols: Regiospecific Synthesis of Alkyl Azides by C–C Bond Cleavage. *Angewandte Chemie International Edition* **2015**, 54 (43), 12692-12696. (c) Zhao, H.; Fan, X.; Yu, J.; Zhu, C., Silver-Catalyzed Ring-Opening Strategy for the Synthesis of β - and γ -Fluorinated Ketones. *Journal of the American Chemical Society* **2015**, 137 (10), 3490-3493. (d) Wang, M.; Wu, Z.; Zhu, C., Ring-opening selenation of cyclobutanols: synthesis of [gamma]-selenylated alkyl ketones through C–C bond cleavage. *Organic Chemistry Frontiers* **2017**, 4 (3), 427-430.
9. (a) Ellman, J. A.; Owens, T. D.; Tang, T. P., N-tert-Butanesulfinyl imines: Versatile intermediates for the asymmetric synthesis of amines. *Accounts of Chemical Research* **2002**, 35 (11), 984-995. (b) Groger, H., Catalytic enantioselective Strecker reactions and analogous syntheses. *Chemical Reviews* **2003**, 103 (8), 2795-2827. (c) Kobayashi, S.; Ishitani, H., Catalytic enantioselective addition to imines. *Chemical Reviews* **1999**, 99 (5), 1069-1094. (d) Wang, J.; Liu, X. H.; Feng, X. M., Asymmetric Strecker Reactions. *Chemical Reviews* **2011**, 111 (11), 6947-6983.
10. (a) Qi, L.; Chen, Y., Polarity-Reversed Allylations of Aldehydes, Ketones, and Imines Enabled by Hantzsch Ester in Photoredox Catalysis. *Angewandte Chemie International Edition* **2016**, 55 (42), 13312-13315. (b) Hu, C.; Chen, Y., Chemoselective and fast decarboxylative allylation by photoredox catalysis under mild conditions. *Organic Chemistry Frontiers* **2015**, 2 (10), 1352-1355. (c) Heitz, D. R.; Rizwan, K.; Molander, G.

A., Visible-Light-Mediated Alkenylation, Allylation, and Cyanation of Potassium Alkyltrifluoroborates with Organic Photoredox Catalysts. *The Journal of Organic Chemistry* **2016**, *81* (16), 7308-7313. (d) Quiclet-Sire, B.; Zard, S. Z., New Radical Allylation Reaction. *Journal of the American Chemical Society* **1996**, *118* (5), 1209-1210. (e) Kamijo, S.; Kamijo, K.; Maruoka, K.; Murafuji, T., Aryl Ketone Catalyzed Radical Allylation of C(sp³)-H Bonds under Photoirradiation. *Organic Letters* **2016**, *18* (24), 6516-6519. (f) Schaffner, A.-P.; Renaud, P., Tin-Free Radical Allylation of B-Alkylcatecholboranes. *Angewandte Chemie International Edition* **2003**, *42* (23), 2658-2660. (g) Le Guyader, F.; Quiclet-Sire, B.; Seguin, S.; Zard, S. Z., New Radical Allylation Reaction of Iodides. *Journal of the American Chemical Society* **1997**, *119* (31), 7410-7411.

11. (a) Giese, B.; He, J.; Mehl, W., Polar effects in radical addition reactions: Borderline cases. *Chemische Berichte* **1988**, *121* (11), 2063-2066. (b) Batchelor, S. N.; Fischer, H., Radical Addition Rates to Alkenes by Time-Resolved CIDNP: 2-Hydroxy-2-propyl Radicals. *The Journal of Physical Chemistry* **1996**, *100* (23), 9794-9799.
12. Wang, J.; Zheng, N., The cleavage of a C-C Bond in cyclobutylanilines by visible-light photoredox catalysis: Development of a [4+2] annulation method. *Angew. Chem., Int. Ed.* **2015**, *54* (39), 11424-11427.
13. (a) Surry, D. S.; Buchwald, S. L., Dialkylbiaryl phosphines in Pd-catalyzed amination: a user's guide. *Chemical Science* **2011**, *2* (1), 27-50. (b) Hartwig, J. F., Evolution of a Fourth Generation Catalyst for the Amination and Thioetherification of Aryl Halides. *Accounts of Chemical Research* **2008**, *41* (11), 1534-1544.
14. Gruhn, A. G.; Reusch, W., Acid-catalyzed reactions of a strained ring nazarov substrate. *Tetrahedron* **1993**, *49* (36), 8159-8168.
15. McLaughlin, M.; Palucki, M.; Davies, I. W., Efficient Access to Azaindoles and Indoles. *Organic Letters* **2006**, *8* (15), 3307-3310